The Pennsylvania State University

The Graduate School

Department of Civil Engineering

A CAPACITY ESTIMATION METHOD FOR TWO-LANE, TWO-WAY HIGHWAYS USING SIMULATION MODELING

A Thesis in

Civil Engineering

by

Joonhyo Kim

Submitted in Partial Fulfillment
of the Requirements
for the Degree of

Doctor of Philosophy

August 2006

The thesis of Joonhyo Kim was reviewed and approved by the following:

Martin T. Pietrucha
Associate Professor of Civil and Environmental Engineering
Thesis Co-Advisor
Chair of Committee

Ageliki Elefteriadou
Associate Professor of Civil and Coastal Engineering
University of Florida
Thesis Co-Advisor
Special Member

Kevin M. Mahoney
Associate Professor of Civil and Environmental Engineering

Eric T. Donnell
Assistant Professor of Civil and Environmental Engineering

Deborah J. Medeiros
Associate Professor of Industrial and Manufacturing Engineering

Andrew Scanlon
Professor of Civil and Environmental Engineering
Head of the Department of Civil and Environmental Engineering

*Signatures are on file in the Graduate School

ABSTRACT

The 2000 HCM (Highway Capacity Manual) suggests the capacity of two-lane, two-way highways to be 3,400 pcph for both directions and 1,700 pcph for one direction. In fact, higher traffic volumes have been observed in previous studies. Also, a single capacity value cannot reflect the variety of traffic, geometric, and driver conditions that may exist on two-lane, two-way highways. In addition, observation of capacity is difficult, so a new simulation model is developed in this study. Capacity of two-lane, two-way highways is estimated using a microscopic simulation model, which is developed with MATLAB 6.5. Due to the absence of capacity data, the newly developed simulator, TWOSIM (Two-lane, two-way highway SIMulator) is compared to existing analytical tools such as TWOPAS and 2000 HCM method for verification of its performance. Using TWOSIM, the capacity (i.e., 100 percent no-passing zone, all passenger cars and commuters, level tangent section, 12’ lane width, 6’ shoulder width) for one direction is estimated to be 2,100 pcph at 60 and 70 mph average free flow speeds, 2,000 pcph at 50 mph average free flow speed, and 1,850 pcph at 40 mph average free flow speed. These estimated capacities are higher than the 2000 HCM’s estimated capacity for one direction. The presence of passing zones was not found to increase capacity. Additional capacity values are estimated to account for the presence of a driveway, a horizontal curve, a grade, and various percentages of trucks in the traffic stream. These treatments were found to reduce capacity (5~38 percent reduction in capacity). Based on the results, recommendations are provided regarding changes in the 2000 HCM, as well as in the model calibration and algorithm improvement of TWOSIM.

TABLE OF CONTENTS

LIST OF FIGURES vii

LIST OF TABLES x

ACKNOWLEDGEMENTS xiii

CHAPTER 1. INTRODUCTION 1
1.1 Background 1
1.2 Objectives 3
CHAPTER 2. LITERATURE REVIEW 4
2.1 Definition of highway capacity 4
2.2 Capacity studies and traffic flow characteristics for two-lane, highways 6
2.2.1 Analytical approaches 7
2.2.2 Empirical approach 10
2.2.3 Two-lane, highway capacity in the U.S Highway Capacity Manual 14
2.3 Factors affecting the capacity of two-lane, two-way highways 15
2.3.1 Overtaking and gap acceptance 16
2.3.2 Opposing volume 18
2.3.3 Heavy vehicles 20
2.3.4 Geometric conditions 23
2.3.5 Passing zones and passing sight distance 24
2.4 Modeling two-lane, two-way highways 24
2.4.1 Arrival headway distributions 24
2.4.2 Car-following models 27
2.5 Existing simulation models 29
2.5.1 TWOPAS (TWO-lane PASsing) 29
2.5.2 TRARR (TRAffic on Rural Roads) 30
2.6 Research findings to date and research needs 32
CHAPTER 3. METHODOLOGY 35
3.1 Field data collection 35
3.2 Development of the simulation model 36
3.3 Estimation of capacity 37
CHAPTER 4. FIELD DATA COLLECTION 38
4.1 Data collection 38
4.1.1 Science Park Road, State College, Pennsylvania 39
4.1.2 Highway 322, State College, Pennsylvania 41
4.2 Data reduction and analysis 43
4.2.1 Science Park Road 43
4.2.2 Highway 322 52
4.3 Summary 61

CHAPTER 5. BASIC TWO-LANE, TWO-WAY HIGHWAY SIMULATOR (TWOSIM I) 62
5.1 Base conditions 62
5.2 Input data 63
5.2.1 Arrival headway distribution 63
5.2.2 Car following model 67
5.3 Verification of basic two-lane, two-way highway simulator (TWOSIM I) 83
5.3.1 Input data 84
5.3.2 Speed-flow-density relationships 89
5.4 Comparison of TWOSIM I to TWOPAS and HCM 2000 91
5.4.1 Comparison of average travel speed 92
5.4.2 Comparison of percent time spent following 94
5.5 Capacity estimation and sensitivity analysis 96
5.5.1 Determination of observation point for the collection of capacity data 96
5.5.2 Arrival demand and arrival rate 97
5.5.3 Estimation of capacity 98
5.6 Sensitivity analysis 100
5.6.1 Capacity vs. average free flow speed 100
5.6.2 Capacity vs. standard deviation of desired speed 101
5.6.3 Capacity vs. delay of safety reaction time 101
5.6.4 Capacity vs. length of study segment 102
5.7 Results 103
CHAPTER 6. TWO-LANE, TWO-WAY HIGHWAY SIMULATOR WITH PASSING ZONE (TWOSIM II) 104
6.1 Development of TWOSIM II model 105
6.1.1 Minimum passing sight distance 105
6.1.2 Passing zone and no-passing zone 107
6.1.3 Available passing sight distance 108
6.1.4 Passing behavior 108
6.1.5 Assumptions of TWOSIM II 109
6.1.6 Implementation of the passing algorithm 113
6.1.7 Verification of TWOSIM II 115
6.2 Comparison to the findings from other studies 121
6.2.1 Comparison of passing time 121
6.2.2 Comparison of passing rate 122
6.3 Estimation of capacity 123
6.4 Sensitivity analysis 126
6.4.1 Passing rates vs. traffic volume and free flow speed 126
6.4.2 Capacity vs. opposing flow 127
6.5 Results 128
CHAPTER 7. TWO-LANE, TWO-WAY HIGHWAY SIMULATOR WITH DRIVEWAY, HORIZONTAL CURVE, AND GRADE (TWOSIM III) 129
7.1 Development of TWOSIM III 130
7.1.1 Driveway 130
7.1.2 Horizontal curve 134
7.1.3 Grades 137

7.2 Verification of TWOSIM III 140
7.2.1 Verification of driveway algorithm 140
7.2.2 Verification of horizontal curve algorithm 142
7.2.3 Verification of grade algorithm 145
7.3 Comparison of TWOSIM III to TWOPAS and HCM 2000 147
7.3.1 Presence of a driveway 148
7.3.2 Presence of a horizontal curve 149
7.3.3 Presence of grades 151
7.3.4 Presence of heavy vehicles 152
7.4 Estimation of capacity 153
7.4.1 Presence of a driveway 153
7.4.2 Presence of a horizontal curve 154
7.4.3 Presence of upgrade section 155
7.5 Sensitivity analysis 155
7.5.1 Superelevation of the horizontal curve 155
7.5.2 Percent of trucks 156
7.5.3 Length of upgrade 158
7.5.4 Horizontal curve at upgrade section 158
7.6 Results 159
CHAPTER 8. CONCLUSIONS AND RECOMMENDATIONS 161
REFERENCES 166
APPENDICES 172
APPENDIX A: SUMMARY OF FIELD DATA 169
Histogram of free flow speeds (Science Park Road) 169
APPENDIX B: IMPLEMENTATION OF TWOSIM 173
Implementation of arrival headway distribution 173
Implementation of Gipps' car-following model in TWOSIM 174
APPENDIX C: CODE OF TWOSIM 196
Example of code in TWOSIM I 196
Input and output data in TWOSIM I 209
APPENDIX D: VERIFICATION OF TWOSIM 212
Regression analysis for average travel speed of the first dummy vehicle 212
Akcelik's M3A headway distribution 212
Maximum acceleration rates 213
Effective size of vehicles 214
Desired speeds 214
APPENDIX E: HYPOTHESIS TEST 216

LIST OF FIGURES

Figure 2-1 Maximum flow rate according to Eq 2-4 (upper curve) and 2-5 (lower curve), Source: (9), pp.12 9

Figure 2-2 Maximum flow versus speed by Johnson and Greenshields, Source: McLean (1989) 12

Figure 2-3 Schematic of resistance forces acting on moving vehicle on a grade, Source: Lan and Menedez (2003) 21

Figure 2-4 Probability and Cumulative density of M3A headway distributions for 800 vph arrivals 26

Figure 3-1 Methodology overview 35

Figure 4-1 Locations of data collection on Science Park Road 39

Figure 4-2 Schematic of site on Science Park Road 40

Figure 4-3 Locations of data collection on Highway 322 42

Figure 4-4 Screen shot of digital stopwatch 44

Figure 4-5 Traffic volume of Science Park Road (Peak hour) 45

Figure 4-6 The histogram of headway distribution (location 2 in Science Park Road) 46

Figure 4-7 Histogram of free flow speeds at non-peak hour (Location 1, Science Park Road) 48

Figure 4-8 Percent time spent following in Science Park Road 51

Figure 4-9 Traffic volume at highway 322 (Nov 6th) 53

Figure 4-10 Traffic volume at highway 322 (Nov 20th) 53

Figure 4-11 Headway distribution at highway 322 (Location 1 Inbound/Pre-game, Nov 20th) 54

Figure 4-12 Headway distribution at highway 322 (Location 2 Inbound/Pre-game, Nov 20th) 54

Figure 4-13 Headway distribution at highway 322 (Location 1 Outbound/Aft-game, Nov 20th) 55

Figure 4-14 Headway distribution at highway 322 (Location 2 Outbound/Aft-game, Nov 20th) 55

Figure 4-15 Histogram of free flow speed at highway 322 56

Figure 4-16 Percent time spent following at highway 322 58

Figure 4-17 Headway vs. speed (HW 322-Inbound) 59

Figure 4-18 Headway vs. speed (hw 322-Outbound) 60

Figure 5-1 Concept of safety constraint in Gipps' car-following model 69

Figure 5-2 Average travel speed vs. flow rate (source: field data & NCHRP 3-55(3)) 79

Figure 5-3 Difference between ATS and FFS vs. flow rate 80

Figure 5-4 Average travel speed vs. directional traffic volume 81

Figure 5-5 Probability density vs. probability of arrival headway 85

Figure 5-6 Speed trend of the first six vehicles 87

Figure 5-7 Speed trend of the first seven vehicles 88

Figure 5-8 Vehicle trajectories at 400 pcph arrival demand 89

Figure 5-9 Speed vs. density 90

Figure 5-10 Speed vs. flow 90

Figure 5-11 Flow vs. density 91

Figure 5-12 Hourly flow rate over segment 96

Figure 5-13 Schematic of arrival demand and arrival rate in TWOSIM I 97

Figure 5-14 Hourly flow rates vs. arrival demand 99

Figure 6-1 Elements of passing sight distance for two-lane, highways 106

Figure 6-2 Circumstances when a driver considers passing 110

Figure 6-3 Circumstances when a driver determines to pass 111

Figure 6-4 Completion of passing 113

Figure 6-5 Trajectories of vehicles in both directions 116

Figure 6-6 Trajectory of passing vehicle 117

Figure 6-7 Trajectories of passing vehicle and opposing vehicle 118

Figure 6-8 Consideration of travel time of opposing vehicle 119

Figure 6-9 Histogram of clearance distances 121

Figure 6-10 Hourly flow rates at 20 percent no-passing zone 124

Figure 6-11 Avarage flow rates under 20 percent no-passing zones vs. 100 percent no-passing zones 125

Figure 7-1 Schematic of deceleration zone 132

Figure 7-2 Speed profile of 200 hp truck with 200 lb/hp at upgrade segment 139

Figure 7-3 Trajectories of vehicles entering and exiting main road 141

Figure 7-4 Histogram of deceleration rate in exiting main road 142

Figure 7-5 Histogram of speeds in exiting main road 142

Figure 7-6 Speed profile of vehicles at 50 feet radius of horizontal curve 143

Figure 7-7 Speed profile of vehicles at 1500 feet radius of horizontal curve 144

Figure 7-8 Trajectory of vehicles when horizontal curve is present 144

Figure 7-9 Speed profile of vehicles at 1500 feet radius of horizontal curve at 4 percent maximum superelevation 145

Figure 7-10 Speed profile at 1 mile 7 percent upgrade section with 10 percent trucks 146

Figure 7-11 Trajectories on the segment with 7 percent upgrade section with 10 percent trucks 146

Figure 7-12 Speed profile at 2 mile 7 percent upgrade section with 10 percent trucks 147

LIST OF TABLES

Table 4-1 Survey points and time at Science Park Avenue 40

Table 4-2 Survey locations and time at highway 322 43

Table 4-3 Traffic volume at Science Park Road 45

Table 4-4 Autocorrelation coefficient at Lag 1 for headways in the field 48

Table 4-5 Maximum flow rates at each location of Science Park Road 49

Table 4-6 Percent time spent following at Science Park Road 50

Table 4-7 Average speed with traffic volume 51

Table 4-8 Maximum flow rates at highway 322 57

Table 4-9 Percent time spent following at highway 322 57

Table 4-10 Headways vs. speed at highway 322 (Inbound/Pre-game) 59

Table 4-11 Headways vs. speed at highway 322 (Outbound/Aft-game) 59

Table 4-12 Average speed with traffic volume 60

Table 5-1 Goodness of fit test for the headway distributions in Science Park Road (peak hour) 65

Table 5-2 Goodness of fit test for the headways in Science Park Road (non-peak hour) 65

Table 5-3 Goodness of fit test for headways in highway 322 66

Table 5-4 Classified maximum acceleration rate of passenger cars in TWOSIM I 71

Table 5-5 Percentile estimates of steady state unexpected deceleration 73

Table 5-6 Braking distance and deceleration rate of vehicles in 2004 and 2005 75

Table 5-7 Result of regression analysis 80

Table 5-8 Comparison of average travel speed from TWOSIM I to TWOPAS and HCM 93

Table 5-9 Comparison of percent time spent following with TWOPAS and HCM 94

Table 5-10 Capacity vs. average free flow speed 100

Table 5-11 Capacity vs. standard deviation of desired speed 101

Table 5-12 Capacity vs. delay of safety reaction time 102

Table 5-13 Capacity vs. length of study segment 102

Table 6-1 Elements of safe passing sight distance for design of two-lane, highways 107

Table 6-2 Minimum passing sight distance (2003 MUTCD) 108

Table 6-3 Updated passenger car performance characteristics in TWOPAS 112

Table 6-4 Statistics of passing time in TWOSIM II 122

Table 6-5 Passing rates in TWOSIM II (Free Flow Speed: 60mph) 123

Table 6-6 Passing rates in TWOSIM II 126

Table 6-7 Capacity at 20 percent no-passing zones with different opposing flow rate 127

Table 7-1 Critical gaps derived from field data for right turns to a major road 133

Table 7-2 Updated truck performance characteristics 140

Table 7-3 Comparison of ATS when a driveway is present 148

Table 7-4 Comparison of PTSF when a driveway is present 149

Table 7-5 Comparison of ATS when a horizontal curve is present 150

Table 7-6 Comparison of PTSF when a horizontal curve is present 150

Table 7-7 Comparison of ATS when an upgrade section is present 151

Table 7-8 Comparison of PTSF when an upgrade section is present 152

Table 7-9 Comparison of ATS when 10 percent of trucks exist in the presence of an upgrade section 152

Table 7-10 Comparison of PTSF when 10 percent of trucks exist in the presence of an upgrade section 153

Table 7-11 Capacity as a function of curb radius of driveway 154

Table 7-12 Capacity as a function of the radius of horizontal curve 154

Table 7-13 Capacity as a function of grade of 1 mile upgrade section 155

Table 7-14 Capacity as a function of the superelevation of horizontal curve 156

Table 7-15 Capacity as a function of the radius of horizontal curve and percent of trucks..... 156

Table 7-16 Capacity as a function of the percent of trucks in the presence of a driveway 157

Table 7-17 Capacity as a function of the percent of trucks at upgrade section 157

Table 7-18 Capacity as a function of the length of upgrade section..... 158

Table 7-19 Capacity as a function of the percent of trucks at horizontal curve on upgrade section 159

ACKNOWLEDGEMENTS

I would like to express my gratitude to all those who gave me the opportunities to complete this thesis. I am deeply indebted to my academic advisor, Dr. Lily Elefteriadou, whose help, simulating suggestions, and encouragement assisted me in writing this thesis. Special thanks go to Dr. Martin T. Pietrucha as committee chair for his advice and care, which helped me follow all of the procedures that I needed to complete my PhD program. Next, I like to thank the members of my dissertation committee for their acceptance of this task and their helpful comments and suggestions in preparing this thesis: Dr. Kevin Mahoney, Dr. Eric Donnell, and Dr. Debora Medeiros.

Special thanks go to Taegyu Kim, Dongmin Lee, and Seokil Bae for providing great help in performing the field surveys. I especially appreciate University of Florida for giving me a chance to participate in projects and gain experience associated with topics relevant to my dissertation. I feel a deep sense of gratitude for my wife, Sarah, for her love and encouragement and especially express my thanks to the Lord for His provision of spiritual food during the period of my studies.

CHAPTER 1. INTRODUCTION

1.1 Background

According to statistics published by the U.S. Federal Highway Administration, two-lane highway facilities represent about 97 percent of the total highway system length in the United States. Two-lane highways account for more than 65 percent of the total non-urban vehicular travel nationwide. Hence, two-lane highways will continue to compose most of the primary inter-urban highway network as well as being the basis of the secondary highway and collector networks (FHWA, 1985).

There have been many attempts to develop capacity estimation models of two-lane, two-way highways during the past decades. Since two-lane, two-way highways represent uninterrupted flow, most capacity models have focused on developing traffic stream models. In the 2000 HCM (Highway Capacity Manual), the capacity of two-lane, two-way highways is given as 1,700 pcph (passenger car per hour) for each direction of travel (3,200 pcph for both directions), which is independent of the directional distribution of traffic on the facility and of site geometry. A single capacity value, however, does not reflect the effect of various driver, geometric, and traffic characteristics, such as opposing flow or the presence of driveways, horizontal curves, grades, and trucks.

According to Harwood, et al. (1999), capacity conditions on two-lane roads are very difficult to observe because very few two-lane highways operate at or near capacity. It is explained that typically a two-lane highway with high volume is widened to four lanes long before the demand approaches capacity. The authors note that higher capacity volumes than ones suggested in the HCM have been observed in the field. Also, Yagar

(1983) and Rozic (1992) suggest that the capacity of two-lane, two-way highways can reach 3,600 pcph or 4,000 pcph for both directions.

Although capacity is regularly observed in other types of facilities, such as freeways, there are additional issues associated with the definition of capacity, as well as where and when it should be measured. Firstly, capacity for freeways has been found to vary even at the same location, from one day to the next, and from one hour to the next (Elefteriadou, 2004). Secondly, capacity could be measured before or after breakdown points (e.g. congestion occurrence), and the current HCM 2000 definition does not specify when capacity should be measured. These issues have not yet been explored for two lane highway facilities.

For the analysis of two lane highways, there are two existing microscopic simulators: TWOPAS (TWO-lane PASsing) and TRARR (TRAffic on Rural Roads). TWOPAS was developed in the United States, and it considers vehicle characteristics as well as highway design parameters in estimating the performance of two-lane highways. It provides outputs, such as average travel speed, percent time spent following, trip time, delay, number of passes, vehicle miles traveled, and travel time. This simulator, however, cannot provide capacity estimates, since its algorithms assume that capacity is a fixed value, equal to 1,700 vph. It does not consider the impacts of any geometric or traffic conditions on capacity and cannot handle oversaturated conditions. Determination of capacity cannot be accomplished by a simple change in the software, as its estimation involves many different model components. TRARR also does not account for intersections and varying traffic flows along the simulated road, and it cannot determine

capacity. Its output includes derived macroscopic traffic measures such as travel times, journey speeds, percent of time spent following and overtaking rates.

In summary, the HCM 2000 suggests the capacity of two-lane highways is 3,200 pcph, however there has been no research evaluating the impacts of geometric and traffic characteristics on that value. Also, there have been studies indicating that the capacity at some locations may be higher than 3,200 pcph. Obtaining an adequate sample of capacity estimates through field data collection for a variety of geometric and traffic conditions has proven to be extremely difficult. None of the existing simulators can be used to estimate capacity for two lane highways. Therefore, this thesis develops a new microscopic simulation model to estimate the capacity for two-lane, two-way highways under a variety of prevailing geometric and traffic conditions.

1.2 Objectives

The objectives of this dissertation are as follows:

- To develop a microscopic simulator for two-lane, two-way highways for estimating capacity under a variety of geometric and traffic conditions;
- To estimate capacity for two-lane, two-way highways under certain conditions: the presence or absence of passing zones, driveways, horizontal curves, and grades;
- To present capacities of two-lane, two-way highways with the conditions noted above combined with other factors, such as speed limit and percentage of trucks.

CHAPTER 2. LITERATURE REVIEW

The definition of capacity has evolved over time, and a thorough understanding of this concept is vital to this research, thus this literature review commences with a discussion on the definition of capacity. The second section deals with capacity studies on two-lane, two-way highways from the perspective of macroscopic traffic flow characteristics. The third section describes factors affecting the capacity of two-lane, two-way highways. The fourth section introduces theories related to vehicle movement for the development of a simulation model. The fifth section discusses existing commercial simulation models for two-lane, two-way highways. The last section summarizes research to date and research needs for the establishment of capacity for two-lane, two-way highways.

2.1 Definition of highway capacity

Capacity studies and the accurate estimation of capacity have been essential in determining the projected or estimated demand when a roadway facility is designed or upgraded. Capacity, however, has been defined in different ways over the past decades. The earliest capacity definition developed by Normann (1942) included the following three types:

- Theoretical lane capacity: the number of vehicles traveling in a single traffic lane that could pass a given point if all drivers traveled at the same speed and no space between vehicles exceeded the distance allowed by the average driver while following another vehicle.
- Possible capacity: the number of vehicles per hour that can travel over long stretches of highway that are free from intersections.
- Practical capacity: a relative value, which is adopted for design purposes.

The 1950 Highway Capacity Manual (1950 HCM) categorized capacity into basic, possible and practical capacity. The possible capacity was separated into two different capacities, basic capacity and possible capacity, depending on the traffic and roadway conditions.

- Basic capacity: the maximum number of passenger cars that can pass a given point on a lane or roadway during one hour under the most nearly ideal roadway and traffic conditions which can possibly be attained.
- Possible capacity: the maximum number of vehicles that can pass a given point on a lane or roadway during one hour under the prevailing roadway and traffic conditions.
- Practical capacity: the maximum number of vehicles that can pass a given point on a roadway or in a designated lane during one hour without the traffic density being so great as to cause unreasonable delay, hazard, or restriction to the drivers' freedom to maneuver under the prevailing roadway and traffic conditions.

In the 1965 HCM, the concept was redefined so that capacity described a given section instead of at a point, as follows: "The maximum number of vehicles which has a reasonable expectation of passing over a given section of a lane or a roadway in one direction (or in both directions for a two-lane or a three-lane highway) during a given time period under prevailing roadway and traffic conditions."

The 1985 HCM used the concept of hourly rate for the capacity. In terms of two-lane highway operations, the essence of the definition did not change between the two manuals. The 1985 HCM defined capacity to be: "The maximum hourly rate at which persons or vehicles can reasonably be expected to traverse a point or uniform section of a

lane or roadway during a given time period under prevailing roadway, traffic and control conditions."

The definition in the 1985 HCM continued to be used in the 2000 HCM. In the 2000 HCM, vehicle capacity is the maximum number of vehicles that can pass a given point during a specified period under prevailing roadway, traffic, and control conditions. These conditions should be reasonably uniform for any section of facility analyzed, because any change in the prevailing conditions changes the capacity of the facility.

Studying highway capacity, Elefteriadou (2004) pointed out that there are different maximum sustained flows depending on when the capacity is observed along a highway. Three different flow parameters (maximum pre-breakdown flow, breakdown flow, and maximum discharge flow) are presented to define capacity for a highway facility. The maximum values of each of them are random variables, possibly normally distributed. She found pre-breakdown flow is often higher than the discharge flow. The transition from non-congested to congested flow is probabilistic and may occur at various flow levels.

In summary, the definition of capacity has evolved over time, and it has suggested that there are stochastic components making it difficult to directly and simply define capacity.

2.2 Capacity studies and traffic flow characteristics for two-lane highways

In the first two parts of this section, analytical and empirical capacity studies of two-lane, two-way highways are reviewed. The analytical approach involves establishing a model to explain certain phenomena. In the empirical approach, models are derived directly

from data and field surveys. The last part of this section presents capacity studies performed to develop and enhance the HCM.

2.2.1 Analytical approaches

Since capacity is considered to have forced flow with uniform speed, the analytical approach focused on the estimation of the maximum theoretical capacity in a single traffic lane during the early twentieth century. The theoretical maximum volume for a single lane by Hammond and Sorenson (1941) was derived to be a function of speed, which implies that the capacity increases with the decrease of spacing (Luttinen, 2001):

$$c = \frac{5280 \quad v}{s} \qquad \textbf{Eq 2-1}$$

where, c = capacity of a single lane (veh/h);

v = speed (mile/h);

s = average vehicle spacing (ft).

$$s = av^2 + bv + c \qquad \textbf{Eq 2-2}$$

where, a, b, c are constants.

av^2 = the distance traveled while the vehicle was braking;

bv = the distance traveled during the driver's perception reaction time; and

c = vehicle length or the spacing adopted when traffic was stationary

In Equation 2-2, the constant a is related to the inverse of friction and grade effects. The constant b is related to perception reaction time at constant speed.

Clayton's maximum theoretical lane volume equation (1941) used the minimum safe time headway to calculate the maximum theoretical lane volume for a two-lane, two-way highway instead of the space mean headway that Wardrop (1952) used. The minimum

safe headway (h_{min}) was equal to the time (T_R) taken to apply the brakes after the preceding vehicle had applied their brakes, plus the time required to travel the length (L) of the vehicle with the current speed v.

$$h_{\min} = T_R + \frac{L}{v} \qquad \textbf{Eq 2-3}$$

where,

T_R = reaction time taken to apply brakes (1 sec);

L = length of vehicle (15 ft); and

v = speed (mph)

Clayton's maximum flow rate equation is as follows:

$$q_{\max} = \frac{3600}{1 + \frac{L}{1.47v}} = \frac{5280v}{1.47v + L} \qquad \textbf{Eq 2-4}$$

where,

q_{max} = maximum flow rate (pcph);

L = length of vehicle (15 ft); and

v = speed (mph)

Equation 2-4 represents the upper curve plotted in Figure 2-1. The capacity established from Equation 2-4 is shown to keep increasing with an increase in speed. Another equation was developed by adding the second order of speed taking into account the safe stopping distance as follows:

$$q_{\max} = \frac{5280v}{L + Av + \frac{v^2}{B}} \qquad \textbf{Eq 2-5}$$

where,

q_{max} = maximum flow rate (pcph);

L = length of vehicle (15 feet);

v = speed (miles per hour);

A =1.47; and

B = 30 (light vehicles) and 20 (heavy vehicles)

Equation 2-5 gives the maximum flow rate as 1,830 veh/h at speed 21 mph when 30 is used for the parameter B (Figure 2-1). Compared with the maximum flow rate from Equation 2-4, Equation 2-5 considers the safe stopping distance and larger spacing and naturally results in lower capacity. Clayton concluded that Equation 2-5 was generally acceptable, although the constants and the power of v vary.

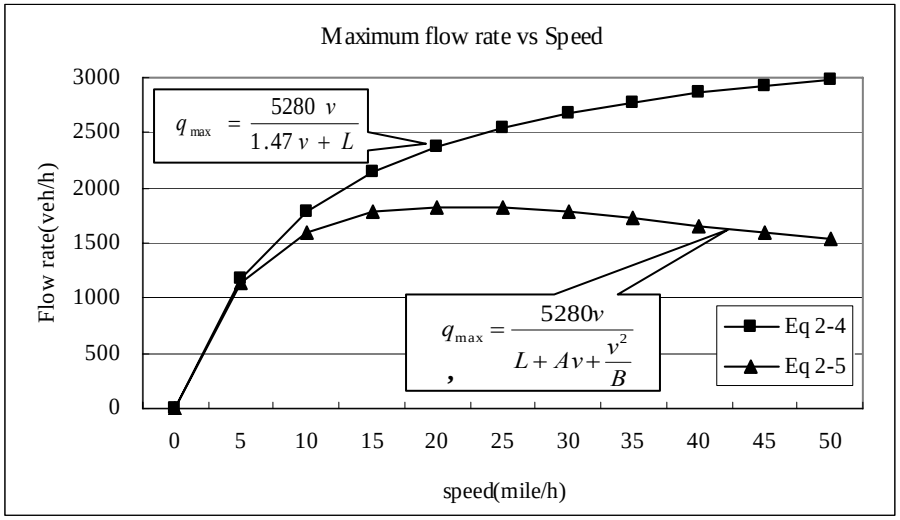

Figure 2-1 Maximum flow rate according to Eq 2-4 (upper curve) and 2-5 (lower curve), Source: (9), pp.12

McLean (1989) suggested a macroscopic stream model is not very relevant or valid for capacity estimation. He pointed out that when platooning is dominant, density alone may not be an adequate descriptor of the spatial nature of the traffic and its effect on traffic stream speed. At the microscopic level, vehicles within platoons would be operating in a car-following mode, while the interactions between platoons are analogous to the interactions between free flow vehicles at much lower densities.

McLean (1989) also mentioned that for conventional interrupted flow, the interruptions are most commonly created by intersections, where the flow of interest must share the road space with cross-traffic. In two-lane, two-way highway operations, opposing lanes are shared between opposing traffic and overtaking vehicles. The opposing traffic delays vehicles wishing to overtake in a manner analogous to cross-traffic with right-of-way at an intersection. Sight distance restrictions create delays in a manner analogous to poorly timed signals, where through vehicles may have to wait even in the absence of cross-traffic. The major differences are that, for two-lane, two-way highway flow, only vehicles wishing to overtake are delayed, and the delay means traveling at a slower speed than their desired speeds. He suggested that two-lane, two-way highway operations might be better conceptualized as being somewhere between the traditional considerations of uninterrupted and interrupted flow.

2.2.2 Empirical approach

According to McLean (1989), Johnson's empirical model (1928) gives some insight about the non-linear relationship between spacing and speed, which is similar to Clayton's second order speed (Eq 2-5). In his study, spacing-speed data of vehicle groups were collected from an aerial survey on a 29 mile section of two-lane highway. He found that clearance (spacing) was proportional to a power of speed:

$$C = 0.5\,V^{1.3} \quad or \quad c = 0.082\,v^{1.3} \qquad \textbf{Eq 2-6}$$

where,

C = inter-vehicle clearance, (ft);
c = inter-vehicle clearance, (m);
V = traffic speed, (mile/h); and
v = traffic speed, (km/h)

This gave the following relationship between maximum theoretical lane volume and traffic speed (average vehicle length 15 feet):

$$Q = \frac{5280V}{0.5V^{1.3} + 15} \quad or \quad Q = \frac{1000v}{0.082v^{1.3} + 4.6} \qquad \textbf{Eq 2-7}$$

where, V = traffic speed (mile/h), v = traffic speed (km/h)

Unlike Johnson's study, Greenshields (1934) used fixed-base photogrammetry to obtain speed and spacing data for vehicles passing an observation point on a two-lane rural highway (McLean, 1989). The spacing data were averaged for each 2 mile/h (3.2 km/h) increment in speed, and Greenshields claimed that the averaged values could be fairly well represented by the straight line as shown in the following equation:

$$S = 21 + 1.1V \quad or \quad s = 6.4 + 0.21v \qquad \textbf{Eq 2-8}$$

where,

S = vehicle spacing, (ft);
s = vehicle spacing, (m);
V = speed, (mile/h); and
v = speed, (km/h)

Johnson's and Greenshields' equations are plotted in Figure 2-2. There is no maximum theoretical lane volume in Greenshields' curve with the first order speed term as that of Clayton's Equation 2-4. Compared with Figure 2-1, Figure 2-2 gives a similar trend in a sense that one curve gives maximum flow rate and the other does not. The difference between the two curves with maximum flow in the two figures is that a different power is used for speed (2 vs. 1.3). The two increasing curves in the two figures have a linear relationship between speed and spacing. Consequently, compared with the curves in Figure 2-1, the curves derived from the empirical study result in higher capacity as shown in Figure 2-2.

Using graphical methods, Normann (1942) plotted the spacings against speed for each road type, and derived the theoretical lane capacity. The results showed that the maximum theoretical lane capacity on a two-lane roadway was 2,000 veh/h in the daytime and about 1,800 vph at night, both being attained at a vehicle speed of about 33 miles per hour. These theoretical lane capacities may be achieved over very short sections of highway that act as bottlenecks.

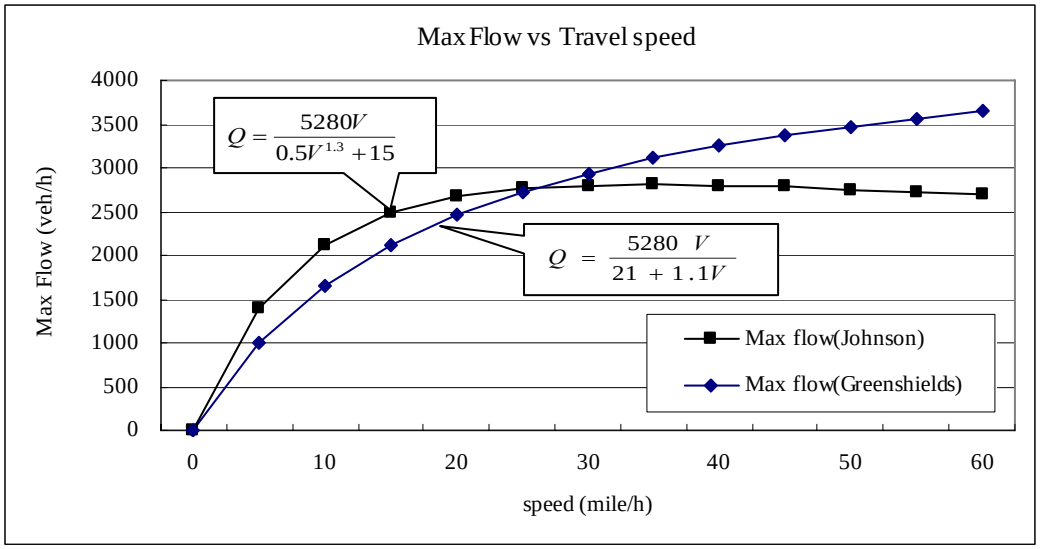

Figure 2-2 Maximum flow versus speed by Johnson and Greenshields, Source: McLean (1989)

Yagar (1983) indicated that there are the cases cited in international studies where observed volumes reach as high as 3,550 vph, which is higher than the capacity given in the 2000 HCM. He suggests that the highest capacity could reach 3,600 veh/h for both directions (1800 veh/h for each direction) under ideal conditions.

Enberg and Pursula (1991) found the relationship between speed and flow was linear based on data collected in Finland. This regression equation for space mean speed as a function of two-way flow rate was as follows:

$$v_s = 99.46 - 0.0051 \times q \qquad \text{Eq 2-9}$$
$$R^2 = 0.473$$

where,

v_s = space mean speed (km/h); and

q = two-way flow rate (veh/h)

To develop a model estimating the capacity of two-lane highways, Rozic (1992) assumed four combinations of traffic flow conditions on two-lane, two-way highways with two types of vehicle positions depending on whether a vehicle was involved in overtaking or not: vehicle file and vehicles involved in overtaking. Vehicle file is defined as vehicles that keep in their own lane, are not involved in overtaking, and are not positioned between two adjacent maneuvers of overtaking vehicles traveling in the same direction. Vehicles involved in overtaking were doing so in either a passive or active manner. Rozic (1992) concluded that the capacity of a two-lane rural highway with a realistic composition of traffic flow in roadway conditions approaching the ideal could be about 2,700 vph in both directions. Since it became apparent during the course of defining the vehicle file that there might be gaps that could be filled with other vehicles, it was realistic to expect that such classifications could yield values exceeding 3,000 vph in both directions. Those gaps are filled if all vehicles in the vehicle file link up in a dynamic way (i.e., if, in the ultimate case, the entire vehicle file becomes a long platoon). In that way the traffic flow on a two-lane, two-way highway was converted into two platoons moving in opposite directions, when the capacity of a single traffic lane was defined, and the capacity of the highway as a whole was the sum of the capacities of two traffic lanes. In this particular research, such an ideal capacity could be assessed at 4,000 pcph in both directions.

Harwood, et al (1999) suggested that a capacity value cited in the HCM should not represent the highest flow rate ever observed on a given facility type; but rather should

represent a value that can reasonably be expected to be served on most facilities under base conditions when demand is sufficient.

2.2.3 Two-lane highway capacity in the U.S. Highway Capacity Manual

The HCM's two-lane highway capacity estimate has evolved over time. The 1950 HCM specified the basic capacity of two-lane highways (possible capacity under ideal conditions) as being 2,000 pcph for both directions, regardless of directional split. The practical capacity under prevailing conditions was obtained by using adjustments reflecting effects of lane width, road alignment, trucks, and grades.

The 1965 HCM indicated that the total capacity under ideal conditions is 2,000 pcph for both directions, regardless of the directional split of traffic, which was equal to the basic capacity in the 1950 HCM. The 1965 Manual gives service volume reduction factors for each level of service considering lane width, lateral obstruction, alignment, and trucks. Unlike the 1950 HCM, the 1965 Manual presented a precise procedure for the computation of two-lane road capacities and service volumes. The capacity under prevailing conditions has determined as:

$$C = 2000\, W_c\, T_c \qquad \textbf{Eq 2-10}$$

where,

W_c = width adjustment factor at capacity; and

T_c = truck adjustment factor at capacity

In the 1985 HCM, the capacity of a two-lane highway under ideal conditions was assumed to vary from 2,000 pcph (directional split 100/1) to 2,800 pcph (directional split 50/50), total, in both directions as a function of the directional distribution of traffic. This

capacity reflects the impact of opposing vehicles on passing opportunities, and therefore on the ability to efficiently fill gaps in the traffic stream.

Compared with the 1985 HCM, the capacity in the 2000 HCM increased from 2,000 pcph to 3,400 pcph for both directions (or 1,700 pcph for each direction). According to the 2000 HCM, for extended lengths of two-lane highway, the capacity will not exceed 3,200 pcph for both directions of travel combined. Harwood et al. (1999) indicated that the revised capacity values of 3,200 pcph for two-way flow and 1,700 pcph for directional flow are much less influenced by directional split than was suggested in the 1985 HCM. Also, they suggest directional split has no influence on flow, the capacity would be twice the capacity for directional flow, which is 3,400 pcph. The recommended two-way capacity value is less than twice the directional capacity value, and this 200 pcph difference between 3,200 and 3,400 pcph represents the influence of directional split on capacity.

2.3 Factors affecting the capacity of two-lane, two-way highways

Many studies have suggested that capacity cannot be estimated simply using the minimum headway. A variety of factors have been found to impact headway distributions; and hence, the maximum flow rate. On two-lane, two-way highways, there are complicated interactions between the environment, the two opposing traffic streams, and driver behavior. This section reviews the impact of factors, such as overtaking and gap acceptance behavior, opposing volume, heavy vehicles, geometric conditions, passing zones, and passing sight distance on the capacity of two-lane, two-way highways.

2.3.1 Overtaking and gap acceptance

Overtaking is an important factor in two-lane, two-way highway operations. When platooning results from a slow moving vehicle, larger gaps exist downstream of the slow vehicle. In this case, whether the larger gap can be filled with the overtaking vehicles from the platoon or not could have an impact on how much capacity would increase.

Wardrop (1952) suggests that the number of desired overtakings increases as the square of the flow for a given distribution of speeds increases. In terms of the frequencies in space (f'_i) and time (f_i) respectively, the total number of overtakings is expressed as follows (McLean, 1989):

$$P = K^2 \sum_{i=1}^{C-1} \sum_{j=i+1}^{C} f_i' f_j' \left(v_j - v_i\right) = Q^2 \sum_{i=1}^{C-1} \sum_{j=i+1}^{C} f_i f_j \left(\frac{1}{v_i} - \frac{1}{v_j}\right) \qquad \textbf{Eq 2-11}$$

where,

P = total number of overtakings;
K = density (vehicles/ unit length of road);
f'_i = the frequencies in space;
f'_j = the frequencies in time; and
v_i = speed (km/h) of vehicle i

Crawford (1963) notes that overtaken and opposing vehicles were driven at equal speeds ranging from 32 to 80 km/h, and subjects were required to overtake if they judged the available gap to be adequate. The equation for the median critical time gap has obtained as follows (McLean, 1989):

$$g_c = 7.2 + 46.5/u \qquad \textbf{Eq 2-12}$$

where,

g_c = the median critical time gap (sec); and

u = the relative (or closing) speed between the overtaken and opposing vehicle (m/s)

Farber and Silver (1967) found that drivers can make reasonable judgments of overtaking distance, but are unable to judge opposing-vehicle speed. From an analysis of co-variance, it was inferred that the drivers were responding to gap-distance rather than gap-time, so acceptance behavior was expressed in terms of distance (McLean, 1989).

Miller and Pretty (1968) used a maximum likelihood method to estimate the parameters for an assumed log-normal distribution of time-critical-gaps (McLean, 1989). Werner and Morrall (1984) showed that the directional split has a significant effect on overtaking. They developed a unified traffic flow theory model demonstrating the interaction of two opposing streams of traffic and the effect that occurred on passing. The model is sensitive at lower volumes and reflects more accurately congestion as perceived by the driver.

McLean (1989) presented the following general findings inferred from reported results on overtaking gap-acceptance behavior:

- Drivers can make reasonable judgments of overtaking distance, but have difficulty in judging opposing-vehicle speed.
- The real gap-acceptance behavior of a driver population lies somewhere between the fully consistent and fully inconsistent driver assumptions.
- There is considerable variability in reported overtaking gap-acceptance results. This is contributed to by regional differences in driver behavior, within-driver variability, between driver variability, and sampling biases inherent in the common method of overtaking gap-acceptance data collection.

- Overtaking gap-acceptance decision making is generally very conservative.
- Overtaking gap-acceptance depends on the overtaken-vehicle type and speed, the gap type (sight distance or opposing vehicle) and the maneuver type (accelerative or flying).

Enberg and Pursula (1991) found that the overtaking density of the traffic flow stream increases with increasing traffic. Wardrop's curve from Equation 2-11 was compared to the curve drawn with the observed data. They found that the equation is usable only for low traffic flows below about 1100 veh/h. At higher flows the calculations according to the equation estimated remarkably more overtakings than actually were done on the road sections that were observed.

2.3.2 Opposing volume

Since opposing volume may impact the overtaking supply and the speed of primary traffic, it is considered as an influential factor on the capacity of two-lane, two-way highways.

Many of the efforts to find a measure of the congestion on a highway have revealed that the mean difference in speed between succeeding vehicles is the best index of possible highway capacity. Normann's (1939) multivariate linear regression model analyzes mean speed difference for successive vehicles in terms of directional flows (McLean, 1989).

$$\Delta V_1 = 6.44 - 0.00324Q_1 - 0.00254Q_0 \ (r^2 = 0.66) \qquad \textbf{Eq 2-13}$$

where,

ΔV_1 = mean speed difference for successive vehicles traveling in the primary direction (mile/h);

Q_1 = flow in primary direction (veh/h);

Q_0 = flow in opposing direction (veh/h); and

r^2 = proportion of variance in the dependent variable attributable to the regression equation

The volumes at which these relations extrapolated to zero mean speed difference were regarded as possible capacities for given road condition. This analysis estimated possible capacities of about 1,940 veh/h at an average speed of 26 mile/h (42 km/h) for two-lane highways with few trucks; 1,500 veh/h at average speed of 26 mile/h for two-lane highways with 17 percent of the traffic being made up by trucks.

Underwood (1964) and Casey and Tindall (1966) found that primary flow has a greater effect on primary direction mean speed than opposing flow does, but there are substantial differences in the absolute and relative values for these effects. Underwood presented the following regression equation (McLean, 1989):

$$V_1 = 77.8 - 0.0087Q_1 - 0.0026Q_0 \quad \textbf{Eq 2-14}$$

where,

V_1 = mean speed for traffic in the primary direction (km/h);

Q_1 = primary direction flow (veh/h); and

Q_0 = opposing direction flow (veh/h)

Casey and Tindall (1966) derived the following regression equation (McLean, 1989):

$$V_1 = 72.6 - 0.0158Q_1 - 0.0087Q_0 \quad \textbf{Eq 2-15}$$

Krumins (1981) presents another equation (McLean, 1989):

$$V_1 = 94.0 - 0.0086Q_1 - 0.0026Q_0 \quad \textbf{Eq 2-16}$$
$$r^2 = 0.46$$
$$V = 94.4 - 0.0060Q \quad \textbf{Eq 2-17}$$
$$r^2 = 0.55$$

where,

V_1 = mean speed for traffic in the primary direction (km/h);

V = mean speed for vehicles traveling in both directions (km/h);

Q_1 = primary direction flow (veh/h);

Q_0 = opposing direction flow (veh/h); and

Q = Q_1+Q_0

On the contrary, Yagar (1983) indicated that capacity in one direction is reasonably independent of opposing volume, except for extreme cases of traffic interference, such as turning movements through gaps in the opposing stream. In addition, he concluded that the capacity of two-lane highways should be based on single lane analysis, as the opposing capacities are not heavily dependent of one another. However, opposing volume can be taken into account in determining capacity for a given direction.

2.3.3 Heavy vehicles

Heavy vehicles have a dominant influence on the development of platoons along two-lane, two-way highways particularly on upgrade segments.

According to Aerde and Yagar (1984), PCEs (passenger car equivalences) for trucks and recreational vehicles were found to be considerably higher than those currently used for most types of standard capacity analyses. McLean (1989) suggested that truck impedance effects vary with the total traffic volume on two-lane, two-way highways. Truck impedance is relatively small because catch-ups are infrequent when traffic flow rate is low and a lot of overtaking opportunities can be provided. Truck impedance gets larger as flow rates increase, so truck impedance is at a maximum for moderate flows and constrains overtaking opportunities where the increased catch-ups and overtaking difficulty associated with trucks could lead to considerable delays for passenger vehicles.

On steep upgrades, the reduction in truck speeds coupled with the lack of overtaking opportunity increases inter-platoon spacing so that the presence of trucks leads to a marked reduction in capacity (McLean, 1989).

Harwood et al. (1999) indicated that the magnitude of the truck and recreational vehicle effects increase progressively for rolling and mountainous terrain, in comparison to level terrain. When all other factors are held at ideal conditions, the presence of 20 percent trucks in the traffic stream decreases capacity to 83 percent of its ideal value for level terrain, 54 percent for rolling terrain, and 28 percent for mountainous terrain.

Lan and Menendez (2003) proposed a new formulation to obtain truck speed profiles. The dynamic, kinematic and operating characteristics of trucks entails the following external resistance forces, including air resistance (F_a), rolling resistance (F_r), skidding resistance (F_s), and grade resistance (F_g), as well as the tractive force delivered by the engine (F_p). Different forms of resistance force, such as inertial resistance and transmission resistance, act against the process of transmitting the engine traction to ground. Figure 2-3 is a schematic of these forces that act on a vehicle on an inclined surface.

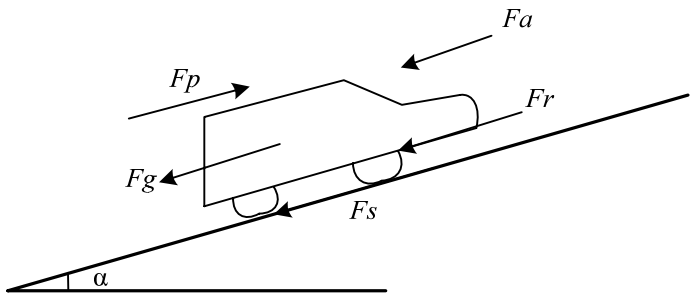

Figure 2-3 Schematic of resistance forces acting on moving vehicle on a grade, Source: Lan and Menedez (2003)

When a vehicle is accelerating, F_s is equal to zero and the net force that drives the effective mass of the vehicle after tractive force is counterbalanced by all the resistance forces is as follows:

$$rF_p - F_a - F_r - F_g = M_e a \qquad \textbf{Eq 2-18}$$

$$F_p = \frac{50P}{u}(lb)$$

$$F_g = W\sin\alpha = W\tan\alpha = WG \text{ (when angle } \alpha \text{ is small)}$$

The effective mass, M_e is a combination of the static mass and the equivalent mass to account for the loss of tractive force due to rotational inertia of the vehicle and driveline components during acceleration. The engine efficiency, *r*, represents the loss of engine power due primarily to the transmission resistance and tire slip. The reduction in engine power due to transmission resistance ranges from 10 percent in high gear, 15 percent in low gear, and 20~25 percent in transmissions with high resistance. A vehicle acceleration rate is estimated using Equation 2-19:

$$\begin{aligned} a &= \frac{1}{M_e}\left(\frac{1{,}000rP}{u} - F_a - F_r - WG\right) \\ &= \frac{M}{M_e}\left(\frac{500r/u}{W/P} - \frac{(F_a + F_r)}{W} - G\right)g \\ &= \left(1.02 - \frac{4.76}{u}\right)\left[\frac{550r/u}{W/P} - (k_r + k_s u) - \frac{k_a u^2}{W} - G\right]g \end{aligned} \qquad \textbf{Eq 2-19}$$

where,

a = acceleration/deceleration rate, ft/s^2;

u = velocity, ft/s;

M/M_e = 0.2, as $u \le 5.9$ ft/s;

1.02 - 4.76/u, as u>5.9 ft/s;

r = engine efficiency factor (0.92);

W = weight of vehicle, lb;

P = power, HP

ρ = air density, lb/ft^3 (= 0.0765 lb/ft^3 at sea level);

C_a = unitless drag coefficient (taken as 0.8);

A = frontal cross section area of the vehicle, ≈ 0.9 (wheel tread)(body height)=0.9(7.85)(11.5) ft^2;

k_r = 0.01;

k_s = 1/14,667, s/ft;

k_a = 0.0764;

G = grade; and

g = gravity constant (=32.17 ft/s^2)

2.3.4 Geometric conditions

The steepness and length of an upgrade segment has an impact on the speed of heavy vehicles, which affects how often the platoon is developed and how long it is. Therefore, geometric conditions are an important factor in capacity studies for two-lane, two-way highway.

Normann (1942) found the desired overtaking rates increase with increasing truck proportion and increasing gradient (decreasing truck speed). He proposed the following formula that relates practical capacities for alignment presenting restrictions on overtaking opportunity to the practical capacity on a level tangent section.

$$V_R = \frac{2000 V_T (1 - R)}{2000 - V_T R} \qquad \textbf{Eq 2-20}$$

where,

V_R = practical capacity on the alignment where all passings are restricted for alignment (veh/h);

V_T = practical capacity on tangent alignment (veh/h) and;

R = ratio of the distance that all passings are restricted to the entire length of the highway

Polus et al. (1991) concluded that the capacity value is sensitive to the geometric characteristics of each site. According to Harwood et al. (1999), there are significant differences among percent time delay versus service volumes to truck percent for each terrain type. There are wider gaps between percent time delay at moderate service volumes in rolling and mountainous terrain.

2.3.5 Passing zones and passing sight distance

The presence of passing zones (and passing sight distance) is another factor that may affect the capacity of two-lane, two-way highways. When vehicles follow a leading slow vehicle, they may want to overtake it and travel at their desired speed. However, if the segment does not provide enough passing sight distance or passing zones, then the following vehicles would not be able to overtake and have to follow in the platoon even when gaps are available. Heimbach et al. (1973) found that a statistically reliable relationship exists between percent of no-passing zone and mean speed.

2.4 Modeling two-lane, two-way highways

Two methods were reviewed for modeling two-lane, two-way highways: arrival headway distributions and car-following models.

2.4.1 Arrival headway distributions

Schuhl's (1955) composite headway model indicates that both free and following vehicle headways are exponentially distributed. Taylor, et al. (1972) found that a model combining negative exponential, inter-bunch headways with a bunch size distribution

provides a good representation of rural traffic (McLean, 1989). According to Gerlough and Huber (1975), Dawson combined the Erlang distribution and the shifted minimum headway to the right and developed the hyper-Erlang ("hyperlang") distribution. May (1990) suggested that the negative exponential distribution for random headway represents the distribution of random time headways. The negative exponential distribution inherently tends to the highest probability of the smallest headways. Due to the unrealistic result that the negative exponential distribution gives the highest probability for headways less than 1 second, the shifted negative exponential was developed to overcome the limitation. May (1990) discussed several models for the intermediate headway state such as a generalized mathematical model, a composite model, and others. The Pearson type III distribution is an example of a generalized mathematical model approach. Depending on two parameters, $\hat{K}$ (user-selected parameter between 0 and ∞ that affect the shape of the distribution) and λ (parameter as a function of the mean time headway and the two user specified parameters), a variety of distributions are possible (Pearson type III, Gamma, Erlang, negative exponential, and shifted negative exponential distribution). The composite model uses the combinations of a normal headway distribution for the vehicles in the car-following or platoon and a shifted negative exponential distribution for the vehicles without interaction.

Luttinen (1992) studied the statistical properties of vehicle time headways. He concluded that on high-standard roads, the vehicles are also more clustered and there is a small positive autocorrelation between consecutive headways. On low-standard roads there is some indication of possible positive autocorrelation under high flow rates.

Sullivan and Troutbeck (1994) studied Cowan's M3 headway distribution for modeling urban traffic flow. They concluded Cowan's M3 dichotomized headway distribution is a useful model for vehicle headways. The M3 model was found to provide an excellent fit to field data using a minimum arrival (intra-bunch) headway. Cowan's M3 headway distribution is found to be much simpler to use and still satisfies the required degree of accuracy in generating the distribution of vehicle headways. The other advantage mentioned here is that the parameters within the model have a physical significance and can be related to the characteristics of traffic flow on the roadway.

Akcelik and Chung (2003) concluded that while the bunched exponential distribution of arrival headways (Cowan's M3) is relatively new and is less common, it has been found to be more realistic than other headway distributions, such as the log normal distribution, negative exponential distribution, and shifted negative exponential distribution. They found that the more commonly used shifted negative exponential (M2) model produced poor predictions for the range of small headways.

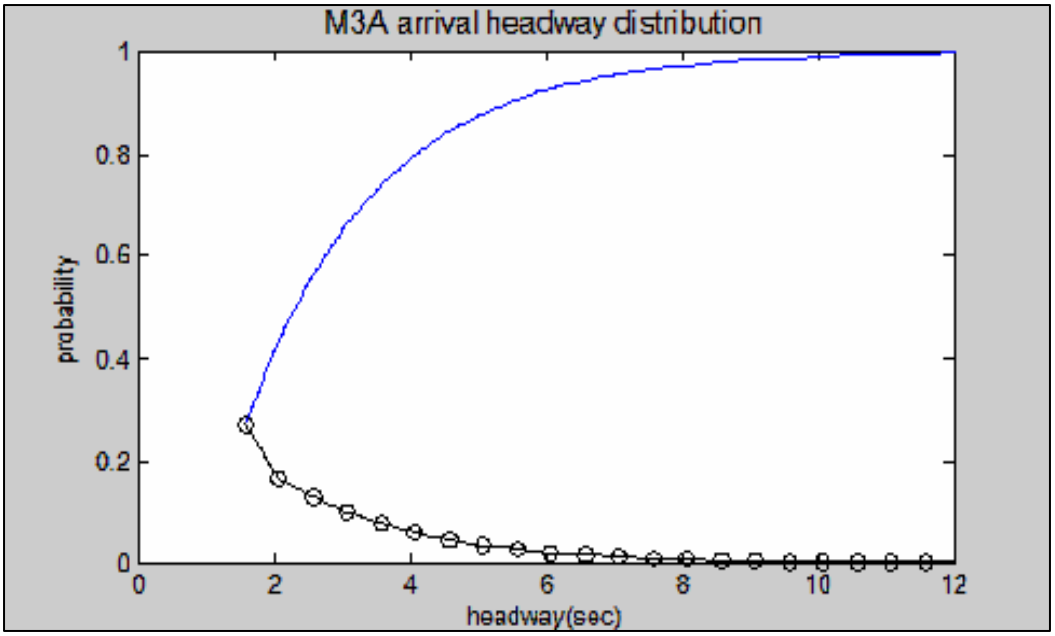

Figure 2-4 Probability and Cumulative density of M3A headway distributions for 800 vph arrivals

They strongly recommended Cowan's M3 instead of the other two exponential models. In presenting their findings, Akcelik developed the proportion of free (unbunched vehicles) as an exponential model (M3A) and compared it to Tanner's linear model for estimating the proportion of free vehicles (M3T). They found that Akcelik's M3A model grounded on Cowan's M3 provided good estimates of arrival headways. Figure 2-4 shows the general shape of the M3 distribution for an arrival flow rate of 800 vph.

2.4.2 Car-following models

According to May (1990), Pipe developed a car-following theory based on the rule in 1950s: " A good rule for following another vehicle at a safe distance is to allow yourself at least the length of a car between your vehicle and the vehicle ahead for every ten miles per hour of speed at which you are traveling." Forbes considered reaction time for the spacing between two consecutive vehicles so that the following driver has to have a time gap that should be equal or greater than the reaction time. General Motors' car-following models considered how a driver responded to the stimuli such as the relative velocity of the lead and following vehicle to select an appropriate acceleration or deceleration. The components in the generalized model are spacing, relative speed, and the speed of the following vehicle.

Gipps (1981) developed a car-following model to explain the speed of the following vehicle. This model selects the minimum of two speeds to be the response of the following vehicle. The equation for two speeds is shown below:

$$v_n(t+\tau) = \min\left\{\begin{array}{l} v_n(t) + 2.5a_n\tau\left(1 - v_n(t)/V_n\right)\left(0.025 + v_n(t)/V_n\right)^{1/2} \\ b_n\tau + \sqrt{\left(b_n^2\tau^2 - b_n\left[2\left[x_{n-1}(t) - s_{n-1} - x_n(t)\right] - v_n(t)\tau - v_{n-1}\left(t^2\right)/\hat{b}\right]\right)} \end{array}\right\} \quad \textbf{Eq 2-21}$$

where,

a_n = the maximum acceleration which the driver of vehicle *n* wishes to undertake;

b_n = the most severe braking that the driver of vehicle *n* wishes to undertake (b_n<0);

s_n = the effective size of vehicle *n*, that is, the physical length plus a margin into which the following vehicle is not willing to intrude, even when at rest;

V_n = the speed at which the driver of vehicle *n* wishes to travel;

$x_n(t)$ = the location of the front of vehicle *n* at time *t*;

$v_n(t)$ = the speed of vehicle *n* at time *t*; and

τ = the apparent reaction time, a constant for all vehicles

The first speed implies that a vehicle will not exceed its driver's desired speed based on the performance of the driver and the vehicle. The second speed reflects the vehicle's safe speed, which increases as the subject vehicle catches up with the lead vehicle and decreases as the subject vehicle becomes closer to the lead vehicle.

Gipps introduced $\hat{b}$ as a safety margin by supposing that the driver makes allowances for a possible additional delay when traveling at $v_n(t+\tau)$, before reacting to the vehicle ahead. This has the effect that the simulated vehicle can brake earlier and gradually reduce braking so that it crawls up to the stop line. A variant of the Gipps model is implemented in AIMSUN (Advanced Interactive Microscopic Simulator for Urban and non-urban Networks). In the development of methodology for assessing adaptive cruise control behavior, Lee and Peng (2002) tested many longitudinal human

driver models developed in the last fifty years. They found Gipps model provides the best fit to data measured in natural driving.

Besides, compared with other car-following models, Gipps' model is seen to reflect driver's behavior in two-lane, two-way highway well in adapting their speed to free flow or congested conditions. For example, the model enables drivers to select their own desired speed in free flow speed conditions and maintain a safe speed in congested condition. Gipps' model is considered a relatively viable model for building an algorithm for a simulation model. Therefore, Gipps' model will be selected to be the car-following model for the simulation developed in this study.

2.5 Existing simulation models

There are two microscopic simulators currently used for the analysis of two-lane, two-way highways: TWOPAS and TRARR. This section introduces these two microscopic simulators.

2.5.1 TWOPAS (TWO-lane PASsing)

The TWOPAS traffic simulation model is used as the traffic analysis module in the Interactive Highway Safety Design Model (IHSDM), which is a decision-support tool with a suite of software analysis tools for evaluating safety and operational effects of geometric decisions on two-lane rural highways (IHSDM, 2003).

According to the Interactive Highway Safety Design Manual (2003), TWOPAS simulates traffic operations on two-lane highways by reviewing the position, speed, and acceleration of each individual vehicle along the highway at 1-sec intervals and advancing those vehicles along the given study section in a realistic manner. The model

takes into account driver preferences, vehicle size and performance characteristics, and the oncoming and same direction vehicles that are in sight at any given time.

The model incorporates realistic passing and pass abort decisions by drivers in two-lane highway passing zones. The model can also simulate traffic operations in passing and climbing lanes added in one or both directions on two-lane highways including lane additions and lane drops. The model does not currently simulate traffic turning on or off the highway at intersections and driveways although work is underway to incorporate this capability (IHSDM, 2003).

In its output, TWOPAS presents flow rates from the simulation, percent time spent following, average travel speed, trip time, traffic delay, geometric delay, total delay, number of passes, vehicle km traveled, and total travel time.

According to IHSDM (2003), TWOPAS is stalled when a traffic volume above 1,700 vph is input as directional volume. This is one of the reasons that a new simulation model is needed for the estimation of capacity.

2.5.2 TRARR (TRAffic on Rural Roads)

According to Koorey (2002), TRARR is a micro-simulation model and models each vehicle individually. Each vehicle is randomly generated, placed at the beginning of the segment and monitored as it travels. Different driver behavior and vehicle performance factors determine how the vehicle simulated reacts to changes in alignment and traffic. TRARR uses traffic flow, vehicle performance, and geometric alignment to establish the speeds of vehicles along the given study segment. TRARR is designed for two-lane rural highways, with occasional passing lane sections. TRARR can calculate travel time, time spent following, and benefits resulting from passing lanes or road realignments.

TRARR uses four main input files to run a simulation and generate output data (Koorey, 2002):

- ROAD: the section of highway in 100 meter increment includes horizontal curvature, gradient, auxiliary (passing) lanes, and no-overtaking lines.
- TRAF: the traffic volume and vehicle mix to be simulated. Other information regarding the simulation time and vehicle speeds is also contained.
- VEHS: the operating characteristics of the vehicle fleet. The relevant details relating to engine power, mass, fuel consumption, and so on are entered into this file.
- OBS: the points along the highway at which to record data of vehicle movements. A range of values including mean speed, travel times, and fuel consumption is presented based on specified observations.

As a modeling tool for the evaluation of rural passing lanes and realignments, TRARR has proved to be an adequate package. However, there are a number of potential drawbacks reported from practice. Koorey (2002) identified the following concerns with TRARR:

- Inability to handle varying traffic flows down the highway, particularly due to major side roads.
- Inability to properly model the effects of restricted speed zones (such as small towns).
- Inability to model congested situations e.g. temporary lane closures or single-lane bridges.

- Difficulty in using field data for calibration, with no automatic calibration assistance built in.
- Difficulties creating and editing road data, particularly for planned new alignments.
- Limited ability to use the same tool to check for speed environment consistency and safety risks.
- Additional effort required in applying results to project evaluations.
- Lack of practical documentation for running typical TRARR applications in New Zealand.
- Lack of a modern interface and associated compatibility issues.

As mentioned above, TRARR does not model congested situations. Therefore, TRARR is not considered an appropriate tool for the analysis of capacity.

Although the two microscopic simulation models each have strengths and weaknesses, TWOPAS is considered to have more advanced functions and generally be more applicable for conditions in the Unites States. Hence, TWOPAS will be compared with the new simulation model developed in this research.

2.6 Research findings to date and research needs

The following are drawn from the literature review:

- The definition of capacity has evolved over time, and it has been suggested that there are stochastic components making it difficult to directly and simply define capacity.
- Many models have been developed using analytical and empirical approaches to estimate the theoretical capacity of two-lane, two-way highways. They are

mainly a function of average vehicle spacing, average speed, and minimum time headway. While the models provide useful insights about the two-lane flow, no general mathematical models can be applied to all situations considering a variety of geometric and traffic conditions.

- Although the 2000 HCM suggests the capacity of a two-lane highway to be 3,400 pcph for both directions and 1,700 pcph for each direction of travel, several studies have shown that there are higher volumes observed on two-lane highways. Some authors indicated that an ideal capacity could reach 3,550 pcph or 4,000 pcph for both directions.
- A variety of factors that may have an impact on the capacity of two-lane, two-way highways were reviewed. Since these factors interact along a given segment, it is difficult to estimate capacity of two-lane, two-way highways using general mathematical models.
- TWOPAS is an existing two-lane, two-way simulation model that is more applicable to the conditions of the United States. However, it cannot estimate capacity.

The following research needs are derived from the research findings:

- Since capacity conditions on two-lane, two-way highways are rarely observed, a model would be appropriate for the estimation of capacity under various geometric and traffic conditions.
- Generally, simulation is a useful technique to model complex systems. Given the difficulty in considering various factors interacting on two-lane, two-way highways, simulation modeling will be used in this research.

- The simulation model should be developed at the microscopic level so that it replicates movement of individual vehicles. The simulation model is expected to incorporate a variety of geometric and traffic conditions including treatments such as the presence of driveways, horizontal curves, grades, and trucks.

CHAPTER 3. METHODOLOGY

Figure 3-1 provides a schematic of the methodology. First, field data were collected to obtain information on the traffic characteristics of two-lane, two-way highways. Second, a microscopic simulation model named TWOSIM (Two-lane, two-way highway SIMulator), was developed and applied for the estimation of capacity. Lastly, using the simulation model, the capacity under various geometric and traffic conditions including special treatments was estimated.

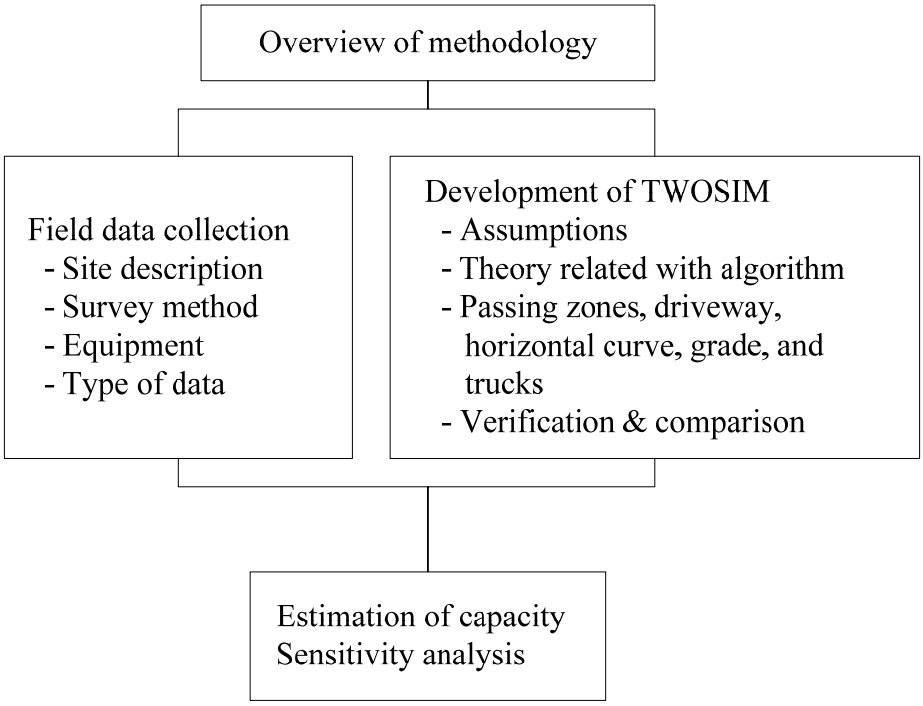

Figure 3-1 Methodology overview

3.1 Field data collection

As mentioned earlier, it has been very difficult to measure capacity because of the rarity of capacity conditions on two-lane, two-way highways. Data collected in the field were applied for the calibration of input parameters in the newly developed simulation model. The following section describes the field data needed and how these data were applied for

the development of the simulation model. The details of data collection are described in Chapter 4.

- For the purposes of this study, the field data to be collected were used in the arrival distribution modeling and in the car-following model. The parameters include vehicle characteristics, geometric conditions, average headways, average free flow speed, and so on. The output from the simulator will provide performance measures such as average travel speed and percent time spent following.

To obtain capacity data, data were collected at weekday peak hours during football game day in State College, PA. The details of the locations are described in Chapter 4. The field data were measured with Nu-metrics Hi-Star traffic sensors, video camera, and a digital stopwatch.

3.2 Development of the simulation model

As discussed in the literature review, there are a variety of factors that affect the performance of two-lane, two-way highways. These factors are calibrated in the development of the simulation model.

The simulation model was developed from the microscopic perspective and replicates each vehicle's movement interacting with other vehicles in traffic at each time step. Internal output data from the simulator included information such as flow rate, speed, density, average travel speed, percent time spent following, and flow rate at any point over a given segment.

MATLAB (student version 6.5) was selected as a tool for developing the simulator. MATLAB is a programming language that is more familiar to the author and a high-level

technical computing language and interactive environment for algorithm development and numerical computation comparable to traditional programming languages such as C, C++, and Fortran. The new simulator was verified by examining graphical output and conducting statistical tests by comparing it two other methods: TWOPAS and 2000 HCM.

The simulation model was developed stage by stage. TWOSIM I (Basic Two-lane, two-way highway SIMulator) was developed with a straight tangent level segment, which does not deal with any opposing traffic and additional traffic entering or exiting within a given segment. Passing is not allowed. TWOSIM II (Basic Two-lane, two-way highway SIMulator and passing algorithm) includes the additional algorithm of overtaking behavior. TWOSIM II can incorporate the interactions between opposing traffic and primary traffic. The final version of TWOSIM, TWOSIM III (Basic Two-lane, two-way highway SIMulator and the algorithm of considering the presence of driveway, horizontal curves, grades, and trucks) includes more advanced options that consider the presence of a driveway, horizontal curves, grades along a given segment, and truck traffic.

3.3 Estimation of capacity

While capacity conditions for two-lane, two-way highways are rarely observed in the field, a simulation model can generate extremely high demand, and replicate capacity conditions. The microscopic simulation model generates location versus time data for each individual vehicle simulated and estimates capacity by measuring the traffic volume at given observation points under capacity conditions. Chapter 5 discusses how capacity conditions are defined, simulated, and estimated in the model.

CHAPTER 4. FIELD DATA COLLECTION

Field data play a vital role in developing a simulation model. Field data were collected to support the model calibration. The following sections describe the data collection and data analysis conducted for this dissertation.

4.1 Data collection

Data collection was conducted at the following sites:

- Science Park Road, State College, Pennsylvania
- Highway 322, State College, Pennsylvania

Science Park Road is classified as an urban two-lane, two-way highway with access at its primary junction (class II according to HCM 2000). On the other hand, highway 322 can be classified as a rural two-lane, two-way highway for mobility rather than access (class I according to HCM 2000). Science Park Road is on hilly terrain with level terrain to some extent and has several driveways providing access to residential and commercial areas. Data were collected at level locations to prevent speeds from being affected by grades. Its posted speed limit is 35 mph.

The study section of highway 322 has a 55 mph posted speed limit, and the data collection took place before and after a football game held at Penn State University in November so that the highest demand could be captured. The two sites do not have passing zones. The following sections describe how and where data collection was performed.

4.1.1 Science Park Road, State College, Pennsylvania

As shown in Figure 4-1, the data collection was conducted at three locations on Science Park Road over two days. There is a signalized intersection to the south of location A and to the north of location C. The other two locations (B and C) further downstream to the north were chosen and located along level tangent sections. Each location is 0.42~0.45 miles away from each other. For this survey, Nu-metrics Hi-Star traffic sensors and video cameras were used.

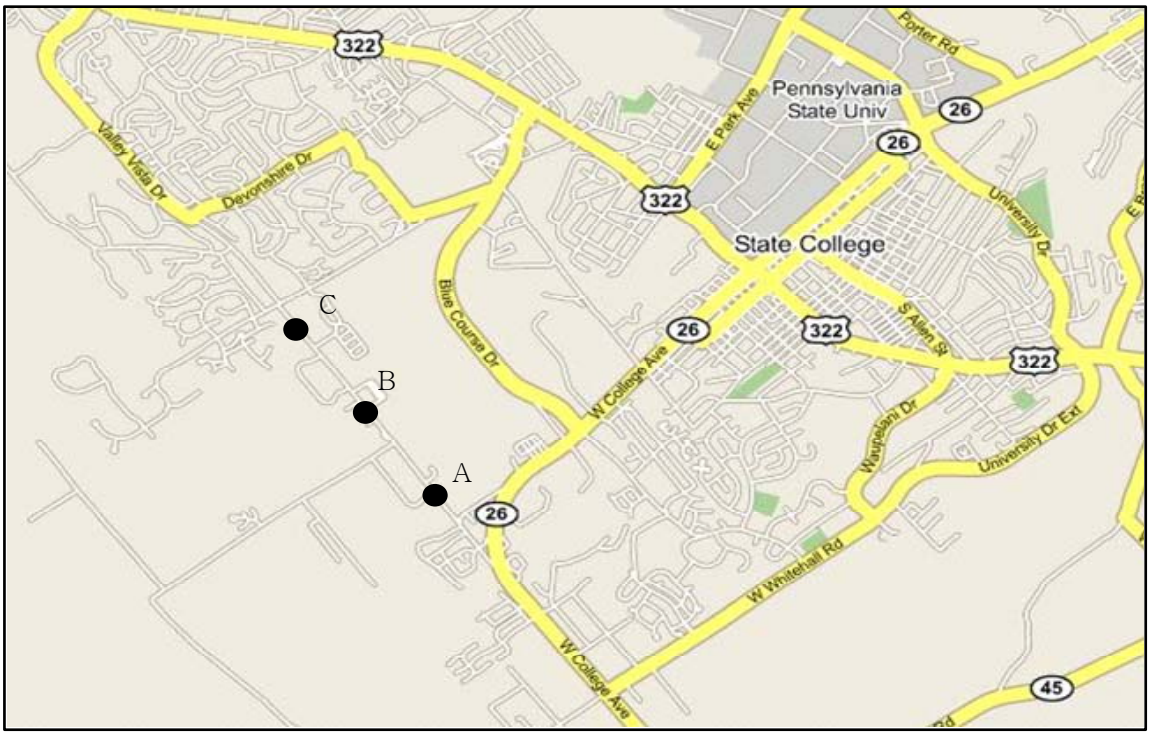

Figure 4-1 Locations of data collection on Science Park Road

Figure 4-2 provides a schematic of the data collection locations. Four Nu-metrics Hi-Star traffic sensors were installed at two locations in both directions each day. On the first day (January 3, 2004), locations A and B were surveyed and on the second day (January 8, 2004), location B and C were surveyed. Therefore, location B was surveyed twice over the two days. Points 1 ~ 4 represent where the Nu-metrics devices were installed on the

3rd of January and points 5 ~ 8 does where Nu-metrics was installed on the 8th of January. Two camcorders were set up away from the roadside where they were inconspicuous so that they did not influence vehicle speeds.

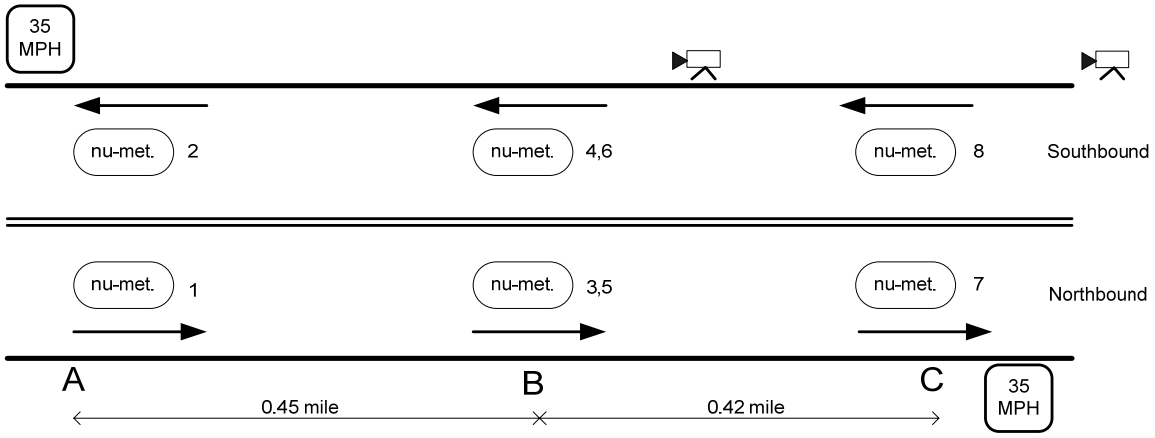

Figure 4-2 Schematic of site on Science Park Road

Table 4-1 shows each point and location of data collection and survey time. Data collection was performed for 3.5 hours during non-peak and peak hours. Each Nu-metrics device installed at each point captured traffic information by direction.

Table 4-1 Survey points and time at Science Park Avenue

Point	Location	Direction	Day	From	To
1	A	Northbound	June 3rd, 2004 (First day)	14:00	17:30
2	A	Southbound		14:00	17:30
3	B[1]	Northbound		14:00	17:30
4	B[1]	Southbound		14:00	17:30
5	B[2]	Northbound	June 8th, 2004 (Second day)	14:00	17:30
6	B[2]	Southbound		14:00	17:30
7	C	Northbound		14:00	17:30
8	C	Southbound		14:00	17:30

Note: [1] This location is named as B1.

[2] This location is named as B2.

By using the nu-metrics devices, video cameras, and wheel measure, the following traffic, vehicle, and geometric characteristics were measured:

- Vehicle counts
- Speed
- Vehicle length
- Headways
- Directional distribution
- Lane and shoulder width
- Terrain type, presence of horizontal/vertical curve

The nu-metrics devices record volume, speed and length of vehicles plus roadway occupancy and generates an electronic file with these data. The device transmits and stores all the data as encoded text file, which can be converted in the personal computer for the analysis. In Science Park Road, each of four nu-metrics device was placed at each site 30 minutes before the device began collecting data.

4.1.2 Highway 322, State College, Pennsylvania

The section of Highway 322 analyzed for this research is located in the south of State College, and many football fans from the south of State College take this route to get to Beaver Stadium to watch football games. This two-lane, two-way highway is a primary arterial connecting major trip generators, which is classified as class I according to HCM 2000. The Class I highway usually serves long-distance trips and motorists expect to travel at relatively high speeds.

The study segment where data collection was conducted does not have passing zones and its posted speed limit is 55 mph. The two locations (1 & 2) on the map are 0.52 mile

apart along the highway. There is no signalized intersection within 1 mile from the survey location of highway 322. The westbound traffic heads to State College, and the eastbound traffic travels out of State College.

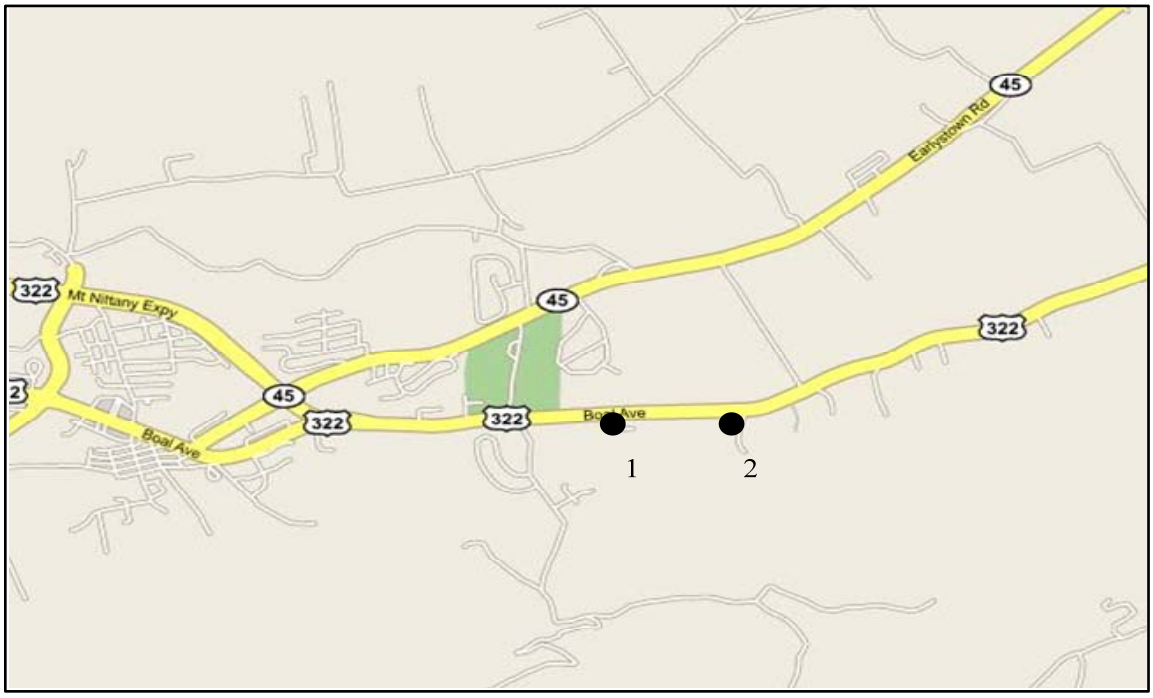

Figure 4-3 Locations of data collection on Highway 322

Two camcorders were positioned in inconspicuous locations so that traffic passing by the data collection locations would not be disrupted by curious motorists. The camcorders captured traffic flow in both directions at the same time. The clocks of the two camcorders were set to synchronize before recording started. The synchronized clock setting is necessary for estimating an accurate travel time between the two locations and travel speed.

The data collection was conducted on a football game day in State College, because these days were considered to be the days with the highest traffic for the year at this

location. Therefore, the data collection was conducted before and after a football game to capture the heaviest traffic traveling toward and away from the stadium.

- ✓ Morning period: From two and half hours earlier than the game starts to half an hour earlier than the game starts (09:30~11:30).
- ✓ Afternoon period: From half an hour earlier than the game expects to end to an hour later than the game ends (15:00~17:00).

Table 4-2 Survey locations and time at highway 322

Date	Locations	Time
Nov. 6th, 2004 (Sat)	1 & 2	9:30~11:30
		15:00~17:00
Nov. 20th, 2004(Sat)	1 & 2	9:30~11:30
		15:00~17:00

Headways were manually measured with a digital stopwatch on a laptop computer as shown in Figure 4-4. The digital stopwatch allows measurement of headway at 1/10 second unit. All the headways can be stored into an electronic file, which was converted with Microsoft Excel for data reduction and analysis.

4.2 Data reduction and analysis

4.2.1 Science Park Road

The Nu-metrics units stored data from the field into an electronic file including information with speed, vehicle length, delay, seconds, and offset. Speed represents spot speed in miles per hour. Vehicle length is represented in feet. All delays are set at zero, as this variable is not used for any purpose in this study. Seconds represent the time when a vehicle passed by the Nu-metrics device, which means time headway. Offset represents

cumulative seconds. The Nu-metrics format data are edited in a Microsoft worksheet to calculate arrival time represented as clock time. Then, traffic volume can be calculated with clock and headway information.

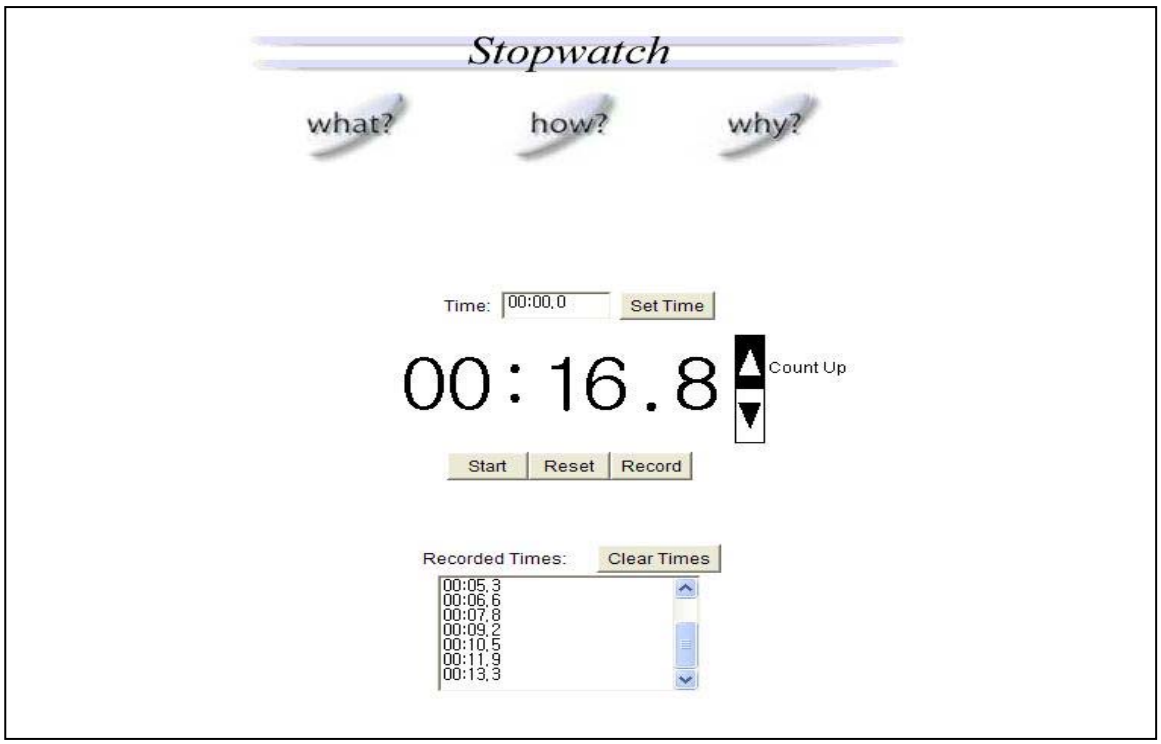

Figure 4-4 Screen shot of digital stopwatch

4.2.1.1 Traffic volume

According to the 2001 Green Book, the overall length of a passenger car, design vehicle is 19 feet, so vehicles longer than 20 feet, allowing 5 percent (1 feet) measuring error, were classified as heavy vehicles. Table 4-3 shows the traffic volumes at peak hour (16:30~17:30) and non-peak hour (14:00~15:00) on Science Park Road. The traffic volumes during peak hours range from 421 vph to 769 vph. Traffic volumes, in the range of 317 vph to 487 vph, were observed during non-peak hour on Science Park Road. The percentage of heavy vehicles is presented in Table 4-3. The traffic volumes observed

during the peak hours on Science Park Road were not found to reach capacity condition, 1,700 pcph per direction according to HCM 2000.

Table 4-3 Traffic volume at Science Park Road

Location	Peak hour (16:30~17:30)		Non-peak hour (14:00~15:00)	
	Traffic volume	Percent of heavy vehicle	Traffic volume	Percent of heavy vehicle
1	582	3.8	373	7.2
2	439	2.7	317	8.2
3	692	3.8	416	5.8
4	457	3.9	377	6.6
5	723	1.7	438	5.5
6	469	3.2	419	7.9
7	421	5.7	377	9.3
8	769	1.0	487	4.3

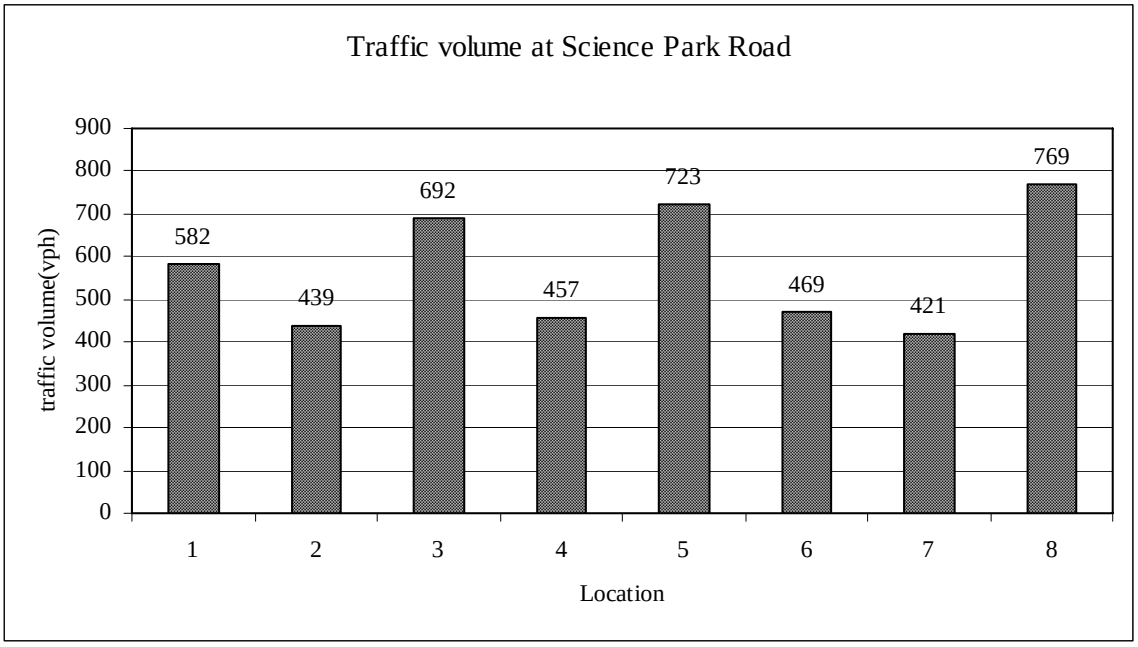

Figure 4-5 Traffic volume of Science Park Road (Peak hour)

4.2.1.2 Arrival headway

Headway distribution

The data were examined to see how headways are distributed when vehicles arrive at the beginning of a two-lane, two-way highway. The purpose of this analysis was to determine what type of headway distribution should be used in the simulation model to be developed as part of this study. As an example, headway distribution during the peak hour (4:30~5:30 pm) along Science Park Road is illustrated in Figure 4-6. The distribution shows the lowest headway group has the highest probability and the other probabilities go lower when headways increase as log-normal or negative-exponential distribution does.

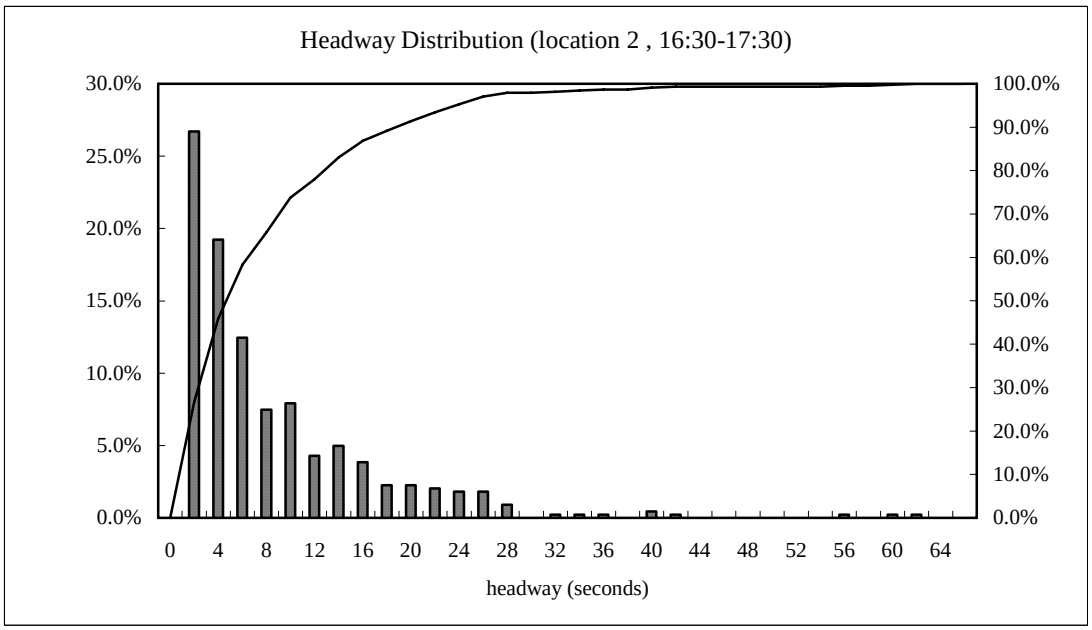

Figure 4-6 The histogram of headway distribution (location 2 in Science Park Road)

Identical and independent distribution of headway

Luttinen (1992) stated that there is a common assumption in analyzing the shape of headway distribution, which is the renewal hypothesis that headways are independent and identically distributed. For verifying the property, the autocorrelation coefficient is estimated. The coefficient is a measure of correlation between observations at given

distances (*lag*) apart. In a sample of *n* observations the estimate of the autocorrelation coefficient at *Lag k* is as shown in Equation 4-1.

When the coefficient estimate is less or equal to zero, the headways are identically and independently distributed. Otherwise, the renewal hypothesis is rejected and there is significance of autocorrelation between successive headways. In this study, the most important coefficient is r_1, so the autocorrelation coefficient at *lag* 1 is calculated with headways from the field. It was found that most locations are shown to have headways not independent and identically distributed except for the locations with negative coefficients. The result indicates that headways on two-lane, two-way highways are influenced by successive vehicles. When the headway of the leading vehicle is less than the average headway, the headways of the vehicles following are also less than the average headway. When such phenomena are predominant, that leads to the positive autocorrelation coefficient of headways.

$$\bar{r}_k = \frac{\sum_{j=1}^{n-k} (T_j - \mu_T)(T_{j+k} - \mu_T)}{\sum_{j=1}^{n} (T_j - \mu_T)^2} \qquad \textbf{Eq 4-1}$$

where,

μ_T = $1/n \sum_{j=1}^{n} T_j$;

T_j = time headway;

k = lag; and

$\bar{r}_k$ = autocorrelation coefficient

Table 4-4 Autocorrelation coefficient at Lag 1 for headways in the field

Site	Autocorrelation coefficient at Lag 1								
Science Park Road	Loc.	1	2	3	4	5	6	7	8
	Coef	0.041	0.004	0.083	0.032	0.144	0.086	0.095	0.157
Highway 322	Loc.	Nov. 6th				Nov. 20th			
		1(in)	2(in)	1(out)	2(out)	1(in)	2(in)	1(out)	2(out)
	Coef	0.137	0.060	0.034	-0.02	0.003	0.002	-0.02	-0.03

4.2.1.3 Free flow speed distribution

Free flow speed implies what speed drivers desire to achieve at low volume conditions (i.e. below 200 vph) without intervention or interaction on the roadway. Therefore, data on free flow speed should be collected when traffic flows are below 200 vph. However, the traffic volume in the non-peak hours along Science Park Road exceeded 200 vph, therefore only speeds with headway longer than 20 seconds were selected for the development of the distribution of free flow speeds.

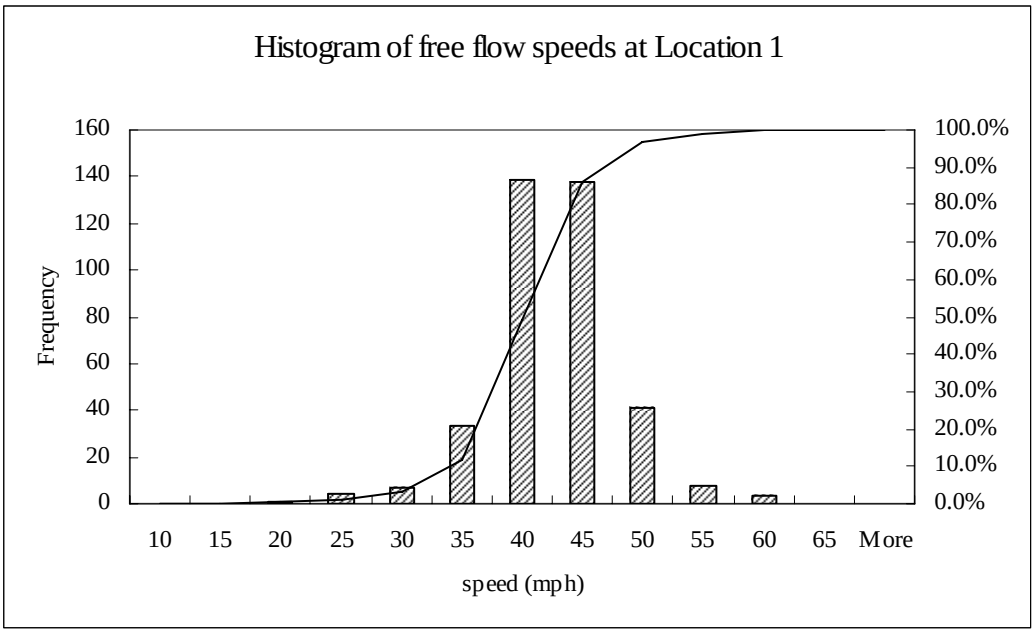

Figure 4-7 Histogram of free flow speeds at non-peak hour (Location 1, Science Park Road)

The mean and standard deviation values of free flow speed were 41.3 mph and 6.6 mph, and the histogram of free flow speeds is as shown in Figure 4-7. The histograms of other locations can be found in Appendix A.

4.2.1.4 Maximum flow rate

In this study, maximum flow rate is defined as the highest flow rate derived from volumes observed during predefined time intervals (e.g., 5 minutes, 10 minutes) that are less than an hour. Flow rates were calculated based on observed volumes for a rolling five minute interval. The maximum flow rate was selected from these calculated rates. Therefore, hourly flow rate is calculated by multiplying five-minute volume by 12, and the calculation is progressed in one minute steps during the entire peak hour. Then, the maximum value is selected among the hourly flow rates over the entire peak hour.

The resulting maximum flow rates on Science Park Road are calculated by each survey location as shown in Table 4-5.

Table 4-5 Maximum flow rates at each location of Science Park Road

Location	Traffic volume (vph)	Maximum flow rate (vph)
1	582	828
2	439	672
3	692	924
4	457	660
5	723	960
6	469	636
7	421	588
8	769	1056

Maximum flow rates are always higher than observed hourly traffic volumes. The maximum flow rate at location 8 was obtained to be 1,056 vph, which implies that there was 125 vehicle observed for a five minute interval.

4.2.1.5 Percent time spent following

Percent time spent following is performance measure of two-lane, two-way highways according to HCM 2000. When the simulation model in this study is developed, comparison of percent time spent following from the simulator, TWOPAS, and HCM 2OOO will be required to determine how well the simulator replicates realistic phenomena occurring in traffic movement on two-lane, two-way highways. According to HCM 2000, the percent time spent following is difficult to measure in the field. As a surrogate measure, the number of headways below 3 seconds is counted, and the ratio is calculated versus total number of headways observed during the same period. Likewise, percent time spent following is calculated with field data. Percent time spent following on Science Park Road is shown in Table 4-6.

Table 4-6 Percent time spent following at Science Park Road

Survey point	1	2	3	4	5	6	7	8
Headways (<3 sec)	251	118	264	133	262	126	126	300
Headways (>=3 sec)	331	321	428	324	461	343	295	469
Total volume (vph)	582	439	692	457	723	469	421	769
Percent time spent following (%)	43.1	26.9	38.2	29.1	36.2	26.9	29.9	39.0

Figure 4-8 illustrates that percent time spent following tends to increase with traffic volume. It is noted that the percent time spent following at location 1 is higher than those of locations with higher traffic volumes. Taking into account the dynamic variability of vehicle movement and location, a point measurement, like this case, does not seem to

fully explain how the tendency of percent time spent following would be and how percent time spent following is related with traffic volume.

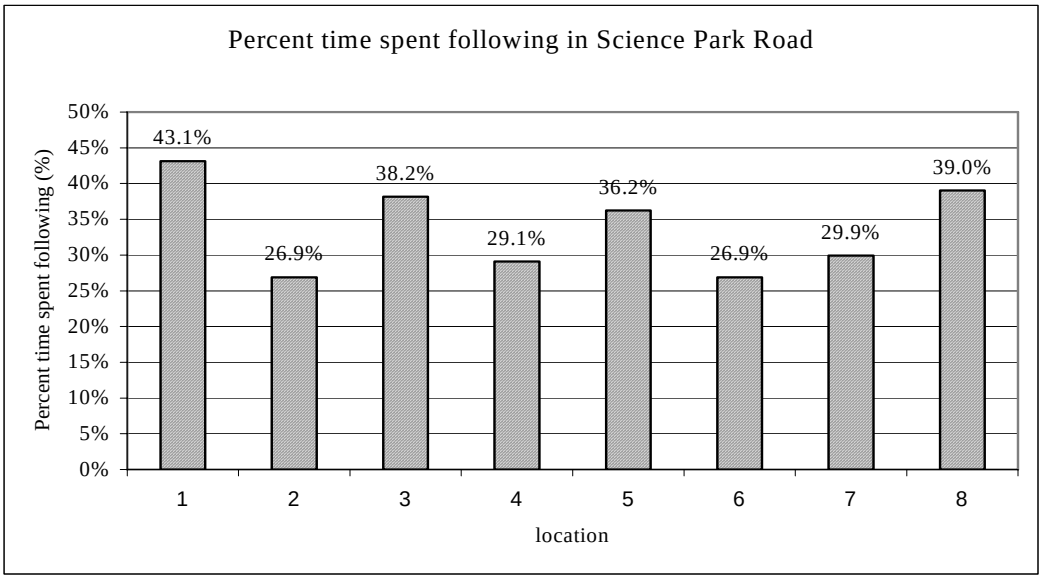

Figure 4-8 Percent time spent following in Science Park Road

4.2.1.6 Average speed

Average speed is calculated with the spot speeds collected with the Nu-metrics devices for each directional traffic volume during the peak hour.

Table 4-7 Average speed with traffic volume

Primary traffic volume (vph)	Opposing volume (vph)	Average speed (mph)	
		Primary direction	Opposing direction
582	439	38.2	40.4
692	457	42.0	39.1
723	469	38.3	39.9
421	769	42.9	35.6

4.2.2 Highway 322

4.2.2.1 Traffic volume

The traffic volumes on highway 322 were observed twice on Nov 6th and 20th. Inbound traffic volume was observed before football game starts and outbound traffic volume was observed around the time football game ends. Location 1 is located west of location 2. Therefore, the inbound volume flows from location 2 to location 1, and outbound volume flows from location 1 to location 2.

Traffic volumes on the 6th of November were 1,330 pcph at location 2 and 1,321 pcph at location 1. Outbound traffic volumes on the same day were 1,363 pcph at location 1 and 1,328 pcph at location 2. There is some discrepancy in traffic volume between the two locations which may be due to vehicles exiting at a mid-block driveway.

Inbound traffic volumes on the 20th of November were 1,173 pcph at location 2 to 1,193 pcph at location 1. Outbound traffic volumes on the same day was 1,353 pcph at location 1 to 1,349 pcph at location 2. The same discrepancy in traffic volumes between the two locations is also observed due to the exiting of traffic through the mid-block driveway.

There was congestion upstream of location 1 when the outbound traffic was observed around the time football game was over. Taking into account the traffic condition upstream, the traffic flow at the observation points was expected to reach very high volumes, near the level of capacity. However, the actual volume was observed to be around 1,350 pcph, which is not regarded as capacity.

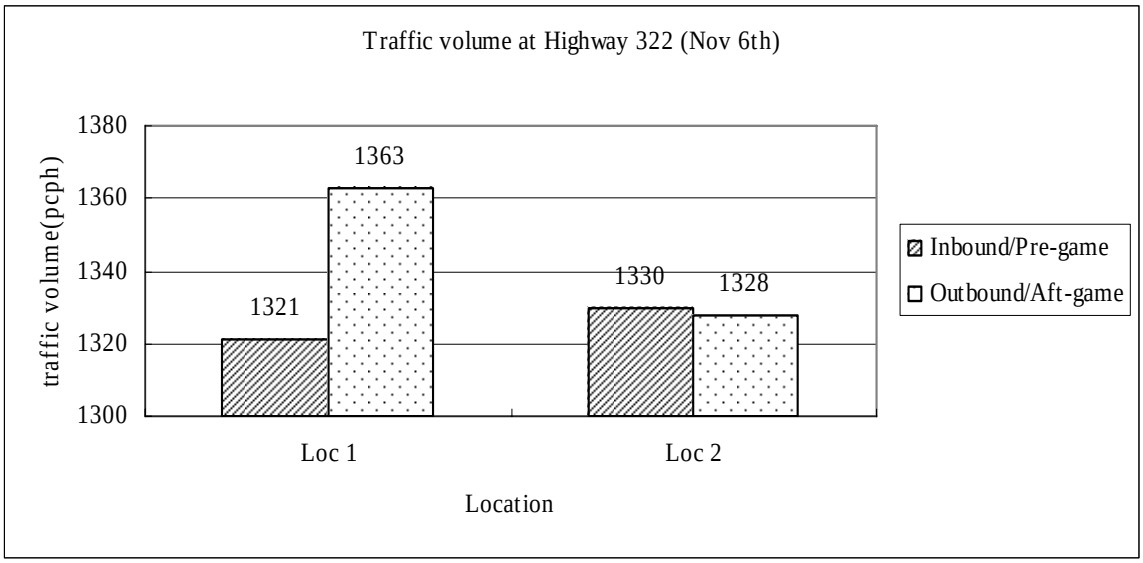

Figure 4-9 Traffic volume at highway 322 (Nov 6th)

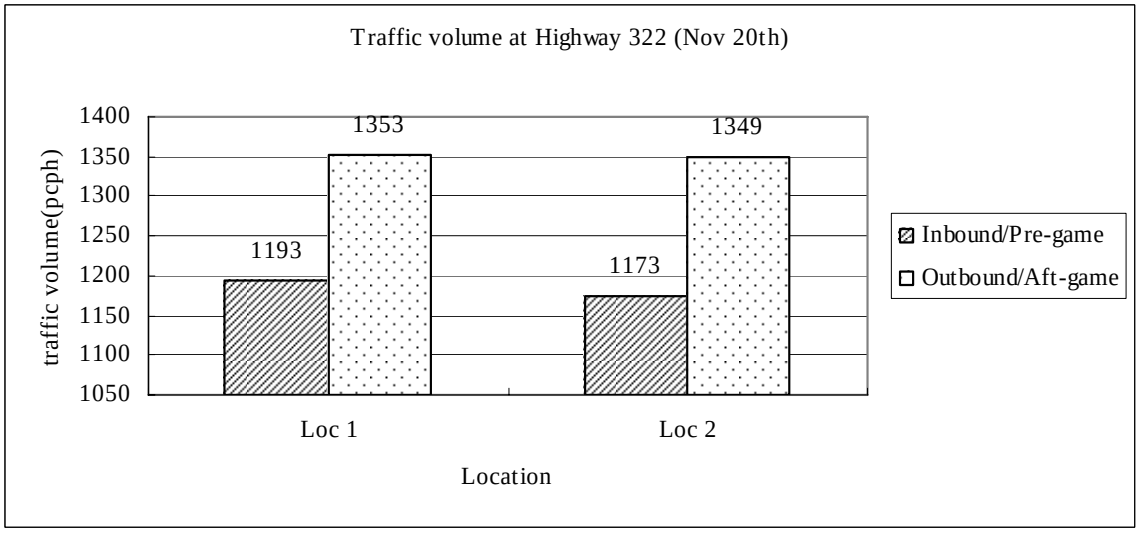

Figure 4-10 Traffic volume at highway 322 (Nov 20th)

4.2.2.2 Headway distribution

Headway data were collected at two locations along highway 322. However, the headway distributions are shown to be close to negative exponential or Akcelik's M3 headway distribution. Figures 4-11~14 show how the distribution of headways at various observation locations.

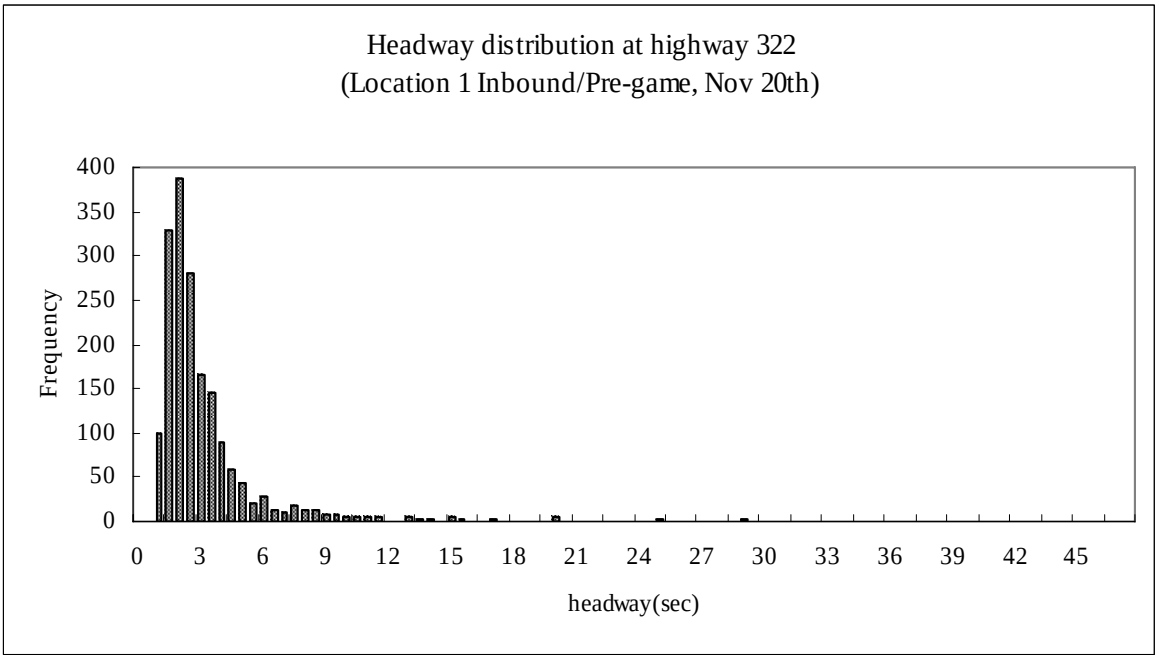

Figure 4-11 Headway distribution at highway 322 (Location 1 Inbound/Pre-game, Nov 20th)

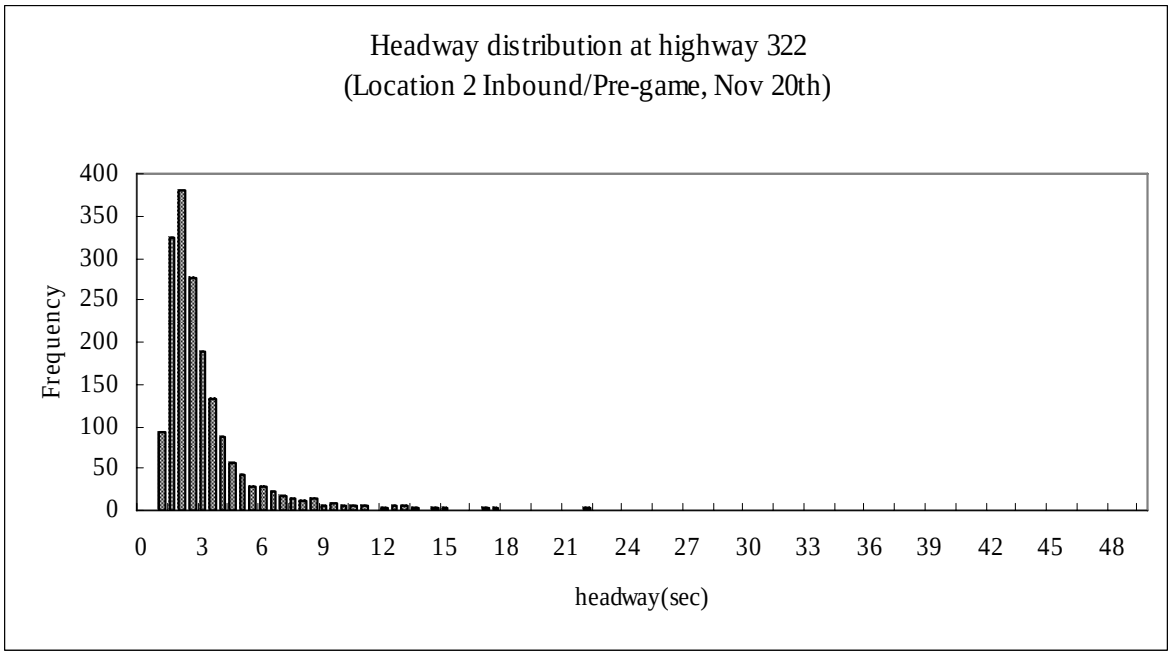

Figure 4-12 Headway distribution at highway 322 (Location 2 Inbound/Pre-game, Nov 20th)

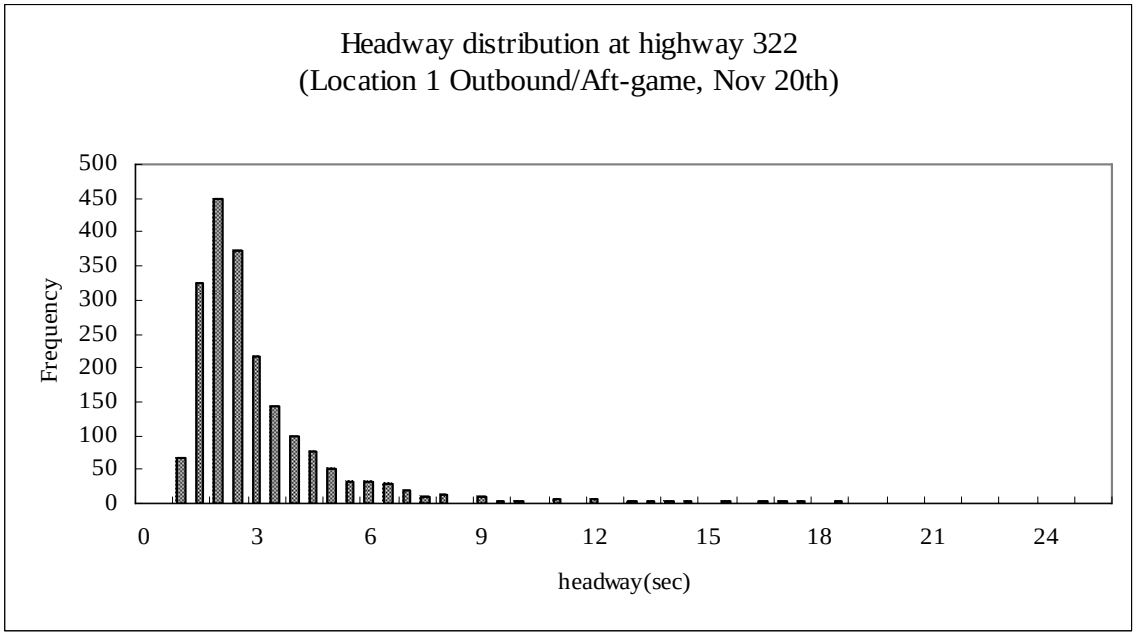

Figure 4-13 Headway distribution at highway 322 (Location 1 Outbound/Aft-game, Nov 20th)

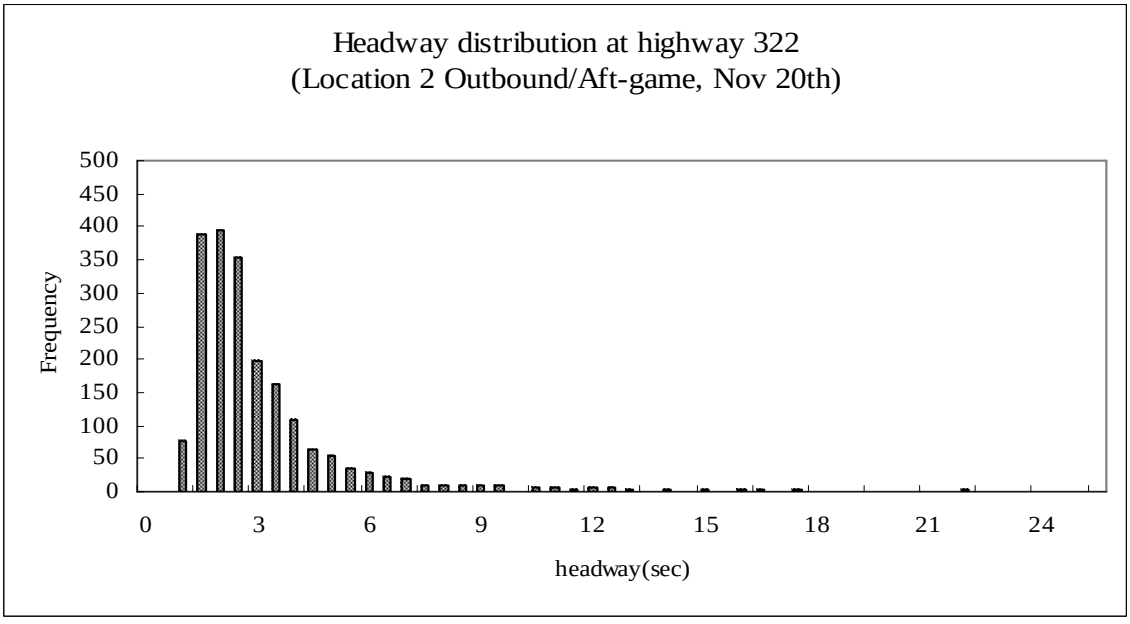

Figure 4-14 Headway distribution at highway 322 (Location 2 Outbound/Aft-game, Nov 20th)

4.2.2.3 Free flow speed distribution

The free flow speed distribution is applied in the simulation model to reflect the desired speed. Free flow speed was observed when traffic volume was low (about 174 vph). Generally, free flow speed distributions are known to follow a normal distribution. The

mean free flow speed was 57.1 mph, 2.1 mph higher than posted speed limit, 55 mph, and the standard deviation was 4.5 mph.

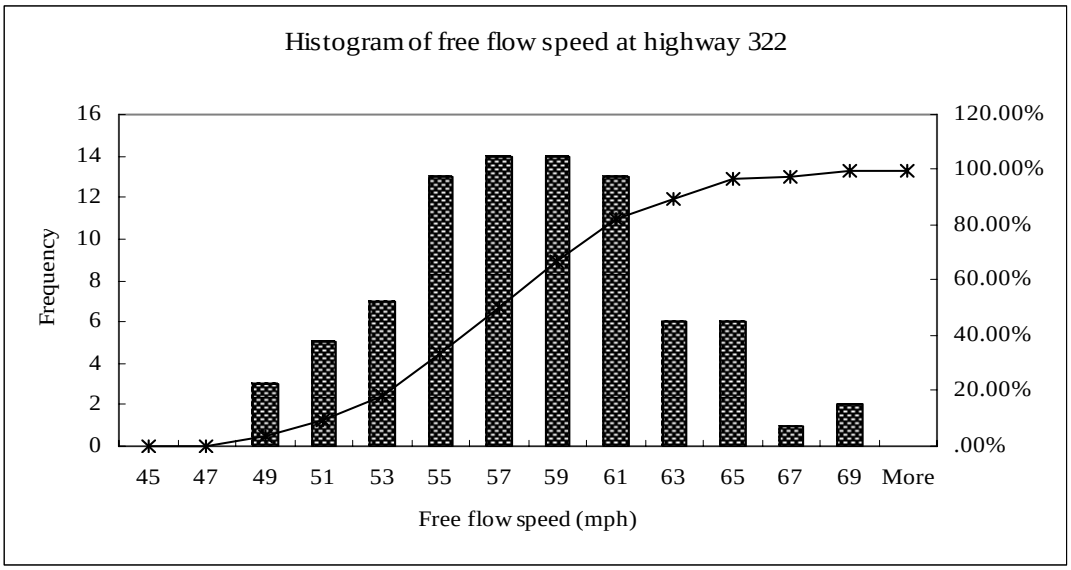

Figure 4-15 Histogram of free flow speed at highway 322

4.2.2.4 Maximum flow rate

The maximum flow rates along highway 322 are calculated in Table 4-8. The maximum flow rate in inbound/pre-game direction is estimated from the traffic observation conducted before the football game started in the morning. The maximum flow rate in outbound/aft-game direction is estimated from the traffic observed around the end of the game in the afternoon. The hourly flow rate is obtained by converting five minute volumes. The resulting table shows that every maximum flow rate at the downstream location is lower than that of the upstream location. Again, the location, whether it is upstream or downstream, is shown to have nothing to do with where the highest maximum flow rate is observed. The maximum flow rates along highway 322 did not reach the capacity suggested by the HCM 2000 even though there was a very high arrival demand at the beginning of the two-lane, two-way highway segment. Through the result

of the analysis of the field data, it was concluded that capacity for two-lane, two-way highways would not be observed without persistent effort under general circumstances.

Table 4-8 Maximum flow rates at highway 322

Direction		Maximum flow rate (vph)
Nov. 6th	Site 2→ Site 1 (Inbound/Pre-game)	1572→1608
	Site 1→ Site 2 (Outbound/Aft-game)	1548→1536
Nov. 20th	Site 2→ Site 1 (Inbound/Pre-game)	1452→1416
	Site 1→ Site 2 (Outbound/Aft-game)	1548→1524

4.2.2.5 Percent time spent following

Percent time spent following is a performance measure of two-lane, two-way highways in the HCM 2000. It is a useful measure as the resulting percent time spent following from the simulator will be compared to that of HCS 2000 and TWOPAS to verify if the simulator developed in this study is a realistic tool.

Table 4-9 Percent time spent following at highway 322

Location	Nov 6th				Nov 20th			
	Inbound		Outbound		Inbound		Outbound	
	1 (dn)	2(up)	1(up)	2(dn)	1(dn)	2(up)	1(up)	2(dn)
Volume (pcph)	1,321	1,330	1,363	1,328	1,193	1,173	1,353	1,349
Percent time spent following (%)	76.7	76.0	72.5	71.5	70.1	70.7	72.8	71.5

Note: *dn* represents downstream location, *up* represents upstream location based on the direction of traffic flow.

Percent time spent following ranges from 70.1 percent to 76.7 percent, which represents the percentage of headways less or equal to 3 seconds when compared to all headways. Looking at the percent time spent following at two successive locations in the

same direction, the percent time spent following is similar and increases or decreases at the downstream.

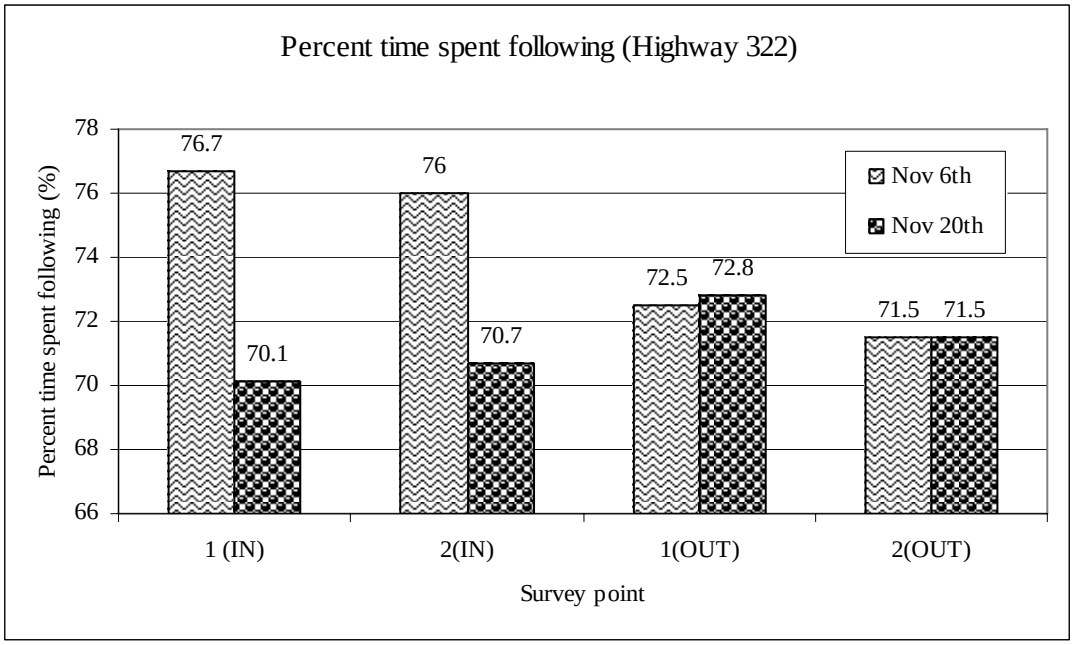

Figure 4-16 Percent time spent following at highway 322

4.2.2.6 Headway vs. speed

This section examines how speeds are distributed at relatively small headways (less than 3 seconds) and how often short headways can be observed in practice. For this analysis, headways less than 3 seconds were selected. The speeds are classified into 10 mph intervals. The mean and standard deviation of headways at each speed class is calculated. Tables 4-10 ~11 show how mean headway is related with different speed class. The count represents the total number of headways analyzed. The mean and standard deviation of spacing is calculated by multiplying the median speed of each class by the mean headway. Generally, average spacing from the bumper to the bumper for two consecutive vehicles ranges from 129.6 feet to 172.0 feet at operating speeds of 40 to 65 mph.

Table 4-10 Headways vs. speed at highway 322 (Inbound/Pre-game)

Headway vs. speed		Speed (mph)		
		<=50	>50 ~ <=60	>60~<=70
Headways	Mean (sec)	1.90	1.85	1.91
	Std dev. (sec)	0.57	0.57	0.53
Count		257	980	24
Spacing	Mean (ft)	129.6	148.3	172.0
	Std dev. (ft)	38.8	45.6	47.7

Table 4-11 Headways vs. speed at highway 322 (Outbound/Aft-game)

Headway vs. speed		Speed (mph)		
		<=50	>50 ~ <=60	>60~<=70
Headways	Mean (sec)	1.90	1.86	1.81
	Std dev. (sec)	0.55	0.57	0.57
Count		719	672	18
Spacing	Mean (ft)	131.2	146.0	163.9
	Std dev. (ft)	37.7	44.8	51.4

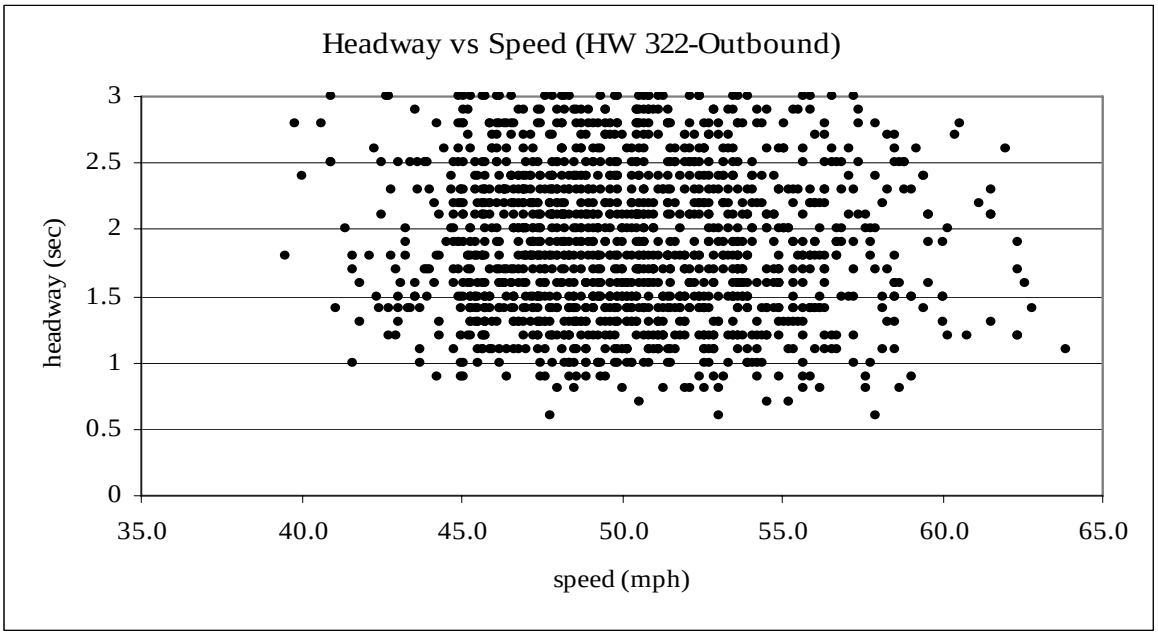

Figure 4-17 Headway vs. speed (HW 322-Inbound)

Figures 4-18~19 show headways plotted with speeds. It shows that small headways occur not only at low speeds but also at high speeds, such as 55 and 60 mph. Some small headways between 0.5 second and 1 second are not considered as normal or safe headways. Such small headways should be avoided in the simulation model for safety purposes. The two figures show small headway can occur at any speed range.

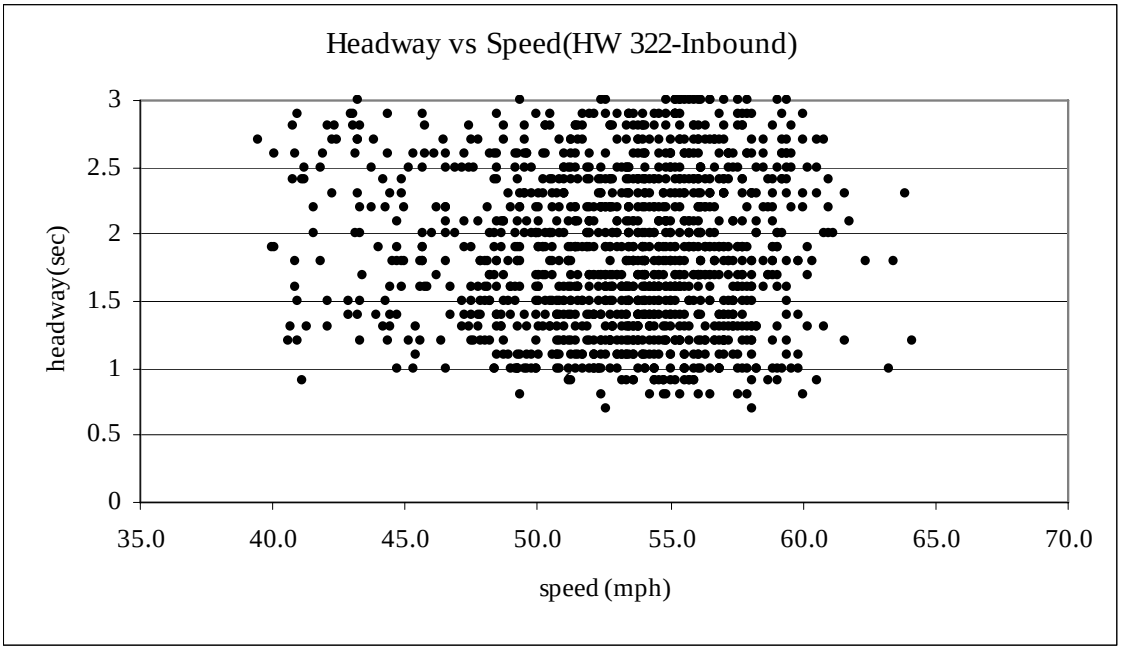

Figure 4-18 Headway vs. speed (hw 322-Outbound)

4.2.2.7 Average speed

Table 4-12 shows that average speed is calculated with the spot speeds estimated using time headway measured with digital stop watch at each directional traffic volume.

Table 4-12 Average speed with traffic volume

Primary traffic volume (vph)	Opposing volume (vph)	Average speed (mph)	
		Primary direction	Opposing direction
1,193	174	51.4	57.1
1,349	172	50.5	57.3

4.3 Summary

Field data collection was performed to calibrate the new microscopic simulation model and to obtain capacity data. The results of the field data collection showed that capacity conditions were not observed. However, various traffic flow characteristics were obtained and applied in the development of the simulation model. For instance, it was determined that the arrival headway distribution followed the M3A distribution, which was selected to be used in the simulation model. Similarly, the free flow speed was found to follow the normal distribution. The average free flow speed was found to be 5 mph higher than the posted speed limit. The mean and variance of the average free flow speed was applied in the simulation model to assign a desired speed to each individual driver in the simulator.

CHAPTER 5. BASIC TWO-LANE, TWO-WAY HIGHWAY SIMULATOR (TWOSIM I)

TWOSIM I replicates only fundamental vehicle movements, such as acceleration/deceleration without considering interactions with opposing vehicles, passing, heavy vehicles, horizontal/vertical alignments, and other factors.

This chapter presents the base conditions used in the basic two-lane, two-way highway simulator (TWOSIM I), what algorithms are employed in it, how the simulator is verified, and what the results of the comparison of TWOSIM I to TWOPAS and HCS^{+} are.

5.1 Base conditions

The basic two-lane, two-way highway simulator (TWOSIM I) is developed under the following base conditions:

- Lane widths greater than or equal to 12 ft.
- Shoulder widths wider than or equal to 6ft.
- 100 percent no-passing zones marked for no-passing.
- All passenger cars (no heavy vehicles and RV).
- Driver population is 100 percent commuters.
- Uninterrupted flow (no stop sign, signal along the segment, no driveway)
- 2 mile length of level terrain in homogeneous condition with no horizontal/vertical curve.
- Opposing traffic is so low that the impact on capacity reduction (200 pcph) can be negligible.

For those conditions, all passenger cars are assumed to have different performance, such as maximum acceleration/deceleration rate. Drivers are assumed to accelerate up to their respective desired speed. Also base conditions assume good weather, good pavement conditions, and no impediments to traffic flow.

5.2 Input data

There are two primary components for the replication of realistic vehicle movements in TWOSIM I: a) arrival headway distribution and b) car-following model.

5.2.1 Arrival headway distribution

First of all, in order to replicate realistic vehicle movements along a two-lane, two-way highway, a certain distribution that can explain how vehicles arrive at the beginning of two-lane, two-way highway segment is required. This section describes how the appropriate distribution for the arrival pattern of vehicles along a two-lane, two-way highway is selected and how the selected distribution is implemented in the simulation model.

5.2.1.1 Selection of arrival headway distribution

Summarizing the research for arrival headway distribution discussed in Chapter 2, Sullivan and Troutbeck (1994) found that a double displaced negative exponential headway distribution models vehicle headways more accurately than the Cowan's M3 distribution (M3) for headways greater than four seconds. However, they concluded that M3 is much simpler to use and still satisfies the required degree of accuracy in generating the distribution of vehicle headways. Luttinen (1999) examined the skewness and kurtosis of M3 distribution and concluded that M3 is a reasonable model for long

headways, but it does not provide a realistic model for short headways. However, he found the overall shape of the distribution fits very well with real headway data. Akcelik and Chung (2003) found that the more commonly used shifted negative exponential (M2) model gave poor predictions for the range of small headways. They strongly recommended M3 instead of the other two exponential models (i.e., shifted negative exponential and negative exponential distribution). Akcelik and Chung improved the M3 distribution by suggesting the proportion of free (unbunched vehicles) as an exponential model (M3A) and developed Akcelik's M3A model. They concluded that the M3A provides good estimates of arrival headways.

The three mathematical distributions discussed above are examined with the arrival headways from the field survey: Log-normal distribution, Negative-exponential distribution, and M3A distribution. For the comparative analysis, two statistical techniques, chi-square (χ^2) and Kolomgorov-Smirnov (*K-S*), can be applied to evaluate how well a measured distribution can be represented by a mathematical distribution. The *K-S* test was not selected in this case because the parameters of the distribution are estimated from sample data and the nonparametric test could give too conservative results. Also, the *K-S* test requires continuous data, but headway data from the Nu-metrics devices used in the field are discrete. When the calculated χ^2_{CALC} is smaller than the χ^2 value, it is concluded that there is significant evidence that the two distributions are identical. If the two compared distributions are statistically equal, then the result is marked "Yes," otherwise it is marked "No" in Table 5-1~3. Among the eight groups of data for Science Park Road, every group shows that there is evidence of a statistical difference between the measured headway distribution and the log-normal distribution.

There are two locations showing that there is no evidence of statistical difference between the measured headways and negative exponential distribution. There are four locations showing that there is no evidence of statistical difference between the measured headways and M3A distribution.

Table 5-1 Goodness of fit test for the headway distributions in Science Park Road (peak hour)

Location	Log-normal distribution			Neg-exponential distribution			M3A distribution		
	χ^2_{CALC}	$\chi^2 value$	Result	χ^2_{CALC}	$\chi^2 value$	Result	χ^2_{CALC}	$\chi^2 value$	Result
1	2262.7	6.0	No	74.2	9.5	No	11.6	11.1	No
2	1001.4	9.5	No	9.3	9.5	**Yes**	5.60	11.1	**Yes**
3	839.3	11.1	No	35.3	9.5	No	23.95	12.6	No
4	806.6	9.5	No	26.9	9.5	No	5.96	11.1	**Yes**
5	517.8	11.1	No	30.6	9.5	No	47.2	12.6	No
6	1021.4	11.1	No	8.65	9.5	**Yes**	3.17	11.1	**Yes**
7	925.7	9.5	No	18.3	9.5	No	4.84	11.1	**Yes**
8	889.6	9.5	No	14.55	9.5	No	15.95	11.1	No

Another goodness of fit test was conducted with headway data during the non-peak hour. As shown in Table 5-2, the M3A distribution gives the best goodness of fit compared with the other two distributions.

Table 5-2 Goodness of fit test for the headways in Science Park Road (non-peak hour)

Location	Log-normal distribution			Neg-exponential distribution			M3A distribution		
	χ^2_{CALC}	$\chi^2 value$	Result	χ^2_{CALC}	$\chi^2 value$	Result	χ^2_{CALC}	$\chi^2 value$	Result
1	646.4	9.5	No	20.5	9.5	No	7.6	11.1	**Yes**
2	1183.6	7.8	No	4.5	9.5	**Yes**	8.4	11.1	**Yes**
3	914.4	7.8	No	11.3	9.5	No	4.4	11.1	**Yes**
4	1214.2	9.5	No	2.3	9.5	**Yes**	15.5	11.1	No
5	746.9	9.5	No	32.1	9.5	No	10.6	12.6	**Yes**
6	1039.4	9.5	No	8.4	9.5	**Yes**	7.67	11.1	**Yes**
7	979.6	11.1	No	11.9	9.5	No	3.4	11.1	**Yes**
8	913.5	9.5	No	19.3	9.5	No	12.9	11.1	No

A comparison test was performed with the headways collected in the highway 322 of State College. All locations were shown to have a shape similar to the exponential or M3A distribution (Appendix A). As a result, only location 3 was found to have the distribution identical to neg-exponential distribution and M3A distribution.

Table 5-3 Goodness of fit test for headways in highway 322

Location	Log-normal distribution			Neg-exponential distribution			M3A distribution		
	χ^2_{CALC}	$\chi^2 value$	Result	χ^2_{CALC}	$\chi^2 value$	Result	χ^2_{CALC}	$\chi^2 value$	Result
1	2784.6	6.0	No	246.2	14.1	No	227.1	15.5	No
2	824.3	6.0	No	55.1	11.1	No	25.71	9.5	No
3	3161.8	6.0	No	313.6	9.5	**Yes**	212.9	11.1	**Yes**
4	2297.1	6.0	No	206.4	12.6	No	107.6	12.6	No
5	3198.4	6.0	No	233.5	14.1	No	900.5	11.1	No
6	3210.0	6.0	No	227.9	18.3	No	866.3	11.1	No
7	3254.6	6.0	No	331.0	14.1	No	743.9	9.5	No
8	2262.7	6.0	No	204.4	18.3	No	1052.9	11.1	No

In summary, the test result indicates that the best fitting distribution for the headways in Science Park Road is the M3A distribution. The negative-exponential distribution is also found to explain the headway distribution of Science Park Road well. Consequently, the M3A distribution is applied to TWOSIM I.

5.2.1.2 Implementation of arrival headway distribution in MATLAB

This section describes how the M3A headway distribution is employed in the simulator. For the implementation of the M3A distribution, the following parameters in the distribution have to be determined: minimum headway, bunching factor, the proportion of free vehicles, decay parameter. Although the study by Akcelik and Chung (2003) suggested the minimum headway for a two-lane, two-way highway to be 1.5 seconds,

TWOSIM I is programmed to select the minimum headway (*delta*) within the range of 1.4 to 1.6 seconds to reflect the randomness of minimum headway in the real world.

When the minimum headway is chosen, the bunching factor (*b*) is specified as suggested by the corresponding publication. The inverse function derived from the M3A distribution gives maximum headway, which truncates the right tail of the distribution to avoid error occurrence when the interpolation function (*interp1*) in MATLAB is executed. Accordingly, the proportion of free vehicles (*phi*) and a decay parameter (*lamda*) is calculated with the given input data and the arrival demand.

After all the parameters are calculated, Akcelik's M3A distribution can calculate the cumulative distribution of headways for each time headway respectively using the following equation.

$$F(t) = 1 - \varphi\, e^{-\lambda(t-\Delta)} \quad for\ t \geq \Delta$$
$$= 0 \quad for\ t < \Delta$$

Eq 5-1

where,

t = headway (sec);

Δ = minimum arrival headway (sec);

φ = proportion of free vehicles; and

λ = a decay parameter

Details on how the arrival headway distribution is implemented in MATLAB can be found in Appendix B.

5.2.2 Car following model

Many different "car-following" models have been proposed to describe driver behavior in a traffic stream. This section describes what car-following model is adopted in TWOSIM I and how the selected model is employed in TWOSIM I.

5.2.2.1 Selection of car-following model

Generally, the car-following model calculates vehicle's acceleration/deceleration or speed taking into account the interaction between successive vehicles. Through the literature review, Gipps' car following model (1981) was selected as the preferred model for replicating a vehicle's movement on a two-lane, two-way highway. The Gipps' car-following model does not allow each driver to exceed his/her desired speed. This reflects the speed trend of the leading vehicle in platoon on a two-lane, two-way highway. According to Lee, et al. (2002), the Gipps' model was found to be most promising model in the development of a longitudinal human driving model that is accurate enough for the evaluation of the impact of adaptive cruise control systems on highway traffic.

As described in Chapter 2 of this dissertation, Gipps (1981) developed a car-following model based on two constraints:

$$v_n(t+\tau) = \min\left\{\begin{array}{l} v_n(t) + 2.5\,a_n\tau\left(1 - v_n(t)/V_n\right)\left(0.025 + v_n(t)/V_n\right)^{1/2} \\ b_n\tau + \sqrt{\left(b_n^2\tau^2 - b_n\left[2\left[x_{n-1}(t) - s_{n-1} - x_n(t)\right] - v_n(t)\tau - v_{n-1}^2(t)/\hat{b}\right]\right)} \end{array}\right\} \qquad \textbf{Eq 5-2}$$

where,

a_n = the maximum acceleration which the driver of vehicle *n* wishes to undertake;

b_n = the most severe braking that the driver of vehicle *n* wishes to undertake;

s_n = the effective size of vehicle *n*, that is, the physical length plus a margin into which the following vehicle is not willing to intrude, even when at rest;

V_n = the speed at which the driver of vehicle *n* wishes to travel;

x_n = the location of the front of vehicle *n* at time *t*;

$v_n(t)$ = the speed of vehicle *n* at time *t*;

τ = the apparent reaction time, a constant for all vehicles; and

$\hat{b}$ = the estimation of the most severe braking deceleration rate, b_{n-1}

The first constraint is that a driver will not exceed his/her desired speed. The second constraint is based on the consideration of braking. The ground concept of the constraint is illustrated in Figure 5-1. If vehicle *n-1*, the lead vehicle, commences braking as hard as desirable at time *t*, it will come to rest at location x_{n-1}^*. Vehicle *n* traveling immediately behind will not react until time $t+\tau$ and consequently will not come to rest before reaching x_n^*.

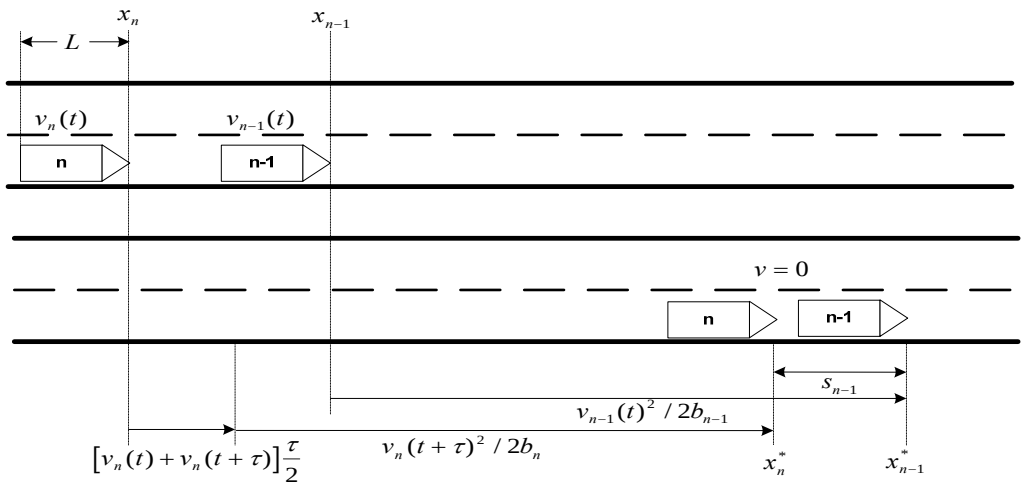

Figure 5-1 Concept of safety constraint in Gipps' car-following model

Therefore, s_{n-1} can be expressed as following equation:

$$s_{n-1} = x_{n-1}^* - x_n^* = [x_{n-1}(t) - v_{n-1}(t)^2/2b_{n-1}] - [x_n(t) + \{v_n(t)+v_n(t+\tau)\}\frac{\tau}{2} - v_n(t+\tau)^2/2b_n] \quad \textbf{Eq 5-3}$$

For the purpose of safety, the driver of vehicle *n* must ensure that $x_{n-1}^* - s_{n-1}$ exceeds x_n^*. However, if this were the governing inequality, the driver of vehicle *n* would have no margin for error. Therefore, Gipps introduced an additional safety margin by supposing that the driver makes allowance for a possible additional delay of θ when traveling at $v_n(t+\tau)$, before reacting to the vehicle ahead. That is, there is a true reaction

time, τ, and a safety reaction time, $\tau + \theta$, that appears in the calculations. Thus, the limitation on braking requires the following equation:

$$x_{n-1}(t) - v_{n-1}(t)^2 / 2b_{n-1} - s_{n-1} \geq x_n(t) + \left[v_n(t) + v_n(t+\tau)\right]\tau / 2 + v_n(t+\tau)\theta - v_n(t+\tau)^2 / 2b_n$$

Eq 5-4

Without the introduction of the parameter θ in this fashion, a single vehicle approaching a stationary object or a stop line would travel at its desired speed until it had to commence maximum braking. The effect of θ is to cause the simulated vehicle to brake earlier and to gradually reduce braking so that it crawls up to the stop line.

According to Gipps, in real traffic, it is possible for the driver of vehicle *n* to estimate all the values in the equation above except b_{n-1} by direct observation. Thus b_{n-1} should be replaced by some estimate $\hat{b}$ to give:

$$-v_n(t+\tau)^2 / 2b_n + v_n(t+\tau)(\tau/2 + \theta) - \left[x_{n-1}(t) - s_{n-1} - x_n(t)\right] + v_n(t)\tau / 2 + v_{n-1}(t)^2 / 2\hat{b} \leq 0$$

Eq 5-5

The relative magnitude of τ and θ are important in determining the behavior of vehicles. It can be shown (Appendix B) that, if θ is equal to $\tau/2$ and the willingness of the previous driver to brake hard has not been underestimated, a vehicle traveling at a safe speed and distance will be able to maintain a state of safety indefinitely. Thus Equation 5-5 can be rewritten as:

$$-v_n(t+\tau)^2 / 2b_n + v_n(t+\tau)(\tau) - \left[x_{n-1}(t) - s_{n-1} - x_n(t)\right] + v_n(t)\tau / 2 + v_{n-1}(t)^2 / 2\hat{b} \leq 0$$

Eq 5-6

Hence,

$$v_n(t+\tau) \leq b_n\tau + \sqrt{\left(b_n^2\tau^2 - b_n[2[x_{n-1}(t) - s_{n-1} - x_n(t)] - v_n(t)\tau - v_{n-1}^2(t)/\hat{b}]\right)} \qquad \textbf{Eq 5-7}$$

This equation is the second limiting condition in calculating Gipps' car-following model as shown in Equation 5-2. When the second speed is the limiting condition for almost all vehicles, congested flow exists with the traffic flowing as fast as the volume of vehicles permit. On the other hand, when the first speed in Equation 5-2 is the limiting condition, the traffic flows freely.

5.2.2.2 Updating parameter values in Gipps' car-following model

Since Gipps' car-following model was developed in 1981, the parameters in the model should be updated with up-to-date vehicle performance data.

Maximum acceleration rate of passenger cars

Since TWOSIM I simulates 100 percent of passenger cars, maximum acceleration rates of passenger cars are introduced at the website (web.missouri.edu/~apcb20/times.html). This website has information on vehicle manufactured between 1970 and 1999. Taking into account the average age of cars in use in 2002, 8.4 years (1), maximum acceleration rates vehicles made in the 1990s should be applied in Gipps' car-following model. Table 5-4 shows arbitrarily classified TWOSIM I car type by maximum acceleration rate.

Table 5-4 Classified maximum acceleration rate of passenger cars in TWOSIM I

TWOSIM I car type	Maximum acceleration rate (ft/s^2)	Percent (%)
1 (Lowest Performance)	6.4~8.0	17.8
2	8.1~10.0	42.6
3	10.1~12.0	3.9
4	12.1~14.0	17.8
5	14.1~16.0	5.7
6	16.1~18.0	7.4
7	18.1~20.0	4.4
8 (Highest Performance)	20.1~23.3	0.4

Source: http://web.missouri.edu/~apcb20/times.html

There are eight types of cars with different maximum acceleration rates and different percentage distributions. It is noted that this percentage does not represent the usage on the roadway but simply a stratified portion by vehicle type in the market. Therefore, it is assumed that the maximum acceleration rate is randomly selected in TWOSIM I based on the percentage.

Estimate of most severe braking deceleration rate

Braking performance is related to a number of factors, including the type and condition of the tires, the condition and type of roadway surface, and the grade of road (Roess et al., pp. 50). There are two types of parameter associated with the most severe deceleration rate in Equation 5-2: b_n and $\hat{b}$. The variable b_n represents the most severe braking deceleration rate that the driver of vehicle n (Figure 5-1) wishes to undertake. Since a deceleration rate is obtained by multiplying maximum acceleration by –2 according to Gipps' car-following model (Equation 5-4) and maximum acceleration rates are updated as above, the most severe braking deceleration of following vehicle n is updated together.

$$b = -2 \times a \qquad \textbf{Eq 5-8}$$

where,

b = most severe braking deceleration rate of following vehicle n (ft/s^2); and

a = maximum acceleration rate of following vehicle n (ft/s^2)

Secondly, in Gipps' car-following model $\hat{b}$ represents the estimate of most severe braking deceleration rate of a lead vehicle *n-1* as shown in Figure 5-1. Gipps' car-following model generates $\hat{b}$ by choosing the minimum value between the two numbers in Equation 5-9. The formula estimates the most severe braking deceleration rate of the

lead vehicle *n-1* to be –3.0 when the most severe braking rate of a following vehicle *n* is less or equal to –3. Otherwise, the formula estimates the value of (*b*-3)/2 to be the most severe braking deceleration rate of the lead vehicle.

$$\hat{b} = \min\left(-3.0, (b-3.0)/2\right)\left(m/s^2\right) \quad \text{Eq 5-9}$$
$$= \min(-9.8, (b-9.8)/2)\,(ft/s^2)$$

where,

b = most severe braking deceleration rate of following vehicle n (ft/s^2);

a = maximum acceleration rate of following vehicle (ft/s^2); and

$\hat{b}$ = estimate of most severe braking deceleration rate of lead vehicle (ft/s^2)

Here, the parameter value (9.8 ft/s^2) in Gipps' car-following model needs to be updated taking into account recent advances in vehicle performance. The 2001 Green Book indicates that braking deceleration rate for an emergency stop is 14.8 ft/s^2. The Revised Monograph on Traffic Flow Theory (1994) introduces research by Fambro, et al. (1994), which provides some steady-state deviations from the empirical data given in Table 5-5.

Table 5-5 Percentile estimates of steady state unexpected deceleration

Deceleration rate	Unexpected	Expected
Mean	-0.55g (17.6 ft/s^2)	-0.45g (14.4 ft/s^2)
Standard deviation	0.07g (2.2 ft/s^2)	0.09g (2.9 ft/s^2)
75th Percentile	-0.43g (13.8 ft/s^2)	-0.36g (11.5 ft/s^2)
90th Percentile	-0.37g (11.9 ft/s^2)	-0.31g (9.9 ft/s^2)
95th Percentile	-0.32g (10.3 ft/s^2)	-0.27g (8.7 ft/s^2)
99th Percentile	-0.24g (7.7 ft/s^2)	-0.21g (6.7 ft/s^2)
g (gravity constant) = 9.8 m/sec^2 = 32.15 ft/s^2		

The second column represents deceleration as responses to an unexpected obstacle or object encountered on a closed course. The third column represents the response of drivers in their own vehicle in which the braking maneuver was anticipated.

The parameter $\hat{b}$, the most severe braking deceleration rate is executed under an emergency. Therefore, the responses to an unexpected object from the Fambro's study are considered as more proper deceleration than the responses to expected condition are. Converting the mean, -0.55g into English units, the mean of deceleration rate is 17.6 ft/s^2. In TWOSIM I, the following equation is applied to estimate the most severe braking rate of a lead vehicle.

$$\hat{b} = \min\left(-17.6, (b - 17.6)/2\right)\left(ft/s^2\right) \qquad \textbf{Eq 5-10}$$

The new equation determines the most severe braking rate of vehicle *n-1* to be 17.6 ft/s^2 unless the most severe braking of vehicle *n* is larger than 17.6 ft/s^2. According to the newly updated equation, the estimate of most severe braking rate of a lead vehicle range from –32.2 ft/s^2 to –17.6 ft/s^2.

The performance of the most recent vehicles (i.e. 2004 & 2005) was found from a website (www.autos.msn.com) shown in Table 5-6, but it includes various passenger car types such as sedan, wagon, and sports utility vehicle. It is noted that the information does not cover all types of passenger cars on the market. The third column of Table 5-6 represents the distance to a full stop from 60 mph. More details about the performance of vehicles from the 1990s and 2000s can be found in Appendix B. Using the distance to stop from a 60 mph initial speed, the deceleration rate, the fourth column in Table 5-6, can be calculated with the following equation based on vehicle dynamics.

$$f = \frac{V^2}{30\,S} \qquad \text{Eq 5-11}$$

$$b = g \cdot f = 32.15\, f = 1.07\,\frac{V^2}{S}$$

where,

f = friction factor;

V = veloctiy (mph);

S = distance to stop (ft);

b = deceleration rate (ft/s^2); and

g = gravity acceleration rate (32.15 ft/s^2)

Table 5-6 Braking distance and deceleration rate of vehicles in 2004 and 2005

Company	Year	Distance (feet)[1]	Deceleration (ft/s^2)
Acura	2005	122 ~ 141	-34.1 ~ -27.5
Audi	2005	132 ~ 135	-29.4 ~ -28.8
Benz	2005	118 ~ 142	-32.9 ~ -27.4
Cadilac	2005	118 ~ 127	-32.9 ~ -30.6
Chevrolet	2005	118 ~ 146	-32.9 ~ -26.6
Chrysler	2005	129 ~ 133	-30.1 ~ -29.2
Dodge	2005	134 ~ 143	-29.0 ~ -27.2
Ford	2005	132 ~ 146	-29.4 ~ -26.6
GMC	2005	147	-26.4
Hyundai	2005	158	-24.6
Jaguar	2005	133	-29.2
Jeep	2005	139 ~ 143	-27.9 ~ -27.2
Kia	2005	129 ~ 147	-30.1 ~ -26.4
Landrover	2005	121	-32.1
Mazda	2005	139	-27.9
Mitsubishi	2005	145 ~ 146	-26.8 ~ -26.6
Pontiac	2005	145	-26.8
Porsche	2005	114	-34.1
Subaru	2005	137 ~ 146	-28.3 ~ -26.6
Toyota	2005	120 ~ 135	-32.4 ~ -28.8
Volkswagen	2004	136 ~ 141	-28.6 ~ -27.5

Note: [1] Distance to stop from 60 mph to 0 mph

The highest deceleration rate is obtained to be -34.1 ft/s^2 from Acura vehicle, which is slightly higher than the highest deceleration rate (-32.2 ft/s^2) modeled in TWOSIM I.

The lowest deceleration rate is -24.6 ft/s^2 for a Hyundai vehicle, which is lower than the lowest severe braking rate (-17.4 ft/s^2).

Delay of safety reaction time

According to Gipps' model, θ (Eq 5-12) was introduced for a further safety margin by supposing that a driver makes allowance for a possible additional delay of θ when traveling at $v_n(t+\tau)$, before reacting to the vehicle ahead. The effect of θ is to cause the simulated vehicle to brake earlier and to gradually reduce braking so that it crawls up to the stop position.

$$x_{n-1}(t) - v_{n-1}(t^2)/2b_{n-1} \geq x_n(t) + \left[v_n(t) + v\ (t+\tau)\right]\tau/2 + v_n(t+\tau)\theta - v_n(t+\tau)^2/2b_n$$

Eq 5-12

Green (2000) redefines perception reaction in more detail to avoid confusion for the purpose of his study. He regards mental processing time as perception time. The mental processing time is the time it takes for the responder to perceive that a signal has occurred and to decide on a response. The combined perception time and movement time is defined to be brake reaction time. The movement time is the time it takes the responder's muscles to perform the programmed movement. Lastly, stopping time is brake reaction time plus device response time, which is the time it takes the physical device to perform its response. Through his overall study about literature regarding reaction time, he found expectancy has the greatest effect. With high expectancy and little uncertainty, the best driver response time is about 0.70 to 0.75 sec, of which 0.2 sec is movement time under circumstances such that drivers can expect what would happen ahead or would be ahead like approaching signalized intersection or stop line with stop sign. With normal and common expectancy, such as brake lights on a lead car, expected times are about 1.25 sec.

This estimate is only valid for a specific set of conditions: brake response to "normal" road events in good weather with high visibility. Last, driver's response time for surprise intrusions is about 1.5 sec, including a 0.3 sec movement time. The surprise intrusion is circumstance such that an object suddenly moves into the driver's path from off the road or another vehicle suddenly cuts across an intersection immediately ahead.

According to Green's study, total reaction time in TWOSIM I is determined between 1.25 second and 1.5 second for allowing safety margin in TWOSIM I. Therefore, each θ for every driver in TWOSIM I is generated in the range from 0.78 to 1.14 as shown in the following calculation:

Total reaction time = $\tau + \theta \times \tau$ = 0.7 + 0.78×0.7 = 1.25 sec

Total reaction time = $\tau + \theta \times \tau$ = 0.7 + 1.14×0.7 = 1.5 sec

Effective size of vehicle

As noted in Equation 5-2, the effective size of the vehicle represents the physical length of the car plus the spacing of vehicle at rest. The average effective size of vehicles suggested in Gipps' car-following model, 21.3 feet (6.5m), is applied in TWOSIM I. According to the 2001 Green Book, the overall length of a passenger car is 19 feet (5.8 m). When the physical length of the vehicle is 19 feet, the remnant is 2.3 feet (21.3-19 = 2.3 feet = 0.7 m), which is considered as an appropriate value for spacing between two successive vehicles at rest. Therefore, it is acceptable that the effective size of vehicle in the original Gipps' model continues to be applied in TWOSIM I. The TWOSIM I will generate the effective size of vehicles randomly from a normal distribution with mean 21.3 ft and standard deviation 1.0 feet.

5.2.2.3 Implementation of car-following model in MATLAB

Predetermination of arrival speed of first vehicle

In implementing TWOSIM I, there are two issues related to the arrival speed of the first vehicle generated in TWOSIM I. Gipps' car-following model cannot calculate the speed for the current time step without knowing the speed in the previous time step. Therefore, an arrival speed has to be given to the first vehicle at its arrival.

The next issue is how to determine the arrival speed of the first vehicle. TWOSIM I's study segment is not shaped as a circle but as a straight pipe type with an entry and exit at both ends. When the study segment is circular, the speed of the first vehicle is influenced immediately by vehicles arriving successively at the segment through a warming-up period, because some vehicles arriving later than the first vehicle immediately travel ahead of the first vehicle and have an impact on the speed of the first vehicle.

However, there is no vehicle at the downstream of the first vehicle in the pipe type segment of TWOSIM I over entire simulation period. Therefore, without an algorithm considering the impact of traffic arrival demand, the first vehicle would always travel at free flow speed and exit the end of segment regardless of traffic demand and so do the following vehicles. To avoid the unrealistic speed trend, there is a need of certain algorithm to determine the speed of the first vehicle to reflect the impact of traffic demand.

For the exploration of such algorithm, the speed-flow relationship of two-lane, two-way highway in NCHRP 3-55(3) is first reviewed. That relationship is:

$$ATS_d = FFS_d - 0.0125\left(V' + V''\right) \qquad \textbf{Eq 5-13}$$

where,

ATS_d = directional average travel speed (mph);

FFS_d = directional free-flow speed (mph);

V' = directional passenger-car equivalent flow rate (pcph);

V'' = passenger car equivalent flow rate for the opposing direction (pcph)

TWOSIM I can apply the relationship to determine what the speed of the first vehicle in simulation would be. In order to determine the value of parameter for TWOSIM I, a regression analysis is conducted using field data and NCHRP 3-55(3) data. These data are combined to obtain appropriate values for each directional flow rate so that the newly developed model can cover two classes of two-lane, two-way highway and estimate average travel speed at a various range of traffic flow. Figure 5-2 plots such data and shows there is decreasing tendency of average travel speed with traffic flow rate. The points with higher average travel speed are from the site with 60 mph free flow speed. The points with lower average travel speed are collected from the site with 45 mph free flow speed. Both groups show that the average travel speed decreases with traffic flow at both directions.

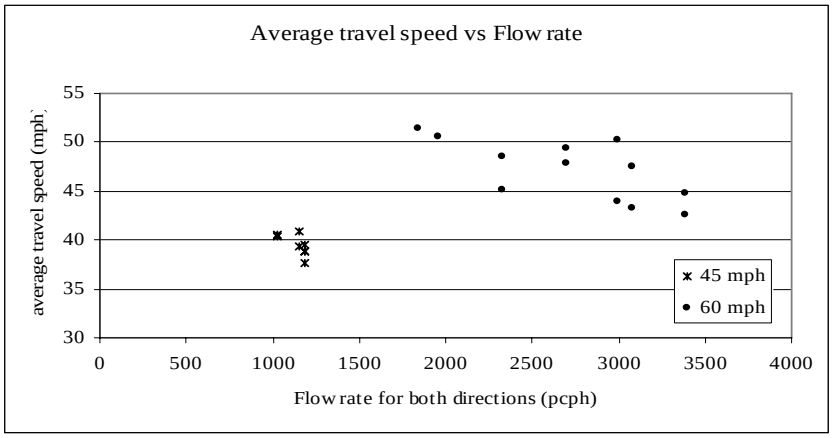

Figure 5-2 Average travel speed vs. flow rate (source: field data & NCHRP 3-55(3))

To obtain a general regression equation and make the same form as Equation 5-12, the dependent variable is defined as the difference between average travel speed and free flow speed. Figure 5-3 shows the relationship of the difference and flow rate in both directions.

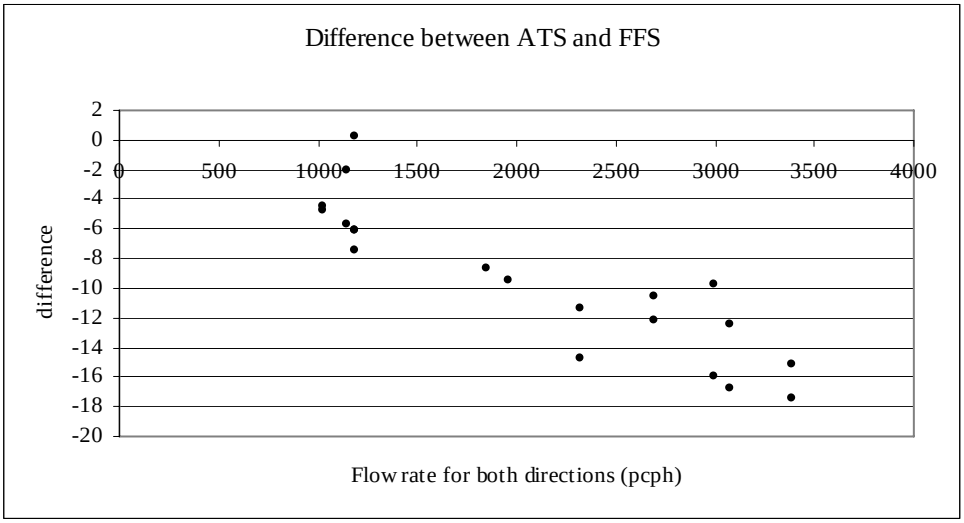

Figure 5-3 Difference between ATS and FFS vs. flow rate

The difference decreases with traffic flow rate for two-lane, two-way highways. Using these dependent values, new coefficients are obtained by conducting a regression analysis. Coefficients are obtained with *p-value* low enough to provide statistical significance. Details on the statistical result of regression can be found in Appendix D. The result indicates that the average travel speed decreases by 0.7 percent of the primary directional volume and 0.3 percent of the opposing directional volume from free flow speed.

Table 5-7 Result of regression analysis

Regression analysis	Coefficient	Standard error	t-stat	p-value
Directional volume	-0.007	0.0010	-6.56	0.0000
Opposing volume	-0.003	0.0011	-2.38	0.0283
R-square: 0.87, Multiple-R: 0.93, Adjusted R-square: 0.81				

The new equation with new values for the coefficients is applied in TWOSIM I as follows. Compared with the relationship in NCHRP 3-55(3), this equation differentiates the impact of traffic flow on the speed by direction:

$$ATS_d = FFS_d - 0.007\,V' - 0.003\,V'' \qquad \textbf{Eq 5-14}$$

where,

ATS_d = directional average travel speed (mph);

FFS_d = directional free-flow speed (mph);

V' = directional passenger-car equivalent flow rate (pcph); and

V'' = passenger car equivalent flow rate for the opposing direction (pcph)

Figure 5-4 shows the linear relationship of directional traffic flow and average travel speed at given free flow speed, 60 mph.

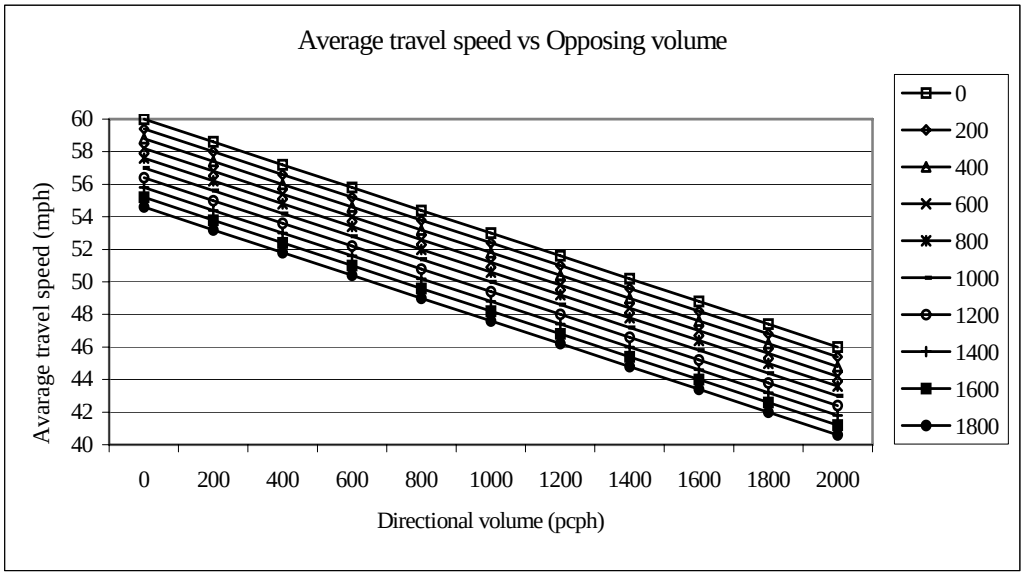

Figure 5-4 Average travel speed vs. directional traffic volume

A variety of different combinations of directional traffic volumes show different average travel speed. The line at the top represents the average travel speed with primary volume varying along x-axis and opposing volume 0 pcph under 60 mph free flow speed.

The second lower line represents the average travel speed with primary volume varying along the x-axis and opposing volume 200 pcph under 60 mph free flow speed. The other lines correspond to different opposing volumes under the same condition of free flow speed and primary direction volume. In TWOSIM I, this trend of average travel speed governs the travel speed of the first vehicle.

The new relationship of average travel speed with traffic flow differentiated by direction is applied to determine travel speed of the first vehicle in TWOSIM I.

Predetermination of initial speed for all vehicles (arrival speed)

All the other vehicles are required to have arrival speed regardless of car-following model similar to the way that the arrival speed of the first vehicle is needed. Then, it is an issue how arrival speed of each vehicle arriving at study segment is determined in TWOSIM I.

There is an assumption that when a vehicle arrives at study segment, its arrival speed is assumed to depend upon the speed of vehicle directly ahead. The arrival speed of the vehicle following is assumed to be 1 mph less than the speed of a lead vehicle at the moment when the following vehicle arrives at the study segment. When the headway between two successive vehicles is longer than 3 sec, the arrival speed of the following vehicle is determined randomly from the normal distribution of desired speed.

This assumption is realistic, because vehicles arriving at the segment with a closely following vehicle ahead can hardly make higher speeds than the speed of the vehicle ahead. Likely, vehicles arriving at the study segment with following the vehicle ahead at moderate distance (at headway longer than 3 seconds) can make its own arrival speed independent of the speed of the vehicle ahead.

At this point, a concern could be raised that the assumption of arbitrary adjustment of arrival speed might be seen to produce an unrealistic flaw in the determination of speed by the car-following model and ultimately potential bias in generating output. TWOSIM I allows the warm-up period and the warm-up zone to be specified for reading outcomes of simulation at a stabilized equilibrium condition. When the warm-up period ends and the analysis period begins, the impact of predetermined arrival speed is significantly reduced and then traffic conditions are governed only by the desired speed and car-following model built in TWOSIM I.

The analysis period is defined as the temporal range beginning at the end of warm-up period and ends after the specified analysis period (i.e., 15 minutes). The analysis zone is defined to begin at the end of warm-up zone (default: 0.5 mile) and ends at the full distance of the analysis zone (i.e., 2 miles). Therefore, the output is collected during the analysis period over the analysis zone in TWOSIM I. It is noted that observing the warm-up period or warm-up zone in TWOSIM I will provide information about how vehicles would behave at the beginning of the segment. The list of required input data and output available from TWOSIM I can be found in Appendix C.

5.3 Verification of basic two-lane, two-way highway simulator (TWOSIM I)

The purpose of model verification is to assure that the conceptual model is reflected accurately in the computerized representation. For verification of TWOSIM I, it is required to closely examine the model output for reasonableness under a variety of settings for the input parameters, check if input parameter values are consistent at the end of the simulation, develop the graphical representation, and verify that what is seen in the graph replicates the actual system.

5.3.1 Input data

5.3.1.1 Random number generation

According to Mills (2003), there have been several random number generators such as the middle square generator, the Fibonacci generator, the Lehmer generator, and the subtract with borrow generator. The middle square generator suggested by Jon Von Neumann in 1946 is shown not to conform to uniformity over the unit interval. The Fibonacci generator was found to fail simple tests for randomness. Lehmer's generator is better than the first two generators and the prime modulus multiplicative linear congruential generator. This generator had been used until the release of MATLAB version 5.0.

After version 5.0, MATLAB used the subtract-with-borrow generator, which is much faster and has longer period length (almost 2^{1492} according to Moler (1995)) than the Lehmer generator. Therefore, the subtract-with-borrow generator has desirable properties of pseudo random number generators such as uniform, lengthy (most lengthy) period, serially uncorrelation, and fastness. TWOSIM uses the subtract-with-borrow generator built in MATLAB 6.5 and 7.0 to generate random numbers for various random variables.

5.3.1.2 Akcelik's M3A headway distribution

Verification of arrival headway distribution in TWOSIM I

Whether the algorithm of M3A distribution built in TWOSIM I works as expected, needs to be verified. To ensure that the algorithm works as expected, χ^2 test is conducted at traffic volume 1,000 vph for the comparative test between the built-in probability and the probability of outcomes generated by the built-in probability. The test aims at showing if the arrival headways generated in TWOSIM I has identical distribution to M3A

distribution. The related statistical analysis is attached at Appendix C. It should be kept in mind that the probability of the arrival headway can vary every run due to stochastic characteristic of assignment. Figure 5-5 illustrates that mathematical probability density of M3A and probability of arrival headways as outcome in TWOSIM I has a similar trend.

5.3.1.3 Gipps' car-following model

Distribution of maximum acceleration rate

TWOSIM I assigns a maximum acceleration for each vehicle according to built-in probability density of Table 5-4. The probability of maximum acceleration rates produced in TWOSIM I is compared with the built-in probability density in TWOSIM I.

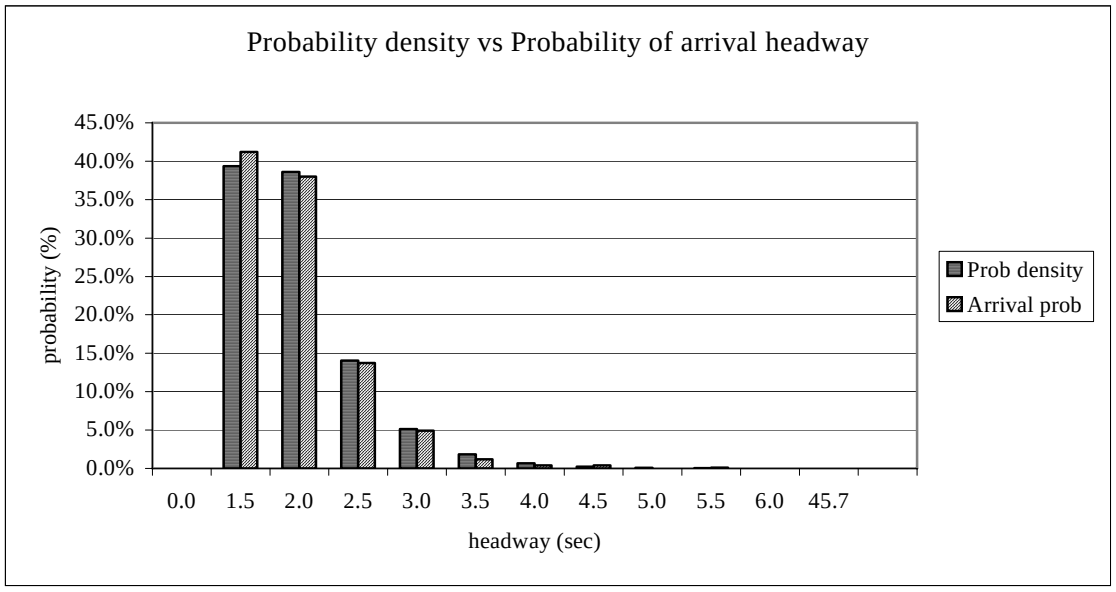

Figure 5-5 Probability density vs. probability of arrival headway

It is shown that there is a similar trend between the two probabilities, which indicates the algorithm assigning maximum acceleration rate built in TWOSIM I works as intended. The slight discrepancy is acceptable and reflects stochastic characteristic in assigning maximum acceleration rate inside TWOSIM I.

Effective size of vehicle

TWOSIM I assigns the effective size of vehicle as a parameter in the car-following model according to a normal distribution. A Chi-square test was conducted to ensure that the corresponding algorithm reproduced the effective size of vehicle according to a normal distribution. The test result shows there is significant evidence that the distribution of the effective size of vehicles generated in MATLAB is identical to a normal distribution. The associated figure is attached in Appendix D.

Desired speed

Desired speed for passenger cars is designed to have a normal distribution in TWOSIM I. A Chi-square test was conducted to determine if there is normality in the desired speed values generated in TWOSIM I. The test result shows that there is significant evidence that the distribution of the desired speed values generated in TWOSIM I are identical to a normal distribution. The associated figure is attached in Appendix D.

Speed trends of vehicles following

To verify Gipps' car-following model, an arbitrarily unrealistic trend of speed is given to the first leading vehicle in a platoon as shown in Figure 5-6. The first vehicle's speed goes up and down like sine function. The speeds of vehicles following over time vary according to the same pattern. In Figure 5-6, the number for each speed curve represents the order of vehicle. When a vehicle ahead accelerates, so does the vehicle following behind unless it reaches its individually desired speed. Likely, when a vehicle ahead decelerates, so does the vehicle following behind unless it reaches its individually desired

speed. As shown in Figure 5-7, the speed trend of platooned vehicles is shown to work as expected.

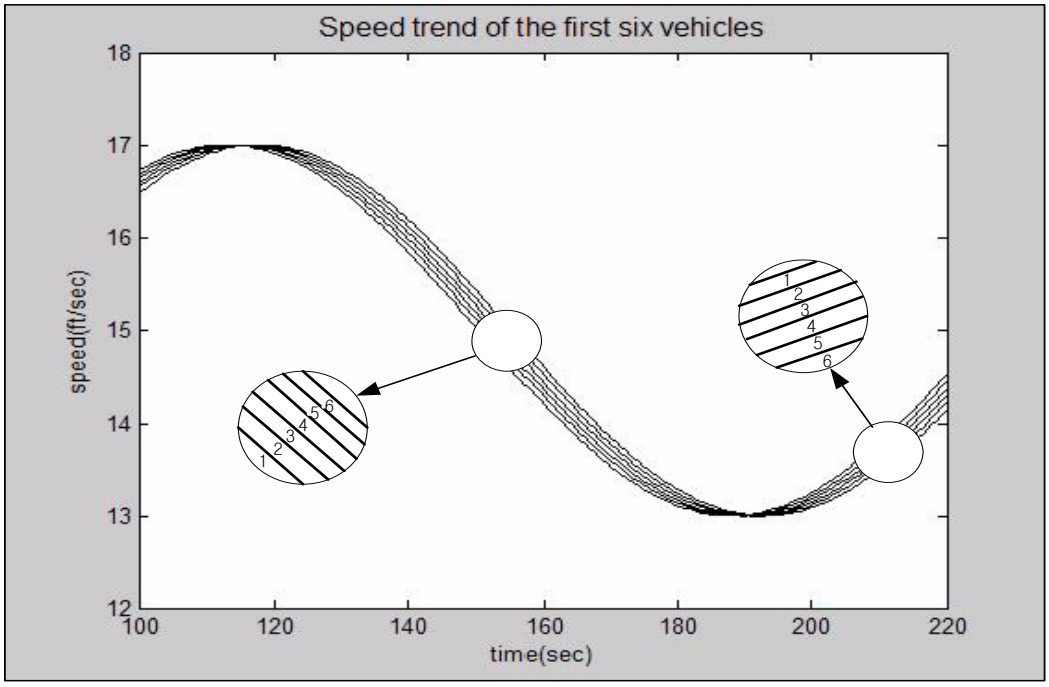

Figure 5-6 Speed trend of the first six vehicles

Now, the first leading vehicle in a group of vehicles achieves a realistic speed. In Figure 5-7, line 1 represents the speed trend of the first leading vehicle in the group as it accelerates after entering the segment at 56 mph, and 10 seconds later, it runs at a constantly desired speed. Five seconds later, the second vehicle arrives at the segment and keeps accelerating up to its desired speed, which is 8 mph higher than the desired speed of the lead vehicle. Immediately, the spacing with the first vehicle gets so close that the second vehicle starts decelerating at 42 seconds and maintains the same speed as the speed of the first vehicle. The third vehicle arrives at speed of 61 mph, higher than its own desired speed of around 56 mph. Thus, the vehicle decelerates instantly but smoothly down to its desired speed. The other vehicles, the 4^{th} ~ 7^{th} vehicle accelerate after entry and cruise at their respective desired speed immediately.

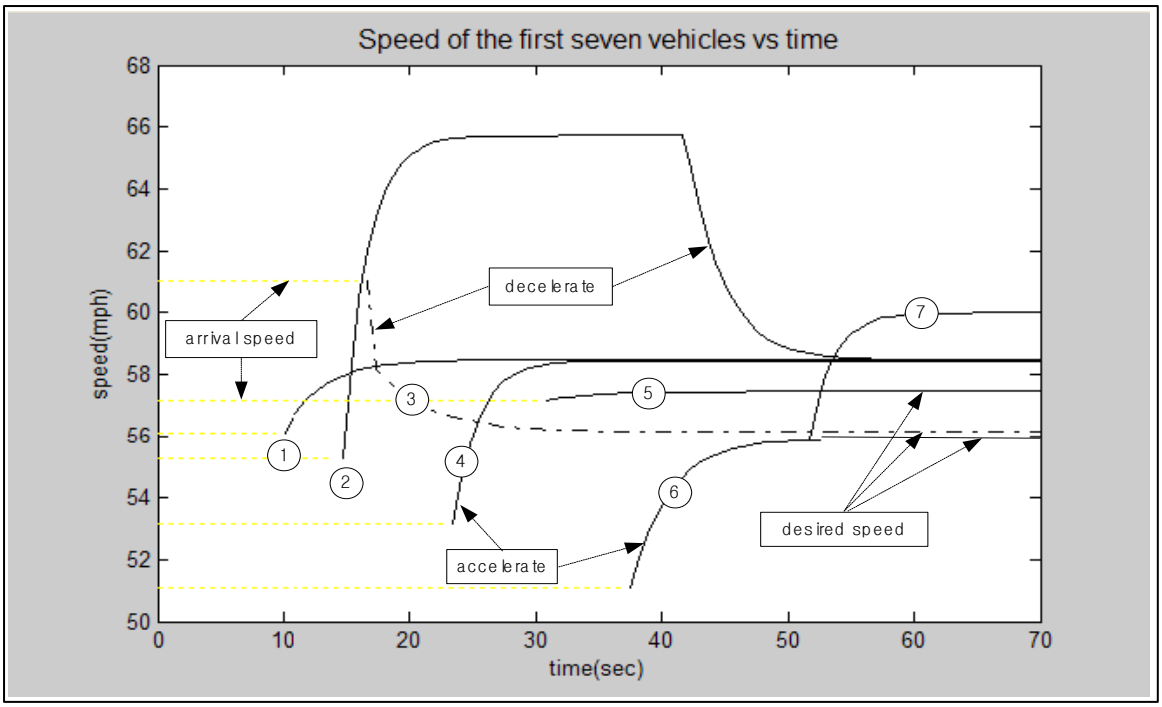

Figure 5-7 Speed trend of the first seven vehicles

Vehicle trajectory in time-space diagram

Completing the previous steps leads to the generation of a speed matrix. Using the speed matrix and a time step, each vehicle's location at each time step can be calculated. Figure 5-8 shows an example of vehicle trajectories in time-space. The x-axis represents time in seconds and the y-axis longitudinal location of the vehicle within the study segment in feet. Thus the slope of each curve represents the speed of each vehicle. The vertical gap represents the space headway between successive vehicles from front to front. In Figure 5-8, condition 1 and 2 show that a vehicle accelerates to catch up with the vehicle ahead. Condition 3 and 4 illustrate that when a vehicle completes catching up with a vehicle ahead, it begins maintaining a safe following distance relevant to the vehicle ahead. Condition 5 shows when a vehicle reaches its desired speed, and it maintains the desired speed and does not desire to accelerate. Condition at 6 represents vehicles platooned

along the study segment. Around condition 7, the spacing between two trajectory lines increases with time, because a lead vehicle with a higher desired speed is accelerating and departing away from an upstream vehicle.

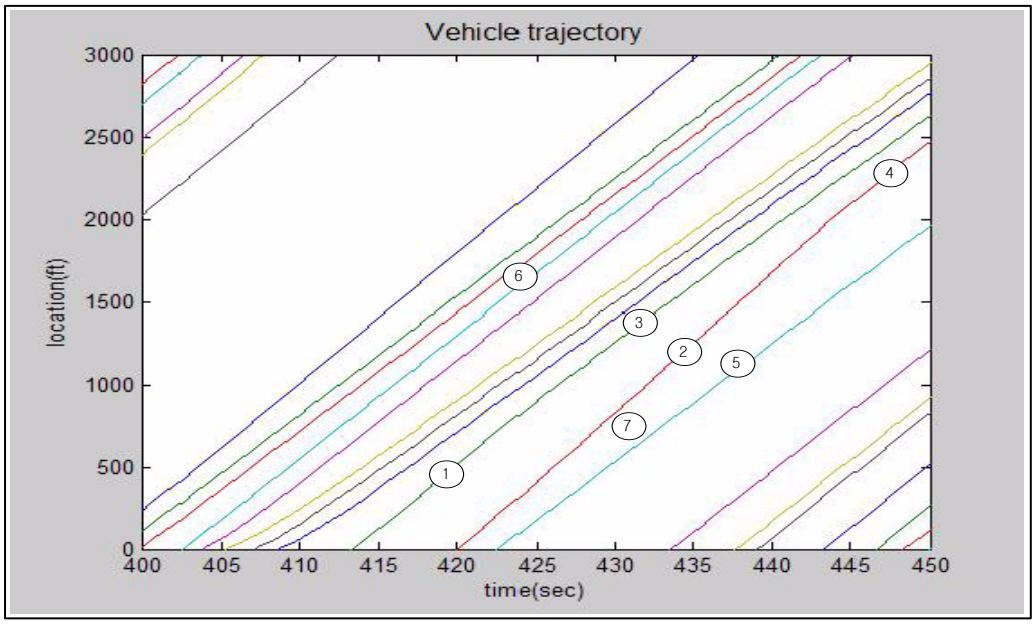

Figure 5-8 Vehicle trajectories at 400 pcph arrival demand

5.3.2 Speed-flow-density relationships

The relationships of the three variables, speed, flow, and density, are analyzed under arrival demand from 500 pcph to 2,400 pcph and average free flow speed 40 mph in base conditions.

Density and space mean speed are collected at every instant over the entire analysis period. Flow rate is obtained by multiplying the density by the space mean speed. Figure 5-9 shows the speed-density relationship. As expected, the speed decreases when density increases. The speed decreases more rapidly at a density above 60 pcpmpl (passenger car per mile per lane). The speed-flow relationship shown in Figure 5-10 follows the typical shape for uninterrupted flow with speed decreasing with flow rate. The arm at the bottom part of the curve represents forced flow. In the flow-density relationship, shown in Figure

5-11, the flow increases until the density increases up to the optimal density (around 75 pcpmpl) and then the flow decreases when the density exceeds the optimal density. The HCM 2000 does not present these relationships of speed, flow, and density for two-lane, two-way highways.

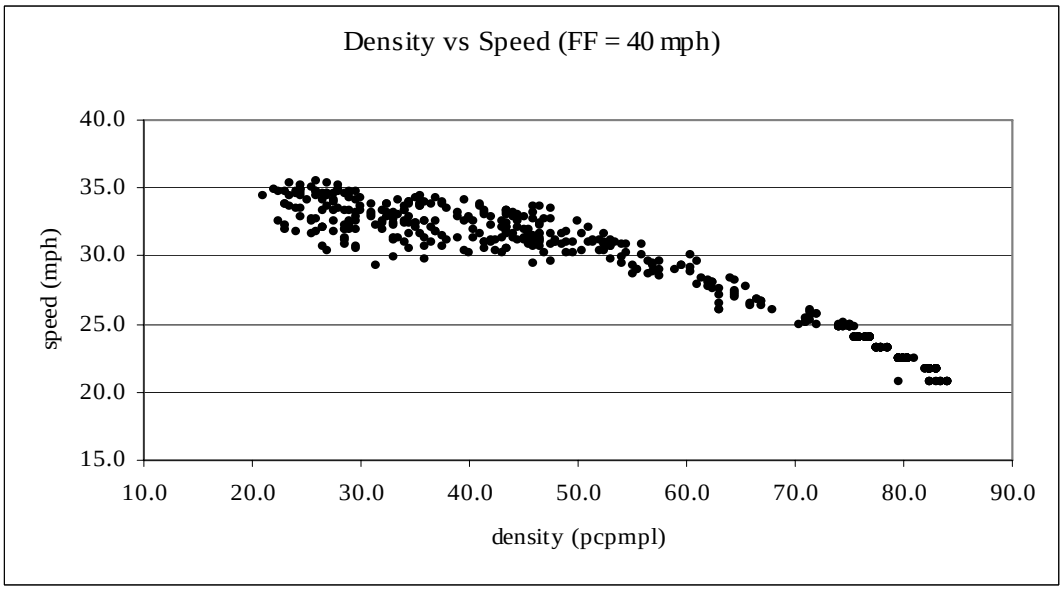

Figure 5-9 Speed vs. density

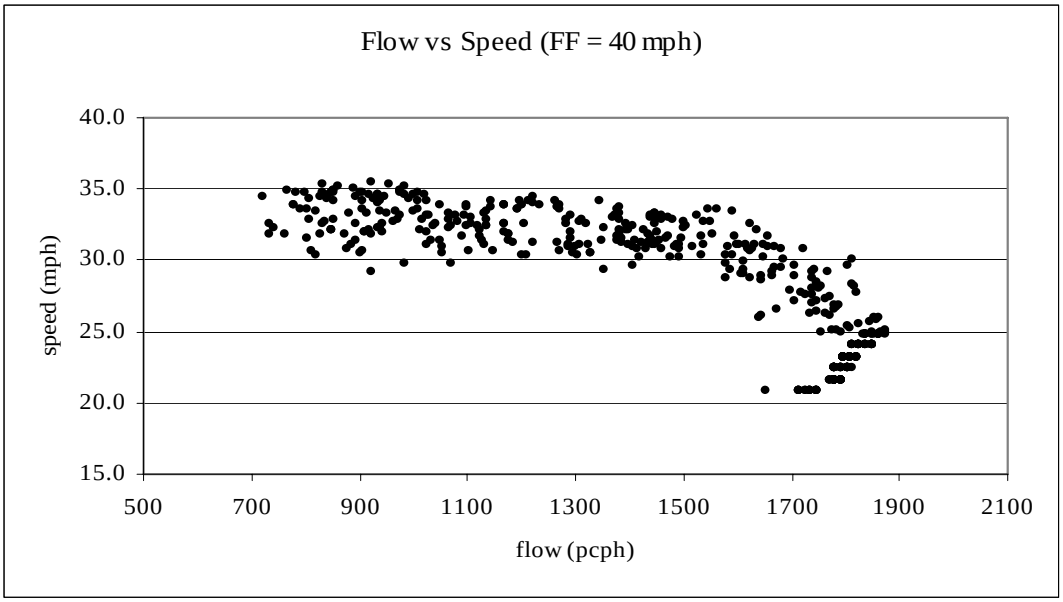

Figure 5-10 Speed vs. flow

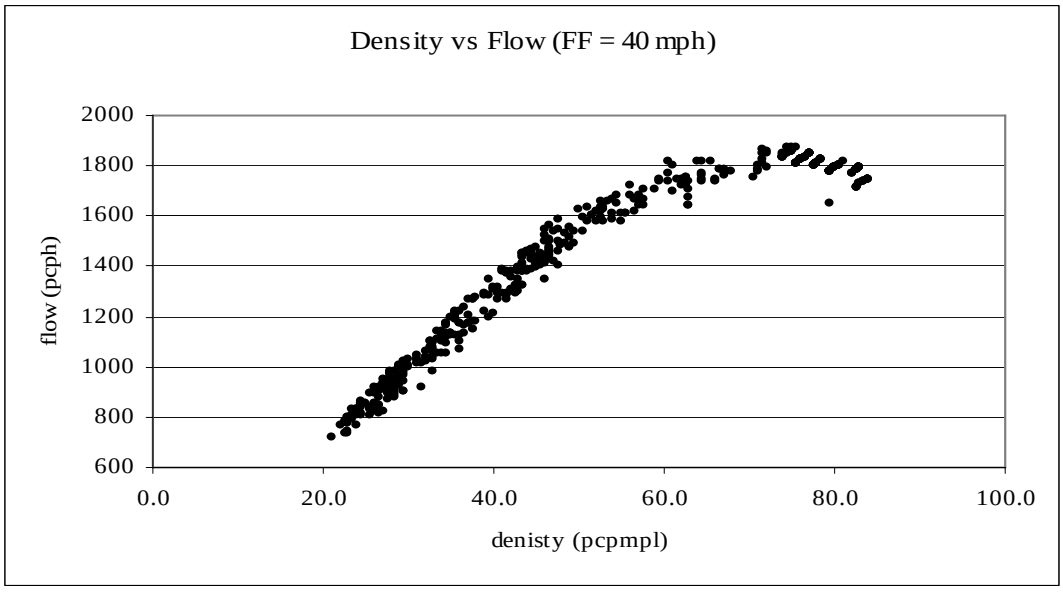

Figure 5-11 Flow vs. density

5.4 Comparison of TWOSIM I to TWOPAS and HCM 2000

For the comparison of TWOSIM I model under the given base conditions, field data should be acquired to estimate the most appropriate parameters in the simulation model. However, the base conditions are hardly ever seen in the field. Due to the unavailability of field data under the base conditions, a comparison of the basic TWOSIM I to TWOPAS and HCM 2000 under base conditions was performed. The input data for TWOPAS and HCM to achieve the same base conditions as TWOSIM I are as follows:

- TWOSIM I : Mean free flow speed 60 mph, standard deviation of desired speed 4 mph, warm-up period 5 min, analysis period 5 min, segment length 2 mile, warm-up zone 0.5 mile, 100 percent no-passing zone, 100 percent passenger cars, no driveways, shoulder width 6.0 ft, lane width 12.0 ft, primary direction volume 500 ~ 1,700 pcph by 200 pcph increment, opposing volume 500 pcph

- TWOPAS : Mean free flow speed 60mph, standard deviation of free flow speed 4mph, warm-up period 5 min, analysis period 5 min, segment length 2 mile, 100 percent no-passing zone, 100 percent passenger cars, no driveways, shoulder width 6.0 ft, lane width 12.0 ft, primary direction volume 500 ~ 1,700 pcph by 200 pcph increment, opposing volume 500 pcph
- HCM 2000 : Free flow speed 60.0 mph, directional analysis, PHF 1.0, truck and RV 0 percent, 100 percent no-passing zone, 100 percent passenger cars, no driveways, access points 0/mi, shoulder width 6.0 ft, lane width 12.0 ft, segment length 2 mile, primary direction volume 500 ~ 1,700 pcph by 200 pcph increment, opposing volume 500 pcph

Comparison analysis is performed with various combinations of directional volume. The primary directional volume varies from 500 to 1,700 pcph by 200 pcph increment, but the opposing volume is set to be 500 pcph. For the comparison, average travel speed and percent time spent following is examined. In the case of TWOSIM I and TWOPAS, each measure is obtained by running the simulation five times and getting the average value of the output. The TWOPAS algorithm can be used with IHSDM (Interactive Highway Safety Design Model, 2003). For the implementation of HCM 2000 methodology, HCS^{+} (Highway Capacity Software by McTrans, 2005) was used.

5.4.1 Comparison of average travel speed

Table 5-8 presents the average travel speed (ATS) and the absolute difference of TWOSIM I from TWOPAS and HCM. There are small absolute differences in ATS between TWOSIM I and TWOPAS ranging from 0.6 to 2.1 mph. The ATSs of TWOSIM

I are similar to those of TWOPAS for all the pairs of traffic volumes. However, the ATSs from TWOSIM I and from TWOPAS are significantly higher than that of HCM and the difference from TWOSIM I ranges from 7.5 to 12.3 mph. In HCM, the value of the ATS does not change when changing the class of highways, however the LOS (level of service) does.

Table 5-8 Comparison of average travel speed from TWOSIM I to TWOPAS and HCM

Flow rate (pcph)			ATS in primary direction (mph)			Absolute difference (mph)	
Primary	Oppos.	Sum	TWOSIM I	TWOPAS	HCM	vs. TWOPAS	vs. HCM
500	500	1,000	57.2	55.4	49.7	1.8	7.5
700	500	1,200	56	53.9	48.3	2.1	7.7
900	500	1,400	55.5	54.7	46.7	0.8	8.8
1,100	500	1,600	54.8	53.7	45.1	1.1	9.7
1,300	500	1,800	54.3	52.6	43.6	1.7	10.7
1,500	500	2,000	53.6	52.3	42.0	1.3	11.6
1,700	500	2,200	52.7	52.1	40.4	0.6	12.3

Next, the significant discrepancy in ATS between TWOSIM I and HCM was examined. TWOSIM I determines the average travel speed of the first vehicle with Equation 5-15, which was developed with field data and data from NCHRP 3-55(3) as mentioned in earlier sections:

$$ATS_d = FFS_d - 0.007\,V' - 0.003\,V'' \qquad \textbf{Eq 5-15}$$

where,

ATS_d = directional average travel speed (mph);

FFS_d = directional free - flow speed (mph);

V' = directional passenger - car equivalent flow rate (pcph); and

V'' = passenger car equivalent flow rate at opposing direction (pcph)

In addition, in TWOSIM I, the average travel speed for the entire traffic stream is obtained by collecting speeds of vehicles generated through the interactions between the vehicles in simulation.

Equation 5-16 is used for the calculation of average travel speed in HCM.

$$ATS = FFS - 0.0076\, v_p - f_{np} \qquad \textbf{Eq 5-16}$$

where,

ATS = directional average travel speed (mph);

FFS = directional free - flow speed (mph);

v_p = passenger - car equivalent flow rate for peak 15 - min period (pcph); and

f_{np} = adjustment for percentage of no - passing zones

While TWOSIM I uses directional flow rate (V', V'') for the calculation of ATS, HCM considers total traffic flow rate (v_p) for the estimation of ATS. As shown in the two equations, the difference in weight of directional volume and the inclusion of an additional adjustment factor (f_{np}) for the percent of no-passing zones in the HCM equation appear to create significant discrepancies in the two average travel speeds.

5.4.2 Comparison of percent time spent following

Table 5-9 shows that absolute difference of percent time spent following (PTSF) between TWOSIM I and TWOPAS ranges from 0.4 to 5.1 percent for various combinations of traffic flows.

Table 5-9 Comparison of percent time spent following with TWOPAS and HCM

Flow rate (pcph)			PTSF in primary direction (%)			Absolute difference (%)	
Primary	Oppos.	Sum	TWOSIM I	TWOPAS	HCM	vs. TWOPAS	vs. HCM
500	500	1,000	46.0	51.0	71.8	5.0	25.8
700	500	1,200	56.3	61.1	81.2	4.8	24.9
900	500	1,400	66.4	71.5	86.8	5.1	20.4
1,100	500	1,600	73.2	78.0	90.8	4.8	17.6
1,300	500	1,800	79.6	82.1	94.2	2.5	14.6
1,500	500	2,000	84.5	84.9	95.0	0.4	10.5
1,700	500	2,200	89.3	85.5	97.7	3.8	8.4

Taking into account the stochastic nature of the two simulation models, TWOSIM I and TWOPAS can be said to have similar trends for percent time spent following for the given traffic flow rates. However, there are significant differences in PTSF between TWOSIM and HCM, which range from 8.4 to 25.8 percent. In HCM, the value of the PTSF does not change when changing the class of highways, however the LOS does.

Since percent time spent following in TWOSIM I is produced by interactions between vehicles during simulation, it is difficult to estimate the PTSF before running a simulation with TWOSIM I. The HCM 2000 presents Equation 5-17 for calculating percent time spent following as a function of traffic flow rate and directional distribution (NCHRP 20-7, 2005):

$$PTSF_d = BPTSF_d + f_{np}\left(\frac{V_d}{V_d + V_o}\right) \qquad \textbf{Eq 5-17}$$

where,

$PTSF_d$ = percent time-spent-following in the direction analyzed;

f_{np} = adjustment for percent no-passing zones in the direction analyzed;

V_d = primary directional passenger-car equivalent flow rate, pcph;

V_0 = opposing directional passenger-car equivalent flow rate, pcph;

$BPTSF_d = 100\left(1 - \exp\left(aV_d{}^b\right)\right)$

where, $BPTSF_d$ = base percent time-spent-following in the direction analyzed;

a, b = values of coefficients used in estimating percent time spent following for directional segments; and

v_p = two-way passenger-car equivalent flow rate, pcph

As shown, two factors, primary directional flow rate and the percent of no-passing zone have an impact on the estimation of PTSF in HCM.

In consequence, TWOSIM I is shown to estimate similar ATSs to those from TWOPAS, but the ATSs are significantly different from those of HCM 2000. Similarly, TWOSIM I gives similar PTSFs to those of TWOPAS, but the PTSFs have significant discrepancy against the PTSFs from HCM 2000. In conclusion, TWOSIM I output is comparable to that of TWOPAS.

5.5 Capacity estimation and sensitivity analysis

5.5.1 Determination of observation point for the collection of capacity data

Figure 5-12 shows how hourly flow rates vary with every observation point over the entire segment in the travel direction when the arrival rate is 2,016 pcph.

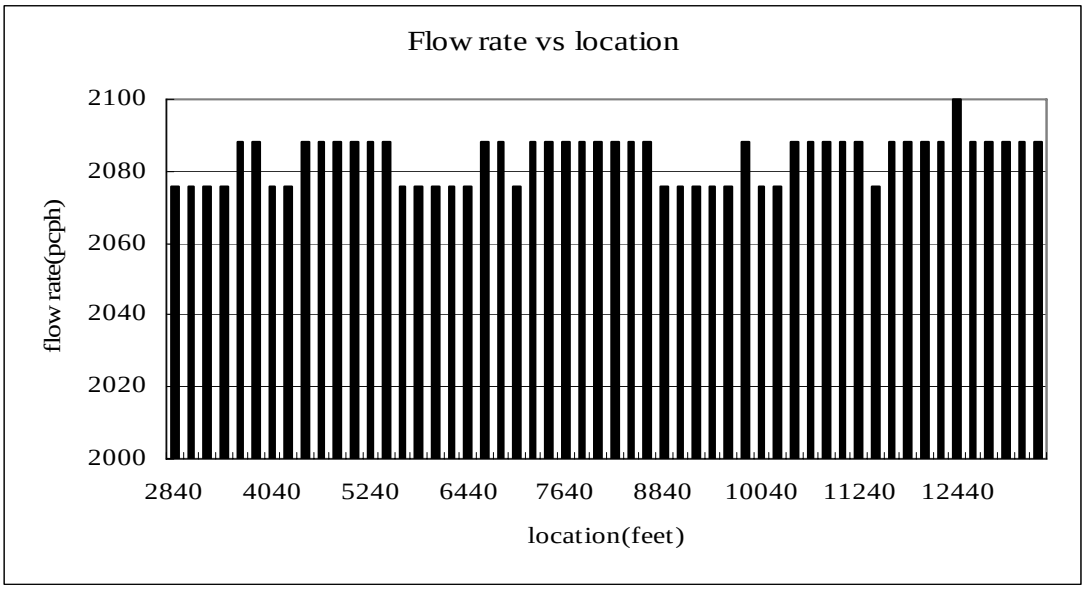

Figure 5-12 Hourly flow rate over segment

The x-axis represents each observation point over the segment every 200 feet, and the y-axis represents the hourly flow rate converted from five minute volumes from one simulation run. The figure shows that the hourly flow rates fluctuate over the entire segment and reach this highest point at 2,100 pcph. The flow rates are shown to fluctuate

over the entire segment for additional runs of simulation, which results from the interactions between vehicles.

Therefore, the exact location for collecting capacity data along two-lane highways does not seem to be important. For the estimation of capacity, the observation point in the middle of the homogeneous segment is selected, and the capacity data will be collected at this location.

5.5.2 Arrival demand and arrival rate

This section presents how capacity is estimated and what the estimated capacity is under base conditions. Prior to the explanation about how the capacity is calculated, it is necessary that two types of traffic volume be defined: arrival demand and arrival rate. Figure 5-13 illustrates the concept of arrival demand and arrival rate.

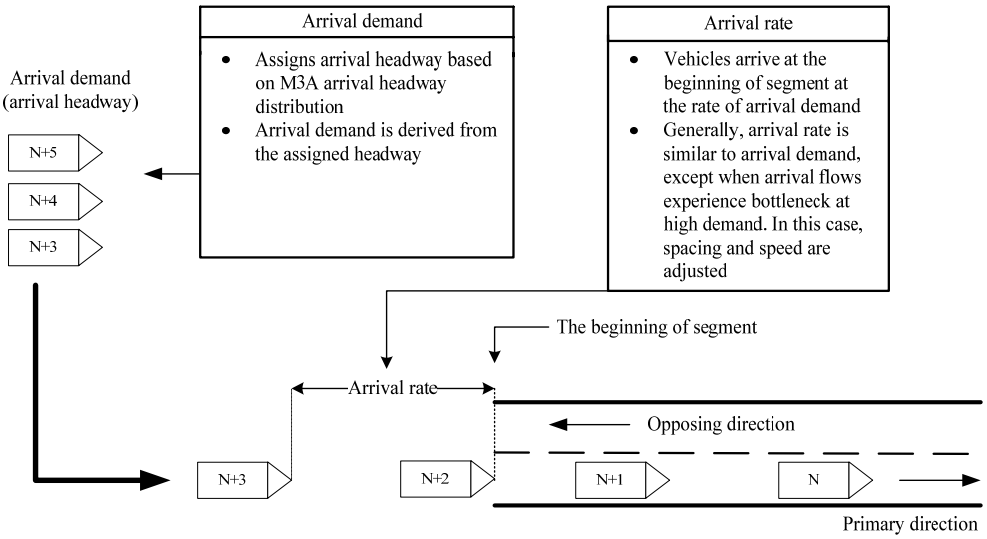

Figure 5-13 Schematic of arrival demand and arrival rate in TWOSIM I

Here, *N* represents the number of vehicles simulated. As shown in Figure 5-13, arrival demand represents the arrival headways assigned to vehicles based on the M3A headway distribution in TWOSIM I. TWOSIM I generates vehicles based on the

headway distribution and the generated vehicles arrive at the beginning of the study segment at each vehicle's own assigned headway.

Since vehicles arrive at the beginning of the study segment based on the headways in TWOSIM I, the arrival demand should be the same as the rate of arrivals, or arrival rate. However, when the arrival demand is high, speed gets lower and congestion occurs prior to arrival at the beginning of the segment. In this case, TWOSIM I adjusts the spacing between two consecutive vehicles prior to their arrival in the beginning of the segment to keep safe spacing between them. As a result, this adjustment leads to a change in the original headway assigned and ultimately makes vehicles arrive at a rate different than the arrival demand. This is the difference between arrival demand and arrival rate.

5.5.3 Estimation of capacity

When arrival demand is high, it is observed that the hourly flow rates do not exceed the given arrival demand. Therefore, capacity is defined as the average of the hourly flow rates, when the arrival demand systematically exceeds the flow rate.

As discussed earlier, an observation point in the middle of the homogeneous segment would be used to obtain capacity data. Five minute volumes observed at this location are converted into an hourly flow rate for the estimation of capacity. Among the hourly flow rates, the flow rates that are systematically less than the given arrival demand are selected and the average of them is estimated to be capacity. This section describes the procedure of estimating capacity in detail.

The hourly flow rates are collected at the selected point in the study segment with different arrival demand in the range from 1,800 pcph to 2,300 pcph and plotted in Figure 5-14. The hourly flow rates are shown to increase with arrival demand, but they stop

increasing at the range of arrival demand from approximately 2,200 to 2,300 pcph. The dotted diagonal line is the imaginary line where flow rates are equal to arrival demand. At arrival demand from 1,700 pcph to approximately 2,200 pcph, some hourly flow rates are higher and others are lower than the given arrival demand (above or below the diagonal line). The flow rates lower than the arrival demand in the same range result from randomness in the simulation. However, when arrival demand reaches above 2,200 pcph, there is no hourly flow rate higher than the given arrival demand. This represents capacity conditions. TWOSIM I estimates capacity by calculating the average of the group of flow rates (circled) less than the given arrival demand.

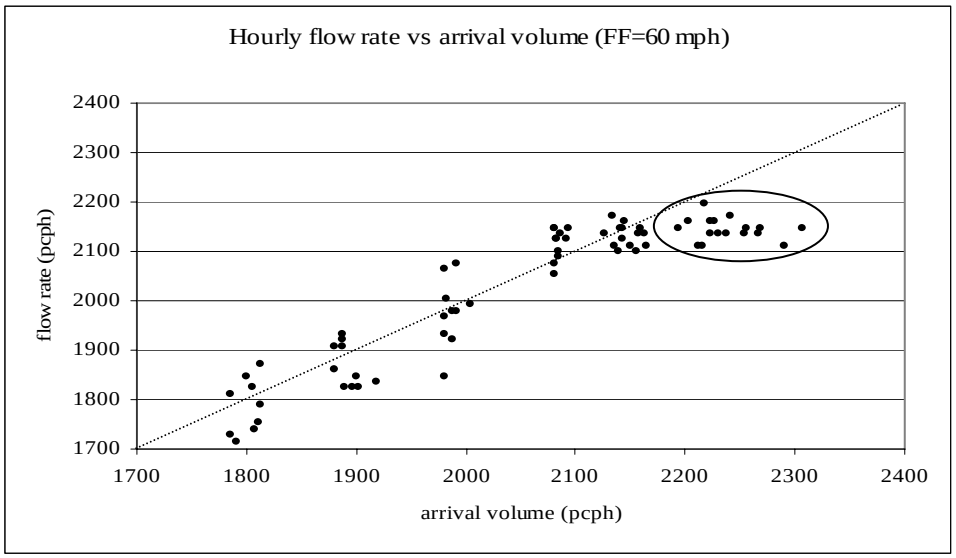

Figure 5-14 Hourly flow rates vs. arrival demand

Using these capacity data, the directional capacity of two-lane, two-way highway at an average free flow speed of 60 mph under the base conditions is estimated to be 2,100 pcph, which is 400 pcph greater than the base capacity of HCM 2000 1,700 pcph/direction.

5.6 Sensitivity analysis

A sensitivity analysis was performed to examine how capacity varies with average free flow speed, standard deviation of free flow speed, length of study segment, and delay of safety reaction time under base conditions.

5.6.1 Capacity vs. average free flow speed

Table 5-10 shows the base capacity estimated using TWOSIM I. For this analysis, TWOSIM was run ten times at each arrival demand, so a total of 70 runs of TWOSIM I were performed for all average free flow speeds to obtain these results. The base capacity ranges from 1,835 pcph to 2,141 pcph with average free flow speed. While HCM 2000 suggests a single value of capacity, it is noted that TWOSIM I produces different capacities for different average free flow speeds.

Table 5-10 Capacity vs. average free flow speed

Capacity (pcph)	Average free flow speed			
	40 mph	50 mph	60 mph	70 mph
	1,835	2,012	2,141	2,096

Statistical testing (using the *t*-test) shows that the base capacity at each average free flow speed is statistically different for each of the free flow speeds. The results of the test can be found in Appendix E.

Given that these results were obtained using simulation, the findings should be verified using field data. The changes in capacity as a function of the average free flow speed may be the result of using Gipps' car-following model, in which operating speed associated with the average free flow speed has influence on the average headway at

capacity. Hence, the use of average free flow speed as an input is likely to have an impact on capacity.

5.6.2 Capacity vs. standard deviation of desired speed

Next, it is examined how capacity varies with the standard deviation of desired speed. Table 5-11 shows that capacity decreases somewhat with an 8 mph standard deviation in desired speed. *T*-test results show there is significant difference between the capacity at the 8 mph standard deviation and the other capacities (see Appendix E for test results). Therefore, it can be concluded that the standard deviation of desired speeds has an impact on the capacity of two-lane, two-way highways. The higher standard deviation the desired speeds have, the lower the capacity is.

Table 5-11 Capacity vs. standard deviation of desired speed

Capacity (pcph)	Standard deviation of desired speed		
	0 mph	4 mph	8 mph
	2,137	2,141	2,053

5.6.3 Capacity vs. delay of safety reaction time

Next, how capacity is related to the delay of safety reaction time (theta), one of the parameters in Gipps' car-following model is examined. The delay of safety reaction time is compared at 0.07, 0.78, and 1.14 seconds, which makes the actual reaction time to be 0.75 seconds for the best driver, 1.25 seconds for normal and common expectancy, and 1.5 seconds for the reaction time for surprise intrusions. For comparison, its standard deviation is assumed to be zero. For example, if the delay of safety reaction time is set to be 0.78, then all the drivers are assumed to have 1.25 second reaction time in TWOSIM I.

Table 5-12 shows how capacity varies with different delay of safety reaction times of drivers at an average desired speed of 60 mph. The statistical test (Appendix E) shows

that there is a significant difference in capacity when the delay of safety reaction for all drivers is changed.

Table 5-12 Capacity vs. delay of safety reaction time

Capacity (pcph)	Delay of safety reaction time (sec)		
	0.07	0.78	1.14
	2,330	2,294	1,988

When all simulated drivers have shorter delay of safety reaction time (0.78), the capacity can reach 2,294 pcph. When all the drivers in TWOSIM I have normal performance, capacity reaches 2,330 pcph. If all vehicles are driven by drivers with 1.14 seconds delay of safety reaction time, the capacity is estimated to be 1,988 pcph. As shown in this result, when the driver population is more likely to consist of drivers with shorter reaction times or shorter delay of safety reaction times, the capacity is found to increase. On the other hand, when the driver population is likely to have longer reaction times or delay of safety reaction times, the capacity is lower.

5.6.4 Capacity vs. length of study segment

Table 5-13 Capacity vs. length of study segment

Capacity (pcph)	Length of study segment (mile)			
	1	2	3	4
	2,124	2,141	2,132	2,134

Table 5-13 shows how the capacity would vary with different lengths of segment. The results of statistical testing (Appendix E) show there is no significant difference among the capacities for four different lengths of segment.

5.7 Results

The results from the sensitivity analysis and capacity estimation with TWOSIM I are summarized as follows:

- The comparison of TWOSIM I and TWOPAS shows that there is no significant difference in average travel speed and percent time spent following between the two programs.
- The results of the comparison between TWOSIM I and HCM 2000 show that there is significant difference in average travel speed and percent time spent following. Similarly, there are significant differences between TWOPAS and the HCM 2000.
- The capacity under the base conditions was found to reach approximately 2,100 pcph at average free flow speeds of 60 mph and 70 mph, 2,050 pcph at 50 mph average free flow speed, and 1,800 pcph at 40 mph average free flow speed.
- The standard deviation of desired speed for two-lane, two-way highways has an impact on capacity.
- Capacity decreases when the delay of safety reaction time increases. When drivers are more likely to consist of drivers with shorter delay of safety reaction time, the capacity is inclined to increase. On the other hand, when more drivers are likely to have longer delay of safety reaction time, the capacity tends to decrease.
- The length of study segment does not have an impact on the capacity of two-lane, two-way highways, when there are no passing zones.

CHAPTER 6. TWO-LANE, TWO-WAY HIGHWAY SIMULATOR WITH PASSING ZONE (TWOSIM II)

Passing is one of the elements that should be included in the estimation of capacity of two-lane, two-way highways. TWOSIM II is an upgraded version of TWOSIM I which includes the passing algorithm.

The passing algorithm of TWOSIM II is based on a behavioral model. The behavioral model considers the nature of the gap-acceptance decision process and the perceptual cues used by drivers in the judgment of gap size (McLean, 1989). McLean introduced three hypotheses as to the stimulus perceived by drivers in making stream-crossing gap-acceptance decisions (McLean, 1989): time hypothesis, distance hypothesis, and modified-time hypothesis. When a driver judges the gap to enter the main stream, he/she perceives the time gap in the main stream based on the time hypothesis, the space gap based on the distance hypothesis, and both gaps in the modified-time hypothesis. TWOSIM II uses the modified-time hypothesis, which considers both the distance between the passing vehicle and the opposing vehicle and the travel time of the opposing vehicle depending on its speed in making a decision about safe passing.

In gap acceptance behavior, there are two types of drivers: inconsistent drivers and consistent drivers. For inconsistent drivers it is assumed that there is variability in making independent gap-acceptance decisions. On the other hand, consistent drivers reject all gaps smaller and accept all gaps larger than their own unique critical gaps (McLean, 1989). A consistent driver assumption is made in TWOSIM II.

This chapter presents essential elements and assumptions for the development of TWOSIM II, verification and comparison of TWOSIM II, sensitivity analysis, and estimation of capacity for a section with passing zones.

6.1 Development of TWOSIM II model

For modeling passing maneuvers in TWOSIM II, there are four essential elements: minimum passing sight distance, passing zone/no-passing zone, available passing sight distance, and passing behavior. Each of these are described in the following sections.

6.1.1 Minimum passing sight distance

The minimum passing sight distance presented in the 2004 Green Book is generally used for highway design. Several studies by Lieberman (1982), Glennon (1988), Sparks (1993), and Hassan (1997) have revised Lieberman's model and developed a passing model to estimate the appropriate passing sight distance. They have suggested new minimum passing sight distances that is less conservative than that of the 2004 Green Book.

According to the Green Book (2004), passing sight distance for design usage should be determined on the basis of the length needed to complete normal passing maneuvers in which the passing driver can determine whether there are potentially conflicting vehicles ahead before beginning the maneuver. The minimum passing sight distance consists of the following four distance components shown in Figure 6-1.

- d_1: distance traversed during perception and reaction time and during the initial acceleration to the point of encroachment on the left lane.
- d_2: distance traveled while the passing vehicle occupies the left lane.
- d_3: distance between the passing vehicle at the end of its maneuver and the opposing vehicle.

- d_4: distance traversed by an opposing vehicle for two-thirds of the time the passing vehicle occupies the left lane, or 2/3 of d_2 above.

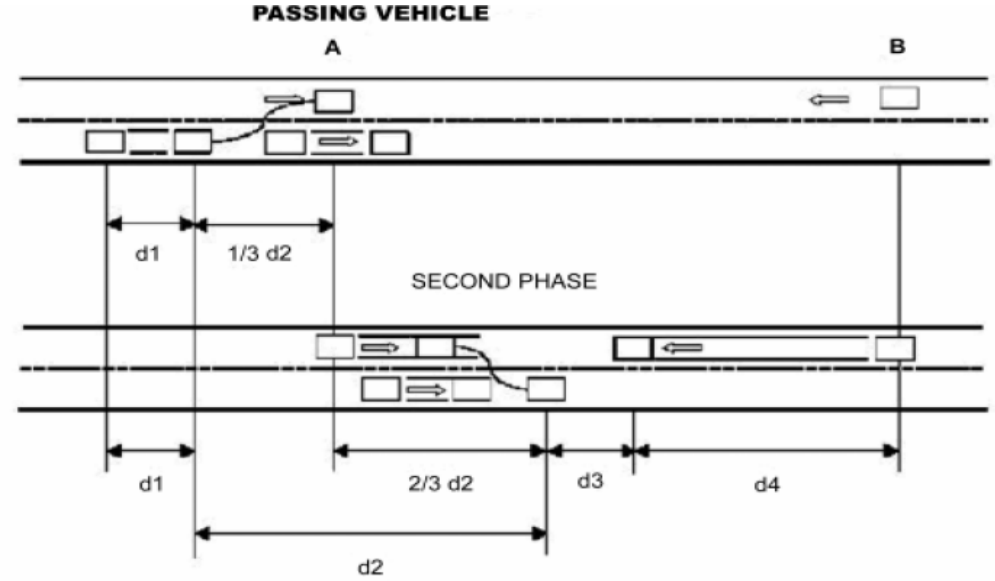

Figure 6-1 Elements of passing sight distance for two-lane highways
(source: A Policy on Geometric Design of Highways and Streets, 2004)

$$d_1 = 1.47 t_1 \left(v - m + a t_1 / 2\right)$$
$$d_2 = 1.47 v t_2$$
$$d_3 = clearance\ length$$
$$d_4 = \frac{2}{3} d_2 \qquad \textbf{Eq 6-1}$$

where,

t_1 = time of initial maneuver (sec);
a = average acceleration (mph/s);
v = average speed of passing vehicle (mph);
m = difference in speed of passed vehicle and passing vehicle (mph); and
t_2 = time passng vehicle occupies the left lane (sec)

Table 6-1 shows fundamental elements of safe passing sight distance for design of two-lane highways.

Table 6-1 Elements of safe passing sight distance for design of two-lane highways

Component of passing maneuver	Metric				US Customary			
	Speed range (km/h)				Speed range (mph)			
	50-65	66-80	81-95	96-110	30-40	40-50	50-60	60-70
	Average passing speed (km/h)				Average passing speed (mph)			
	56.2	70.0	84.5	99.8	34.9	43.8	52.6	62
Initial maneuver:								
a = average acceleration[a]	2.25	2.3	2.37	2.41	1.4	1.43	1.47	1.5
t_1 = time (sec)[a]	3.6	4.0	4.3	4.5	3.6	4	4.3	4.5
d_1 = distance traveled	45	66	89	113	145	216	289	366
Occupation of left lane:								
t_2 = time (sec)a	9.3	10.0	10.7	11.3	9.3	10	10.7	11.3
d_2 = distance traveled	145	195	251	314	477	643	827	1030
Clearance length:								
d_3 = distance traveled	30	55	75	90	100	180	250	300
Opposing vehicle:								
Total distance, $d_1+d_2+d_3+d_4$	97	130	168	209	318	429	552	687
	317	446	583	726	1040	1468	1918	2383

[a] For consistent speed relation, observed values adjusted slightly.

Note: In the metric portion of the table, speed values are in km/h, acceleration rates in km/h/s, and distances are in meters. In the U.S. customary portion of the table, speed values are in mph, acceleration rates in mph/sec, and distances are in feet.

Source: Exhibit 3-5, pp. 120. A Policy on Geometric Design of Highways and Streets, 2004. American Association of State Highway and Transportation Officials.

Passing sight distance increases as speed goes up. The clearance length against the opposing vehicle when passing is completed ranges between 100 to 300 feet. TWOSIM II uses the minimum passing sight distance suggested by the Green Book because it is used for highway design and also because it is relatively straightforward to implement in a simulator.

6.1.2 Passing zone and no-passing zone

Passing zones and no-passing zones are specified to allow or prohibit passing in each direction of a given study segment. The Manual on Uniform Traffic Control Devices (MUTCD, 2003, pg. 3B-5) specifies “where the distance between successive no-passing zones is less than 120 m (400 ft), no-passing markings should connect the zones.” The MUTCD presents minimum passing sight distances with speed limit as shown in Table 6-

2. The minimum passing sight distance increases with the speed limit. Therefore, the length of passing zone specified as input data in TWOSIM II should satisfy the minimum passing sight distance depending on the posted speed limit.

Table 6-2 Minimum passing sight distance (2003 MUTCD)

85^{th} percentile or Posted or Statutory speed limit (mph)	Minimum passing sight distance (feet)
25	450
30	500
35	550
40	600
45	700
50	800
55	900
60	1,000
65	1,100
70	1,200

Source: Table 3B-1, pp. 3B-9. 2003 Edition MUTCD. Federal Highway Administration.

6.1.3 Available passing sight distance

Available passing sight distance is defined as the sight distance available to a driver attempting to pass at a given location and time during the simulation. TWOSIM II estimates the available passing sight distance of a driver considering overtaking a slower lead vehicle. This chapter deals only with level and tangent sections and the available passing sight distance is always provided to a driver considering passing.

6.1.4 Passing behavior

TWOSIM II's passing behavior is assumed to follow the concept for the safe passing sight distance in the 2004 Green Book. The assumptions in the Green Book are as follows:

- The overtaken vehicle travels at uniform speed.

- The passing vehicle decelerates and trails the overtaken vehicle when it enters a passing section.
- When the passing section is reached, the passing driver needs a short period of time to perceive the clear passing section and to react to start his or her maneuver.
- Passing is accomplished under what may be termed a delayed start and a hurried return in the face of opposing traffic. The passing vehicle accelerates during the maneuver, and its average speed during the occupancy of the left lane is 15 km/h [10 mph] higher than that of the overtaken vehicle.
- When the passing vehicle returns to its lane, there is a suitable clearance length between it and an oncoming vehicle in the opposing lane.

6.1.5 Assumptions of TWOSIM II

TWOSIM II's passing model consists of the assumptions of safe passing sight distance in the 2004 Green Book. The model is built using the following assumptions, in two stages: 1st stage - determine to pass, 2nd stage – passing.

6.1.5.1 1st Stage (Determine to pass)

The stage for determining to pass consists of two steps: considering passing and deciding to pass. Although a driver desires to overtake, if there is no available passing sight distance or gap, the driver has to decide against overtaking. Therefore, at the first step, a driver desiring to pass has to consider if all the circumstances provide appropriate conditions for safe passing. The circumstances for considering passing are as follows:

- When a vehicle is following a slower lead vehicle within a 3 second headway, the driver in the following vehicle is assumed to consider passing.

- The length of passing zone available should be equal to or greater than d_1+d_2 (Figure 6-1 and 6-2).
- The desired speed of a driver wishing to pass should be 5 mph greater than that of the slower lead vehicle. Also, the desired speed of the slower lead vehicle should be lower than that of a vehicle ahead of it.

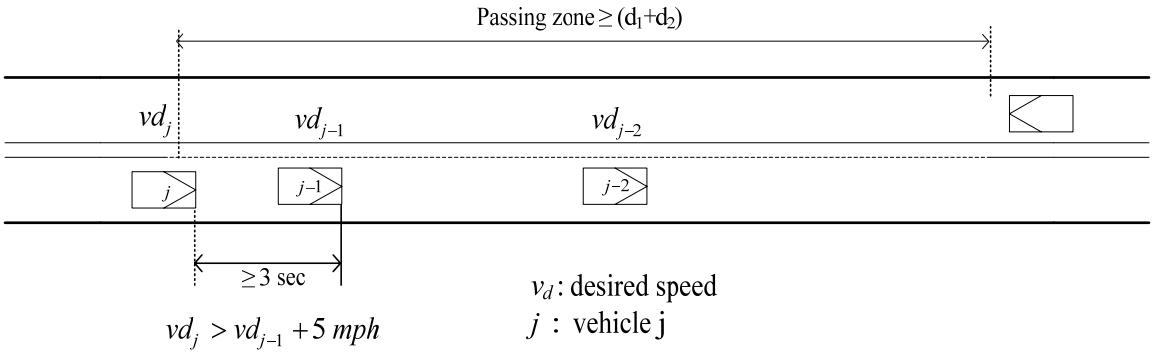

Figure 6-2 Circumstances when a driver considers passing

Then, a driver is assumed to determine to pass under the following circumstances:

- The distance between the oncoming vehicle in the opposing lane and the subject vehicle (*j* in Figure 6-3) considering passing should be greater than the minimum passing sight distance.
- There must be a gap between the slower lead vehicle (*j-1* in Figure 6-3) and the vehicle ahead of it (*j-2* in Figure 6-3) large enough for a passing vehicle to return to the right lane after passing. The time headway between the two is assumed to be longer than 5 seconds.
- A vehicle is located in the analysis zone during the analysis period. The following vehicle should be located in the passing zone
- Passing more than one vehicle at a time is not allowed.

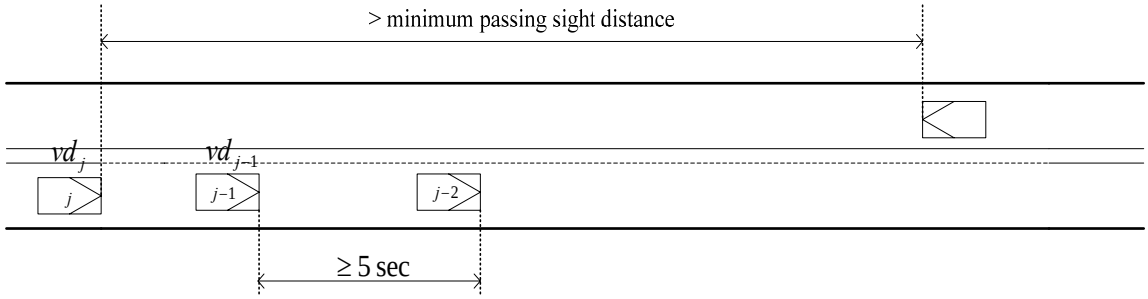

Figure 6-3 Circumstances when a driver determines to pass

6.1.5.2 2nd Stage (Passing)

Acceleration rate in passing

When a driver determines to pass as described in the previous stage, the vehicle initiates passing in TWOSIM II. While a driver is passing a vehicle, the driver should accelerate to higher speed than the speed of the passed vehicle. It then passes the vehicle and returns to the right lane. This section describes how TWOSIM II models the acceleration rate of a vehicle when passing.

Lieberman (1982) developed a simplified acceleration formula for calculating acceleration of a vehicle in passing, so that the formulation can still retain the dependence of acceleration on vehicle speed as shown in Equation 6-2:

$$\bar{a} = a_{\max}\left\{1 - \left[\left(v + m/2\right)/v_{\max}\right]\right\} \qquad \textbf{Eq 6-2}$$

where,

$\bar{a}$ = average acceleration (ft/s^2);

a_{max} = maximum acceleration achievable at zero speed (ft/s^2);

v = speed of passed vehicle (ft/s);

m = speed difference, passing versus impeder vehicles, at critical position (mph); and

v_{max} = maximum speed achievable at zero acceleration (ft/s)

The formulation explains what acceleration rate a vehicle can have at average speed while a vehicle is passing. The numerator ($v+m/2$) represents an average speed between the speed at the beginning of the passing maneuver (v) and the target highest speed ($v+m$) at the end of the passing maneuver. Therefore, the resulting acceleration is the average of acceleration rates that a vehicle achieves in passing from the initial speed to the highest speed at the end of passing. The average acceleration rate is applied to calculate speed at each time step while passing is undertaken.

The equation requires the difference (m) between the speed of passed vehicle and the highest speed of the passing vehicle. The maximum passing speed is limited so that the maximum speed is not 15 mph higher than his/her own desired speed. The speed difference between the passed vehicle and the passing vehicle is assumed to range between 10 mph and 15 mph.

The updated maximum speed of passenger cars used in TWOPAS is presented in NCHRP 3-55(3) (1998) as shown in Table 6-3.

Table 6-3 Updated passenger car performance characteristics in TWOPAS

TWOPAS Vehicle Type	Percent of Passenger Car population	Original Maximum Acceleration (ft/sec^2)	Updated Maximum Acceleration (ft/sec^2)	Original Maximum Speed (ft/sec)	Updated Maximum Speed (ft/sec)
9	10.0	9.277	11.17	109.14	112.8
10	15.0	9.766	11.99	114.89	117.8
11	20.0	10.089	12.77	118.69	121.1
12	25.0	10.429	13.22	122.69	127.0
13	30.0	11.281	14.10	131.78	142.7

Source: Table 5.9:3, pp. 41. TWOPAS Model Improvements, 1998.

TWOSIM II applies the highest maximum speed, 142.7 ft/s (97.3 mph) which has the highest usage, to be the maximum speed in calculating the acceleration rate when passing.

Additional assumptions in passing and completion of passing

When passing is in progress, the passed vehicle, the following vehicle behind the passing vehicle, and the oncoming vehicle in the opposing lane are assumed to maintain their speed.

Passing is completed when the distance from the front of passing vehicle and the front of passed vehicle is longer than or equal to three or four times the effective size of the passing vehicle. In Figure 6-4, when a passing vehicle (*j*) is three or four times the length of effective size ahead of the passed vehicle (*j-1*), the passing vehicle returns to the right lane and completes passing. Aborting the passing maneuver is not allowed in TWOSIM II, and the opposing traffic is not allowed to pass.

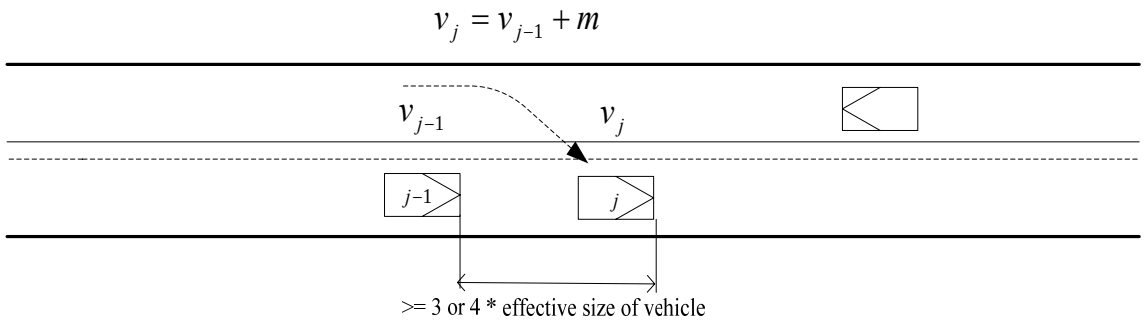

Figure 6-4 Completion of passing

6.1.6 Implementation of the passing algorithm

6.1.6.1 Modeling vehicles in the opposing lane

Opposing vehicles are modeled with the same methodology as the vehicles in the primary direction. A 0.5 mile warm-up zone and a 2 mile study section are assumed in the simulation. The beginning of the section for the opposing lane is 2×0.5+2 miles = 15,840 feet, which is the end of the primary direction. Therefore, every vehicle in the opposing

lane enters the simulation at the 15,840 feet location. As each vehicle in the opposing lane travels, its location expressed numerically decreases.

6.1.6.2 Modeling passing vehicles

Vehicle status

In addition to the assumptions presented above in TWOSIM II, the status of each vehicle relative to passing is monitored and recorded. The specification of vehicle status enables TWOSIM II to collect statistics associated with passing maneuvers as an output. The status of each vehicle in the primary direction is defined as follows:

- 0: vehicle travels in the primary lane normally or considers passing.
- 1: vehicle decides to pass and initiates passing at travel lane.
- 2: vehicle is passing at opposing lane.
- 3: passing vehicle returns to primary lane and completes passing.
- 5: opposing vehicle is facing oncoming passing vehicle on the way in appropriately safe distance.

Vehicle status 0 is possible for vehicles in both directions. Vehicle status 1 to 3 is given only to passing vehicles and vehicle status 5 is given only to opposing vehicles.

The length of the passing zone is calculated and built in a lookup table in TWOSIM II so that the length of the passing zone available can be calculated in the study segment, particularly whenever a vehicle is considering passing and requires the estimation of the passing zone length.

Speed difference

In determining the AASHTO passing sight distance (Equation 6-1) as well as the average acceleration of passing (Equation 6-2), there is one element that affects minimum passing sight distance and that is the speed difference (m) between the speed of the passing vehicle and the speed of the passed vehicle. The 2004 Green Book indicates it should not be less than 10 mph. Therefore, TWOSIM II uses the speed difference randomly in the range of 10 to 15 mph.

Interaction between primary traffic and opposing traffic

The traffic in the opposing lane and the primary lane is simulated simultaneously at every time step during the entire simulation period. Since every vehicle over the entire segment is considered at every time step, a passing event can occur at any moment or at any location as long as the passing condition is satisfied. The TWOSIM II code can be found in Appendix B.

6.1.7 Verification of TWOSIM II

6.1.7.1 Opposing vehicles

First, the movement of opposing vehicles is verified. As mentioned earlier, the opposing vehicles are modeled in the same way as the primary traffic. The only difference is the beginning of the study segment for opposing vehicles is equal to the end of the study segment for primary traffic.

Figure 6-5 shows the trajectories of opposing vehicles and primary vehicles together. The primary traffic volume is 1,200 pcph and the opposing traffic volume is 200 pcph. More dense trajectories going upward represent primary traffic at a higher rate, and the

less dense trajectories downward represent the opposing traffic at 200 vph. The opposing traffic is shown to start traveling at 15,840 feet and their location reduces as they travel.

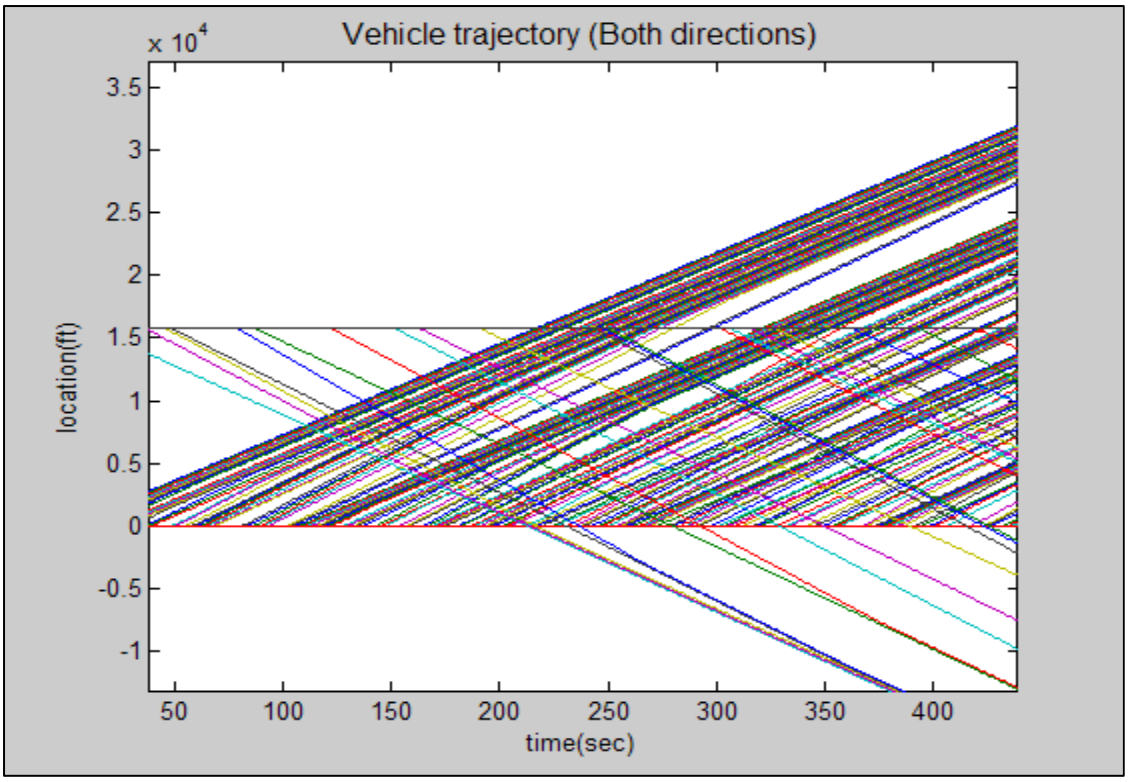

Figure 6-5 Trajectories of vehicles in both directions

6.1.7.2 Passing trajectories

Next, to verify that the passing maneuvers are executed as programmed in TWOSIM II, a graphic output of individual passing activity was examined. Figure 6-6 shows the trajectory of a passing vehicle for which passing starts at 301 sec and ends at 312 sec. Along the x-axis, two solid vertical lines were drawn to indicate time points of time when the driver starts considering passing and when he/she completes passing. The horizontal gap between the two vertical lines represents the passing time, which is approximately 12 seconds. Two horizontal lines along the y-axis represent the location where passing is

considered and completed. The vertical gap between the two horizontal lines represents passing distance, which is approximately 1,250 feet.

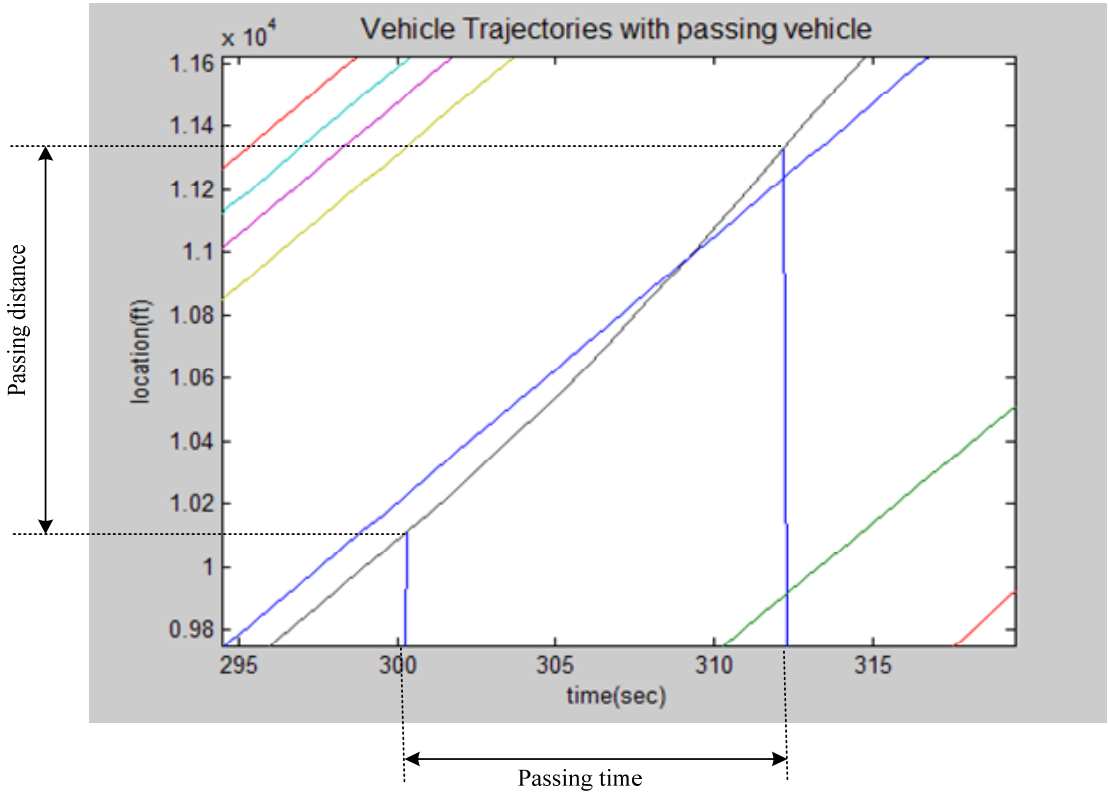

Figure 6-6 Trajectory of passing vehicle

Figure 6-7 shows the trajectories of passing vehicles and opposing vehicles, and primary traffic together. The vertical distance along the y-axis between the opposing vehicle and passing vehicle represents clearance when passing is completed. This distance is an important element to verify whether TWOSIM II implements the passing maneuver safely. There are some vehicles following the slower lead vehicle, which do not attempt to pass even if there are adequate gaps.

6.1.7.3 Minimum clearance between opposing vehicle and passing vehicle

Through the process of verification using graphical output, it was found that the passing vehicle was too close to the opposing vehicle. This limited clearance occurred because

the decision about attempting to pass was made simply by the distance calculated by the criteria in AASHTO's Green Book without considering the clearance against the opposing vehicle when passing is completed. The distance criteria in considering passing does not guarantee safe execution of the passing maneuver particularly in cases when the opposing vehicle travels at high speed.

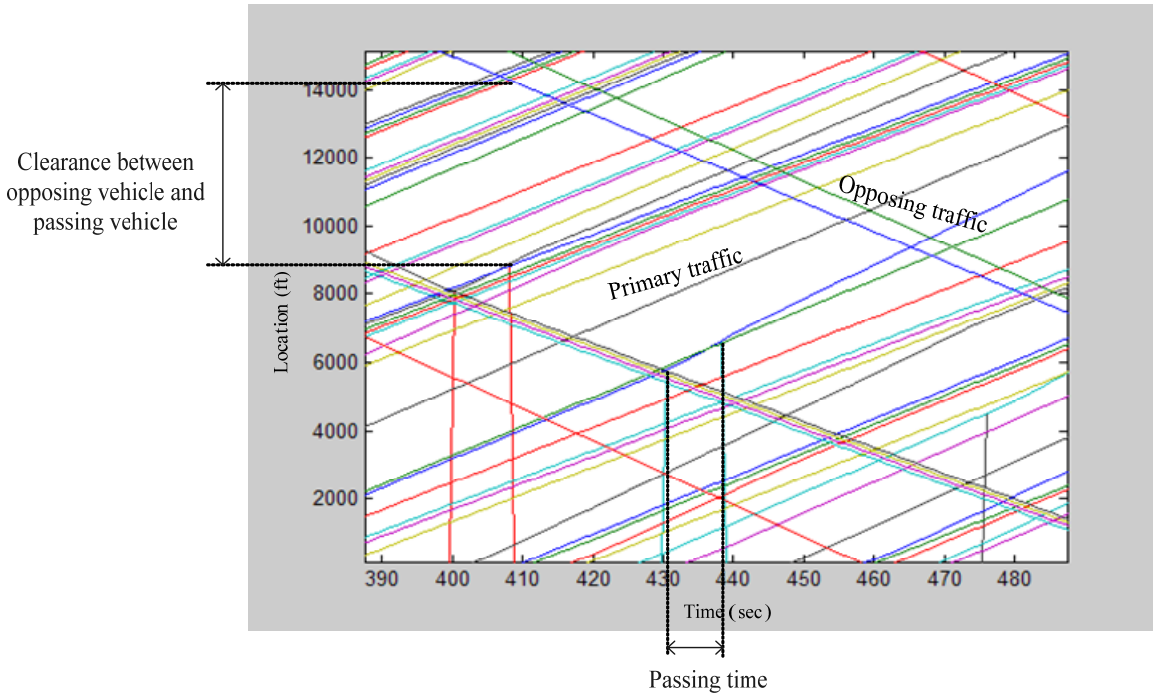

Figure 6-7 Trajectories of passing vehicle and opposing vehicle

Therefore, it is necessary to include another criterion to reflect the speed of opposing vehicles or the travel time of the opposing vehicle while passing is executed.

To achieve a safe passing maneuver, the travel time of the opposing vehicle during passing is considered. The estimated clearance should be greater than the clearance (d_3) presented in the Green Book's passing sight distance formula so that passing can be executed safely without a risk of collision. Figure 6-8 illustrates the concept.

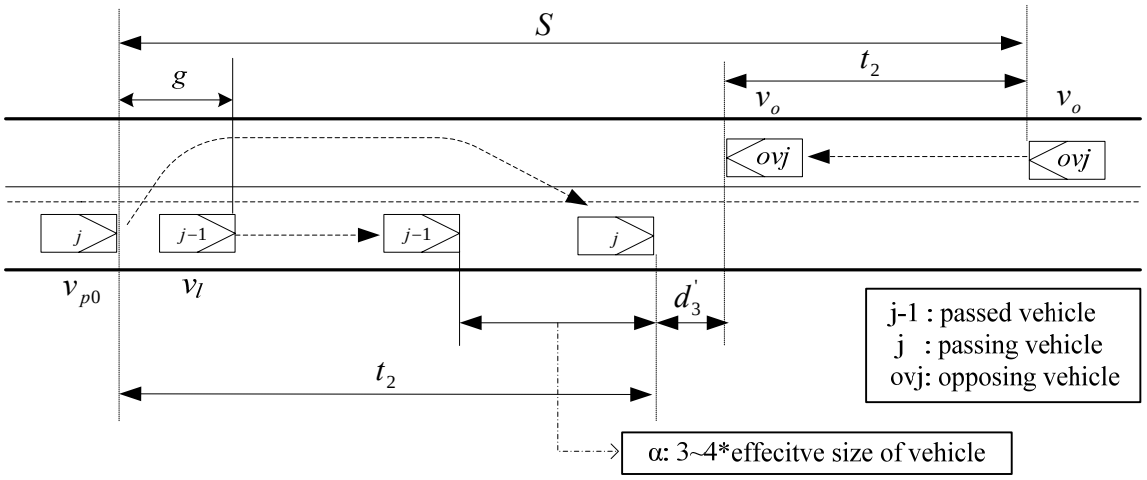

Figure 6-8 Consideration of travel time of opposing vehicle

Parameter d_3 (Equation 6-1) in the Green Book is defined as the distance from center to center of each car. Parameter d_3' represents the clearance distance from head to head of each vehicle, which is always smaller than d_3.

In Figure 6-8, time, t_2 is the duration of travel on the right lane. During t_2, the opposing vehicle travels over a certain distance, which depends on the speed of the opposing vehicle. The clearance between the opposing vehicle and the passing vehicle at this moment can be expressed as d_3' (Figure 6-8).

The concept is expressed by Equation 6-3~4. The clearance distance when passing is completed should be equal or greater than the d_3 suggested by AASHTO.

$$S - (g + v_l t_2 + \alpha s + d_3' + v_o t_2) \geq d_3 \qquad \textbf{Eq 6-3}$$

where,

S = distance between opposing vehicle and passing vehicle when passing is commenced, (ft);

g = distance between the bumper of passed vehicle and the bumper of passing vehicle, (ft);

v_l = speed of passed vehicle, (ft/s);

v_0 = speed of opposing vehicle, (ft/s);

t_2 = time for passing at left lane or time for opposing vehicle to travel from commencement of passing to the completion of passing, (sec);

d'_3 = clearance between the bumper of opposing vehicle and the bumper of passing vehicle when passing is completed, (ft);

d_3 = clearance in AASHTO PSD, (ft)

a = acceleration rate in passing, (ft/s^2);

s = effective size of vehicle, (ft); and

α = multiplier to the effective size of vehicle, (3~4)

t_2 is given by the following equation:

$$t_2 = \frac{\left(v_1 - v_{po}\right) \pm \sqrt{\left(v_1 - v_{po}\right)^2 + 2a\left(g + \alpha s\right)}}{a} \qquad \textbf{Eq 6-4}$$

where,

v_{p0} = speed of passing vehicle, (ft/s)

The equation calculates the clearance between two vehicles when passing is completed, considering the time for passing and the opposing vehicle's speed.

6.1.7.4 Clearances when passing is completed

Clearances between the opposing vehicle and the passing vehicle when passing is completed are examined to consider how the simulator replicates clearance distances. Each run of TWOSIM II generates a clearance distance for each passing maneuver executed. The clearance distances are plotted in Figure 6-9. It shows that all the clearances are distributed above approximately 100 feet. Therefore, passing is executed safely in TWOSIM II.

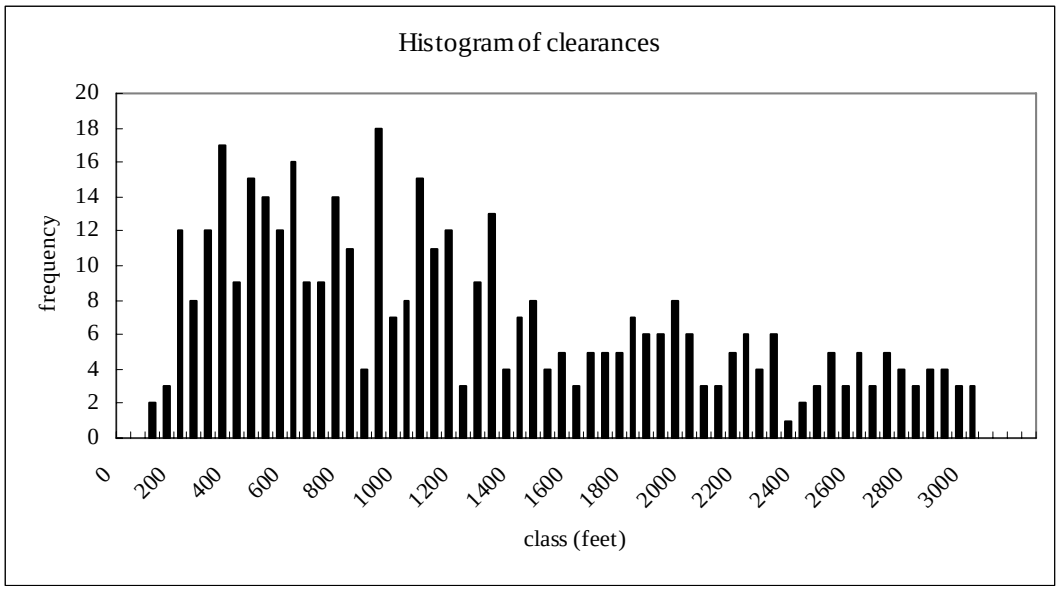

Figure 6-9 Histogram of clearance distances

6.2 Comparison to the findings from other studies

Comparison to findings from other studies is conducted to evaluate the operational performance of TWOSIM II with passing activities on two-lane, two-way highways. Passing time and passing rate from TWOSIM II are compared with the field data from other studies.

6.2.1 Comparison of passing time

Comparison of the time for executing a passing maneuver in TWOSIM II with passing time published in the 2004 Green Book and other studies is made to evaluate the performance of the simulator.

The passing time in TWOSIM II represents the travel time of a passing vehicle from when passing is initiated to when passing is completed. Table 6-4 shows average passing time in TWOSIM II by speed range. The passing time increases with the speed range.

The average passing time over the entire speed range is obtained to be 10.7 seconds and the standard deviation is 2.6 seconds.

Table 6-4 Statistics of passing time in TWOSIM II

Speed range	40~50 mph	50~60 mph	60~70 mph	Overall
Average	10.2	11.5	14.0	10.7
Standard deviation	1.6	1.8	2.5	2.6

This value for mean passing time was compared to those measured in previous research. According to McLean (1989), Troutbeck (1981) found average passing time ranges between 9.2 and 10.6 seconds in the speed range, 60~80 km/h.

More recently, Polus, et al. (2000) evaluated the passing process on rural two-lane, two-way highways by videotaping six tangent two-lane highway sections from high vantage points and from a helicopter hovering above one site. This study indicates the average passing time is 10.87 seconds and its standard deviation is 3.40 seconds (Polus, et al., 2000, Table 1). Based on these statistics from the estimate, the passing time in TWOSIM II is consistent with the previous empirical studies.

6.2.2 Comparison of passing rate

Next, the average passing rate in TWOSIM II is compared to that in other studies. The average passing rate during a five minute analysis period in ten iterations is presented at the third column of Table 6-5 and converted into a 60 minute passing rate in the fourth column. There are 101 passing maneuvers executed in an hour for a volume of 600 pcph and 200 pcph in the primary and opposing direction volumes respectively. The passing rate increases when the primary volume increases up to 1,200 pcph. It decreases when the primary volume exceeds 1,200 pcph.

The percent of passing vehicles among the total traffic volume in the primary direction also increases when the primary volume increases up to 800 pcph. It decreases when the primary direction volume exceeds 800 pcph.

Table 6-5 Passing rates in TWOSIM II (Free Flow Speed: 60mph)

Directional Traffic volume (pcph)		Passing rates (number of passes/1.6mile)		Percent of passing (%) (a / b×100 %)
Primary (a)	Opposing	5 min	60 min (b)	
600	200	8.4	101	16.8
800	200	11.4	137	17.1
1000	200	13.2	158	15.8
1200	200	14.3	172	14.3
1400	200	12.6	151	10.8
1600	200	11.5	138	8.6

NCHRP 3-55(3) (1998, pp. 32) indicates the data on passing rate are very scarce. In the field, it is difficult to measure passing time. Although there are passing rates measured in the field through the existing studies according to McLean (1989, pg. 295~296), the data are still limited and they show a conflicting trend. Therefore, it is difficult to derive a consistent trend from the values for the comparison with the passing rates from TWOSIM II. In consequence, these empirical values cannot be adequately compared to the passing rates from TWOSIM II.

6.3 Estimation of capacity

The capacity of two-lane, two-way highways is estimated using TWOSIM II. Every input is the same as that used in TWOSIM I except for the presence of passing zones and the interactions between directional traffic. Capacity is estimated with 20 percent no-passing zones under base conditions.

Since the total length of the study segment is 2 miles, the length of the passing zone is 1.6 miles with 0.2 miles of no-passing zones at each end. Figure 6-10 shows the hourly flow rates observed in the middle of the segment as a function of arrival demand.

The capacity is obtained to be 2,109 pcph at an average free flow speed 60 mph. This is estimated as the average of hourly flow rates, which do not exceed the given arrival demand. This estimated capacity is identical to the capacity in TWOSIM I where no passing zones were present. The result implies that the presence of a 20 percent no passing zone does not have an impact on the capacity of two-lane, two-way highways. This may be because the high traffic flow in the primary direction does not provide any gaps for passing.

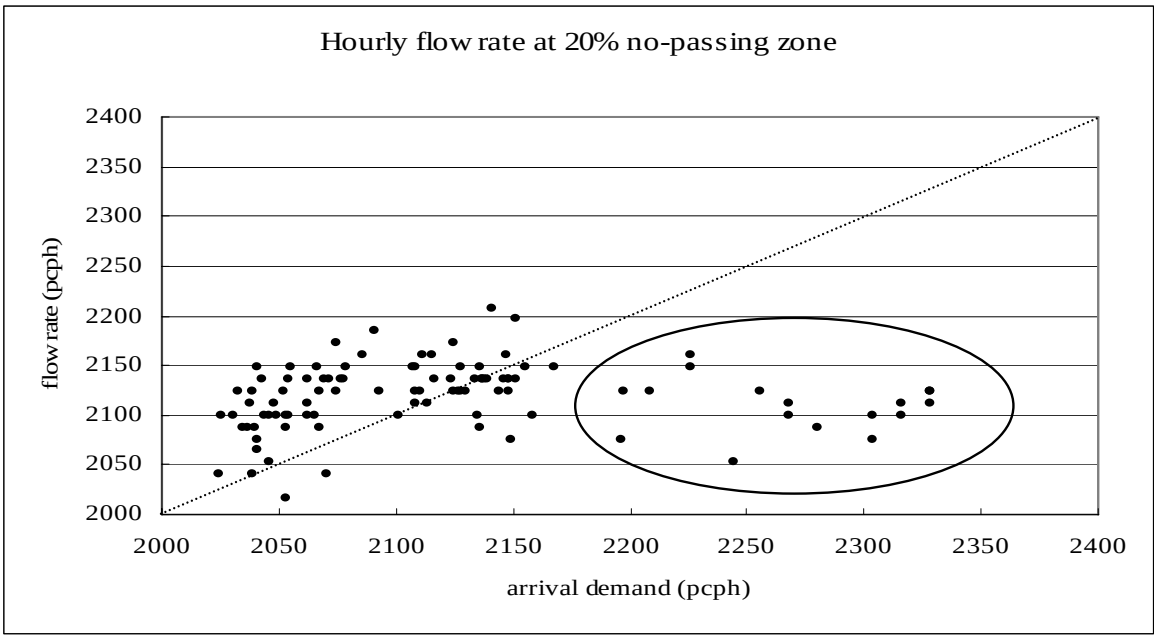

Figure 6-10 Hourly flow rates at 20 percent no-passing zone

To verify the unavailability of passing gaps at a high traffic level, an experiment was conducted with a lower arrival demand (1,700 pcph) to examine whether there is a significant increase in the flow rate downstream with the presence of a passing zone. This

experiment was conducted using constant arrival demand and 30 runs of simulations for two cases: 20 percent no-passing zones and 100 percent no-passing zones.

Average flow rates for the 30 runs are plotted by location in the travel direction in Figure 6-11. The figure shows the average flow rates under 20 percent no-passing zones are somewhat higher than the flow rates under 100 percent no-passing zones over most of the study segment. The average flow rate in the middle of the study segment under 20 percent no-passing zones is 1,780 pcph and that under 100 percent no-passing zones is 1,740 pcph. The null hypothesis that there is no difference between two means was rejected because *p*-value was 0.0053 (Appendix E). The result shows there is a statistically significant difference between the two means. Therefore, it is concluded that the presence of a passing zone has increasing impact on traffic flow rate when traffic flow is not at capacity conditions. Since the passing vehicles fill up the larger gaps downstream of the slower vehicles, the flow rates under 20 percent no-passing zones are shown to be slightly higher.

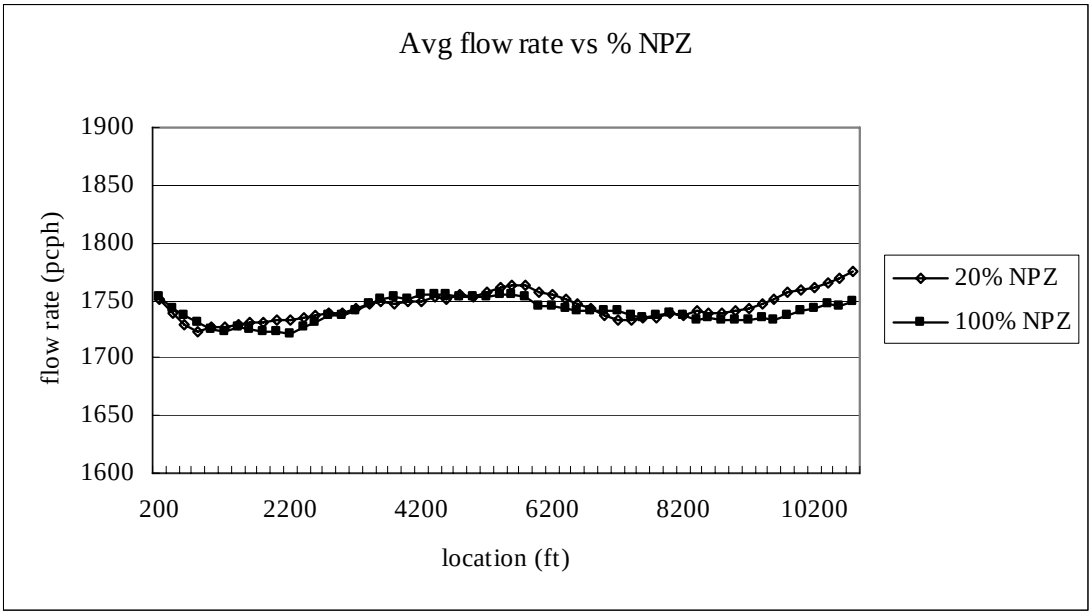

Figure 6-11 Avarage flow rates under 20 percent no-passing zones vs. 100 percent no-passing zones

Average travel speed is also found to be significantly different between the two cases (*p*-value: 5.5e-6, Appendix E). The average travel speed when a 20 percent no-passing zone is present is 1 mph higher than that of a segment with 100 percent no-passing zone.

In consequence, it is found that the presence of a passing zone results in better operating conditions at flow rates below capacity, but does not increase the capacity of the section.

6.4 Sensitivity analysis

A sensitivity analysis was performed to evaluate how passing rate varies with different combinations of traffic flow as well as with free flow speed with 20 percent no-passing zones and how capacity varies with different opposing flow rates.

6.4.1 Passing rates vs. traffic volume and free flow speed

The variability of passing rate with different average free flow speeds and traffic volumes was investigated. The passing rates in the primary direction with different average free flow speeds, 40 mph, 50 mph, and 60 mph, are presented at Table 6-6.

Table 6-6 Passing rates in TWOSIM II

Directional Traffic Volume (pcph)		Passing Rate (number of passes/1.6 mi/h)		
Primary	Opposing	40 mph	50 mph	60 mph
600	200	230 (2.3)	163 (1.6)	101
800	200	288 (2.1)	214(1.6)	137
1000	200	**319 (2.0)**	239 (1.5)	158
1200	200	281(1.6)	**245** (1.4)	**172**
1400	200	305 (2.0)	222 (1.5)	151
1600	200	265 (1.9)	192 (1.4)	138

Note: ( ) represents the ratio of passing rate to the passing rate at 60 mph

The passing rate increases with the primary direction volume up to a certain level (which varies by free flow speed) and then starts to decrease. The passing rate decreases when the primary direction volume is higher than 1,000 pcph under an average free flow speed of 40 mph and higher than 1,200 pcph under average free flow speeds of 50 and 60 mph. As expected, the higher the primary traffic flow, the higher the demand for passing. On the other hand, the higher the primary traffic flow, the lower the supply of passing opportunities (Morrall, et al., 1986).

The results also show that the passing rate decreases with an increase in the average free flow speed. This trend occurs because lower free flow speeds makes average travel times longer so that the durations that vehicles are exposed to the passing opportunity gets longer. Another reason is that the shorter passing time at lower free flow speed provides traffic with more opportunities for passing.

6.4.2 Capacity vs. opposing flow

The variability of capacity with different opposing flow rates was also examined. Table 6-7 shows how the capacity with 20 percent no-passing zones varies with the opposing flow rate.

Table 6-7 Capacity at 20 percent no-passing zones with different opposing flow rate

Traffic volume (pcph)		Capacity (pcph)
Primary (arrival demand)	Opposing	
2,300	200	2,103
	400	2,096
	600	2,091
	800	2,073
	1,000	2,066

Table 6-7 shows that capacity is not significantly affected by different amounts of opposing flow rates when 20 percent no-passing zones are present.

6.5 Results

The results of TWOSIM II are summarized as follows:

- Compared to the previous studies, passing times from TWOSIM II were found to have a range equivalent to the range from previous field studies.
- Passing rate increases with the primary traffic volume when the opposing volume is constant. However, the passing rate decreases with primary traffic volume when the traffic volume exceeds 1,000 pcph (40 mph) and 1,200 pcph (50 or 60 mph).
- Passing rate is found to decrease with increasing average free flow speed.
- Both the capacity with 100 percent no-passing zones and the capacity with 20 percent no-passing zones is estimated to be 2,100 pcph. The presence of passing is found to have no impact on the capacity of two-lane, two-way highways.
- The capacity is not significantly affected with an increasing opposing flow rate.

CHAPTER 7. TWO-LANE, TWO-WAY HIGHWAY SIMULATOR WITH DRIVEWAY, HORIZONTAL CURVE, AND GRADE (TWOSIM III)

TWOSIM III is an upgraded version of TWOSIM I with the addition of an algorithm considering the effect of the presence of a driveway and horizontal and vertical alignment.

When a driveway exists on a two-lane, two-way highway, the deceleration of a vehicle entering a driveway causes delay to the through vehicles on the mainline. A vehicle entering the main road from the driveway may also have an impact on the traffic flow. In TWOSIM III, these interruptions on the main line traffic caused by vehicles exiting or entering are investigated as a factor that they affect the capacity of two-lane, two-way highways.

Horizontal and vertical alignment is also likely to have an impact on capacity. Particularly, the speed of heavy vehicle is susceptible to horizontal and vertical alignment changes.

First, this chapter presents the development of TWOSIM III. Secondly, verification of TWOSIM III is performed using graphic output and other findings from previous publications. Next, the capacity of two-lane, two-way highways under a combination of factors and treatments is estimated. Finally, the results of sensitivity analysis are presented, followed by the conclusions of this chapter.

7.1 Development of TWOSIM III

This section describes the assumptions made and the analytic equations applied to model the acceleration/deceleration behavior of vehicles at around a driveway, a horizontal curve, and up or down a grade by vehicle type.

7.1.1 Driveway

7.1.1.1 Exiting the main road

Exiting vehicles decelerate to leave safely the main road with an appropriate level of comfort. The following section discusses the deceleration rate and speed of the vehicles. Left turn from a driveway into main road and from the main road into a driveway is not considered.

Deceleration rate for right-turns

Bonneson (1997) determined deceleration rates used to model right-turn behavior using field data. The deceleration rates of passenger cars range from 5.9 to 6.9 ft/s^2 (4.0 mph/s to 4.7 mph/s). In TWOSIM III, the average deceleration rate is selected randomly from a range with average deceleration rate 4.2 mph/s and standard deviation 0.1 mph/s. These were selected to be conservative in choosing the deceleration rate.

Exiting speed of right-turning vehicle

Bonneson (1997) also discussed speed when a vehicle exits the main road. As the right-turning vehicle approaches the driveway, it begins decelerating from its running speed, u, to its desired turn speed, u_{rt}. The desired turn speed, u_{rt}, is assumed to be dependent of the turning radius according to the research by Richards (as reported by Stover and Koepke,

1988). They have shown that right turn speed is related to curb return radius and driveway width in a linear manner. Based on an examination of Richard's findings, the following relationship was developed by Bonneson (for a 12-m driveway width):

$$u_{rt} = 3.59 + 0.196 R_c \, (S..I.\, units) \quad \textbf{Eq 7-1}$$

$$u_{rt} = 3.59 + 0.643 R_c \, (U.S.\, units) \quad \textbf{Eq 7-2}$$

where,

u_{rt} = right-turn speed (ft/s); and

R_c = curb radius (ft)

TWOSIM III applies the exiting speed model to calculate the average right-turn speed of a vehicle making a right turn to exit the main line. The right-turn speed is assumed to be normally distributed with a standard deviation of 1.0 mph/s.

These equations are applied only to passenger cars. There is no previous study about developing right turn speed model for heavy vehicles. However, it is obvious that heavy vehicles take a lot more time to decelerate and make a right turn exiting into a driveway. Therefore, it is assumed that the exiting speed and deceleration rate of heavy vehicles are estimated to be 50 percent of those of passenger cars in TWOSIM III.

Radius of driveway

AASHTO's Green Book (2004, Exhibit 9-19) presents edge-of-traveled way designs for right angle turns at intersections. The radius of a simple curve for right turn roadways is determined as a function of design vehicle type. TWOSIM III uses three types of driveway radius: 20, 30, and 45 feet.

Deceleration zone

To determine when a vehicle starts decelerating, a new term is defined called deceleration zone. The deceleration zone is defined to be the area where a vehicle exiting the main road initiates deceleration until it exits the main line. Figure 7-1 illustrates the deceleration zone.

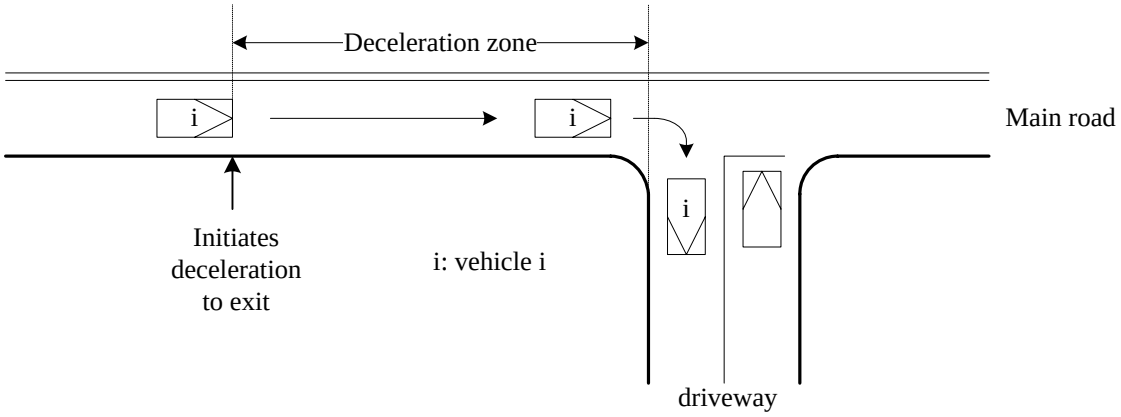

Figure 7-1 Schematic of deceleration zone

The length of deceleration zone can be calculated by the equation of motion:

$$L = \frac{v^2 - v_x^2}{2a} \qquad \textbf{Eq 7-3}$$

where,

L = length of deceleration zone (ft);

v = running speed (ft/s);

v_x = exiting speed (ft/s); and

a = deceleration rate (ft/s^2)

7.1.1.2 Entering vehicle

An entering vehicle is assumed to only make right turns in TWOSIM III. An entering vehicle enters the main road when there is a gap available, the size of which may vary with individual drivers. After he/she enters the main road, he/she starts accelerating to

reach an adequate speed. TWOSIM III models the behavior of entering vehicles as described in the following section.

Entering speed

In TWOSIM III, the vehicle starts from rest, enters the main road and continues to accelerate up to an adequate speed adapting to the flow of the main stream based on Gipps' car-following model. Therefore, Gipps' car-following model generates the speed of each vehicle entering the main line.

Gap acceptance

It is assumed that a driver decides to merge into the main line from the driveway based on the time gap to an oncoming vehicle upstream of driveway. Although most previous studies about critical gap focus on the behavior in making a left turn or crossing an unsignalized intersections, Lerner, et al. (2005) present the results of a study regarding critical gaps for right turning vehicles to merge onto a major road as shown in Table 7-1.

Table 7-1 Critical gaps derived from field data for right turns to a major road

Vehicle type	Critical gap (sec)	
	Raff method	Logistic regression
Passenger car	6.3	6.5
Single-unit truck	8.4	9.5
Combination truck	10.7	11.3

AASHTO currently uses 6.5 sec for right turning drivers. Lerner, et al. (2005) indicate that critical gaps are longer by 0.1 second per percent upgrade for right turns.

TWOSIM III uses the critical gaps as determined by a logistic method shown in Table 7-1, because they are more conservative than Raff method. TWOSIM III applies

the critical gap by vehicle type and generates individual gaps stochastically. The standard deviation is assumed to be 1.7 sec.

The algorithm of accepting or rejecting gaps in TWOSIM III is employed as follows. When there is a vehicle waiting at the driveway, first, the algorithm calculates the travel time that the closest oncoming vehicle would require from its current location to the centerline of the driveway. If the travel time is longer than the critical gap of the driver at driveway, then he/she starts entering the main road. Otherwise, he/she waits until there is an available gap. The driver is assumed to have his/her own constant critical gap and has a consistent behavior in accepting the gap.

7.1.1.3 Additional assumptions

Additional assumptions used in replicating vehicles entering or exiting the main road are as follows:

- The driveway is at a right angle to the right hand side of the main road.
- When a vehicle exits, the time to round the curb depends on the length of the vehicle and its speed. Considering their time, the delay for the main line vehicles due to the vehicle exiting is more reasonably taken into account.

7.1.2 Horizontal curve

According to the AASHTO Green Book (2004), roadway curves are designed based on an appropriate relationship between the design speed and curvature and the relationship with superelevation and side friction. When a vehicle moves in a circular path, it undergoes a centripetal acceleration that acts toward the center of curve. This acceleration is sustained by a component of the vehicle's weight related to the roadway

superelevation, by the side friction developed between the vehicle's tires and the pavement surface, or by a combination of the two. Based on these elements, TWOSIM estimates the speed of a vehicle traveling along a horizontal curve.

7.1.2.1 Geometric features

TWOSIM can model only a single horizontal curve. The reason for this is not only because the objective of this simulation model is to estimate the capacity based on the presence of a horizontal curve but also because coding a single curve is simpler than doing multiple curves. The superelevation is given as an input and the speed along the curve is determined using a previously developed model, which is described in the next section.

7.1.2.2 Speed model at horizontal curve

For the selection of a horizontal curve speed model, the study by Bonneson (1999) was examined. His study describes an analysis of the relationship between vehicular speed and side friction demand on horizontal curves. As result of this study, the prediction model of curve speed is presented as follows:

$$V_c = 63.5\,R\left(-B+\sqrt{B^2+\frac{4c}{127R}}\right) \le V_a(Metric) \qquad \textbf{Eq 7-4}$$

with

$$c = \frac{e}{100} + 0.256 + \left(B - 0.0022\right)V_a(Metric) \qquad \textbf{Eq 7-5}$$

$$B = 0.0133 - 0.0074\,I_{TR} \qquad \textbf{Eq 7-6}$$

where,

V_a = 85th percentile approach speed (km/h or mph);

V_c = 85^{th} percentile curve speed (km/h or mph);

R = radius of curve (m or ft);

B = adjustment of parameter depending on the facility type;

I_{TR} = indicator variable (=1.0 for turning roadways; 0.0 otherwise); and

e = superelevation rate (%)

The metric equations are converted into equations in US customary units as follows:

$$V_c = 12.1\,R\left(-B+\sqrt{B^2+\frac{4c}{38.7R}}\right) \le V_a\,(US\ Customary) \qquad \textbf{Eq 7-7}$$

$$c = \frac{e}{100} + 0.256 + 1.6\left(B - 0.0022\right)V_a\,(US\ Customary) \qquad \textbf{Eq 7-8}$$

There are other models for passenger vehicles in TWOPAS that are clarified by grade and type of vertical curve (Fitzpatrick, et al., 2000). These models are more complicated to code in TWOSIM than the model is developed by Bonneson (1999).

Since TWOSIM applies this equation only to horizontal curves, I_{TR} in Equation 7-6 is always zero and B is constant and equal to 0.0133. These equations are used when the curve speed is lower than the approach speed.

According to Bonneson (1999), the calibrated model was verified by being compared with similar models from three previous efforts and shown to be in very good agreement with existing models. According to the author, the benefit of the proposed speed model offers a human-behavior-based explanation for driver curve speed choice. Since TWOSIM III uses this model, the horizontal curve speed of an individual vehicle would vary depending on its approach speed.

In applying this model, the transition of superelevation is ignored. In TWOSIM III, when a driver approaches a horizontal curve, he/she decelerates when his/her own

approach speed is higher than the curve speed, and enters the horizontal curve at the speed estimated with this model. It is assumed that the vehicle accelerates again when it passes 2/3 of the length of the curve.

Fitzpatrick, et al. (2000) do not provide a speed equation for heavy vehicles due to unavailability of data for reasonable analysis. They determined that there is a similarity in speed trends between passenger cars and heavy vehicles at horizontal curve.

In TWOSIM III, the following equation (Equation 7-9), estimating design speed of curve (AASHTO, 2004), is used for the calculation of curve speed of heavy vehicles. It is not only because of the unavailability of curve speed data for heavy vehicles, but also because it yields more conservative speeds than using the equation by Bonneson (1999).

$$V = \sqrt{15R\left(0.01e_{\max} + f_{\max}\right)} \qquad \textbf{Eq 7-9}$$

where,

V = design speed of curve (mph);
R = radius of curve (feet);
e_{max} = maximum superelevation (%); and
f_{max} = maximum side friction factor

7.1.3 Grades

According to the Green Book (2004), nearly all passenger cars can readily negotiate grades as steep as 4 to 5 percent without an appreciable loss in speed below that normally maintained on level roadways, except for cars with high weight/power ratios, including some compact and subcompact cars. Speeds of most passenger cars are influenced on grades higher than 5 percent. Trucks generally increase speed by up to about 5 percent on downgrades and decrease speed by 7 percent or more on upgrades as compared to their

operation on level terrain (Green Book, 2004). Therefore, a speed model for heavy vehicles is needed to reflect the effect of grades on the traffic stream.

In building the algorithm that considers grades, the deflection or the transition of two different grades is ignored, because the effect of speed reduction along a vertical curve is considered to be negligible and also because the estimation of capacity with TWOSIM III focuses on a segment with sustained grades.

7.1.3.1 Acceleration/deceleration model of passenger car on grades

According to Lan and Menendez (2003), the difference in acceleration/deceleration rate (Equation 7-11) between level terrain and terrain on grades is $M/M_e \times gG$. This factor will be applied to calculate maximum acceleration and deceleration of passenger car in Gipps' car-following model. When a passenger car is traveling upgrade, its acceleration rate is decreased by the amount of "$M/M_e \times gG$" and increased by the same amount on a downgrade. Likewise, when a passenger car is on a downgrade, its deceleration is decreased by the amount of "$M/M_e \times gG$" and increased by the same amount on an upgrade.

7.1.3.2 Acceleration/deceleration model of trucks on grades

Lan and Menendez (2003) developed an acceleration/deceleration model for trucks on grades, which is described section 2.3.3 in more detail. TWOSIM III selects this model to be the acceleration/deceleration model for trucks because it has been verified as a well-defined formulation to obtain truck speed profiles based on the nominal dynamic, kinematic, and operating characteristics of trucks on grades.

For verification of this model, the speed profile of 200 hp truck with 200 lb/hp is plotted in Figure 7-2. When the initial speed of truck is 60.0 mph, speed tends to get lower over the distance of the upgrade segment. The decreasing rate of speed over the distance is higher on steeper grades of upgrade segment. After traveling a long distance up the grade, truck speed does not get lower and has crawl speed constantly. TWOSIM III applies this acceleration/deceleration model to the simulation of trucks on grades as well as on level terrain.

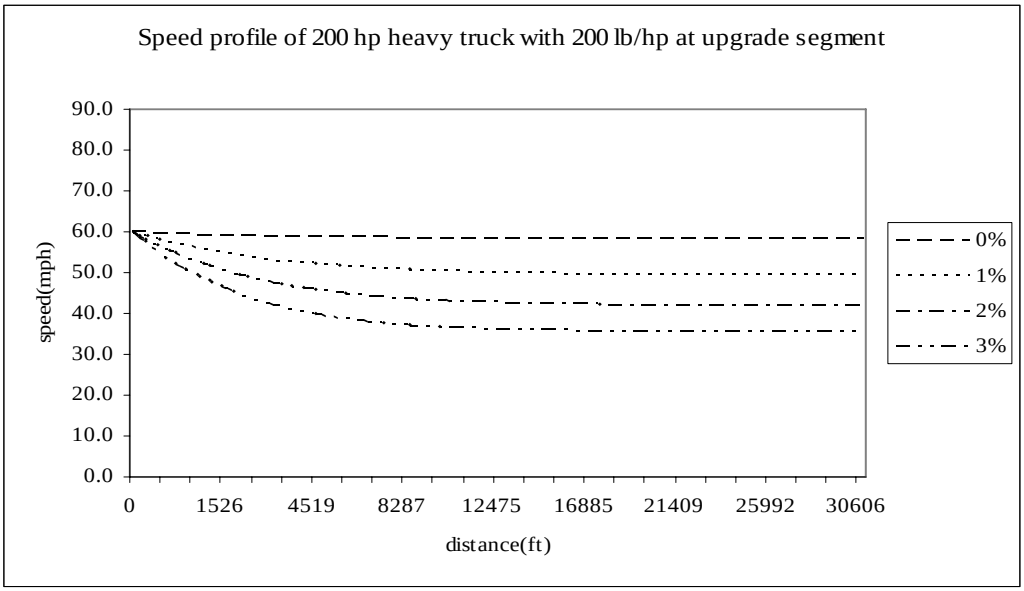

Figure 7-2 Speed profile of 200 hp truck with 200 lb/hp at upgrade segment

7.1.3.3 Performance characteristics of trucks

Leiman, et al. (1998) present the vehicle characteristics of the four types of truck used in TWOPAS. They updated the original weight to net horsepower values to the new ones shown in the third column in Table 7-2. TWOSIM III uses the updated types of truck because this information is the most recent and the targeted population of trucks is grounded on two-lane, two-way highway traffic.

Table 7-2 Updated truck performance characteristics

TWOPAS	Percent of truck	Original weight to net	Updated weight to net
1	12.0	266.0	228.0
2	25.6	196.0	176.0
3	34.0	128.0	140.0
4	28.4	72.0	76.0

7.2 Verification of TWOSIM III

It has been verified that TWOSIM III can replicate vehicles exiting and entering main road and vehicles on horizontal curve or grade. The verification was performed step by step using a graphical output method. The first step focuses on vehicles exiting and entering the main road. The second step examines how vehicles behave at horizontal curves. Thirdly, the behavior of vehicles on grade was verified. The second and third step were verified with the behavior of trucks.

7.2.1 Verification of driveway algorithm

7.2.1.1 Trajectories of vehicles exiting and entering main road

Figure 7-3 shows the trajectories of vehicles entering and exiting the main road in a time-space diagram.

The trajectory of an entering vehicle shows that it starts accelerating as soon as it gets out of driveway located at 10,560 feet and catches up with the vehicle ahead of it. The entering vehicle enters the main road when there is an acceptable gap available. The trajectory of the exiting vehicle shows that it decelerates and exits the main road. Due to the deceleration of the exiting vehicle, the vehicles following through the main road also are shown to decelerate until the exiting vehicle completes its turning maneuver. The vertical lines of exiting and entering vehicles represent that they are located at the

driveway before entering or after exiting. The figure shows that the entering and exiting maneuvers are executed reasonably.

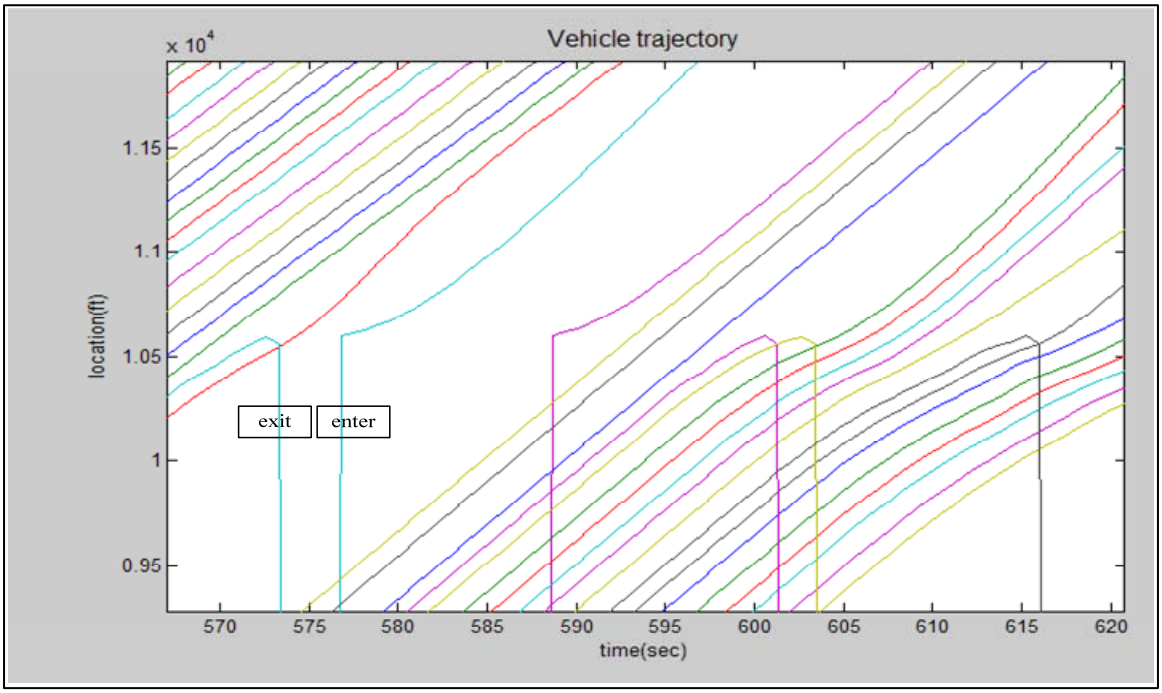

Figure 7-3 Trajectories of vehicles entering and exiting main road

7.2.1.2 Deceleration rate and speed of exiting vehicles

The resulting output for deceleration rates and exit speeds from the TWOSIM III simulation are plotted in Figures 7-4 and 7-5.

Figure 7-4 represents the histogram of deceleration rates that exiting vehicles have to employ to make a right turn to and exit the main road. The mean deceleration rate is 4.2 mph/s and the standard deviation is 0.1 mph/s. These statistics are equivalent to the mean and standard deviation input in TWOSIM III.

Figure 7-5 shows the histogram of exit speeds. The mean exit speed is 11.2 mph and the standard deviation is 0.9 mph. According to Equation 7-2, the average exiting speed is calculated to be 11.2 mph for a 20 feet radius driveway. Therefore, the algorithm on exiting vehicles works as coded.

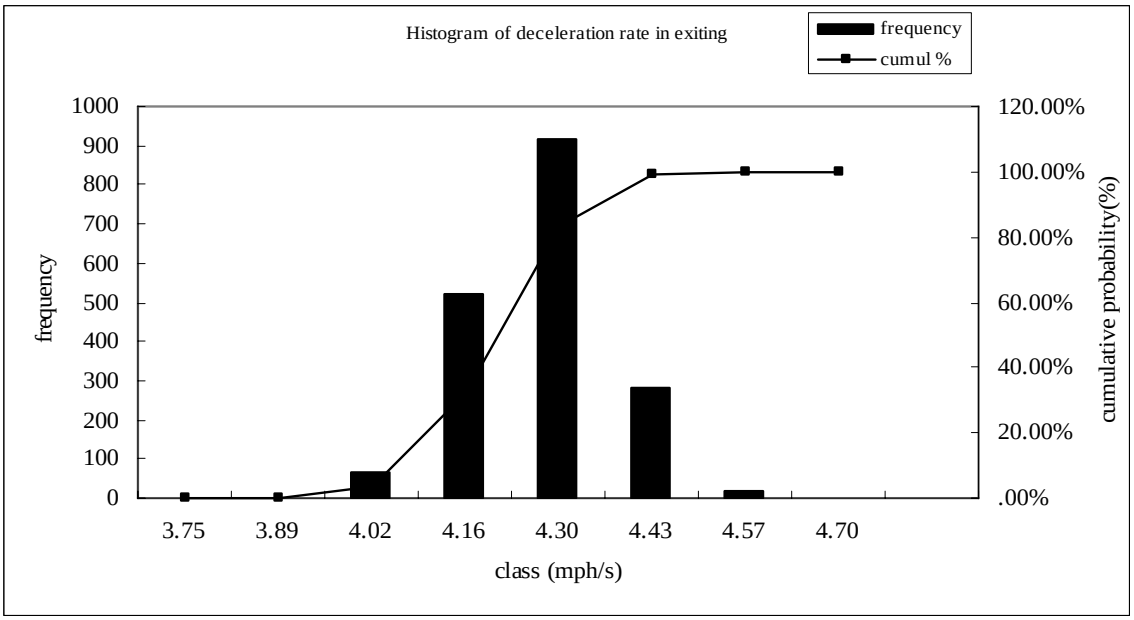

Figure 7-4 Histogram of deceleration rate in exiting main road

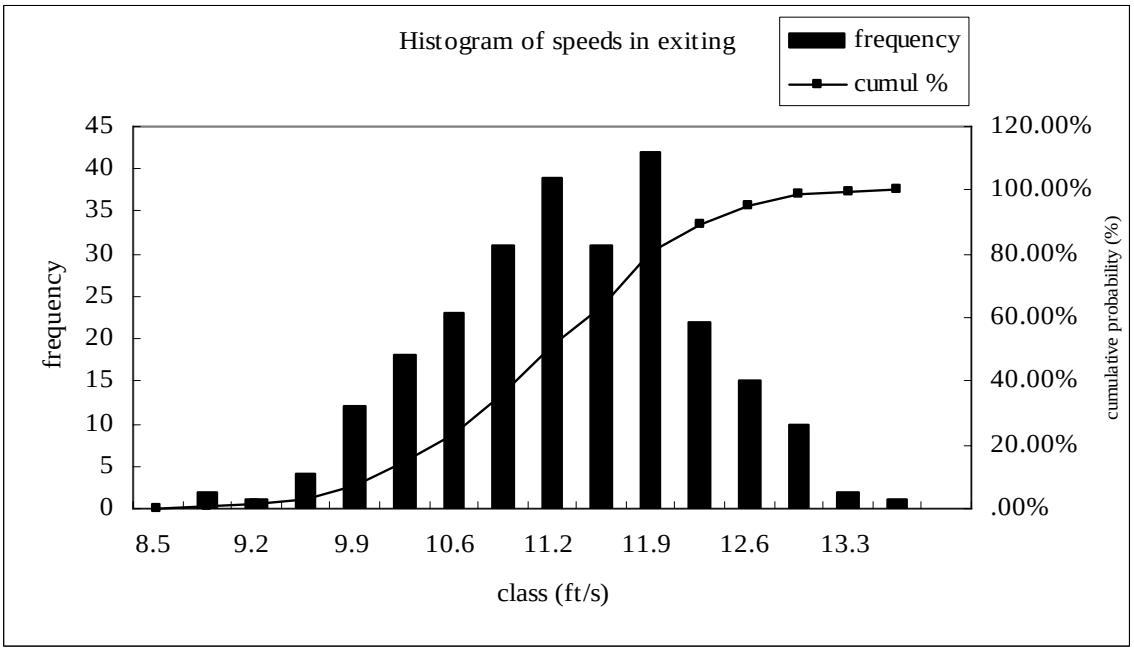

Figure 7-5 Histogram of speeds in exiting main road

7.2.2 Verification of horizontal curve algorithm

The speed profile of vehicles in a horizontal curve is shown at Figure 7-6. In this figure, the radius of the horizontal curve was set to be 50 feet with maximum superelevation 10

percent, so that the speed change can be more clearly shown. The x-axis represents location, and the y-axis is the speed of each vehicle. The vertical lines along the x-axis represent the beginning and end of the horizontal curve. The figure shows vehicles decelerate when approaching the curve and accelerate again when they are about to exit the curve. Since the radius is 50 feet, most curve speeds are concentrated in the range between 20 mph and 25 mph along the curve. When traveling over the curve, the speed profiles are mostly flat similar to TWOPAS's simulated average spot speed (Leiman, et al., 1998, Figure 5.10:2~3).

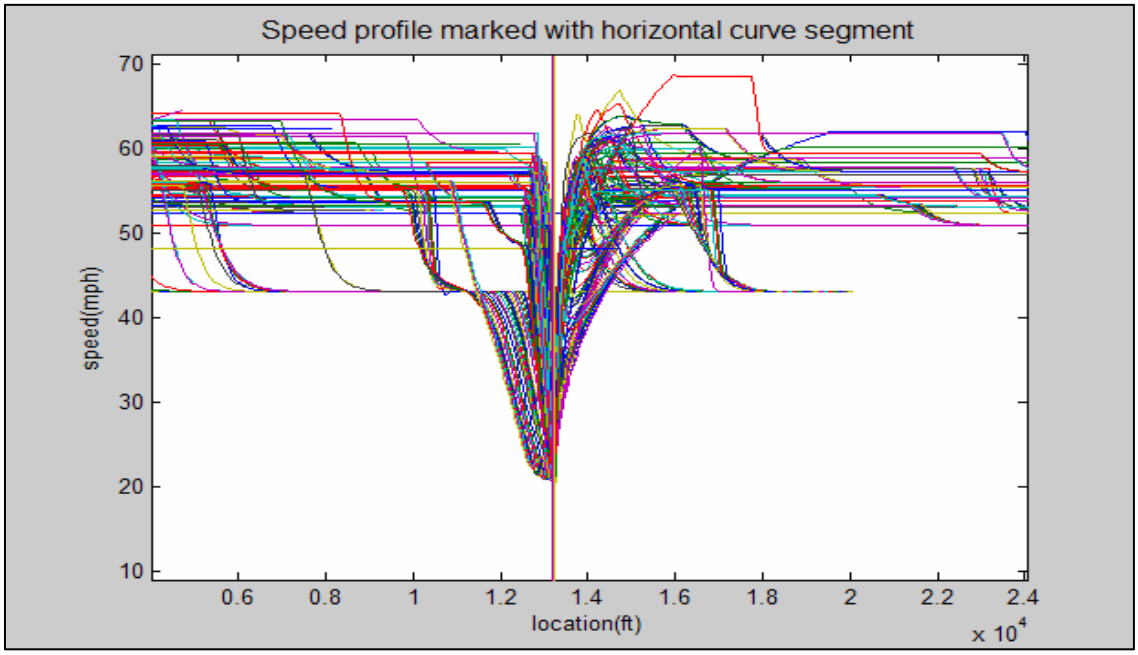

Figure 7-6 Speed profile of vehicles at 50 feet radius of horizontal curve

Figure 7-6 also shows some speed profiles that are shaped like letter "V." This trend of speed along the horizontal curve occurs because the speed of the vehicle ahead is lower than its own curve speed and this speed has to decrease and then increase again based on the car-following model. TWOPAS does not create this kind of speed profile, but TWOSIM III does.

Figure 7-7 shows curve speeds at 1,500 feet radius of horizontal curve that are distributed in the range 43 mph to 58 mph. The length of curve is higher due to the larger radius, but the other conditions are set to be same as those of Figure 7-6.

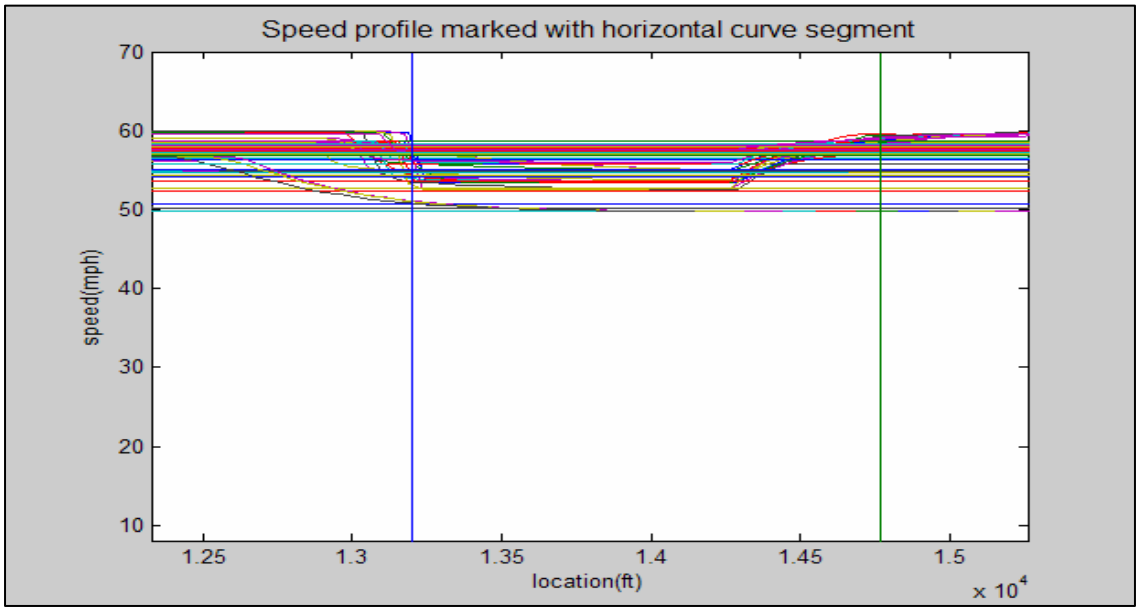

Figure 7-7 Speed profile of vehicles at 1500 feet radius of horizontal curve

Due to the presence of the horizontal curve, the speed reduction occurs at the location where the curve is present as shown in Figure 7-8.

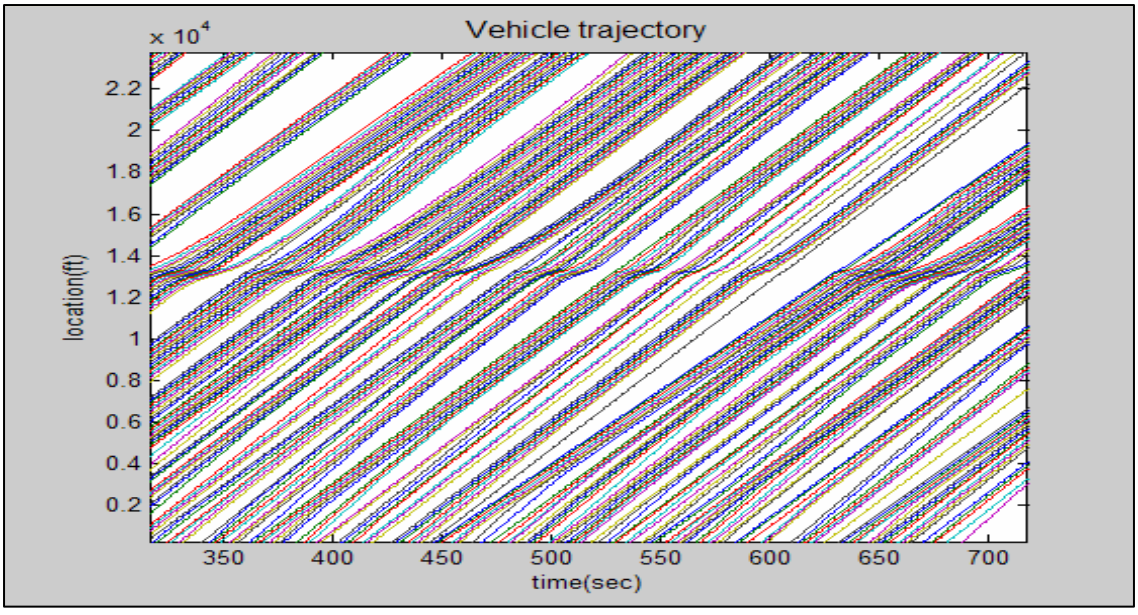

Figure 7-8 Trajectory of vehicles when horizontal curve is present

Next, the maximum superelevation is decreased to 4 percent from 10 percent (Figure 7-7). There are lower speeds in Figure 7-9 due to the smaller superelevation.

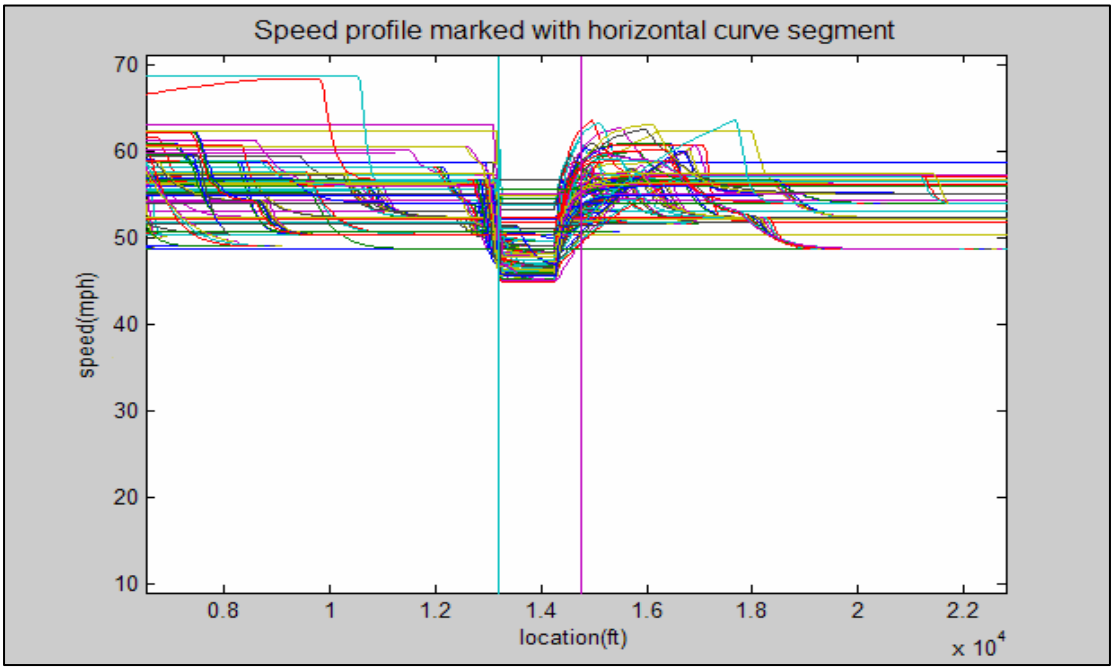

Figure 7-9 Speed profile of vehicles at 1500 feet radius of horizontal curve at 4 percent maximum superelevation

Since a centripetal acceleration that acts toward the center of curvature is less effectively sustained by a component of the vehicle's weight related to the superelevation, lower curve speeds are obtained at a 4 percent maximum superelevation when compared with the case of 10 percent maximum superelevation in the previous example. The curve speeds are distributed in the range between 45 mph and 55 mph. In consequence, TWOSIM III is verified to replicate speed of vehicle when a horizontal curve is present.

7.2.3 Verification of grade algorithm

The speed distribution on grade is examined in this section. Figure 7-10 shows the speed profiles along a 1 mile, 7 percent upgrade section with 10 percent trucks. The two vertical lines along the x-axis represent the beginning and the end of the section.

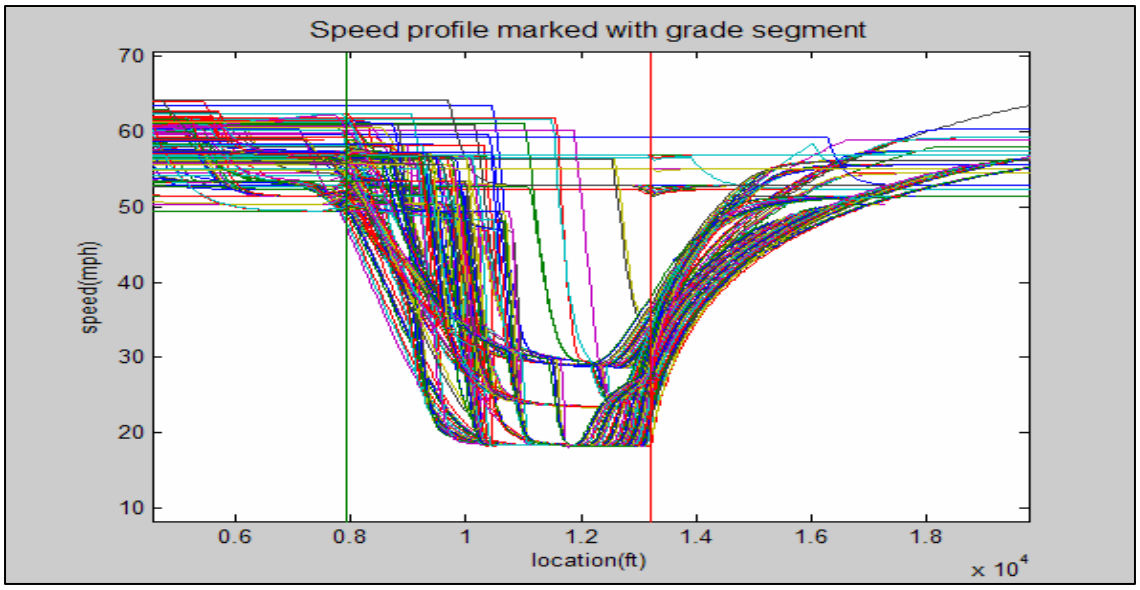

Figure 7-10 Speed profile at 1 mile 7 percent upgrade section with 10 percent trucks

Speeds start decreasing after vehicles enter the upgrade section. The lowest speed is due to a heavy truck, which forces the following vehicles to keep the same speed. After the end of the upgrade section, vehicles accelerate at level terrain.

In Figure 7-11, the two horizontal lines represent the beginning and the end of the upgrade section. Trucks with slower speeds create platoon along the upgrade section.

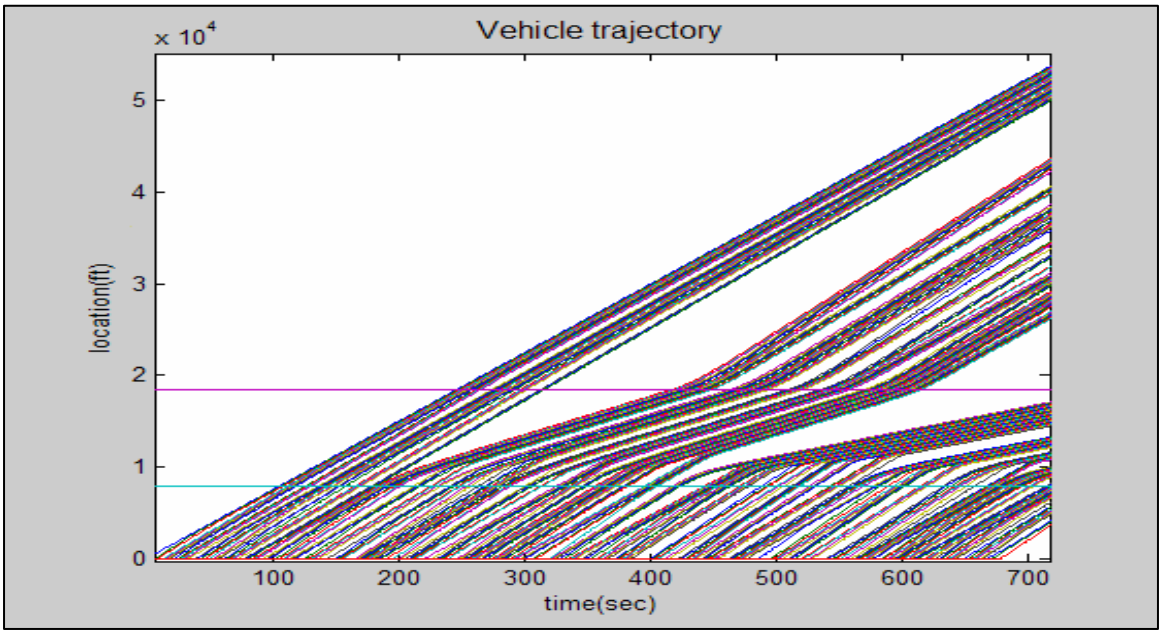

Figure 7-11 Trajectories on the segment with 7 percent upgrade section with 10 percent trucks

Next, the upgrade section is converted into a downgrade and the respective speed profile is shown in Figure 7-12. Compared to Figure 7-10, there is no substantial speed reduction in Figure 7-12, but some speeds decrease due to the decreased deceleration rate.

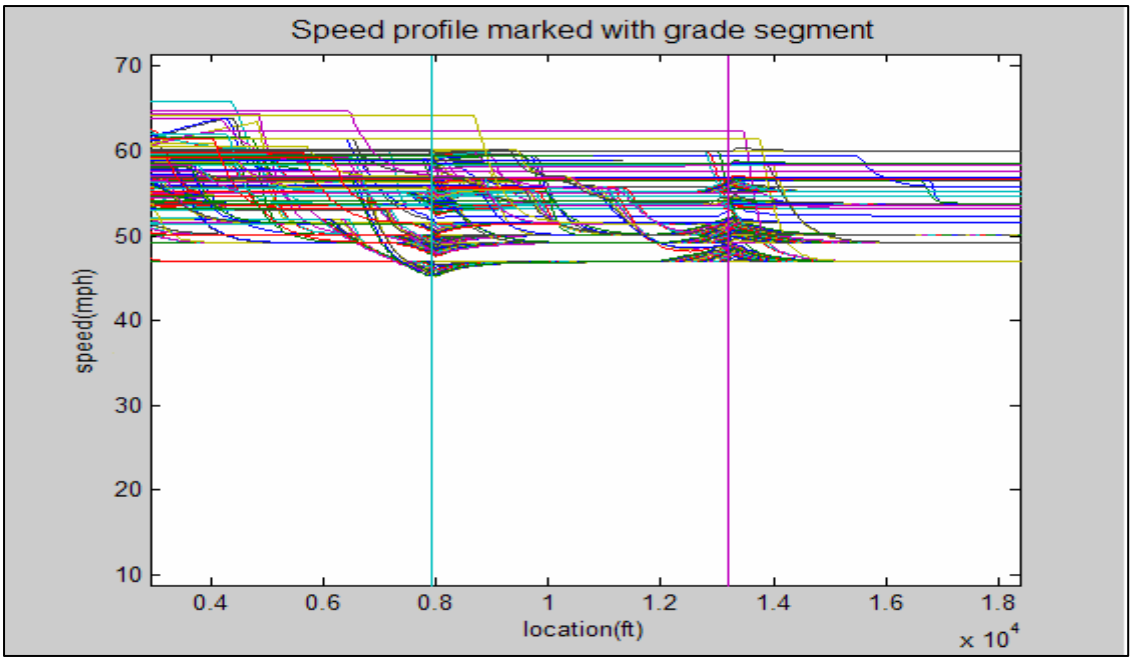

Figure 7-12 Speed profile at 2 mile 7 percent upgrade section with 10 percent trucks

7.3 Comparison of TWOSIM III to TWOPAS and HCM 2000

Since the presence of driveways and horizontal curves are not considered in the HCM 2000 methodology, TWOPAS is compared to TWOSIM III, while the HCM 2000 is compared with TWOSIM III for the grade algorithm only.

The input data required for the analysis of the presence of driveways in TWOPAS is driveway density. The input data in TWOSIM III are the radius of the right turn curb, location, width of lane and shoulder, percent of exit traffic, percent of trucks, and traffic volume. Comparing the input data for the two simulators, TWOSIM III is considered to analyze the presence of driveway by more logical methodology because it uses more detailed data associated with the vehicle dynamics.

7.3.1 Presence of a driveway

The effect of the presence of a driveway along a two-lane, two-way highway is compared using TWOSIM III and TWOPAS. The driveway is located at 1 mile downstream from the beginning of 4 mile study segment. This segment has 100 percent no-passing zones and base conditions are assumed. The driveway curb radius is 30 feet.

In this comparison, only the location of the driveway and permitted turning direction of traffic at the driveway is input in TWOPAS, while the location of driveway, its curb radius, traffic volume at driveway, and percent of exit or entry volume are input in TWOSIM III.

Table 7-3 shows the results of the comparison of average travel speed between TWOSIM III and TWOPAS when a driveway is present. The absolute difference of ATS between the two simulators decreases with total flow rate. There is no significantly large difference between the two simulators in estimating average travel speed with the presence of a driveway along a two-lane, two-way highways. Generally, TWOSIM III's speeds are higher than those from TWOPAS.

Table 7-3 Comparison of ATS when a driveway is present

Flow rate (vph)			ATS in primary direction (mph)		Absolute difference (mph)
Primary	Opposing	Sum	TWOSIM III	TWOPAS	
700	500	1,200	58.6	54.5	4.1
900	500	1,400	57.4	54.0	3.4
1,100	500	1,600	55.7	53.5	2.2
1,300	500	1,800	54.4	52.2	2.2
1,500	500	2,000	53.0	52.2	0.8
1,700	500	2,300	51.7	51.6	0.1

Percent time spent following (PTSF) is also estimated using TWOSIM III and TWOPAS, and the results are shown at Table 7-4. PTSF increases with total traffic flow rate for both simulators. The absolute difference decreases with total traffic flow rate. The PTSFs from TWOPAS are higher than those from TWOSIM III.

Table 7-4 Comparison of PTSF when a driveway is present

Flow rate (vph)			PTSF in primary direction (%)		Absolute difference (%)
Primary	Opposing	Sum	TWOSIM III	TWOPAS	
700	500	1,200	66.4	70.7	4.3
900	500	1,400	72.7	77.9	5.2
1,100	500	1,600	77.7	81.2	3.4
1,300	500	1,800	82.0	85.9	3.9
1,500	500	2,000	84.9	85.8	1.0
1,700	500	2,300	88.5	88.5	0.0

In conclusion, TWOSIM III is found to give similar performance measures results when compared to TWOPAS in analyzing two-lane, two-way highways when a driveway is present.

7.3.2 Presence of a horizontal curve

For the comparison of the horizontal curve algorithm in TWOSIM III, the results of multiple runs of simulation with TWOSIM III are compared with those of TWOPAS.

The horizontal curve starts 2 miles downstream from the beginning of the 4 mile study segment. There is a 100 percent no-passing zone. Its maximum superelevation is 10 percent and its normal crown is -2 percent. The radius of the curve is 1000 ft and its central angle is 60 degree, so its length is 523.6 ft.

Table 7-5 shows average travel speed from TWOSIM III and TWOPAS when there is a horizontal curve. The result shows that two simulators give no significantly large difference in average travel speed when horizontal curve is present.

Table 7-5 Comparison of ATS when a horizontal curve is present

Flow rate (vph)			ATS in primary direction (mph)		Absolute difference (mph)
Primary	Opposing	Sum	TWOSIM III	TWOPAS	
700	500	1,200	56.1	53.2	2.9
900	500	1,400	54.8	53.0	1.8
1,100	500	1,600	54.1	52.1	2.1
1,300	500	1,800	53.3	51.2	2.1
1,500	500	2,000	52.8	50.7	2.1
1,700	500	2,300	51.0	50.3	0.7

Table 7-6 presents percent time spent following from TWOSIM III and TWOPAS when there is a horizontal curve by different combinations of traffic flow rate. The absolute differences in PTSF between the two simulators are smaller for traffic flow rates other than that of 1,200 pcph. Mostly the two simulators are found to give similar PTSFs when there is a horizontal curve.

Table 7-6 Comparison of PTSF when a horizontal curve is present

Flow rate (vph)			PTSF in primary direction (%)		Absolute difference (%)
Primary	Opposing	Sum	TWOSIM III	TWOPAS	
700	500	1,200	62.2	72.1	9.9
900	500	1,400	71.7	76.3	4.6
1,100	500	1,600	79.2	81.0	1.8
1,300	500	1,800	84.8	84.6	0.2
1,500	500	2,000	88.6	86.7	1.9
1,700	500	2,300	91.7	88.4	3.3

Based on the comparison of ATS and PTSF, TWOSIM III is found to give comparable performance measures as TWOPAS when a horizontal curve is located along a two-lane, two-way highway.

7.3.3 Presence of grades

Comparison of TWOSIM III with TWOPAS and HCS is performed for an upgrade segment of 1 mile length of 7 percent upgrade. The section starts 1 mile downstream of the study segment. The remaining sections are level terrain with average free flow speeds of 60 mph. There are 100 percent passenger cars and 100 percent no-passing zones. As mentioned previously, the vertical curve at the beginning and the end of the upgrade section is ignored.

Table 7-7 presents ATS from TWOSIM III, TWOPAS, and HCS. The average travel speed of the entire study segment is estimated to be similar for the two simulators. TWOSIM III is found to give comparable estimates of ATS to TWOPAS, while it has a significantly large difference against the HCS.

Table 7-7 Comparison of ATS when an upgrade section is present

Flow rate (pcph)			ATS in primary direction (mph)			Absolute difference (mph)	
Primary	Opposing	Sum	TWOSIM III	TWOPAS	HCS	vs. TWOPAS	vs. HCS
700	500	1,200	55.7	54.6	47.7	1.1	8.0
900	500	1,400	54.2	54.1	46.0	0.1	8.2
1,100	500	1,600	54.3	53.6	44.3	0.7	10.0
1,300	500	1,800	53.3	53.0	42.6	0.4	10.7
1,500	500	2,000	52.6	52.0	40.9	0.6	11.7
1,700	500	2,200	50.7	52.0	39.2	1.3	11.5

Table 7-8 shows the PTSF from TWOSIM III, TWOPAS and HCS. TWOSIM III gives higher PTSF than TWOPAS when an upgrade section is present. TWOSIM III's PTSFs are closer to that of the HCS than TWOPAS's PTSFs are. Mostly, HCS gives higher PTSF than those of TWOSIM III and TWOPAS. Compared with TWOPAS, TWOSIM III is more likely to have platoons when there is an upgrade section.

Table 7-8 Comparison of PTSF when an upgrade section is present

Flow rate (pcph)			PTSF in primary direction (%)			Absolute difference (%)	
Primary	Opposing	Sum	TWOSIM III	TWOPAS	HCS	vs. TWOPAS	vs. HCS
700	500	1,200	66.0	60.0	75.9	6.0	9.9
900	500	1,400	75.3	68.7	79.6	6.5	4.3
1,100	500	1,600	78.9	71.2	83.3	7.7	4.4
1,300	500	1,800	85.1	76.2	86.6	8.9	1.5
1,500	500	2,000	90.1	82.4	88.7	7.7	1.4
1,700	500	2,200	92.9	83.3	98.7	9.6	5.8

7.3.4 Presence of heavy vehicles

Traffic flow with 10 percent of trucks along a 4 percent upgrade section is simulated to compare TWOSIM III and TWOPAS. The other conditions are the same as the base conditions.

Table 7-9 Comparison of ATS when 10 percent of trucks exist in the presence of an upgrade section

Flow rate (vph)			ATS in primary direction (mph)		Absolute difference (mph)
Primary	Opposing	Sum	TWOSIM III	TWOPAS	
700	500	1,200	54.3	52.2	2.0
900	500	1,400	53.1	50.7	2.4
1,100	500	1,600	52.4	49.0	3.5
1,300	500	1,800	51.0	49.4	1.6
1,500	500	2,000	49.3	46.8	2.6
1,700	500	2,300	47.7	44.7	2.9

Table 7-9 presents average travel speed from TWOSIM III and TWOPAS when there are heavy vehicles at an upgrade section. The two simulators give similar ATS.

Table 7-10 presents PTSFs from TWOSIM III and TWOPAS when there are heavy vehicles at an upgrade section. Mostly, TWOSIM III gives higher PTSFs than TWOPAS when an upgrade section and trucks are present. Compared with TWOPAS, TWOSIM III is more likely to create platoons.

Table 7-10 Comparison of PTSF when 10 percent of trucks exist in the presence of an upgrade section

Flow rate (vph)			PTSF in primary direction (%)		Absolute difference (%)
Primary	Opposing	Sum	TWOSIM III	TWOPAS	
700	500	1,200	67.6	65.1	2.5
900	500	1,400	74.1	73.2	0.9
1,100	500	1,600	80.2	77.9	2.3
1,300	500	1,800	86.4	81.4	4.9
1,500	500	2,000	90.5	83.9	6.7
1,700	500	2,300	93.4	87.1	6.3

7.4 Estimation of capacity

7.4.1 Presence of a driveway

Table 7-11 shows when a driveway is present and other conditions are the same as the base conditions, the capacity is found to range between 1,850 to 1,890 pcph, as a function of given radius of curb. There is no significant difference in capacity between different curb radii from statistical testing standpoint (Appendix E). The slightly higher capacities of longer curb radii may be due to the higher right turning speed. The results show that

the presence of a driveway has significant impact on the capacity of two-lane, two-way highways.

Table 7-11 Capacity as a function of curb radius of driveway

Curb radius (ft)	Capacity (pcph)
20	1,850
30	1,890
45	1,890

7.4.2 Presence of a horizontal curve

Table 7-12 shows the estimated capacities of two-lane, two-way highways when a horizontal curve is present. For this estimation, the maximum superelevation is 10 percent and the maximum friction factor is 0.12.

The results of the statistical test (Appendix E) show that a horizontal curve with a very small radius (100 feet) for a 60 mph average free flow speed has significant reduction in the capacity compared with the other radii. When the horizontal curve radius is greater or equal to 500 feet, the capacity is similar to that of a tangent segment.

Table 7-12 Capacity as a function of the radius of horizontal curve

Curve radius (ft)	Capacity (pcph)
100	1,750
300	1,980
400	2,040
500	2,100
1000	2,100

7.4.3 Presence of upgrade section

For the estimation of the capacity with an upgrade section, it is given that there is 1 mile upgrade section with 10 percent trucks and 90 percent passenger cars. Three different grades are evaluated.

Table 7-13 presents the estimated capacity with grade. The capacity, 1,870 pcph at 4 percent grade decreases at steeper grades, such as 6 percent and 8 percent. It shows that the capacity decreases with the grade of the upgrade section. The reduction of truck speeds is shown to have significant impact on the capacity of two-lane, two-way highways (Appendix E).

Table 7-13 Capacity as a function of grade of 1 mile upgrade section

Grade (%)	Capacity (vph)
4	1,870
6	1,670
8	1,460

7.5 Sensitivity analysis

A sensitivity analysis is performed next to examine the impact of various parameters on capacity.

7.5.1 Superelevation of the horizontal curve

When a horizontal curve with 500 feet radius is present under the base conditions, the capacity is found to increase with superelevation of the curve as shown in Table 7-14. It was found that there is significant difference in capacities when the maximum superelevation of horizontal curve varies (Appendix E). Therefore, the greater

superelevation allows for higher vehicle speeds and leads to a higher capacity for two-lane, two-way highways.

Table 7-14 Capacity as a function of maximum superelevation of horizontal curve

Superelevation (%)	Capacity (pcph)
4	1,600
7	1,940
10	2,100

7.5.2 Percent of trucks

How capacity varies with the percentage of trucks along a horizontal curve, a section with a driveway, and an upgrade section was examined.

7.5.2.1 Presence of horizontal curve

Table 7-16 shows the capacities estimated with different percentages of trucks along a horizontal curve. It was found that there were significant differences in capacities when the radius of horizontal curve varied in combination with varying percentages of trucks.

Table 7-15 Capacity as a function of the radius of horizontal curve and percent of trucks

Curve radius (ft)	Capacity (vph)		
	0 percent trucks	10 percent trucks	20 percent trucks
100	1,750	1,670	1,570
500	2,100	1,990	1,870
1000	2,100	2,050	1,940

As expected, the capacities decrease with increasing percentage of trucks for any given radius of the horizontal curve. The capacities increase with the radius of horizontal curve for a given percentage of trucks. The operating speed is found to decrease with the percentage of trucks and increase with the radius of curve.

7.5.2.2 Percent of trucks at the presence of driveway

Table 7-17 shows the capacities with different percentages of trucks at a section with a driveway. From the result of statistical testing (Appendix E), the capacity is found to decrease with an increasing percentage of trucks when a driveway is present. At zero percent trucks, the two curb radii give the same capacity. When the percentage of trucks increases, the capacities between the two curb radii are shown to be slightly different.

Table 7-16 Capacity as a function of the percent of trucks in the presence of a driveway

Driveway curb radius (ft)	Capacity (vph)		
	0 percent trucks	10 percent trucks	20 percent trucks
30	1,890	1,720	1,620
45	1,890	1,760	1,680

7.5.2.3 Percent of trucks on upgrade section

Table 7-18 shows the capacities estimated for different percentages of trucks along a 1 mile upgrade section.

Table 7-17 Capacity as a function of the percent of trucks at upgrade section

Grade (%)	Capacity (vph)		
	10 percent trucks	20 percent trucks	30 percent trucks
4	1,870	1,740	1,690
6	1,670	1,530	1,480
8	1,460	1,330	1,250

From statistical testing (Appendix E), it was found that grade has a significant impact on capacity Also, the capacity decreases with an increasing percentage of trucks.

7.5.3 Length of upgrade

How the capacity varies with the length of a 6 percent upgrade section. Traffic consists of 10 percent of trucks was examined. Table 7-19 shows that the capacity decreases with the length of the upgrade section.

Table 7-18 Capacity as a function of the length of upgrade section

Grade (%)	Capacity (vph)		
	0.6 mile	1 mile	1.4 mile
6	1,760	1,670	1,450

7.5.4 Horizontal curve at upgrade section

The capacity of a section with a horizontal curve on an upgrade is examined next. The section tested has a horizontal curve with 500 feet radius, and is on a 6 percent upgrade section. The algorithm in TWOSIM III selects the lower speed between two speeds estimated on the basis of horizontal curve and upgrade.

The statistical test shows that there is significant difference in capacity when the percentage of trucks varies when a horizontal curve is present (Appendix E). As expected, the capacity is found to decrease with an increasing percentage of trucks. Compared with the capacity with the presence of a horizontal curve on level terrain (Table 7-16), the capacity with the presence of a horizontal curve on an upgrade section decreases more with an increasing percentage of trucks. The capacity with 100 percent cars at a 500 foot horizontal curve on 6 percent upgrade is the same as the capacity (2,100 pcph) for base conditions.

Table 7-19 Capacity as a function of the percent of trucks at horizontal curve on upgrade section

Percent of trucks	Capacity (vph)
0	2,100
10	1,640
20	1,530

7.6 Results

Using TWOSIM III, several capacity volumes are estimated considering elements such as the presence of a driveway, the presence of a horizontal curve, grade, and the presence of trucks. The following are concluded:

- When there are no trucks in the traffic stream:
  - ✓ Capacity is found to decrease with the presence of a driveway (10 to 12 percent reduction in capacity), a horizontal curve with radius less than 500 ft (3 to 17 percent reduction in capacity), and an upgrade section (11 to 30 percent reduction in capacity for a 4 to 8 percent grade respectively).
  - ✓ Capacity increases with the maximum superelevation (8 percent to 24 percent reduction in capacity) of horizontal curve.
- When there are trucks in the traffic stream:
  - ✓ Capacity decreases with an increasing proportion of trucks (10 to 20 percent) in the traffic stream when there is a driveway (10 to 23 percent reduction in capacity).
  - ✓ Capacity decreases with an increasing proportion of trucks (10 to 20 percent) in the traffic stream when there is a horizontal curve (3 to 26 percent reduction in capacity).

- ✓ Capacity decreases with an increasing proportion of trucks (10 to 30 percent) in the traffic stream when there is an upgrade section (11 to 40 percent reduction in capacity).
- ✓ When the truck percentage is constant, the capacity is found to increase with the radius of the horizontal curve.
- ✓ Capacity at 10 percent trucks is found to decrease as the length of the upgrade section (16 percent, 21 percent, and 31 percent reduction in capacity for 0.6, 1.0, and 1.4 mile) increases.
- ✓ The presence of a horizontal curve and/or an upgrade results in a capacity reduction which is particularly pronounced when trucks are present. For example, for a horizontal curve with a 500 foot radius, and a 6 percent upgrade, the capacity decreased by 22 percent for 10 percent trucks, and by 27 percent for 20 percent trucks.

CHAPTER 8. CONCLUSIONS AND RECOMMENDATIONS

In this dissertation, a microscopic simulator (TWOSIM) was developed to estimate the capacity of two-lane, two-way highways. Capacity estimation for two-lane highways using field data has not been possible because there are a very limited number of sites operating at capacity. Also, existing simulators use capacity as an input and cannot be used or modified to determine capacity. A list of input and output data for TWOSIM can be found in Appendix C. TWOSIM has been verified to replicate stochastic, two-lane flow at the microscopic level and estimates the capacity under a variety of traffic conditions associated with passing maneuvers, the presence of a driveway, the presence of a horizontal curve, upgrade/downgrade, and the presence of trucks.

The conclusions of the research are as follows:

- The capacity of two-lane, two-way highways was found to be a function of average free flow speed. The capacity ranges from 1,800 pcph to 2,100 pcph at an average free flow speed of 40 mph to 70 mph. Compared with the single directional capacity (1,700 pcph) in HCM 2000, this study found higher capacity values
- It was found that the presence of a passing zone does not affect capacity. This happens because at high traffic volume, there are very few passing opportunities available in the primary traffic stream. Simulation with lower traffic volumes showed that the presence of a passing zone clearly contributes to the enhancement of operating conditions, with an increase in the average travel speed.

- The directional capacity was independent of the opposing flow rate. Based on the results of this study, the capacity for both directions should be twice the directional capacity (i.e., 4,200 pcph). In reality, it is a very rare phenomenon that both directions reach capacity conditions at the same time and observing such a condition has never been reported.
  - When there are no trucks in the traffic stream:
    - ✓ Capacity was found to decrease with the presence of a driveway (10 to 12 percent reduction in capacity), a horizontal curve with radius less than 500 ft (3 to 17 percent reduction in capacity), and an upgrade section (11 to 30 percent reduction in capacity for a 4 to 8 percent grade respectively).
    - ✓ Capacity increased with the maximum superelevation (8 percent to 24 percent reduction in capacity) of horizontal curve.
  - When there are trucks in the traffic stream:
    - ✓ Capacity decreased with an increasing proportion of trucks (10 to 20 percent) in the traffic stream when there is a driveway (10 to 23 percent reduction in capacity).
    - ✓ Capacity decreased with the increasing proportion of trucks (10 to 20 percent) in the traffic stream when there is a horizontal curve (3 to 26 percent reduction in capacity).
    - ✓ Capacity decreased with the increasing proportion of trucks (10 to 30 percent) in the traffic stream when there is an upgrade section (11 to 40 percent reduction in capacity).

- ✓ When truck percentage was constant, the capacity was found to increase with the radius of the horizontal curve.
- ✓ Capacity at 10 percent trucks was found to decrease as the length of the upgrade section (16 percent, 21 percent, and 31 percent reduction in capacity for 0.6, 1.0, and 1.4 mile) increased.
- ✓ The presence of a horizontal curve and/or an upgrade resulted in a capacity reduction which was particularly pronounced when trucks were present. For example, for a horizontal curve with 500 feet radius, and a 6 percent upgrade, the capacity decreased by 22 percent for 10 percent trucks, and by 27 percent for 20 percent trucks.

The following recommendations are suggested:

- Since the capacity under the base conditions in the simulator changes with average free flow speed, it is recommended additional field studies be conducted to verify these results.
- In addition, since TWOSIM's capacities are found to be higher than HCM's capacity and independent of the proportion of passing zones, it is recommended that HCM's capacity be reevaluated.
- Since capacity is found to vary with particular treatments using TWOSIM, it is recommended that HCM presents varying capacities as a function of the geometric and traffic conditions.
- It is recommended that HCM provide the following guidelines on capacity reduction due to various factors.

- ✓ In the presence of a driveway, capacity is likely to decrease by 10 to 23 percent when 0 to 20 percent trucks exist.
- ✓ In the presence of a horizontal curve, capacity is likely to decrease by 3 to 26 percent when 0 to 20 percent of trucks exist.
- ✓ In the presence of a 1 mile upgrade section at 4 ~ 8 percent slope, capacity is likely to decrease by 11 to 40 percent when 0 to 20 percent of trucks exist.

- It is recommended that the capacity of two-lane, two-way highways be expressed only in directional terms, because it is extremely rare that both directions could reach capacity conditions at the same time.
- The algorithm of TWOSIM needs to be enhanced so that it can estimate capacity reflecting the presence of multiple driveways or multiple horizontal curves, different types of drivers (e.g., commuters, degree of aggressiveness, etc), or geometric factors, such as lane and shoulder width. The model can also be enhanced to consider weather factors.
- Some parameters in the TWOSIM model (e.g., safety reaction time, gap acceptance behavior in attempting to pass) need to be calibrated with more extensive data collection.
- It is recommended that the car-following model be improved with the development of a model reflecting the behavior of a passenger car driver around large trucks. The uncomfortable feeling of a passenger car driver due to lack of sight distance and the truck's slower speed particularly on an upgrade section may have an impact on capacity.

- Associated with truck traffic, it is recommended that field data for investigating trucks' exit speeds and right-turn speeds around a driveway be collected and a truck speed model along a horizontal curve be developed.

REFERENCES

Aerde, M. V. and Yagar, S. *Capacity, speed and platooning vehicle equivalents for two-lane rural highways*. Transportation Research Records 971, pp. 58-67. 1984.

Akcelik, R. and Chung, E. *Calibration of the bunched exponential distribution of arrival headways*. Akcelik & Associates Pty Ltd. June 2003 (Reprint with minor revisions: Akcelik, R. and Chung, E. Calibration of the bunched exponential distribution of arrival headways. Road and Transport Research 3 (1), pp. 42-59. 1994)

American Association of State Highway and Transportation Officials. *A Policy on Geometric Design of Highways and Streets*. 2004.

Aycin, M. F. and Benekohal, R. F. *Linear acceleration car-following model development and validation*. Transportation Research Record No. 1644, pp. 10-19. 1998.

Banks, J., Carson, J. S., Nelson, B. L., and Nicol, D. M. *Discrete-event system simulation*. Prentice Hall, Inc. 2001.

Bonneson, J. A. *Delay to major-street through vehicles due to right turn activity*. Transportation Research . –A, Vol. 32, No. 2, pp. 139-148, 1998.

Bonneson, J. A. *Side friction factor and speed as controls for horizontal curve design.* Journal of Transportation Engineering. 1999.

Davis, S.C. and Diegel, S. W. *Transportation Energy Databook, Edition 24.* U.S. Department of Engergy. 2004.

Elefteriadou, L. *Chapter 8. Highway capacity*. Handbook of Transportation Engineering. McGrow-Hill. 2004

Enberg, A. and Pursula, M. *Traffic flow and level of service on high-class two-lane rural roads in Finland*. Highway Capacity and Level of Service, Brannolte(ed). 1991.

Fambro, D. et al. *Determination of Factors Affecting Stopping Sight Distance*. Working Paper I: Braking Studies (DRAFT) National Cooperative Highway Research Program, Project 3-42, 1994.

Federal Highway Administration. *Manual on Uniform Traffic Controls Devices*. 2003.

Gartner, N.H., Messer, C.J., and Ruthi, *A. Revised Monograph on Traffic Flow Theory*. Federal Highway Administration, 1994.

Fitzpatrick, K., Elefteriadou, L., Harwood, D. W., Collins, J. M., McFadden, J., Anderson, I. B., Krammes, R. A., Irizarry, N., Parma, K. D., Bauer, K. M., and Passetti, K. *Speed prediction for two-lane, two-way rural highways*. Federal Highway Administration. Turner-Fairbank Highway Research Center. August, 2000.

Gerlough, D. L. and Huber, M. J. *Traffic flow theory: A monograph*. Transportation Research Board, National Research Council, Washington D.C. pp. 17-41. 1975

Gipps, P. G. *A behavioral car-following model for computer simulation*. Transportation Research B. vol. 15B, pp. 105-111. 1981

Green, M. *" How long does it take to stop?" Methodological Analysis of Driver Perception-Brake Times*. Transportation Human Factors, 2(3), 195-216. 2000.

Hammond, H. F. and Sorenson, L. J. (ed.). *Traffic Engineering Handbook*. New York: Institute of Traffic Engineers and National Conservation Bureau. 1941.

Harwood, D. W., May, A. D., Anderson, I. B., Leiman, L., and Archilla, A.R. *Capacity and Quality of Service of Two-Lane Highways*. (NCHRP Final Report 3-55(3)). n.a.: Midwest Research Institute, University of California-Berkeley. 1999.

Hassan, Y., Halim, A. O. A. E., Easa, S. M. *Design considerations for passing sight distance and passing zones*. International symposium on highway geometric design practices. 1998.

Harwood, D. W. and Glennon, J. C. *Passing sight distance design for passenger car and trucks*. Transportation Research Record No. 1208, pp. 59-69. 1989.

Heimbach, C. L., Khasnabis, S., and Chao, G. C. *Relating no-passing zone configurations on rural two-lane highways to throughput traffic*. Highway Research Record, pp. 9-19. 1973.

Interactive highway safety design model (IHSDM). Traffic analysis module (TAM) engineer's manual. Federal Highway Administration and Turner-Fairbank Highway Research Center (TFHRC). Mar. 7, 2003.

Koorey, G. *Assessment of Rural Road Simulation Modeling Tools*. IPENZ Transportation Group Technical Conference. 2002.

Lan, C. and Menendez, M. *Truck speed profile models for critical length of grade*. Journal of Transportation Engineering. ASCE/July/August. 2003.

Lee, K. and Peng, H. *A longitudinal human driving model for adaptive cruise control performance assessment*. Proceedings of IMECE 2002: Symposium on Advanced Automotive Technologies. Nov. 17-22, 2002.

Leiman, L., Archilla, A. R., and May, A. D. *TWOPAS Model Improvements*. University of California Berkeley, California. 1998. NCHRP Project 3-55(3).

Lerner, N., Llaneras, R., Smiley, A., and Hanscom, F. *Comprehensive Human Factors Guidelines for Road Systems*. National Cooperative Highway Research Program. March, 2005.

Lieberman, E. B. *Model for calculating safe passing sight distances on two-lane rural roads*. Transportation Research Record No. 869, pp. 70-76. 1982.

Luttinen, R. T. *Properties of Cowan's M3 Headway distribution*. Transportation Research Record 1678, 1999.

Luttinen, R. T. *Statistical Properties of Vehicle Time Headways*. Transportation Research Record No. 1365, pp. 92-98. 1992.

Luttinen, R. T. *Traffic Flow on Two-lane Highways An overview*. TL Consulting Engineers, LTD. 2001.

Marsaglia, G. and Zaman, A., *A new class of random number generators*. Annals of Applied Probability, 3, pp. 462-480. 1991.

Marsaglia, G. *Random numbers fall mainly in the planes.* Proceedings of the National Academy of Sciences, 61, pp. 25-28. 1968.

May, A. D. *Traffic flow fundamentals*. Prentice Hall. Inc., Englewood Cliffs, N.J. 1990.

McLean, J. R. *Two-Lane Highway Traffic Operations: Theory and Practice*. New York: Gordon and Breach Science Publishers. 1989.

Middleton, D. *Truck accommodation design guidance: designer workshop.* Texas Transportation Institute. October. 2003.

Mills, A. *Random number generators-a brief assessment of those available*. 2003.

Modifications to HCM 2000 Chapters 12 and 20 for Compatibility of the Two-Way Segment and Directional Segment Procedures for Two-lane Highways. NCHRP 20-7, 2005.

Moler, C. *Numerical Computing with MATLAB*. 2005

Moler, C. *Random thoughts*. MATLAB News and Notes. 1995.

Normann, O. K. *Results of highway capacity studies*. Public Roads. vol. 23, no. 4, pp. 57-81. 1942.

Normann, O.K. and Walker, W.P. *Highway Capacity: Practical applications of research*. Public Roads, 25(10), pp. 201-234. 1949a.

Normann, O.K. and Walker, W.P. *Highway capacity: Practical applications of research. Public Roads*, 25(11), pp. 237-277. 1949b.

Polus, A., Craus, J., and Livneh M. *Flow and capacity characteristics on two-lane rural highways*. Transportation Research Records 1320, pp. 128-134. 1991.

Polus, A., Livneh, M., and Frischer B. *Evaluation of the passing process on two-lane rural highways*. Transportation Research Records No. 1701, pp. 53-60. 2000.

Prisk, C.W. *Passing practices on rural highways*. Proceedings of the US Highway Research Board, 21, pp. 366-78. 1941.

Roess, R. P., McShane, W. R., and Prassas, E. S. *Traffic Engineering*. Prentice Hall. 1998.

Rozic, P. *Capacity of two-lane, two-way rural highways: the new approach*. Transportation Research Records 1365, pp. 19-29. 1992.

Saal, C. C. *Hill-climbing ability of motor trucks*. Public Roads, pp. 33-54. 1941.

Sparks, Gordon A., Nuedorf, Russell D., Robinson, J. B. L., and Good, Don. *Effect of vehicle length on passing operations*. Journal of Transportation Engineering. Vol. 119, No 2, pp. 272-283. 1993.

St. John, A. D. *Nonlinear truck factor for two-lane highways*. Transportation Research Records 615, pp. 49-53. 1976.

Sullivan, D. P. and Troutbeck, R. J. *The use of Cowan's M3 headway distribution for modeling urban traffic flow*. Traffic Engineering and Control, pp. 445-450, July/August 1994

Taylor, M. A. P., Miller, A. J. and Ogden, K. W. *A comparison of some bunching models for rural traffic flow*. Transportation Research, vol. 8, pp. 1-9. 1972.

Transportation Research Board 1985. *Highway Capacity Manual*. (Special Report 209). Washington, D.C. National Research Council.

Transportation Research Board 2000. *Highway Capacity Manual*. Washington D.C. National Research Council. HCM 2000, metric units.

Transportation Simulation Systems. *AIMSUN microscopic traffic simulator: a tool for the analysis and assessment of ITS systems*. 2001.

Wang, Y. and Cartmell, M. P. *New model for passing sight distance on two-lane highways*. Journal of Transportation Engineering. 1998.

Wardrop, J. G. *Some theoretical aspects of road traffic research*. Proceedings of the Institution of Civil Engineers, vol. 1, pp. 325-378. With discussion. 1952.

Werner, A. and Morrall, J. F. *A unified traffic flow theory model for two lane rural highways*. Tribune Des Transports vol.1-3. 1984.

Yagar, S. *Capacities for two-lane highways*. Australian Road Research, 13(1). 1983.

Zhang, X. and Jarrett, D. F. *Stability analysis of the classical car-following model*. Transportation Research Board vol. 31, No. 6, pp. 441-462. 1997

Zhang, Y., Owen, L.E. and Clark, J.E. *Multiregime approach for microscopic traffic simulation*. Transportation Research Record No. 1644, pp. 103-115. 1998

APPENDICES

APPENDIX A: SUMMARY OF FIELD DATA

APPENDIX B: IMPLEMENTAION OF TWOSIM

APPENDIX C: CODE, INPUT & OUTPUT OF TWOSIM

APPENDIX D: VERIFICATION OF TWOSIM

APPENDIX E: HYPOTHESIS TEST

APPENDIX A: SUMMARY OF FIELD DATA

Histogram of free flow speeds (Science Park Road)

Free flow speed distribution in Science Park Road, State College, PA (01/03/04 and 01/08/04)

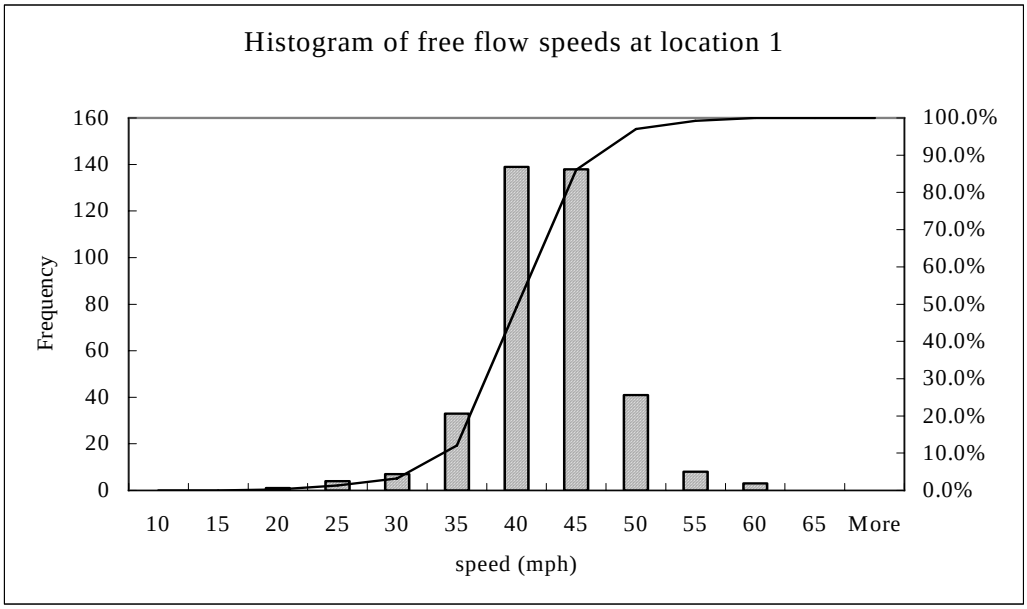

Figure A-1 Histogram of free flow speeds at location 1 (Science Park Road)

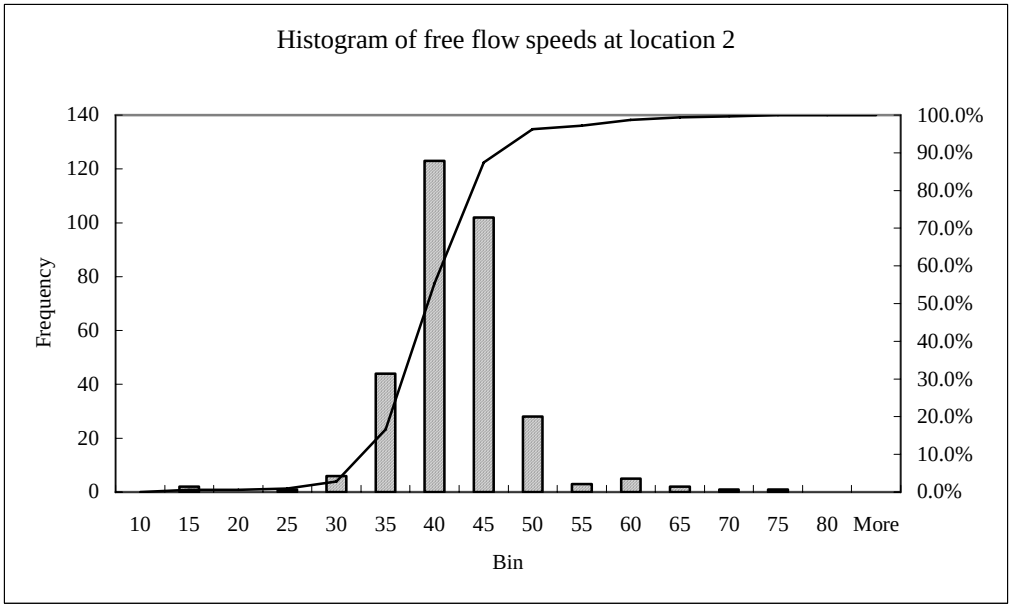

Figure A-2 Histogram of free flow speeds at location 2 (Science Park Road)

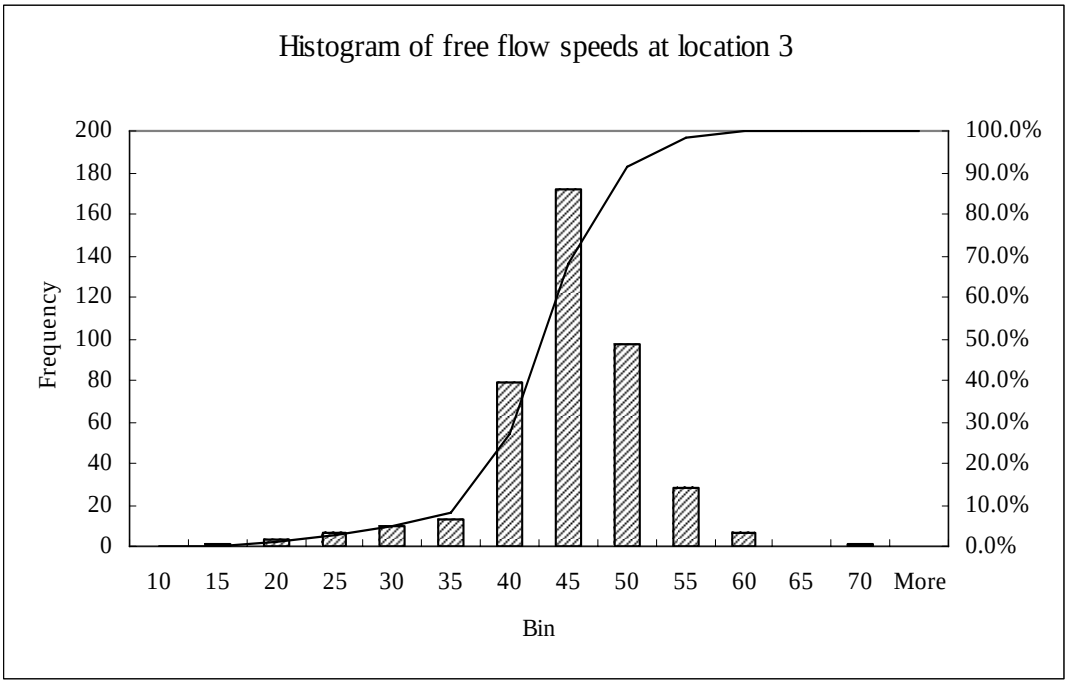

Figure A-3 Histogram of free flow speeds at location 3 (Science Park Road)

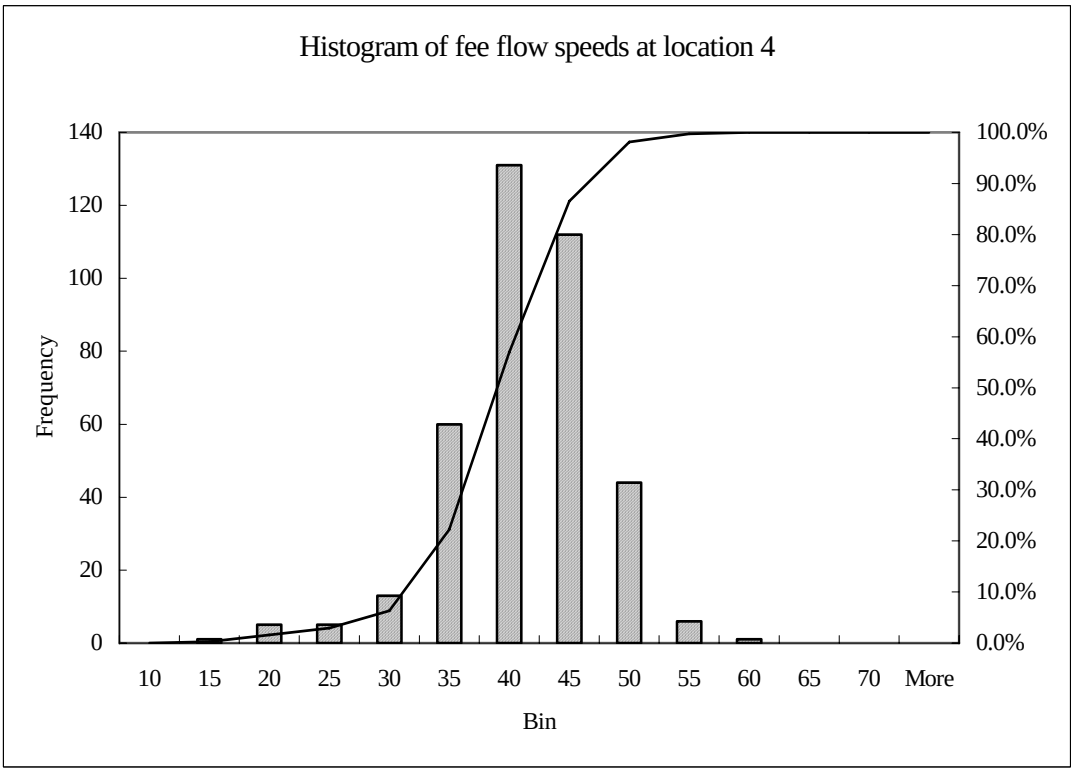

Figure A-4 Histogram of free flow speeds at location 4 (Science Park Road)

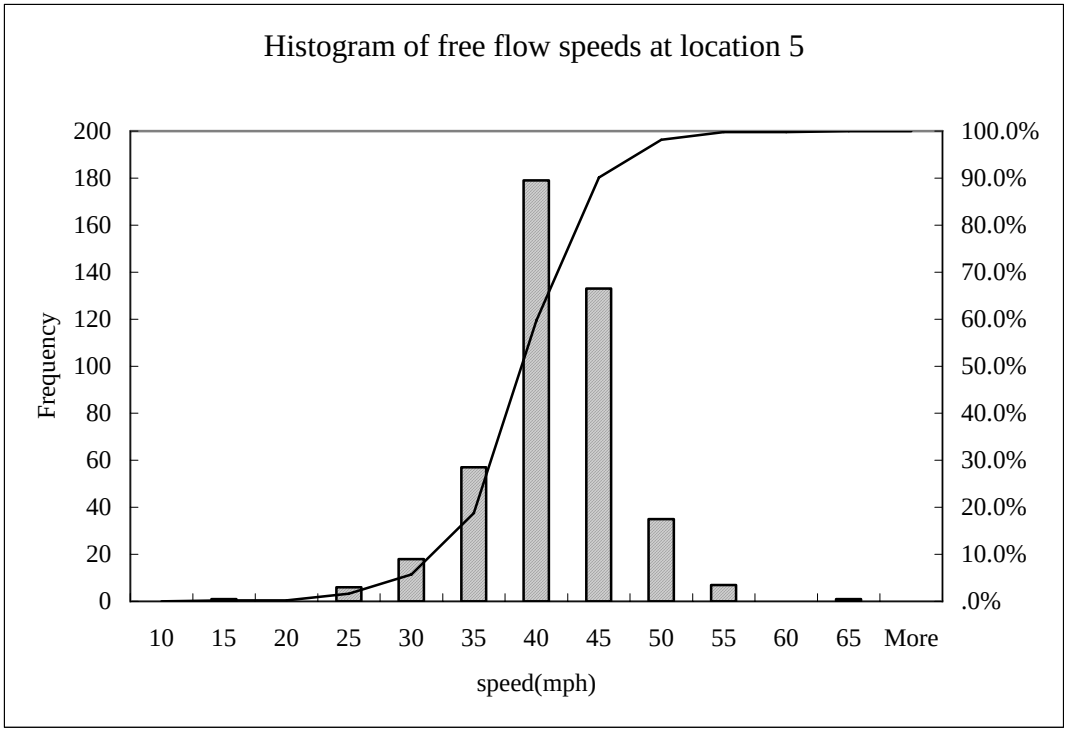

Figure A-5 Histogram of free flow speeds at location 5 (Science Park Road)

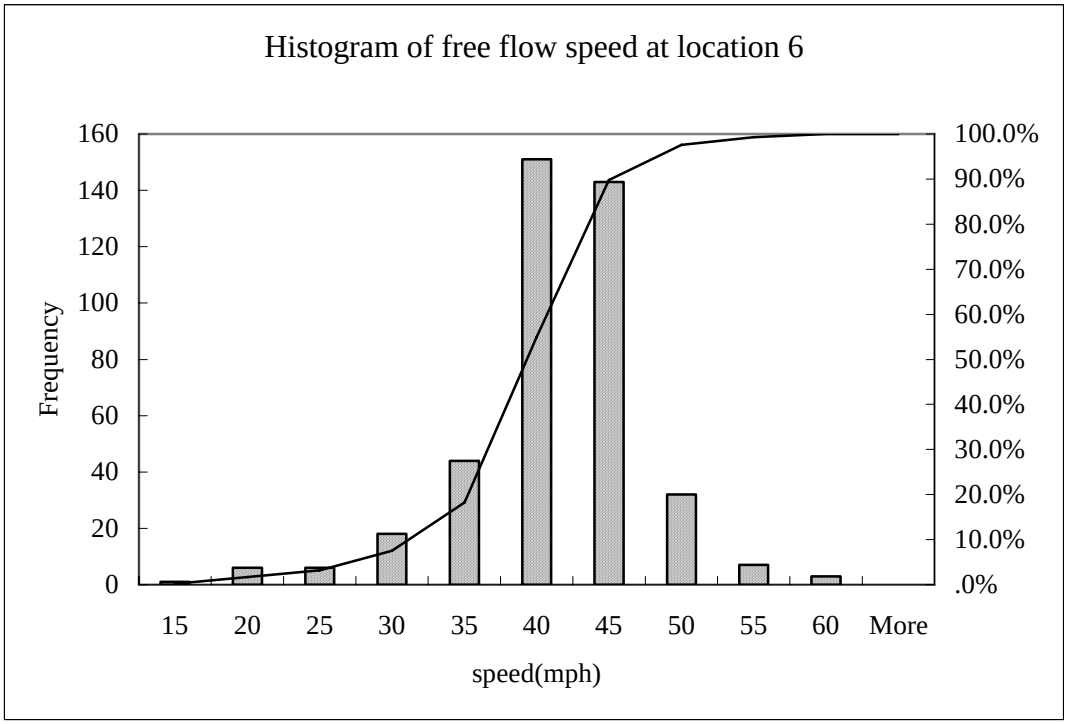

Figure A-6 Histogram of free flow speeds at location 6 (Science Park Road)

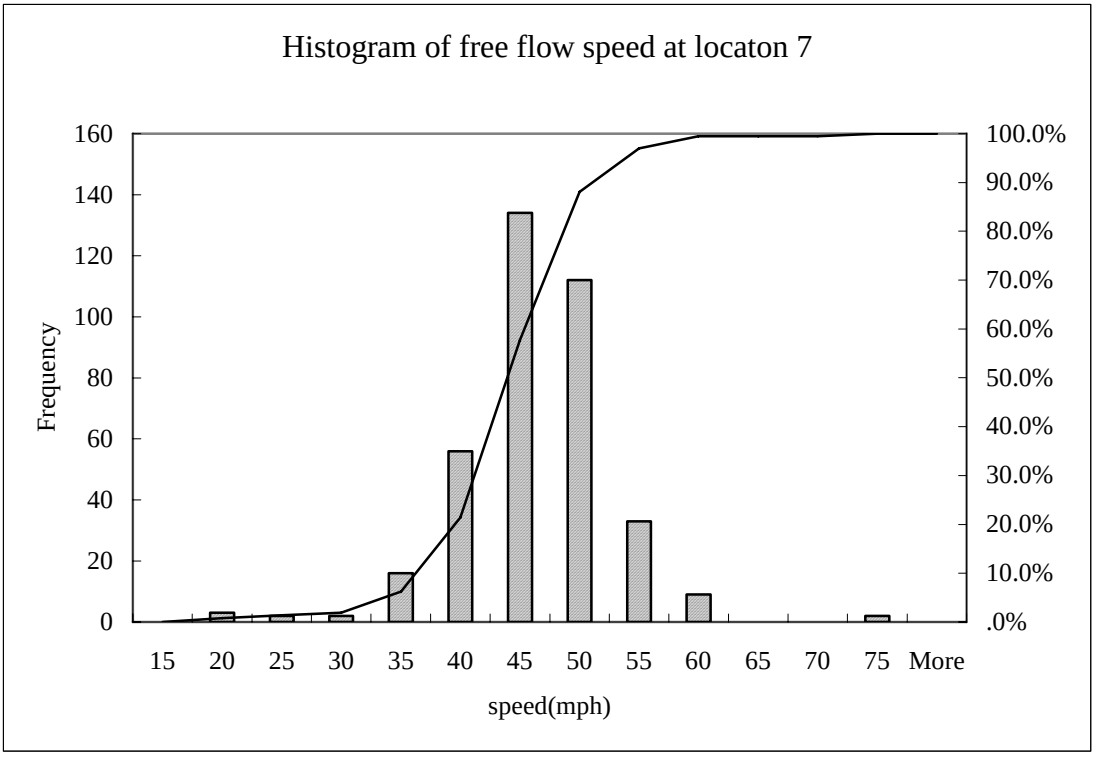

Figure A-7 Histogram of free flow speeds at location 7 (Science Park Road)

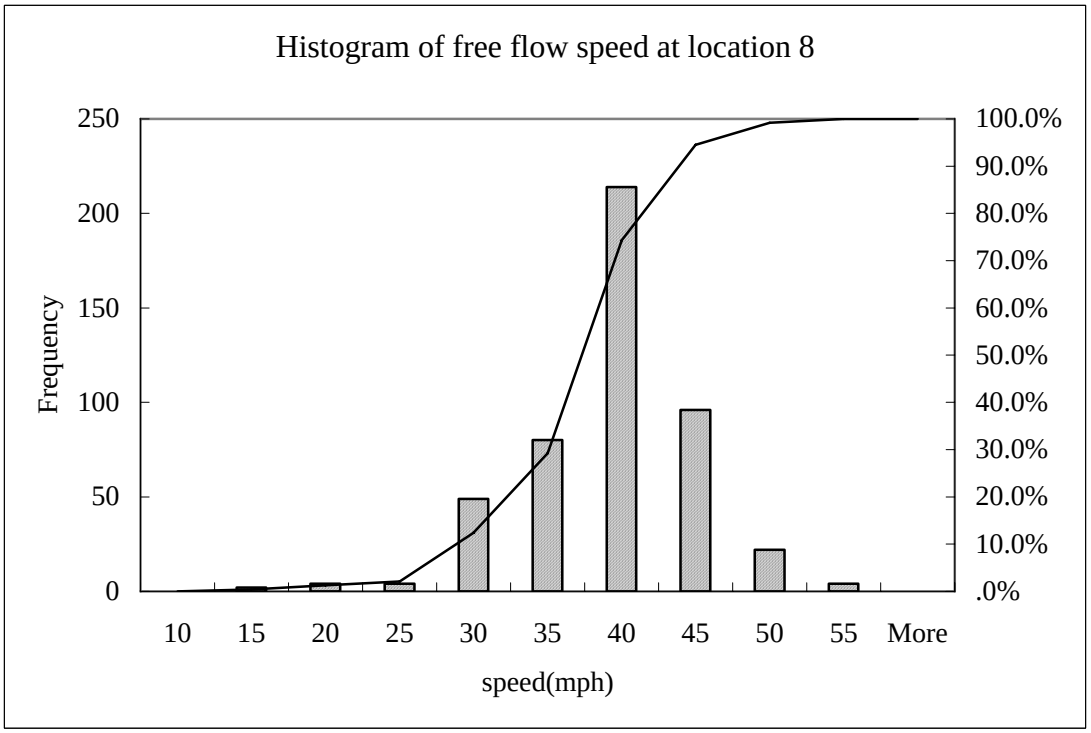

Figure A-8 Histogram of free flow speeds at location 8 (Science Park Road)

APPENDIX B: IMPLEMENTATION OF TWOSIM

Implementation of arrival headway distribution

This section describes how MATLAB determines each generated vehicle's time headway and assigns it based on Akcelik's M3A headway distribution. In Figure B-1, when a vehicle *i* is generated by the simulation, any random value (r_i) between 0 and 1 is assigned to the vehicle *i* as shown in the most left rectangle. On its right, a lookup table of cumulative density (F_i) combined with time headway (t_i) by 0.5 second increment is established.

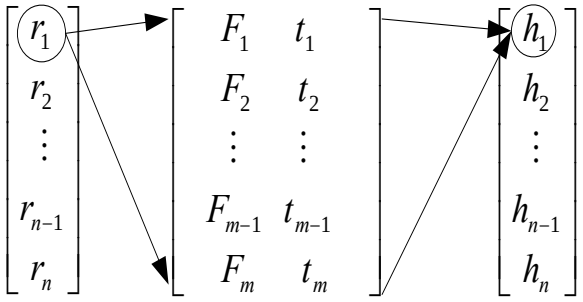

where,

r_i = *random number of vehicle i*;

F_j = *cumulative density at time step j*, $(0 \sim 1)$;

t_j = *time at time step j*,

$(t_1 = 0, t_2 = \Delta, t_3 = \Delta + \alpha(3-2), \cdots t_m = \Delta + \alpha(m-2))$;

h_i = *headway of vehicle i*;

$i = 1,\ldots,n,\ j = 1,\ldots,m$;

n = *total number of cars simulated*;

m = max*imum number of steps*;

Δ = min*imum arrival headway* (sec*onds*); *and*

α = *time increment* (0.5 sec)

Figure B- 1 Concept of *interp1* function in assigning arrival time headway in MATLAB

The *interp1* function of MATLAB uses the cumulative density function and interpolates to find the respective time headway. The time headway obtained by the *interp1* function is assigned to each vehicle. The sum of time headways in the order of arrival represents each vehicle's arrival time.

Implementation of Gipps' car-following model in TWOSIM

Maximum acceleration rate

A matrix (Table 5-4) was built into MATLAB as a lookup table so that *interp1* function in MATLAB can match and assign randomly maximum acceleration rate to each vehicle simulated in TWOSIM.

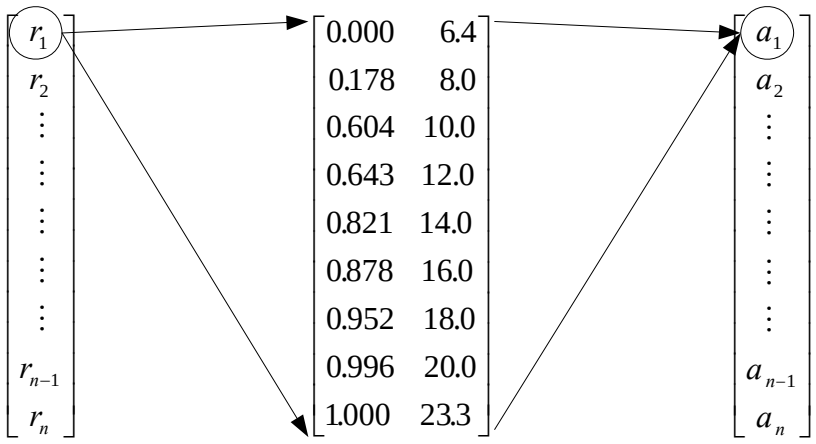

where,

r_i = *random number of vehicle i*;

a_i = max*imum acceleration rate* (ft/s^2);

$i = 1,\ldots,n$; *and*

n = *total number of cars simulated*

Figure B- 2 Diagram of assigning maximum acceleration rate using *interp1* function in MATLAB

Counting number of vehicles over analysis zone and analysis period

This section describes how TWOSIM finds the number of vehicles within a given time period in Figure 5-8. Using *interp1* function of MATLAB, TWOSIM is able to generate time data, which contains when each vehicle passes by a given observation point. The observation points are specified every 100 ft along a given study segment. Therefore, the same number of time vectors as the number of observation points are generated and stored in TWOSIM.

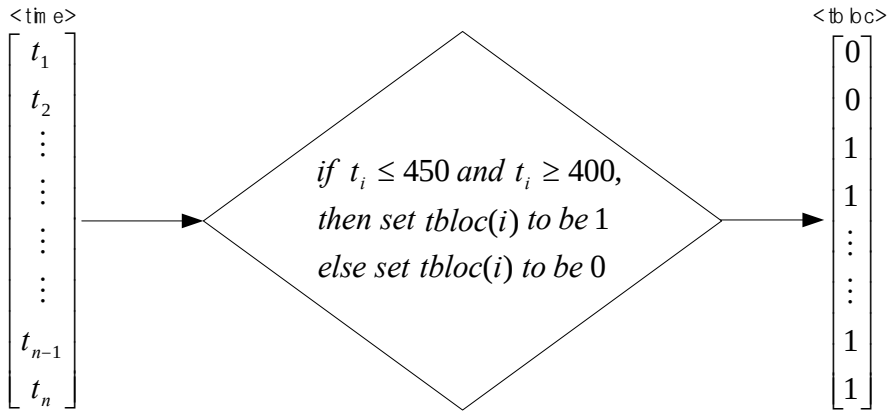

Figure B- 3 Concept of finding instant when vehicle observed at given observation point

Using a *time* column vector, if arrival time of each vehicle falls within a given analysis time (e.g., 400 ~ 450 second), then TWOSIM stores it as 1 at *tbloc* vector. Otherwise, it is stored as 0. The same number of *tbloc* column vectors as the number of observation points are stored.

In consequence, the sum of each column vector, *tbloc* represents the number of vehicles passing by a given location during a given analysis period.

Vehicle performance data

Table B- 1 Vehicle acceleration rates

Year	Make	Model	(0-60)	(1/4 Mile)	acceleration	acceleration
			Sec	sec	ft/ss	ft/ss
1990	Acura	Integra 3-Dr GS	9.2	16.8	9.6	9.4
1990	Acura	Integra GS	8.9	16.6	9.9	9.6
1990	Acura	Legend Coupe	9	17	9.8	9.1
1990	Audi	V8	9.3	17	9.5	9.1
1990	Audi	V8 Quattro	9.3	16.9	9.5	9.2
1990	Audi	Quattro Coupe	8.8	16.5	10.0	9.7
1990	BMW 3	18is	8.8	16.5	10.0	9.7
1990	BMW 3	25i	7.8	16	11.3	10.3
1990	BMW 5	25i	8	16.1	11.0	10.2
1990	BMW 5	35i	8.6	16.5	10.2	9.7
1990	BMW 7	35i	10.3	17.4	8.5	8.7
1990	Buick	LeSabre Limited	9.5	17.1	9.3	9.0
1990	Buick	Regal Limited	9.1	16.8	9.7	9.4
1990	Cadillac	Allante	7.9	16.1	11.1	10.2
1990	Cadillac	Sedan de Ville	8.8	16.6	10.0	9.6
1990	Chevrolet	Beretta GT	8.6	16.4	10.2	9.8
1990	Chevrolet	Beretta GTZ	7.7	16.1	11.4	10.2
1990	Chevrolet	Camaro IROC-Z	5.8	14.4	15.2	12.7
1990	Chevrolet	Camaro Z28	6.5	15	13.5	11.7
1990	Chevrolet	Corvette	5.7	14.3	15.4	12.9
1990	Chevrolet	Corvette ZR-1	4.4	12.8	20.0	16.1
1990	Chevrolet	Lumina APV	12.2	18.7	7.2	7.5
1990	Chevrolet	Lumina Euro Sedan	9.9	17.3	8.9	8.8
1990	Chrysler	LeBaron GTC	7.2	15.8	12.2	10.6
1990	Dodge	Daytona ES	8.4	16.2	10.5	10.1
1990	Eagle	Talon TSi AWD	6.8	15.1	12.9	11.6
1990	Ferrari	348 tb	6	14.3	14.7	12.9
1990	Ford	Escort GT	8.9	16.8	9.9	9.4
1990	Ford	Mustang LX 5.0	6.4	14.9	13.8	11.9
1990	Ford	Probe GT	7.6	16	11.6	10.3
1990	Ford	Probe LX	8.2	16.2	10.7	10.1
1990	Ford	Thunderbird SC	7.4	15.8	11.9	10.6
1990	Ford	Geo Prizm GSi	10	17.3	8.8	8.8
1990	Honda	Accord EX	10	17.2	8.8	8.9
1990	Hyundai	Excel GLS	12.5	18.6	7.0	7.6
1990	Infiniti	M30 Coupe	10	17.4	8.8	8.7
1990	Infiniti	Q45	7.2	15.4	12.2	11.1
1990	Jaguar	XJ6 Sovereign	9	16.8	9.8	9.4
1990	Jaguar	XJ6 Vanden Plas	9.2	16.9	9.6	9.2
1990	Lexus	LS 400	8.1	16.1	10.9	10.2
1990	Lincoln	Continental	11.4	18.4	7.7	7.8
1990	Lincoln	Town Car	10.2	17.5	8.6	8.6
1990	Lotus	Esprit Turbo SE	5.1	13.7	17.3	14.1
1990	Mazda	929 S	10	17.5	8.8	8.6

continued

Year	Make	Model	(0-60)	(1/4 Mile)	acceleration	acceleration
			Sec	sec	ft/ss	ft/ss
1990	Mazda	Miata	9.4	16.9	9.4	9.2
1990	Mazda	MX-5 Miata	9.5	17	9.3	9.1
1990	Mazda	Protege	9.1	16.8	9.7	9.4
1990	Mazda	Protege LX	8.9	16.8	9.9	9.4
1990	Mazda	RX-7 GTU	8.6	16.7	10.2	9.5
1990	Mazda	RX-7 Turbo II	6.3	14.9	14.0	11.9
1990	Merce	des-Benz 300E	8.7	16.8	10.1	9.4
1990	Merce	des-Benz 300E 4Matic	9.2	17	9.6	9.1
1990	Merce	des-Benz 300SL	9.1	17	9.7	9.1
1990	Merce	des-Benz 500SL	6.4	14.9	13.8	11.9
1990	Mercury	ry Sable GS	10.1	17.5	8.7	8.6
1990	Mitsubishi	Eclipse GS-T	7.4	15.9	11.9	10.4
1990	Mitsubishi	Eclipse GSX	6.9	15.2	12.8	11.4
1990	Nissan	240SX SE	8.8	16.5	10.0	9.7
1990	Nissan	300ZX	7.1	15.5	12.4	11.0
1990	Nissan	300ZX Turbo	6.5	15	13.5	11.7
1990	Nissan	300ZX Twin Turbo	5.6	14.1	15.7	13.3
1990	Oldsmobile	Cutlass Calais Quad 442	7.7	16.1	11.4	10.2
1990	Oldsmobile	Silhouette	11.6	18.4	7.6	7.8
1990	Oldsmobile	Trofeo	9.7	17.1	9.1	9.0
1990	Plymouth	Laser RS Turbo	6.9	15.4	12.8	11.1
1990	Pontiac	Formula Firehawk	4.9	13.4	18.0	14.7
1990	Pontiac	Grand Am Quad 4	7.3	15.8	12.1	10.6
1990	Pontiac	Grand Prix STE	7.7	15.6	11.4	10.8
1990	Pontiac	Sunbird Turbo	7.8	16	11.3	10.3
1990	Porsche	911 Carrera 2	5.4	14	16.3	13.5
1990	Porsche	911 Speedster	6	14.5	14.7	12.6
1990	Porsche	944 S2	6.7	14.7	13.1	12.2
1990	Saab	900 Turbo SPG	8.5	16.3	10.4	9.9
1990	Saab	9000 S	9.2	16.8	9.6	9.4
1990	Subaru	Legacy LS	10.5	17.4	8.4	8.7
1990	Toyota	Celica All-Trac	7.5	15.7	11.7	10.7
1990	Toyota	Celica GT-S	10.5	17.6	8.4	8.5
1990	Toyota	MR2 Turbo	6.2	14.7	14.2	12.2
1990	Volkswagen	Corrado	9.3	16.8	9.5	9.4
1990	Volkswagen	Corrado G60	8.9	16.5	9.9	9.7
1990	Volkswagen	Jetta GLI 16V	9	16.6	9.8	9.6
1990	Volkswagen	Passat GL	10.5	17.6	8.4	8.5
1990	Volvo	740 Turbo Wagon	7.8	16.1	11.3	10.2
1991	Acura	Legend Coupe	8.8	16.7	10.0	9.5
1991	Acura	Legend LS	7.9	16.1	11.1	10.2
1991	Acura	Legend Sedan	8.3	16.2	10.6	10.1
1991	Acura	Legend Sedan LS	8.1	16.1	10.9	10.2

continued

Year	Make	Model	(0-60)	(1/4 Mile)	acceleration	acceleration
			Sec	sec	ft/ss	ft/ss
1991	Acura	NSX	5.8	14.4	15.2	12.7
1991	Audi	90 Quattro 20V	9.4	16.9	9.4	9.2
1991	Audi	V8	6.8	15.1	12.9	11.6
1991	Audi	Quattro - 20	7.2	15.4	12.2	11.1
1991	BMW 3	18is	10	17.3	8.8	8.8
1991	BMW 5	25i	8.4	16.2	10.5	10.1
1991	BMW 7	50iL	6.5	14.8	13.5	12.1
1991	BMW 8	50i	7.4	15.6	11.9	10.8
1991	BMW M	5	6.5	14.9	13.5	11.9
1991	Buick	Park Avenue Ultra	9.6	17.1	9.2	9.0
1991	Buick	Riviera Convertable	11	17.8	8.0	8.3
1991	Cadillac	Brougham	9.4	17.1	9.4	9.0
1991	Cadillac	STS	8.6	16.6	10.2	9.6
1991	Chevrolet	Beretta GTZ	7.7	16.1	11.4	10.2
1991	Chevrolet	Corvette L98	5.3	13.9	16.6	13.7
1991	Chevrolet	Corvette Roadster	5.6	14.1	15.7	13.3
1991	Chevrolet	Lumina Z34	7.5	15.8	11.7	10.6
1991	Dodge	Spirit R/T	6.5	15	13.5	11.7
1991	Dodge	Stealth ES	7.1	15.6	12.4	10.8
1991	Dodge	Stealth R/T Turbo	6	14.5	14.7	12.6
1991	Ferrari	Mondial t Cabrio	6.6	15	13.3	11.7
1991	Ford	Crown Victoria LX	9.9	17.4	8.9	8.7
1991	Ford	Mustang GT	7.3	15.6	12.1	10.8
1991	Ford	Taurus SHO	7.7	16.2	11.4	10.1
1991	Ford	Thunderbird LX	9	16.7	9.8	9.5
1991	Honda	Accord EX Wagon	9.4	17	9.4	9.1
1991	Honda	Civic EX Sedan	9.7	17.2	9.1	8.9
1991	Honda	CRX Si	8.7	16.5	10.1	9.7
1991	Hyundai	Scoupe	11.9	18.4	7.4	7.8
1991	Infiniti	G20	8.6	16.6	10.2	9.6
1991	Infiniti	Q45	7.3	15.6	12.1	10.8
1991	Isuzu	Impulse XS	9.3	16.9	9.5	9.2
1991	Isuzu	Stylus XS	9.6	17	9.2	9.1
1991	Jaguar	XJR-15	4.5	12.6	19.6	16.6
1991	Lamborghini	Diablo	4.4	13.2	20.0	15.2
1991	Lotus	Elan SE	6.6	15.2	13.3	11.4
1991	Lotus	Turbo Esprit X-180R	4.6	13.2	19.1	15.2
1991	Mazda	Miata	9.1	16.7	9.7	9.5
1991	Mazda	MX-5 Miata	9.5	17	9.3	9.1
1991	Mazda	RX-7 Conv.	8.8	16.7	10.0	9.5
1991	Mazda	RX-7 Infini IV	7	14.9	12.6	11.9
1991	Mercedes-Benz	300CE 24V	8.5	16.6	10.4	9.6
1991	Mercedes-Benz	300SE	9.2	17	9.6	9.1

continued

Year	Make	Model	(0-60)	(1/4 Mile)	acceleration	acceleration
			Sec	sec	ft/ss	ft/ss
1991	Mercedes-Benz	500SL	6.1	14.4	14.4	12.7
1991	Mercury	Capri XR2	8.3	16.3	10.6	9.9
1991	Mercury	Cougar XR7	9.4	17.1	9.4	9.0
1991	Mercury	Tracer LTS	8.7	16.7	10.1	9.5
1991	Mitsubishi	3000GT SL	8.5	16.4	10.4	9.8
1991	Mitsubishi	3000GT VR-4	5.3	13.8	16.6	13.9
1991	Mitsubishi	Diamante LS	9	16.7	9.8	9.5
1991	Mitsubishi	Galant VR-4	7.3	15.6	12.1	10.8
1991	Nissan	240SX SE	7.9	16.1	11.1	10.2
1991	Nissan	300ZX 2+2	7.5	15.9	11.7	10.4
1991	Nissan	300ZX Turbo(auto)	7	15.4	12.6	11.1
1991	Nissan	NX 2000	7.8	16.1	11.3	10.2
1991	Oldsmobile	Bravada	12.1	18.5	7.3	7.7
1991	Oldsmobile	Ninety Eight	9.7	17.2	9.1	8.9
1991	Pontiac	Firebird Formula	6.5	14.8	13.5	12.1
1991	Pontiac	Trans Am Conv.	7	15.4	12.6	11.1
1991	Pontiac	Grand Prix STE	8.7	16.5	10.1	9.7
1991	Pontiac	Grand Prix GTP (auto)	8.4	16.3	10.5	9.9
1991	Porsche	911 Carrera 2 Tiptronic	6.9	15	12.8	11.7
1991	Porsche	911 Turbo	4.9	13.4	18.0	14.7
1991	Porsche	928 GT	5.9	14.3	14.9	12.9
1991	Porsche	928 S4	6.2	14.7	14.2	12.2
1991	Porsche	Turbo	4.6	12.9	19.1	15.9
1991	Saab	900 S Cabriolet	10.7	17.7	8.2	8.4
1991	Saab	9000 CD	9.7	17.1	9.1	9.0
1991	Saab	9000 Turbo	6.8	15.2	12.9	11.4
1991	Saturn	Coupe	8.6	16.6	10.2	9.6
1991	Saturn	SL2	8.6	16.5	10.2	9.7
1991	Subaru	Legacy Sport Sedan	8.5	16	10.4	10.3
1991	Toyota	Celica GT Conv.	9.8	17.1	9.0	9.0
1991	Toyota	Corolla LE	10.2	17.5	8.6	8.6
1991	Toyota	MR2	8.5	16.3	10.4	9.9
1991	Toyota	Paseo	10	17.3	8.8	8.8
1991	Toyota	Previa LE	12.5	18.8	7.0	7.5
1991	Toyota	Supra Turbo	7.1	15.6	12.4	10.8
1991	Toyota	Tercel LE	11.7	18.3	7.5	7.9
1991	Volkswagen	GTI 16V	8.4	16.8	10.5	9.4
1992	Acura	Integra GS-R	6.8	15.4	12.9	11.1
1992	Acura	Legend LS	7.9	16.1	11.1	10.2
1992	Acura	NSX	5.6	13.9	15.7	13.7
1992	Acura	Vigor GS	8.6	16.6	10.2	9.6
1992	Acura	Vigor LS	7.7	16.1	11.4	10.2
1992	Audi	80	9.7	17.5	9.1	8.6

continued

Year	Make	Model	(0-60)	(1/4 Mile)	Acceleration	acceleration
			Sec	sec	ft/ss	ft/ss
1992	Audi	90 Quattro	8.2	16.3	10.7	9.9
1992	Audi	100	8.4	16.5	10.5	9.7
1992	Audi	100 CS	9.6	17.2	9.2	8.9
1992	Audi	100 S	9.4	17.2	9.4	8.9
1992	Audi	S4	6.1	14.9	14.4	11.9
1992	BMW 3	18i	9.7	17.2	9.1	8.9
1992	BMW 3	25i	7.8	15.8	11.3	10.6
1992	BMW 5	25i	9.6	17.5	9.2	8.6
1992	BMW 8	50i	7.3	15.6	12.1	10.8
1992	Buick	LeSabre Limited	8.8	16.6	10.0	9.6
1992	Buick	Regal GS	9	17	9.8	9.1
1992	Buick	Skylark GS	10.3	17.6	8.5	8.5
1992	Cadillac	Allante	6.7	14.9	13.1	11.9
1992	Cadillac	Eldorado TC	8.2	16.5	10.7	9.7
1992	Cadillac	STS	8.1	16.2	10.9	10.1
1992	Chevrolet	Camaro Z28	6.7	15.2	13.1	11.4
1992	Chevrolet	Caprice Classic LTZ	10.3	17.4	8.5	8.7
1992	Chevrolet	Corvette LT1	5.7	14.1	15.4	13.3
1992	Chevrolet	Corvette ZR-1	5.6	13.9	15.7	13.7
1992	Chevrolet	Lumina APV	11.4	18.4	7.7	7.8
1992	Dodge	Spirit ES	11	17.9	8.0	8.2
1992	Dodge	Stealth R/T Turbo	5.7	14.2	15.4	13.1
1992	Dodge	Viper RT/10	4.8	13.1	18.3	15.4
1992	Eagle	Summit AWD Wagon	11	17.9	8.0	8.2
1992	Eagle	Talon TSi AWD	6.7	15.2	13.1	11.4
1992	Ferrari	512 TR	4.7	12.9	18.7	15.9
1992	Ferrari	F40	3.8	11.8	23.2	19.0
1992	Ford	Crown Victoria LX	9.5	17.1	9.3	9.0
1992	Ford	Escort LX-E	9.3	17	9.5	9.1
1992	Ford	Mustang LX 5.0	6.2	14.8	14.2	12.1
1992	Ford	Probe GT	7.9	16	11.1	10.3
1992	Ford	Taurus LX	9.4	17	9.4	9.1
1992	Ford	Taurus SHO	7.5	15.4	11.7	11.1
1992	Ford	Taurus LX Wagon	10.9	17.9	8.1	8.2
1992	Ford	Tempo GLS	10.2	17.6	8.6	8.5
1992	Honda	Accord EX	9.8	17.4	9.0	8.7
1992	Honda	Civic EX Sedan	9.4	17	9.4	9.1
1992	Honda	Civic Si	8.5	16.4	10.4	9.8
1992	Honda	Civic Si Hatchback	8.4	16.5	10.5	9.7
1992	Honda	Prelude Si 4WS	7.8	15.9	11.3	10.4
1992	Hyundai	Elantra GLS	10.5	17.7	8.4	8.4
1992	Infiniti	J30	8.9	16.7	9.9	9.5
1992	Infiniti	J30t	9.2	16.8	9.6	9.4

continued

Year	Make	Model	(0-60)	(1/4 Mile)	acceleration	acceleration
			Sec	sec	ft/ss	ft/ss
1992	Isuzu	Impulse RS	7.7	15.8	11.4	10.6
1992	Jaguar	XJS	8.3	16.3	10.6	9.9
1992	Lamborghini	Diablo	4.5	13.3	19.6	14.9
1992	Lexus	ES 300	8.6	16.6	10.2	9.6
1992	Lexus	LS 400	8	16	11.0	10.3
1992	Lexus	SC 300	7.8	15.8	11.3	10.6
1992	Lexus	SC 400	7.2	15.4	12.2	11.1
1992	Lincoln	Mark VII LSC	7.8	16.2	11.3	10.1
1992	Mazda	929	8.9	16.7	9.9	9.5
1992	Mazda	MX-3 GS	9.2	16.8	9.6	9.4
1992	Mercedes-Benz	190E 2.3	11.4	18.4	7.7	7.8
1992	Mercedes-Benz	300E	8.6	16.6	10.2	9.6
1992	Mercedes-Benz	400E	7.6	15.8	11.6	10.6
1992	Mercedes-Benz	500E	6.2	14.6	14.2	12.4
1992	Mercedes-Benz	500SEL	7.4	15.7	11.9	10.7
1992	Mercury	Sable LS	9.6	17.4	9.2	8.7
1992	Mitsubishi	3000GT VR-4	5.8	14.3	15.2	12.9
1992	Mitsubishi	Diamante LS	8.9	16.6	9.9	9.6
1992	Mitsubishi	Eclipse GSX	7	15.3	12.6	11.3
1992	Nissan	300ZX Turbo	5.7	14.2	15.4	13.1
1992	Nissan	Maxima SE	7.3	15.7	12.1	10.7
1992	Nissan	Sentra SE-R	8.1	16.2	10.9	10.1
1992	Oldsmobile	Achieva SC	7.3	15.9	12.1	10.4
1992	Oldsmobile	Achieva SCX	8	16.2	11.0	10.1
1992	Plymouth	Acclaim	11.2	17.9	7.9	8.2
1992	Plymouth	Laser RS Turbo	7.1	15	12.4	11.7
1992	Plymouth	Sundance Duster	8.4	16.3	10.5	9.9
1992	Ponitac	Bonneville SSE	9.5	17	9.3	9.1
1992	Pontiac	Bonneville SSEi	8.1	16.1	10.9	10.2
1992	Pontiac	Grand Am GT	7.5	15.9	11.7	10.4
1992	Porsche	968	5.9	14.4	14.9	12.7
1992	Saab	9000 S	10	17.4	8.8	8.7
1992	Saab	9000 Turbo	7.5	15.9	11.7	10.4
1992	Saturn	Coupe SC	8.4	16.4	10.5	9.8
1992	Subaru	SVX	7.3	15.5	12.1	11.0
1992	Toyota	Camry SE	7.7	16	11.4	10.3
1992	Toyota	Camry XLE	11.2	18.2	7.9	8.0
1992	Toyota	Paseo	10.3	17.6	8.5	8.5
1992	Volkswagen	Corrado SLC	6.8	15.3	12.9	11.3
1992	Volkswagen	Passat GL	10.9	17.8	8.1	8.3
1992	Volvo	850 GLT	9.1	16.6	9.7	9.6
1992	Volvo	940 SE	9.2	17	9.6	9.1
1992	Volvo	940 Turbo	8.9	16.8	9.9	9.4

continued

Year	Make	Model	(0-60)	(1/4 Mile)	acceleration	acceleration
			Sec	sec	ft/ss	ft/ss
1992	Volvo	960	8.9	16.5	9.9	9.7
1993	Acura	Integra GS-R	6.5	15.2	13.5	11.4
1993	Acura	Legend Coupe	7.5	15.9	11.7	10.4
1993	Acura	Legend Coupe LS	7.3	15.7	12.1	10.7
1993	Acura	Legend LS	6.7	15.4	13.1	11.1
1993	Acura	NSX	5.6	13.9	15.7	13.7
1993	Audi	90 CS Quattro Sport	8.8	16.7	10.0	9.5
1993	Audi	100 S	8.9	17	9.9	9.1
1993	Audi	100 CS Quattro Wagon	11.2	18	7.9	8.1
1993	Audi	S4	6.5	15.1	13.5	11.6
1993	Audi	V8 Quattro	7.2	15.6	12.2	10.8
1993	BMW 3	25i	8.4	16.5	10.5	9.7
1993	BMW 3	25is	7.4	15.7	11.9	10.7
1993	BMW 5	25i Touring	10	17.8	8.8	8.3
1993	BMW 5	35i	8.2	16.3	10.7	9.9
1993	BMW 5	40i	6.9	15.3	12.8	11.3
1993	BMW 7	40i	6.8	15.3	12.9	11.3
1993	BMW 7	50iL	7.7	15.8	11.4	10.6
1993	BMW 8	50i	7.2	15.6	12.2	10.8
1993	BMW M	5	6.2	14.6	14.2	12.4
1993	Buick	Roadmaster	9	16.9	9.8	9.2
1993	Cadillac	ETC	6.7	15	13.1	11.7
1993	Cadillac	Fleetwood Brougham	9.2	16.9	9.6	9.2
1993	Cadillac	Fleetwood	10	17.5	8.8	8.6
1993	Cadillac	STS	7.2	15.4	12.2	11.1
1993	Chevrolet	Camaro V-6	9	16.6	9.8	9.6
1993	Chevrolet	Camaro Z28	5.8	14.4	15.2	12.7
1993	Chevrolet	Caprice Classic	8.5	16.6	10.4	9.6
1993	Chevrolet	Corvette LT1	5.3	13.9	16.6	13.7
1993	Chevrolet	Corvette ZR-1	5.2	13.6	16.9	14.3
1993	Chrysler	Concorde	8.7	16.2	10.1	10.1
1993	Dodge	Daytona IROC R/T	6.3	14.8	14.0	12.1
1993	Dodge	Intrepid ES	8.8	16.5	10.0	9.7
1993	Dodge	Viper RT/10	4.5	13.2	19.6	15.2
1993	Eagle	Vision ESi	10.4	17.7	8.5	8.4
1993	Eagle	Vision TSi	8.9	16.6	9.9	9.6
1993	Ferrari	348 tb Serie Speciale	5.6	14	15.7	13.5
1993	Ferrari	348 Spider	5.6	14.1	15.7	13.3
1993	Ford	Escort GT	8.4	16.5	10.5	9.7
1993	Ford	Escort LX Wagon	12.8	19.1	6.9	7.2
1993	Ford	Mustang Cobra	5.9	14.5	14.9	12.6
1993	Ford	Mustang GT(auto)	8	16.1	11.0	10.2
1993	Ford	Probe GT	7.5	15.8	11.7	10.6

continued

Year	Make	Model	(0-60)	(1/4 Mile)	acceleration	acceleration
			Sec	sec	ft/ss	ft/ss
1993	Ford	Taurus GL	11.1	18	7.9	8.1
1993	Ford	Taurus SHO	7.5	17	11.7	9.1
1993	Geo Metro	LSi Convertible	13.8	19.4	6.4	7.0
1993	Geo Prizm	LSi	10.7	17.7	8.2	8.4
1993	Geo Storm	GSi	8.7	16.7	10.1	9.5
1993	Honda	Accord LX	10.1	17.6	8.7	8.5
1993	Honda	Civic Coupe EX	8.4	16.5	10.5	9.7
1993	Honda	Civic del Sol Si	8.8	16.8	10.0	9.4
1993	Hyundai	Scoupe Turbo	8.3	16.3	10.6	9.9
1993	Infiniti	J30t	9	16.8	9.8	9.4
1993	Infiniti	iti Q45	7.5	15.6	11.7	10.8
1993	Jaguar	XJ12 Sedan	7.5	15.9	11.7	10.4
1993	Jaguar	XJR-S Coupe	7	15.2	12.6	11.4
1993	Jaguar	XJS Coupe	7.8	15.9	11.3	10.4
1993	Lexus	GS 300	9.2	16.8	9.6	9.4
1993	Lexus	LS 400	8.2	16.2	10.7	10.1
1993	Lexus	SC 300	7.4	15.7	11.9	10.7
1993	Lexus	SC 400	7.2	15.4	12.2	11.1
1993	Lincoln	Mark VIII	7.1	15.4	12.4	11.1
1993	Lotus	Esprit Turbo S4	4.8	13.3	18.3	14.9
1993	Mazda	626 ES	7.7	16	11.4	10.3
1993	Mazda	626 LX (auto)	11.4	18.3	7.7	7.9
1993	Mazda	MX-3	10.3	17.6	8.5	8.5
1993	Mazda	MX-6 LS	7.4	15.7	11.9	10.7
1993	Mazda	RX-7	5.5	14	16.0	13.5
1993	Mazda	RX-7 R1	5.3	13.9	16.6	13.7
1993	Mercedes-Benz	300CE Conv.	8.1	16.1	10.9	10.2
1993	Mercedes-Benz	400E	7.2	15.4	12.2	11.1
1993	Mercedes-Benz	500E	6.3	14.7	14.0	12.2
1993	Mercedes-Benz	600SEC	6.5	14.8	13.5	12.1
1993	Mercedes-Benz	600SEL	6.6	15.2	13.3	11.4
1993	Mitsubishi	3000GT VR-4	5.3	14	16.6	13.5
1993	Mitsubishi	Diamante Wagon	10.1	17.5	8.7	8.6
1993	Mitsubishi	Eclipse GSX	6.8	15.2	12.9	11.4
1993	Mitsubishi	Galant GS	8.3	16.4	10.6	9.8
1993	Mitsubishi	Galant LS	9.4	17.2	9.4	8.9
1993	Mitsubishi	Mirage Coupe LS	11	18	8.0	8.1
1993	Nissan	240SX Convertible	9.6	17.3	9.2	8.8
1993	Nissan	240SX SE	8.4	16.3	10.5	9.9
1993	Nissan	300ZX Turbo	5.2	13.8	16.9	13.9
1993	Nissan	Altima SE	8.2	16.4	10.7	9.8
1993	Nissan	Altima GXE (auto)	9.6	17.2	9.2	8.9
1993	Nissan	NX 1600	9.9	17.3	8.9	8.8

continued

Year	Make	Model	(0-60)	(1/4 Mile)	acceleration	acceleration
			Sec	sec	ft/ss	ft/ss
1993	Nissan	Sentra SE-R	7.6	15.8	11.6	10.6
1993	Oldsmobile	Cutlass Conv.	8.5	16.5	10.4	9.7
1993	Pontiac	Bonneville SLE	8.6	16.5	10.2	9.7
1993	Pontiac	Firebird Firehawk	4.9	13.5	18.0	14.5
1993	Pontiac	Firebird Formula	6.1	14.7	14.4	12.2
1993	Pontiac	Firebird Trans Am	6.3	14.8	14.0	12.1
1993	Pontiac	Sunbird SE Conv.	9.2	16.7	9.6	9.5
1993	Pontiac	Sunbird	9.2	16.7	9.6	9.5
1993	Porsche	911 RS America	5.3	13.8	16.6	13.9
1993	Porsche	911 Turbo 3.6	4.4	12.7	20.0	16.4
1993	Porsche	928 GTS	6.1	14.5	14.4	12.6
1993	Porsche	968	6.6	14.9	13.3	11.9
1993	Porsche	Carrera 2 Cabr.	6	14.4	14.7	12.7
1993	Saturn	SC1	11.5	18.3	7.7	7.9
1993	Saturn	SW2 Wagon	9.3	17.1	9.5	9.0
1993	Subaru	Impreza L	10.6	17.9	8.3	8.2
1993	Subaru	Impreza L Wagon	12.7	19	6.9	7.3
1993	Subaru	Impreza LS AWD	12.1	18.8	7.3	7.5
1993	Subaru	SVX	8.7	16.2	10.1	10.1
1993	Toyota	Camry LE	11	18.2	8.0	8.0
1993	Toyota	Corolla DX	9.3	17	9.5	9.1
1993	Toyota	Corolla DX Wagon	10.8	17.9	8.1	8.2
1993	Toyota	MR2 Turbo	6.1	14.7	14.4	12.2
1993	Toyota	Paseo	10.1	17.8	8.7	8.3
1993	Toyota	Supra Turbo	4.9	13.4	18.0	14.7
1993	Volks	wagen Cabriolet	11.2	18.1	7.9	8.1
1993	Volks	wagen Corrado SLC	6.9	15.5	12.8	11.0
1993	Volks	wagen Passat GLX	8.5	16.6	10.4	9.6
1993	Volvo	850 GLT	9.4	17.3	9.4	8.8
1994	Acura	Integra GS-R	7.1	15.5	12.4	11.0
1994	Acura	Integra LS	7.6	16	11.6	10.3
1994	Acura	NSX	5.3	13.6	16.6	14.3
1994	Audi	Cabriolet	9.7	17.1	9.1	9.0
1994	BMW 3	18is	10.1	17.5	8.7	8.6
1994	BMW 3	25i	7.4	15.5	11.9	11.0
1994	BMW 3	25is	7.2	15.9	12.2	10.4
1994	BMW 3	25i Conv.	7.3	15.9	12.1	10.4
1994	BMW 5	30i	7	15.5	12.6	11.0
1994	BMW 5	30i Touring	8.9	16.7	9.9	9.5
1994	BMW 5	40i	7.9	16	11.1	10.3
1994	BMW 7	40iL	7.7	15.9	11.4	10.4
1994	BMW 7	50iL	7.7	15.9	11.4	10.4
1994	BMW 8	40Ci	7.4	15.6	11.9	10.8

continued

Year	Make	Model	(0-60)	(1/4 Mile)	acceleration	acceleration
			Sec	sec	ft/ss	ft/ss
1994	BMW 8	50CSi	5.8	14.1	15.2	13.3
1994	BMW 8	50i	6.3	14.9	14.0	11.9
1994	Buick	Park Avenue Ultra	7.3	15.5	12.1	11.0
1994	Cadillac	DeVille Concours	7.8	15.8	11.3	10.6
1994	Chevrolet	Camaro Z28	5.7	14.2	15.4	13.1
1994	Chevrolet	Camaro Z28 Conv.	6.2	14.5	14.2	12.6
1994	Chevrolet	Corvette LT1(auto)	5.5	14.1	16.0	13.3
1994	Chevrolet	Corvette ZR-1	4.7	13.1	18.7	15.4
1994	Chevrolet	Impala SS	7.1	15.4	12.4	11.1
1994	Chrysler	Cirrus LXi	10.3	17.5	8.5	8.6
1994	Chrysler	LHS	8.7	16.5	10.1	9.7
1994	Dodge	Intrepid	10.3	17.5	8.5	8.6
1994	Ferrari	456 GT	4.8	13.3	18.3	14.9
1994	Ford	Escort LX Sedan	11.1	17.8	7.9	8.3
1994	Ford	Mustang Cobra	6.9	15.3	12.8	11.3
1994	Ford	Mustang GT	6.7	15.1	13.1	11.6
1994	Ford	Probe GT	7.5	15.3	11.7	11.3
1994	Ford	Taurus GL	10	17.5	8.8	8.6
1994	Ford	Taurus LX	9.2	17	9.6	9.1
1994	Ford	Thunderbird LX	8.5	16.4	10.4	9.8
1994	Honda	Accord EX	9.3	17.1	9.5	9.0
1994	Honda	Accord EX Coupe	9.2	16.9	9.6	9.2
1994	Honda	Civic del Sol VTEC	7.4	15.8	11.9	10.6
1994	Honda	Civic EX Sedan	8.8	16.8	10.0	9.4
1994	Honda	Prelude VTEC	7.2	15.1	12.2	11.6
1994	Infiniti	G20t	8.4	16.5	10.5	9.7
1994	Infiniti	Q45t	7.2	15.4	12.2	11.1
1994	Jaguar	XJ12	7.7	15.9	11.4	10.4
1994	Kia	Sephia GS	10.2	17.5	8.6	8.6
1994	Lexus	ES 300	8.7	16.6	10.1	9.6
1994	Lexus	GS 300	9.4	16.8	9.4	9.4
1994	Mazda	Miata	9.7	17	9.1	9.1
1994	Mazda	Millenia S	7.6	15.8	11.6	10.6
1994	Mazda	MX-5 Miata	8.8	16.6	10.0	9.6
1994	Mazda	MX-6 LS	7.6	15.8	11.6	10.6
1994	Mazda	RX-7	5.3	14	16.6	13.5
1994	Mazda	RX-7 Touring	6	14.5	14.7	12.6
1994	Mercedes-Benz	500SL	6.3	14.6	14.0	12.4
1994	Mercedes-Benz	600SEL	6.7	14.9	13.1	11.9
1994	Mercedes-Benz	C220	8.7	16.9	10.1	9.2
1994	Mercedes-Benz	C280	7.8	16.1	11.3	10.2
1994	Mercedes-Benz	C280 (auto)	8.4	16.5	10.5	9.7
1994	Mitsubishi	3000GT VR-4	5.7	14.2	15.4	13.1

continued

Year	Make	Model	(0-60)	(1/4 Mile)	acceleration	acceleration
			Sec	sec	ft/ss	ft/ss
1994	Mitsubishi	bishi Mirage Coupe LS	8.7	16.6	10.1	9.6
1994	Nissan	300ZX Turbo	6	14.4	14.7	12.7
1994	Nissan	Altima GXE	9.4	16.9	9.4	9.2
1994	Nissan	Maxima SE (auto)	8.8	16.7	10.0	9.5
1994	Nissan	Sentra SE-R	7.4	15.8	11.9	10.6
1994	Oldsmobile	Eighty Eight LSS	8	16.5	11.0	9.7
1994	Oldsmobile	Silhouette	9.7	17.2	9.1	8.9
1994	Plymouth	Neon Highline	8.4	16.3	10.5	9.9
1994	Pontiac	Firebird Formula	5.8	14.1	15.2	13.3
1994	Pontiac	Grand Am SE	11.5	18.2	7.7	8.0
1994	Porsche	911 Carrera	5.2	13.8	16.9	13.9
1994	Porsche	911 Speedster	5.4	14	16.3	13.5
1994	Porsche	911 Turbo 3.6	4.5	12.9	19.6	15.9
1994	Saab	900 SE	7.9	15.8	11.1	10.6
1994	Saab	9000 Aero	7.4	15.7	11.9	10.7
1994	Toyota	Camry SE Coupe	8.1	16.1	10.9	10.2
1994	Toyota	Celica GT	8.4	16.4	10.5	9.8
1994	Toyota	Celica GT Coupe	8.5	16.4	10.4	9.8
1994	Toyota	MR2	6.2	14.8	14.2	12.1
1994	Toyota	Supra	6.9	15.2	12.8	11.4
1994	Toyota	Supra Turbo	5.3	13.7	16.6	14.1
1994	Volks	wagen Corrado SLC	7.2	15.6	12.2	10.8
1994	Volks	wagen Golf III GL	9.8	16.7	9.0	9.5
1994	Volks	wagen Jetta III GL	10.1	17.6	8.7	8.5
1994	Volks	wagen Passat GLX (auto)	8.9	16.9	9.9	9.2
1994	Volvo	850 Turbo Sedan	7.1	15.3	12.4	11.3
1994	Volvo	850 Sportwagon Turbo	7.4	15.5	11.9	11.0
1995	Audi	A6	9.2	16.9	9.6	9.2
1995	BMW 3	18i	8.8	16.6	10.0	9.6
1995	BMW 3	18i Conv.	9.7	17.4	9.1	8.7
1995	BMW 3	18ti	8.9	16.6	9.9	9.6
1995	BMW 3	25i	7.7	16	11.4	10.3
1995	BMW 3	25i Conv.	9.1	16.9	9.7	9.2
1995	BMW 5	40i	6.2	14.8	14.2	12.1
1995	BMW 7	40i	8.4	16.6	10.5	9.6
1995	BMW 7	40iL	7.9	16	11.1	10.3
1995	BMW 7	50iL	6.3	14.8	14.0	12.1
1995	BMW M	3	6.2	14.6	14.2	12.4
1995	BMW M	3 Lightweight	5.3	13.9	16.6	13.7
1995	Buick	Regal GS	8.2	16	10.7	10.3
1995	Buick	Riviera	7.8	15.9	11.3	10.4
1995	Buick	Roadmaster Limited	6.7	15	13.1	11.7
1995	Cadillac	DeVille Concours	6.9	15.2	12.8	11.4

continued

Year	Make	Model	(0-60)	(1/4 Mile)	acceleration	acceleration
			Sec	sec	ft/ss	ft/ss
1995	Cadillac	ETC	6.6	14.8	13.3	12.1
1995	Cadillac	STS	6.4	14.7	13.8	12.2
1995	Chevrolet	Camaro Z28	5.7	14.2	15.4	13.1
1995	Chevrolet	Camaro 3800	7.4	15.7	11.9	10.7
1995	Chevrolet	Cavalier LS	10.9	18	8.1	8.1
1995	Chevrolet	Corvette LT1	5.2	13.7	16.9	14.1
1995	Chevrolet	Corvette ZR-1	4.9	13.1	18.0	15.4
1995	Chevrolet	Impala SS	7	15.4	12.6	11.1
1995	Chevrolet	Lumina	9.5	17	9.3	9.1
1995	Chevrolet	Lumina LS	9.5	17	9.3	9.1
1995	Chevrolet	Monte Carlo	7.8	16	11.3	10.3
1995	Chevrolet	Monte Carlo Z34	7.8	15.5	11.3	11.0
1995	Chrysler	Cirrus LXi	9.4	17.2	9.4	8.9
1995	Chrysler	New Yorker	8.9	16.7	9.9	9.5
1995	Chrysler	Sebring LX	8.6	16.6	10.2	9.6
1995	Dodge	Avenger	10	17.1	8.8	9.0
1995	Dodge	Avenger ES	9.3	17.1	9.5	9.0
1995	Dodge	Neon Sport Coupe	8	16.2	11.0	10.1
1995	Dodge	Stratus ES	9.4	17	9.4	9.1
1995	Eagle	Talon TSi	6.4	15.1	13.8	11.6
1995	Ferrari	333 SP	3.6	11.3	24.4	20.7
1995	Ferrari	456 GT	5.1	13.4	17.3	14.7
1995	Ferrari	F355 Berlinetta	4.7	12.8	18.7	16.1
1995	Ford	Contour SE	9.5	17.2	9.3	8.9
1995	Ford	Mustang 3.8	9.9	17.3	8.9	8.8
1995	Ford	Mustang Cobra R	5.2	13.8	16.9	13.9
1995	Ford	Taurus SHO	7.7	15.8	11.4	10.6
1995	Ford	Thunderbird SC	7	15.2	12.6	11.4
1995	Geo Metro	LSi	12.7	18.8	6.9	7.5
1995	Honda	Accord LX	8.5	16.5	10.4	9.7
1995	Honda	Accord LX V-6	9.1	17.1	9.7	9.0
1995	Honda	Civic EX	8.8	16.8	10.0	9.4
1995	Honda	Odyssey EX	10.3	18.3	8.5	7.9
1995	Honda	Prelude VTEC	6.7	15.1	13.1	11.6
1995	Hyundai	Accent	11.2	18.2	7.9	8.0
1995	Hyundai	Sonata GLS	9.8	17.5	9.0	8.6
1995	Infiniti	I30	7.8	16	11.3	10.3
1995	Infiniti	Q45t	7.9	16.2	11.1	10.1
1995	Jaguar	XJR	6.6	14.9	13.3	11.9
1995	Lamborghini	Diablo VT	4.7	13.2	18.7	15.2
1995	Lexus	ES 300	8.4	16.4	10.5	9.8
1995	Lexus	LS 400	7.4	15.5	11.9	11.0
1995	Lexus	SC 400	7	15.2	12.6	11.4

continued

Year	Make	Model	(0-60)	(1/4 Mile)	acceleration	acceleration
			Sec	sec	ft/ss	ft/ss
1995	Lincoln	Continental	7.7	15.9	11.4	10.4
1995	Lincoln	Mark VIII	7.6	15.8	11.6	10.6
1995	Mazda	626 LS V-6	9.5	17.4	9.3	8.7
1995	Mazda	Millenia S	8	16	11.0	10.3
1995	Mazda	Protege ES	8.7	16.6	10.1	9.6
1995	Mazda	Protege LX	10.6	17.8	8.3	8.3
1995	Mazda	RX-7 R2	5.3	14.1	16.6	13.3
1995	Mercedes-Benz	C36	6	14.5	14.7	12.6
1995	Mercedes-Benz	C280	7.9	16	11.1	10.3
1995	Mercedes-Benz	Cabriolet (auto)	8.7	16.5	10.1	9.7
1995	Mercedes-Benz	E420 (auto)	7.1	15.3	12.4	11.3
1995	Mercury	Grand Marquis LS	8.4	16.3	10.5	9.9
1995	Mitsubishi	3000GT VR-4	5.4	13.5	16.3	14.5
1995	Mitsubishi	Eclipse GS	9	16.6	9.8	9.6
1995	Mitsubishi	Eclipse GS-T	6.4	15	13.8	11.7
1995	Mitsubishi	Eclipse GSX	6.4	14.9	13.8	11.9
1995	Nissan	200SX SE-R	8.2	16.4	10.7	9.8
1995	Nissan	240SX SE	8.3	16.1	10.6	10.2
1995	Nissan	240SX SE-R	8	15.8	11.0	10.6
1995	Nissan	300ZX Turbo	5.5	13.9	16.0	13.7
1995	Nissan	Maxima SE	7.4	15.7	11.9	10.7
1995	Nissan	Sentra GLE	11	18.1	8.0	8.1
1995	Nissan	Sentra GXE	9.6	17.3	9.2	8.8
1995	Oldsmobile	Aurora	8.2	16.3	10.7	9.9
1995	Plymouth	Neon Sport	8.4	16.3	10.5	9.9
1995	Pontiac	Bonneville SE	7.1	15.4	12.4	11.1
1995	Pontiac	SLP Firehawk	5.3	13.9	16.6	13.7
1995	Pontiac	Firebird Formula	6.7	15.1	13.1	11.6
1995	Pontiac	Firebird Trans Am	5.6	14	15.7	13.5
1995	Porsche	911 Cabriolet	6.4	14.5	13.8	12.6
1995	Porsche	911 Carrera	5.3	13.8	16.6	13.9
1995	Saab	900 Turbo Coupe	6.8	15.2	12.9	11.4
1995	Subaru	Legacy L Wagon	10.9	17.7	8.1	8.4
1995	Toyota	Avalon	7.8	15.8	11.3	10.6
1995	Toyota	Avalon XLS (auto)	8.5	16.5	10.4	9.7
1995	Toyota	Camry LE	8	16	11.0	10.3
1995	Toyota	Camry LE V-6 (auto)	8.4	16.3	10.5	9.9
1995	Toyota	Corolla DX	10.2	17.6	8.6	8.5
1995	Toyota	MR2 Turbo	6.2	14.8	14.2	12.1
1995	Toyota	Supra Turbo	5.1	13.5	17.3	14.5
1995	Toyota	Tercel DX	11.2	18.4	7.9	7.8
1995	Volkswagen	GTI VR6	7.1	15.5	12.4	11.0
1995	Volkswagen	Jetta III GLX	7.7	16.1	11.4	10.2

continued

Year	Make	Model	(0-60)	(1/4 Mile)	acceleration	acceleration
			Sec	sec	ft/ss	ft/ss
1995	Volkswagen	Passat GLX	9.5	17.2	9.3	8.9
1995	Volvo	850 T-5R	6.6	15	13.3	11.7
1996	Acura	3.2TL	8.1	16.4	10.9	9.8
1996	Acura	Integra GS-R	7.1	15.5	12.4	11.0
1996	Acura	Integra SE	7.9	16.1	11.1	10.2
1996	Acura	NSX	5.2	13.8	16.9	13.9
1996	Acura	NSX-T	5.8	14.3	15.2	12.9
1996	Acura	SLX Premium Pkg.	11.1	18.1	7.9	8.1
1996	Audi	A6 Quattro Wagon	10.1	17.5	8.7	8.6
1996	Audi	A4	8.9	16.8	9.9	9.4
1996	BMW 3	18ti	8.4	16.4	10.5	9.8
1996	BMW 3	28i Sport	6.4	15	13.8	11.7
1996	BMW 5	25i Touring	8.8	16.8	10.0	9.4
1996	BMW 5	40i Sport	5.8	14.4	15.2	12.7
1996	BMW 7	40i	7.7	15.9	11.4	10.4
1996	BMW 7	50iL	6.4	14.7	13.8	12.2
1996	BMW M	3 Automatic	6.7	15.3	13.1	11.3
1996	BMW M	3 Luxury	6.6	14.9	13.3	11.9
1996	Cadillac	DeVille Concours	7.2	15.4	12.2	11.1
1996	Cadillac	STS	6.4	14.7	13.8	12.2
1996	Chevrolet	Camaro Z28	5.7	14.1	15.4	13.3
1996	Chevrolet	Camaro Z28 SS	5.3	13.8	16.6	13.9
1996	Chevrolet	Cavalier LS	8.3	16.1	10.6	10.2
1996	Chevrolet	Corvette Collectors'	4.9	13.3	18.0	14.9
1996	Chevrolet	Corvette Grand Sport	4.7	13.3	18.7	14.9
1996	Chevrolet	Impala SS	7.3	15.6	12.1	10.8
1996	Chrysler	Sebring JXi Conv.	10	17.4	8.8	8.7
1996	Dodge	Neon Highline	9.1	16.8	9.7	9.4
1996	Dodge	Viper RT/10	5	13.2	17.6	15.2
1996	Ferrari	F355 Spider	4.9	13.4	18.0	14.7
1996	Ford	Mustang Cobra	5.5	14	16.0	13.5
1996	Ford	Taurus	8.7	16.5	10.1	9.7
1996	Ford	Taurus GL	10	17.5	8.8	8.6
1996	Ford	Taurus LX Wagon	8.9	16.7	9.9	9.5
1996	Honda	Accord EX V-6	8.8	16.8	10.0	9.4
1996	Honda	Civic Coupe HX	9.4	17.1	9.4	9.0
1996	Honda	Civic EX Sedan	10.5	17.6	8.4	8.5
1996	Honda	Civic LX Sedan	9.4	17.2	9.4	8.9
1996	Infiniti	I30t	7.7	15.8	11.4	10.6
1996	Isuzu	Hombre XS	12.1	18.8	7.3	7.5
1996	Jaguar	XJ6	7.6	15.8	11.6	10.6
1996	Kia	Sephia LS	10.7	18	8.2	8.1
1996	Lexus	LX 450	10.4	17.8	8.5	8.3

continued

Year	Make	Model	(0-60)	(1/4 Mile)	acceleration	acceleration
			Sec	sec	ft/ss	ft/ss
1996	Lincoln	Mark VIII	7.2	15.4	12.2	11.1
1996	Lotus	Esprit S4S	4.7	13.3	18.7	14.9
1996	Mazda	Miata	8.7	16.6	10.1	9.6
1996	Mercedes-Benz	C220	9	16.9	9.8	9.2
1996	Mercedes-Benz	C280 Sport	7.3	15.8	12.1	10.6
1996	Mercedes-Benz	E320	7.1	15.4	12.4	11.1
1996	Plymouth	Breeze (auto)	12.5	18.9	7.0	7.4
1996	Plymouth	Breeze	9.9	17.5	8.9	8.6
1996	Pontiac	Bonneville SE	7.7	15.8	11.4	10.6
1996	Pontiac	Firebird Formula	5.8	14.3	15.2	12.9
1996	Pontiac	Grand Am SE	8.6	16.5	10.2	9.7
1996	Pontiac	Sunfire GT	7.9	15.9	11.1	10.4
1996	Porsche	911 Targa	5	13.5	17.6	14.5
1996	Porsche	911 Turbo	3.7	12.1	23.8	18.0
1996	Saab	900 S	8.4	16.3	10.5	9.9
1996	Saturn	SL1	9.7	17.2	9.1	8.9
1996	Subaru	Legacy Outback	9.8	17.4	9.0	8.7
1996	Toyota	Paseo	9.5	17	9.3	9.1
1996	Volvo	850 GLT	8.8	16.6	10.0	9.6
1996	Volvo	850 R	6.9	15.3	12.8	11.3
1997	Acura	2.2CL	8.9	16.7	9.9	9.5
1997	Acura	Integra Type R	7	15.3	12.6	11.3
1997	Acura	NSX-T	4.8	13.3	18.3	14.9
1997	Audi	A8 Quattro	6.7	15	13.1	11.7
1997	BMW 5	28i (auto)	7.5	15.8	11.7	10.6
1997	BMW 5	28i (manual)	6.8	15.3	12.9	11.3
1997	BMW 5	40i	6.2	14.6	14.2	12.4
1997	BMW M	3 Sedan	5.5	14	16.0	13.5
1997	BMW Z	3 2.8	6.2	14.7	14.2	12.2
1997	Buick	Regal GS	6.6	15	13.3	11.7
1997	Buick	Regal LS	7.8	16	11.3	10.3
1997	Cadillac	Catera	8.5	16.5	10.4	9.7
1997	Chevrolet	Corvette	4.7	13.3	18.7	14.9
1997	Dodge	Viper GTS	4	12.2	22.0	17.7
1997	Ferrari	456 GTA	4.9	13.3	18.0	14.9
1997	Ferrari	F355 Berlinetta	4.8	13.2	18.3	15.2
1997	Ford	Escort LX Sedan	10.9	18.1	8.1	8.1
1997	Infiniti	Q45t	7.5	15.7	11.7	10.7
1997	Jaguar	XJR	6.8	15.1	12.9	11.6
1997	Jaguar	XK8 Conv.	6.7	15	13.1	11.7
1997	Lexus	ES 300	8	16.1	11.0	10.2
1997	Mercedes-Benz	C36	5.9	14.4	14.9	12.7
1997	Mercedes-Benz	SLK230	6.9	15.2	12.8	11.4

continued

Year	Make	Model	(0-60)	(1/4 Mile)	acceleration	acceleration
			Sec	sec	ft/ss	ft/ss
1997	Mercury	Sable LS	8.4	16.4	10.5	9.8
1997	Mitsubishi	3000GT VR-4	4.8	13.6	18.3	14.3
1997	Mitsubishi	Diamante LS	8.1	16.1	10.9	10.2
1997	Nissan	200SX SE-R	7.8	16.1	11.3	10.2
1997	Nissan	Maxima SE	7.1	15.5	12.4	11.0
1997	Porsche	911 Turbo	3.7	12.3	23.8	17.4
1997	Porsche	911 Turbo S	3.6	11.9	24.4	18.6
1997	Porsche	Boxster	6	14.5	14.7	12.6
1997	Subaru	Legacy Outback Ltd.	9.1	17	9.7	9.1
1997	Toyota	Supra Turbo	5.1	13.6	17.3	14.3
1998	Audi	A6 Quattro	8.7	16.6	10.1	9.6
1998	BMW 3	28is	6.2	14.7	14.2	12.2
1998	BMW 5	40i Sport	5.5	14	16.0	13.5
1998	BMW M	Roadster	5.1	13.7	17.3	14.1
1998	BMW M	3 Sedan	5.5	14	16.0	13.5
1998	Cadillac	DeVille Concours	6.9	15.1	12.8	11.6
1998	Cadillac	STS	6.8	15.1	12.9	11.6
1998	Chevrolet	Camaro Z28	5.2	13.7	16.9	14.1
1998	Chevrolet	Camaro Z28 SS	5.2	13.6	16.9	14.3
1998	Chevrolet	Corvette Convertible	5.1	13.5	17.3	14.5
1998	Chevrolet	Lumina LTZ	7.6	15.8	11.6	10.6
1998	Chevrolet	Monte Carlo Z34	7.5	15.7	11.7	10.7
1998	Chrysler	Concorde LXi	8.1	16	10.9	10.3
1998	Chrysler	Sebring JXi Conv.	10.2	17.6	8.6	8.5
1998	Dodge	Intrepid	8.9	16.7	9.9	9.5
1998	Dodge	Viper GTS	4.1	12.2	21.5	17.7
1998	Dodge	Viper RT/10	4.1	12.3	21.5	17.4
1998	Ferrari	355 F1	4.6	13	19.1	15.6
1998	Ferrari	ri 456M	5.2	13.5	16.9	14.5
1998	Ford	Escort ZX2	7.4	15.7	11.9	10.7
1998	Ford	Mustang Cobra SVT	5.4	14	16.3	13.5
1998	Honda	Accord LX	7.8	16.1	11.3	10.2
1998	Honda	Civic GX (CNG.)	11.9	18.1	7.4	8.1
1998	Hyundai	Tiburon FX	8.4	16.5	10.5	9.7
1998	Isuzu	Amigo	8	16.1	11.0	10.2
1998	Jaguar	XJ8 L	6.7	15	13.1	11.7
1998	Jaguar	XJR	5.2	13.7	16.9	14.1
1998	Lexus	GS 300	7.6	15.7	11.6	10.7
1998	Lexus	GS 400	5.8	14.3	15.2	12.9
1998	Lexus	LS 400	6.3	14.8	14.0	12.1
1998	Lincoln	ln Town Car Touring Sedan	7.9	16.1	11.1	10.2
1998	Lotus	Esprit V8 Turbo	4.4	12.8	20.0	16.1
1998	Mazda	626 LX	9.1	17	9.7	9.1

Year	Make	Model	(0-60)	(1/4 Mile)	acceleration	acceleration
			Sec	sec	ft/ss	ft/ss
1998	Mercedes-Benz	A160	10.3	17.7	8.5	8.4
1998	Mercedes-Benz	C43	5.8	14.4	15.2	12.7
1998	Mercedes-Benz	CLK320	6.8	15.2	12.9	11.4
1998	Mercedes-Benz	E430 Sport	6.2	14.6	14.2	12.4
1998	Mercedes-Benz	ML320	8.9	16.8	9.9	9.4
1998	Nissan	Altima	8.2	16.4	10.7	9.8
1998	Oldsmobile	Intrigue	7.7	15.8	11.4	10.6
1998	Pontiac	Bonneville SE	7.3	15.5	12.1	11.0
1998	Pontiac	Firebird Formula	5.3	13.8	16.6	13.9
1998	Pontiac	Firebird Trans Am	5.1	13.4	17.3	14.7
1998	Pontiac	Sunfire SE Conv.	7.9	16	11.1	10.3
1998	Saab	95	7.2	15.4	12.2	11.1
1998	Toyota	Camry LE V-6 (auto)	7.8	15.9	11.3	10.4
1998	Toyota	Corolla LE	10.3	17.6	8.5	8.5
1998	Volkswagen	Beetle	9.7	17.2	9.1	8.9
1998	Volkswagen	Passat GLS	7.9	16.1	11.1	10.2
1998	Volvo	C70	6.4	14.9	13.8	11.9
1998	Volvo	S70 T5	6.4	14.9	13.8	11.9
1998	Volvo	V70 XC	7.8	15.9	11.3	10.4
1999	Acura	3.2TL	7.4	15.7	11.9	10.7
1999	BMW 3	28i	6.9	15.2	12.8	11.4
1999	BMW 7	50iL	7.3	15.5	12.1	11.0
1999	BMW M	Coupe	5.4	13.8	16.3	13.9
1999	Chevrolet	Corvette Hardtop	4.8	13.3	18.3	14.9
1999	Chrysler	300M	7.9	16	11.1	10.3
1999	Chrysler	300M w/ Perf. Pkg.	7.7	15.9	11.4	10.4
1999	Ford	Mustang Cobra SVT	5.4	13.9	16.3	13.7
1999	Ford	Mustang Convertible V6	8.6	16.5	10.2	9.7
1999	Ford	Mustang GT	5.5	14.1	16.0	13.3
1999	Honda	Accord Coupe LX V-6	7.4	15.8	11.9	10.6
1999	Honda	Civic Si	7.2	15.7	12.2	10.7
1999	Hyundai	Sonata GLS	10.3	17.5	8.5	8.6
1999	Lexus	LX 470	9.4	17.2	9.4	8.9
1999	Lexus	RX 300	8.8	16.8	10.0	9.4
1999	Mazda	626 LX	7.5	15.7	11.7	10.7
1999	Mazda	Miata	7.9	15.9	11.1	10.4
1999	Mercedes-Benz	C230 Komp.	7.6	15.7	11.6	10.7
1999	Mercedes-Benz	CLK430	6.5	14.8	13.5	12.1
1999	Mercedes-Benz	CL600	6.2	14.4	14.2	12.7
1999	Mercedes-Benz	ML320	9	16.8	9.8	9.4
1999	Mercedes-Benz	ML430	8.2	16.4	10.7	9.8
1999	Mercury	Cougar	7.7	16	11.4	10.3
1999	Mitsubishi	Galant GTZ	9	16.7	9.8	9.5
1999	Plymouth	Prowler	5.8	14.4	15.2	12.7

continued

Year	Make	Model	(0-60)	(1/4 Mile)	acceleration	acceleration
			Sec	sec	ft/ss	ft/ss
1999	Pontiac	Grand Am GT	7.7	15.9	11.4	10.4
1999	Porsche	911 Carrera	4.9	13.4	18.0	14.7
1999	Satrun	SC2	8.5	16.5	10.4	9.7
1999	Toyota	Camry Solara SE	7.1	15.6	12.4	10.8
1999	Volkswagen	Bettle GLS (1.8 T)	7.6	15.9	11.6	10.4
1999	Volkswagen	Beetle GLS (2.0)	9.7	17.3	9.1	8.8
1999	Volkswagen	Beetle GLS (1.9 TD)	11.1	17.9	7.9	8.2
1999	Volkswagen	Jetta GLS	7.8	16	11.3	10.3

Table B- 2 Vehicle deceleration rates

Company	Model	year	0-60 time	1/4 mile time	1/4 mile speed	braking 60-0	decel
			seconds	seconds	mph	ft	f/ss
Volkswagen	Passat w8	2004	6.86	15.14	93	141	27.5
Volkswagen	Passat wagon 4motion	2004	8.54	16.43	87.1	136	28.6
Volkswagen	Passat sedan TDI	2004	9.79	17.39	80.8	141	27.5
Acura	RL	2005	6.92	15.42	93.1	122	31.8
Acura	RSX	2005	7.54	16.04	89.7	141	27.5
Acura	TL Dynamic	2005	6.74	14.98	97.7	114	34.1
Audi	A4	2005	7.39	15.83	91.4	135	28.8
Audi	A8	2005	6.89	15.19	97.25	132	29.4
Cadilac	CTS-V	2005	5.3	13.65	110.6	118	32.9
Cadilac	STS	2005	6.21	14.69	97.7	127	30.6
Chevrolet	Cobalt	2005	8.17	16.37	87.6	140	27.7
Chevrolet	Corvette	2005	4.67	12.96	115.7	118	32.9
Chevrolet	Equinox	2005	9.09	17.07	82.3	142	27.4
Chevrolet	Malibu maxx	2005	7.99	16.22	87.4	146	26.6
Chrysler	300c	2005	6.06	14.52	100.8	130	29.9
Chrysler	300 limited	2005	8.07	16.23	89.1	137	28.3
Chrysler	Crossfire srt-6	2005	4.92	13.35	110.1	129	30.1
Chrysler	Crossfire roadster	2005	6.7	15.09	95.2	133	29.2
Chrysler	PT cruiser	2005	8.23	16.51	85.5	130	29.9
Dodge	Caravan	2005	9.83	17.51	80.6	143	27.2
Dodge	Magnum	2005	6.19	14.64	99.9	134	29.0
Ford	Escape	2005	11.99	18.86	75.2	144	27.0
Ford	Focus ST	2005	8.26	16.36	87.5	146	26.6
Ford	Focus ZXW	2005	10.3	17.74	79.9	136	28.6
Ford	Freestyle	2005	8.39	16.6	86.8	137	28.3
Ford	Mustang	2005	5.25	13.85	104.5	132	29.4
Gmc	Envoy SLT	2005	8.39	16.44	86.2	147	26.4
Hyundai	Accent5	2005	9.93	17.56	79	158	24.6
Jaguar	S-type	2005	6.44	14.88	98.3	133	29.2
Jeep	Grand Cherokee	2005	6.74	15.21	92.7	139	27.9
Jeep	Liberty	2005	11.83	18.51	74.3	143	27.2
Kia	Spectra5 5M	2005	8.78	16.81	84.4	129	30.1
Kia	Spectra5 4A	2005	10.05	17.57	80.3	147	26.4
Landrover	LR3	2005	8.7	16.79	85.1	121	32.1
Mazda	Tribute	2005	12.33	19.06	75.5	139	27.9
Mercedes benz	C55	2005	4.94	13.37	109.9	118	32.9
Mercedes benz	E320	2005	7.77	16	90.6	142	27.4
Mitsubishi	Diamante LS	2005	8.88	16.77	86.2	145	26.8
Mitsubishi	Lancer sportback	2005	8.98	17.12	82.7	146	26.6
Nissan	Pathfinder LE	2005	7.33	15.8	89.7	140	27.7
Pontiac	G6 GT	2005	8.01	16.21	87.8	145	26.8
Porsche	911 carrera	2005	4.3	12.75	112.6	114	34.1
Subaru	Legacy	2005	5.66	14.31	96.9	142	27.4

continued

company	Model	year	0-60 time	1/4 mile time	1/4 mile speed	braking 60-0	decel
			seconds	seconds	mph	ft	f/ss
Subaru	Legacy wagon	2005	7.29	15.72	92.4	139	27.9
Subaru	Outback 2.5 GT	2005	5.66	14.17	97.9	141	27.5
Subaru	Outback 3.0 R VDC	2005	8.29	16.58	87.2	137	28.3
Subaru	Outback 2.5i limited	2005	10.26	17.79	79	146	26.6
Toyota	Camry solara	2005	7.51	15.88	90.8	135	28.8
Toyota	Corolla	2005	7.5	15.96	90.5	120	32.4

Calculation of speed in the car-following model

Speed is estimated for each vehicle each time step. The algorithm is executed inside a double loop computing the speed of all vehicles during the entire analysis time. For example, in the loop, the speed of the second vehicle at the second time step is calculated using the speed of the first and second vehicles in the previous time step. Then the speed of the third vehicle at the second time step is estimated and so on. When the speeds of every vehicle the second time are computed, the speeds at the third time step are estimated. The estimation continues until the end of the predefined analysis period. Consequently, a very large matrix including the speed information of vehicles by time step is created. Using the speed matrix, TWOSIM calculates each vehicle's location by time step, which provides information for estimating headways and various outputs such as maximum hourly flow rate, percent time spent following, and average travel speed.

APPENDIX C: CODE OF TWOSIM

Example of code in TWOSIM I

```
clear all;
rand('state',sum(100*clock)); %random number generator;
car=900;
minarrival=1000; %minimum arrival rate(vph), maximum=2700 vph
maxarrival=1000; %maximum arrival rate(vph), maximum=2700 vph
opparrival=200;%Opposing flow rate
spdlim=55;%speed limit
sd=spdlim+5;%free flow speed
car0=car;%create unchangeable name for car
aggdrv=0; %proportion of aggressive drivers
rndrv=rand(car,1);
drv=[];%assing driver type (for the future)
for i=1:car;
      if rndrv(i)<=aggdrv;
            drv(i)=1;
      else
            drv(i)=0;
      end
end
tcar=[];
avgtheta=0.78;%avarage of further safety margin, additional delay of
reaction,default(0.78)
stdtheta=0.5; %margin of theta=0.36sec
itrmax=1;%Number of iterations
wtime=5;%warming up time(minutes)
calt=5;%time period to be calculated for time-based maximum flow(minutes)
totalt=12; %analysis period(minutes):must be equal to or greater than
wtime+calt(minutes)
segleng=2;%the length of highway to be analyzed(mile)
warmzone=0.5; %the length of warming up zone for both ends(mile)
mintime=wtime*60;%mininum time of analysis period
maxtime=(wtime+calt)*60;%maximum time of analysis period
totleng=segleng+2*warmzone; %total rlength of simulated highway(m)
obsint=200; %observation point interval(ft) for time-based maximum flow
obsins=20; %observation instant interval(sec) for space-based maximum flow
arrivalinc=100; %increment of arrival rate for simulation
arrivals=[minarrival:arrivalinc:maxarrival];
[mar nar]=size(arrivals);
col=0;
TBMAXFLOW=zeros(itrmax+1,(maxarrival-minarrival)/arrivalinc+1);
SBMAXFLOW=zeros(itrmax+1,(maxarrival-minarrival)/arrivalinc+1);
```

```
PTSF=[];%the initial value of PTSF
sumtb2mat=[];%the initial matrix of sumtb2
qflow=[];%flow
uspeed=[];%space mean speed
kdensity=[];%density
flowbyobs=[]; %store flowrate by observation
MTSPEED=[];%Average time-mean-speed
MSSPEED=[];%Average space-mean-speed
VerAkcelik=[];%Mean headway of arrivals and its volume
MPTSF=[];%Average percent time spent following
MATS=[];%Average travel speed
SUMMARY=[];%Summarized output
CAL=[];%Calibration output (arrival vol, avg travel speed, PTSF)
FLOWVSPTSFVSSPEED=[];%Flow vs PTSF
MEANARRH=[];%Mean arrival headway
FLOWRATE=[];%Hourly flow rate at observation point
for iarrival=1:nar;%Multiple arrivals
    arrival=arrivals(1,iarrival);
    col=iarrival;
    TBMAXFLOW(1,col)=arrival;
    SBMAXFLOW(1,col)=arrival;
    qflow1=[];
    uspeed1=[];
    kdensity1=[];

    %Akcelik M3A headway distribution
    for itr=1:itrmax;%loop for multiple iterations
        delta=1.4+rand*.2; %minimum headway
        while delta>3600/arrival
            delta=1.4+rand*.2;%maximum allowable demand=3600/1.4=2571vph
        end
        beta=0.6;%bunching factor, default=0.6 for single lane case
        vmx=3600/delta; %maximum flow allowable in Cowan's M3
        q=arrival/3600; %flow rate,veh/sec
        %maximum headway obtained by truncating the right tail to avoid error of
        interp1 function
        tmx=delta-((1-delta*q)*(beta*delta*q+log(10e-35)))/(exp(-beta*delta*q)*q);
        tinc=.5; %time step increment
        th=[0 (delta:tinc:tmx)]'; %built time axis in headway distribution
        phi=exp(-beta*delta*q); %calculate proportion of free(unbunched) vehilces
        lamda=phi*q/(1-delta*q); %decay parameter
        cdf=1-phi*exp(-lamda*(th-delta)); %cumulative density function
        tmax=min(find(cdf>0.9999)); %find minimum index of time making cdf 1
        [m,n]=size(cdf); %calculate size of cdf matrix
        cdf(tmax+2:m)=[];%delete the rows above prob =0.9999
        th(tmax+2:m)=[];%delete the rows above prob=0.9999
```

```
cdf(tmax+1)=1;%boundary adjustment, set the end of cdf to be 1
th(tmax+1)=tmx;%set the end of time axis to be max headway(tmx)
[mcdf,ncdf]=size(cdf);%calculate size of new cdf
pdf=[0;cdf(2);diff(cdf(2:end))];

%Plot M3A arrival headway distribution
        figure(1)
        plot(th(2:end),cdf(2:end),'b-',th(2:end),pdf(2:end),'ko-')
        xlabel('headway(sec)')
        ylabel('probability')
        title('M3A arrival headway distribution','Fontsize',12)
        legend('cdf','pdf')
        grid on;
        axis([0 12 0 1]);

         %Assign arrival headway to each vehicle
           hvol=-1;
              while hvol<arrival-20 | hvol>arrival+20;
              r=rand(car,1); %generating random number for creating
              headways
              id=[1:car];
              hi= [interp1(cdf(:,1),th(:,1),r)];
              headway=zeros(1,car)';
              headwaycum=zeros(1,car)';
              for i=1:car;
                    for j=1;
                          headway(i,j)=[max(hi(i,j),delta)];
                    end
              end
              MEANARRH1=mean(headway);%Mean arrival headway
              MEANARRH=[MEANARRH MEANARRH1];%Mean arrival
              headway
              %create cumulative headway matrices and calcualte
              %arrival demand
              for i=2:car;
                    for j=1;
                          headwaycum(1,1)=headway(1,1);
                          headwaycum(i,j)=headwaycum(i-1,j)+headway(i,j);
                    end
                 end
                 begin=max(find(headwaycum<wtime*60));
                 ending=min(find(headwaycum>(wtime+calt)*60));
              hvol=3600*(car0-1)/headwaycum(end);% arrival demand
           end
      MEANARRH1=mean(headway);%Mean arrival headway
      MEANARRH=[MEANARRH MEANARRH1];%Mean arrival headway
```

```
%Assign maximum acceleration which the driver wishes to undertake
rdma=rand(car,1);
matable=[6.4 0;8 0.178; 10 0.604;12 0.643;14 0.821;16 0.878; 18 0.952;20
0.996;23.3 1];
a=(interp1(matable(:,2),matable(:,1),rdma(:,1)))';%choose acceleration rate
randomly
maccel=mean(a);%mean acceleration rate
%MEAN=11.9ft/ss(5.6m/ss), STDEV=3.04ft/ss(0.3m/ss)

%Assign most severe braking deceleration by normal distribution
%most severe braking b=c*a (c used to be -2)
c=-2;%Default=-2
b=a.*c;

%Assign effectiv size of vehicle
%the physical length plus a margin into which the following vehicle is not
willing to intrude, even when at rest
ms=21.2;    %Default=21.2ft(6.5m)
stds=1.0;%Default=1.0ft(0.3m)
s=(ms+stds*randn(car,1))';%effective size of vehicle at primary direction

%Assign reaction time
rt=0.7;%Default=0.7

%Make theta stochastic to reflect aggresiveness of driver
theta=zeros(car,1);
for i=1:car
      if drv(i)==1; %aggressive driver
            theta(i)=avgtheta;
      else %nonaggressive driver
            theta(i)=avgtheta+stdtheta*rand(1);
      end
end

%Create time step matrix
t=(0:rt:totalt*60+rt)';% seconds
[mt,nt]=size(t);

%Assign bhat
b1=-17.6;%2001 AASHTO d=14.8ft/ss for emergency, default=-17.6
b2=(b-17.6)/2;
bhat=min(b1,b2);

%Assign desired speed
%sd=60;%mean desired speed(mph) or Posted speed limit
```

```
stdsd=4; %4.97mph, standard deviation of desired speeds=10.5ft/s(3.2m/sec,
15.4mph)
vd=(sd+stdsd*randn(car,1))'*1.46667;%random desired speed for each vehicle

%Create the demand responsive speed of initial vehicle by
uf=sd;%free flow speed(mph)
isd=(sd-0.007*arrival-0.003*opparrival)*1.46667;
insd=isd*ones(car,1);%arrival speed of all the other vehicles

%Create initial speed of every vehicle at the first time step,which is
%equal to desired speed of each vehicle's
speed=zeros(mt,car);

%Create speed distribution of the initial vehicle
for i=1:mt;
      speed(i,1)=insd(1);
end

%Plot speed of initial vehicle
figure(2);
            iniv=speed(:,1);
            plot(t,iniv);
            xlabel('time(sec)');
            ylabel('speed(ft/sec)');
            title('Speed of initial vehicle vs. time','Fontsize',12);
            grid on;

%Create location of the first vehicel at every time step
loc=zeros(mt,car);
for i=2:mt;
      loc(i,1)=[loc(i-1,1)+rt*speed(i-1,1)];
end

%Creat location of each vehicel at every time step
%And calculate speed based on Gipps' car-following model
for i=2:mt;%time step
      display('This program is running now. Please do not close window. Sorry
      and Thanks!!')
      for j=2:car;%order of car to be analyzed
            if headwaycum(j)>=t(i,1);%if this vehicle does not arrive at starting
            point yet
                  loc(i,j)=0;
                  speed(i,j)=0;
            else %if this vehicle arrived at starting point
                  if (t(i,1)-headwaycum(j,1))<rt;%right after this vehicle arrives at
                  starting point(the vehicle does not proceed one time step period)
```

```
                    if headway(j)<=3;
                        speed(i,j)=speed(i,j-1)-1*1.46667;%the initial speed
                        1mph less than the speed of the vehicle ahead
                        if speed(i,j)>vd(j);%if arrival speed is greater than
                        desired speed
                            speed(i,j)=vd(j);
                        else
                        end
                    else
                        speed(i,j)=insd(j);%if yes, select the arrival speed
                        given average travel speed
                    end
                    loc(i,j)=(t(i,1)-headwaycum(j))*speed(i,j);
                else %more than one time step after the vehicle arrived at
                starting point
                    if loc(i-1,j-1)-loc(i-1,j)<s(j-1); %s(j-1);%if the headway
                    distance is less than s as soon as it arrives
                        loc(i-1,j)=loc(i-1,j-1)-headway(j)*s(j-1);
                    else
                    end
                    loc(i,j)=loc(i-1,j)+rt*speed(i-1,j);
                    speed(i,j)=min((speed(i-1,j)+2.5*a(j)*rt*...
                        (1-speed(i-1,j)/vd(j))*sqrt(0.025+speed(i-1,j)/...
                        vd(j))),(b(j)*(0.5*rt+theta(j)*rt)+sqrt(b(j)^2*
                        (0.5*rt+theta(j)*rt)^2-b(j)*...
                        (2*(loc(i-1,j-1)-s(j-1)-loc(i-1,j))-speed(i-1,j)*...
                        rt-speed(i-1,j-1)^2/bhat(j))));
                end
            end
        end
    end
    %zero location is changed into nonzero negative location for interploation
    function
    adj=zeros(car,1);
    for j=2:car;
        adj(j,1)=max(find(loc(:,j)==0));
    end
    for j=2:car;
        for i=1:mt;
            if i<=adj(j,1) & adj(j,1)<mt;
                loc(i,j)=loc(adj(j,1)+1,j)-(t(adj(j,1)+1,1)-t(i,1))*speed(1,1);
            else
            end
        end
    end
```

```
%adjust number of cars to be simulated to avoid error
for i=1:car-1;
      locmaxtime(i)=interp1(t(:,1),loc(:,i+1),(wtime+calt)*60+30);
end
car=min(find(locmaxtime<=warmzone*5280))+1;
speed(:,car+5:end)=[];%delete beyond car
loc(:,car+5:end)=[];%delete beyond car
                        figure(3);
                        plot(t,speed);
                        xlabel('time(sec)');
                        ylabel('speed(ft/sec)');
                        title('Speed of vehicle vs. time','Fontsize',12);
                        grid on;
                        figure(4);
                        plot(t,speed(:,1:7));
                        xlabel('time(sec)');
                        ylabel('speed(fps)');
                        title('Speed of the first several vehicles vs.
                        time','Fontsize',12);
                        grid on;
                        axis([0 150 floor(isd-40) ceil(isd+30)]);
                        figure(4);
                        plot(t,speed(:,1:20)/1.46667);
                        xlabel('time(sec)');
                        ylabel('speed(mph)');
                        title('Speed of the first seven vehicles vs.
                        time','Fontsize',12);
                        grid on;
                        axis([0 400 50 70]);

                        figure(4);
                        plot(t(1:15),SP(1:15,1),'y:',t(16:end),SP(16:end,1),'k-
                        ',t(1:22),SP(1:22,2),'y:',t(23:end),SP(23:end,2),'k-
                        ',t(1:25),SP(1:25,3),'y:',t(26:end),SP(26:end,3),'k-
                        .',t(1:35),SP(1:35,4),'y:',t(36:end),SP(36:end,4),'k-
                        ',t(1:46),SP(1:46,5),'y:',t(47:end),SP(47:end,5),'k-
                        ',t(1:56),SP(1:56,6),'y:',t(57:end),SP(57:end,6),'k-
                        ',t(1:77),SP(1:77,7),'y:',t(78:end),SP(78:end,7),'k-');
                        xlabel('time(sec)');
                        ylabel('speed(mph)');
                        title('Speed of the first seven vehicles vs.
                        time','Fontsize',12);
                        grid off;
                        axis([0 70 50 68]);

%Time-based maximum flow rate
```

```
maxtb=(segleng+warmzone)*5280;
mintb=warmzone*5280;

%Determine the interval of observation time
if interp1(loc(:,end),t(:,1),mintb)<maxtime;
      disp('The last vehilce does not reach the starting point of analysis zone at
      maxtime. Therfore increase car appropriately')
else
end
if interp1(loc(:,2),t(:,1),maxtb)>mintime;
      disp('The first vehicle has already passed the end of analysis zone at
      mintime. Therefore increase warm-up time/mintime or reduce speed of the
      first vehicle')
else
end

stb=(mintb:obsint:maxtb+obsint)';%Specify the observation points
stb=[0;stb;maxtb];
[mtb,ntb]=size(stb); %add original Maxtb in the stb matrice
tbloc1=zeros(mtb,car-1);
tbloc2=zeros(mtb,car-1);
for i=1:mtb;
      for j=1:car-1;
            tbloc1(i,j)= [interp1(loc(:,j+1),t(:,1),stb(i,1))];%find a time that a
            vehicle arrives at given observation point
            tbloc1speed(i,j)=[interp1(loc(:,j+1),speed(:,j+1),stb(i,1))];%find a
            speed that a vehicle runs at given observation point
            %Find the corresponding time observed at given observation point
            if tbloc1(i,j)>=mintime & tbloc1(i,j)<=maxtime-
            15/tbloc1speed(i,j);%since a location represents
                  %the location of the front ofvehicle n at time t, so subtract
                  occupancy time of the vehicle at the last moment
                  tbloc2(i,j)=1;%if a vehicle falls within the analysis time slot,
                  then it is set to be 1
            else
                  tbloc2(i,j)=0;%if a vehicle does not fall within the analysis time
                  slot, then it is set to be 0
            end
      end
end
sumtb1=[sum(tbloc2')'];%number of vehicles observed during analysis period
sumtb2=[sumtb1*3600/(maxtime-mintime)];%time-based flow rate

%Create time mean speed matrix
%Find speed of each vehicle at each observation point
tbspeed=zeros(mtb, car-1);
```

```
este=zeros(mtb,car-1); %if there is speed >0, then it will be 1, otherwise 0
for j=1:car-1;
    for i=1:mtb;
        if [interp1(loc(:,j+1),speed(:,j+1),stb(i,1))]<=0;
            tbspeed(i,j)=0;
        else
            tbspeed(i,j)= [interp1(loc(:,j+1),speed(:,j+1),stb(i,1))];%Find the
            corresponding speed at given point
        end
        if tbspeed(i,j)>0;
            este(i,j)=1;
        else
            este(i,j)=0;
        end
    end
end
MTSPEED1=sum(tbspeed')./sum(este')/1.46667;%spot speed at each obs point
MTSPEED2=mean(MTSPEED1);%average spot speed
STDMTSPEED2=std(MTSPEED1);%standard deviation of average spot speed
MTSPEED=[MTSPEED;MTSPEED1];%average spot speed vector with
iterations
if MTSPEED2==NaN;
    error('The vehicles at almost end does not reach the end of analysis
    segment. Therfore increase totalt')
else
end

%Average Travel Speed Calculation based
tt=zeros(car-1,1);%calculate travel time of each vehicle over analyzed segment
trspeed=zeros(car-1,1);%average travel speed of each vehicle over analyzed
segment
    for i=1:car-1;
        tt(i,1)=interp1(loc(:,i+1),t(:,1),(warmzone+segleng)*5280)-
        interp1(loc(:,i+1),t(:,1),warmzone*5280);
        trspeed(i)=segleng*5280/tt(i,1)/1.46667;
    end
    trmax=max(find(trspeed>0));
    trspeed(trmax+1:end)=[];
    MATS1=mean(trspeed);%average travel speed
    STDMATS1=std(trspeed);%standard deviation of average travel speed
    MATS=[MATS;MATS1];%average travel speed vector with iterations

%The flow at zero location is excluded here.
FLOWRATE=[FLOWRATE;sumtb2'];%collect flow rates at any point
TBMAXFLOW1=[max(sumtb2(2:end))];%Time-based maximum flow
TBMAXFLOW(itr+1,col)=TBMAXFLOW1;%When to choose maximum flow,
```

```
exclude the number at zero point
MTBFLOW=mean(sumtb2(2:end));%mean time-based hourly flow rate
STDMTBFLOW=std(sumtb2(2:end));%standard deviation of time-based
hourly flow rate
%Record flow rate at each point
flowbyobs=[flowbyobs sumtb2];

%Space-based Maximum flow rate
%Create matrice for time observation point
ssb=(mintime:obsins:maxtime)';%Specify the observation points
[msb,nsb]=size(ssb);
sbloc1=zeros(msb,car-1);%spot speed initial matrice
for j=1:car-1;
      for i=1:msb;
            sbloc1(i,j)= [interp1(t(:,1),loc(:,j+1),ssb(i,1))];%Find the
            corresponding loction observed at given point of time
      end
end

%Create matrice for evaluating if the vehicle is located within the observed
space, dx
sbloc2=zeros(msb, car-1);
for i=1:msb;
      for j=1:car-1;
            if sbloc1(i,j)>=mintb+s(j+1) & sbloc1(i,j)<=maxtb;%excluding the
            vehicle overlap the beginning point of the obs space
                  sbloc2(i,j)=1;%if a vehicle falls into the observed space, then it
                  is set to be 1
            else
            end
      end
end

%sum of number of vehicles at the given observation instant
sumsb1=sum(sbloc2')';
%Calculate density
density=sumsb1*5280/(maxtb-mintb);%veh/mi/ln

%Create space mean speed matrix
%Find speed of each vehicle at each observation instant
sbspeed=zeros(msb, car-1);
for j=1:car-1;
      for i=1:msb;
            if [interp1(t(:,1),speed(:,j+1),ssb(i,1))]<0;
                  sbspeed(i,j)=0;
            else
```

```
                    sbspeed(i,j)= [interp1(t(:,1),speed(:,j+1),ssb(i,1))];%Find the
                    corresponding speed at given point
                end
            end
        end
        spmspeed0=sbspeed.*sbloc2;
        sms=sum(spmspeed0')./sumsb1/1.46667;%space mean speed

        %Space based flow rate
        sbflow=sms.*density;%vph, alt space based flow
        MSSPEED1=mean(sms);%average space-mean-speed
        STDMSSPEED1=std(sms);%standard deviation of space-mean speed
        MSSPEED=[MSSPEED;MSSPEED1];%average space-mean-speed vector
        with iterations
        SBMAXFLOW1=max(sbflow);%Space-based maximum flow(vph)
        SBMAXFLOW(itr+1,col)=SBMAXFLOW1; %vph
        MSBFLOW=mean(sbflow);%mean space-based hourly flow rate
        STDMSBFLOW=std(sbflow); %standard deviation of space-based hourly flow
rate

        %Create macro viewpoint result for one arrival flow rate
        qflow1=[qflow1;sbflow(:,1)];%vph
        uspeed1=[uspeed1;sms(:,1)]; %mph
        kdensity1=[kdensity1;density(:,1)];%veh/mi/lane

        %Kill the dummy locations of primary vehicles
        pos=zeros(mt,car);
        for i=1:mt;
            for j=1:car;
                if loc(i,j)<0;
                    pos(i,j)=0;
                else
                    pos(i,j)=loc(i,j);
                end
            end
        end

                        figure(5);
                        plot(t,pos,t,mintb.*ones(mt),t,maxtb.*ones(mt)...
                            ,mintime.*ones(mt),loc(:,1),(maxtime-
                            .3).*ones(mt),loc(:,1));
                        xlabel('time(sec)');
                        ylabel('location(ft)');
                        title('Vehicle trajectory','Fontsize',12);

        %Create headway matrix for each observation point
```

```
hw=diff(tbloc1');
[rowhw,colhw]=size(hw);
diffhw=abs(headway(3:car,1)-hw(:,1));
maxdiffhw=max(diffhw);
sumdiffhw=sum(diffhw);
spacing=-diff(sbloc1');
[mx,nx]=size(spacing);
spacings=[];
speeds=[];
headways=[];
negloc=zeros(nx,1);%locate negative location
for i=1:nx;
      negloc(i)=max(find(sbloc1(i,:)>0));
end
for i=1:nx;
      spacing(negloc(i):end,i)=0;
end
for i=1:nx;
      spacings=[spacings;spacing(:,i)];
      speeds=[speeds;tbloc1speed(:,i+1)];
      invhw=hw';
      headways=[headways;invhw(:,i)];
end
zer=find(spacings==0);
[zi,zj]=size(zer);
sortspc=sort(spacings);
sortspc(1:zi)=[];

MEANH1=mean(hw);%average headway for observations per obs location
MEANH=3600/TBMAXFLOW1; %globally average headway for all the
headways over entire observations
spacingmin=min(sortspc);%minimum spacing
spacingmean=mean(sortspc);%mean spacing

            figure(6);
            plot(stb(2:end),spacing(2:end,490));
            xlabel('location(ft)');
            ylabel('spacing(ft)');
            title('The change of spacing','Fontsize',12);
            axis([400 430 0 6000]);

%Verification of Akcelik M3A headway distribution
%check arrival volume and mean headway of arrivals(to make sure if
%warmzone is set to be zero)
VerAkcelik=[VerAkcelik;sumtb2(1) MEANH1(2)];
```

```
        %Calculate percent time spent following
        pTSF1=isfinite(hw);%if there is NaN, returns zero, otherwise one
        denPTSF=sum(pTSF1);%Calculate total number of headways at each obs point
        for i=1:rowhw;
            for j=1:colhw;
                if hw(i,j)<=3;
                    pTSF1(i,j)=1;
                else
                    pTSF1(i,j)=0;
                end
            end
        end
        nomPTSF=sum(pTSF1);%Calculate total number of headways less or equal to
        3 seconds
        pTSF0=(nomPTSF./denPTSF)';%Calculate PTSF
        PTSF=[PTSF pTSF0(2:end)];%Create PTSF for every iteration
        MPTSF1=mean(pTSF0(2:end));%Mean PTSF
        STDMPTSF1=std(pTSF0);%Standard deviation of PTSF
        MPTSF=[MPTSF;MPTSF1];
        tcar=[tcar; car];
       SUMMARY1=[aggdrv    car sd hvol opparrival sumtb2(1) sumtb2(2)
       sumtb2(floor(mtb/2)) sumtb2(end) mean(sumtb2(2:end)) TBMAXFLOW1
      SBMAXFLOW1 MTBFLOW STDMTBFLOW MSBFLOW STDMSBFLOW
      MATS1 STDMATS1 MSSPEED1 STDMSSPEED1 MPTSF1 STDMPTSF1
      MEANH spacingmean spacingmin];%Summarized output
      SUMMARY=[SUMMARY;SUMMARY1];%Summarized output for all the
iterations
FLOWVSPTSFVSSPEED1=[sumtb2(2:end,1) pTSF0(2:end,1)
MTSPEED(1,2:end)'];%flow vs. PTSF
FLOWVSSPTSFVSSPEED=[FLOWVSPTSFVSSPEED;FLOWVSPTSFVSSPEED1];%
flow vs. PTSF
        CAL1=[sumtb2(1) MATS1 MPTSF1];%Calibration output
        CAL=[CAL;CAL1];
                figure(7);
                plot(stb,pTSF0);
                xlabel('location(ft)');
                ylabel('PTSF');
                title('The change of PTSF','Fontsize',12);
                axis([400 430 0 6000]);
        carsim=car;%number of cars simulated
        car=car0;%initial number of cars
    end
    %this script has to be modified when multiple arrivals are run.
    PTSF=[stb(2:end) PTSF];
    %Create macro viewpoint result for multiple arrivals
    qflow=[qflow;qflow1]; %vph
```

```
    uspeed=[uspeed;uspeed1]; %mph
    kdensity=[kdensity;kdensity1]; %veh/mi/ln
end
```

Input and output data in TWOSIM I

Input data

Category	Input data	Description
Simulation options	Number of iterations	Integer (1,2,…)
	Warm-up time	Integer (minute)
	Analysis time	Analysis period for data collection, integer (minute)
	Warm-up zone	Length of warm up zone, integer (mile)
	Observation interval	Length of observation area, integer (ft)
Traffic	Primary volume	Traffic volume in the primary direction (vph)
	Opposing volume	Traffic volume in the opposing direction (vph)
	Driveway volume	Volume entering from the driveway (vph)
	Exit percent	Percent of traffic exiting the main road and entering the driveway (decimal)
	Speed limit	Posted speed limit (mph)
	Percent of trucks	Percent of trucks (decimal)
Geometry	Location of driveway	Integer (mile)
		Integer (ft)
	Driveway curb radius	Length of analysis segment, integer (mile)
	Length of segment	Length of grade segment, integer (mile)
	Length of grade segment	

continued

Category	Input data	Description
Geometry	Location of grade segment	Location of the beginning of grade segment, integer (mile)
	Radius of horizontal curve	Radius of horizontal curve, integer (ft)
	Central angle of curve	Angle made by curve, (degree)
	Location of horizontal curve	Location of the beginning of curve, integer (mile)
	Length of passing zone	Length of passing zone, integer (mile)
	Beginning of passing zone	Location of the beginning of passing zone, integer (mile)

Output data

Category	Output data	Description
Traffic	Probability density of M3A arrival headway distribution	Probability density of M3A arrival headway distribution developed with the given arrival volume
	Arrival headways	Headways of individual vehicles simulated (sec)
	Arrival time	Arrival time of each vehicle simulated (sec)
Vehicle	Maximum acceleration rate	(ft/s^2)
	Most severe deceleration rate	(ft/s^2),
	Types of passenger cars	1 ~ 8 (Table 5-4)
	Types of trucks	5 ~ 7 (5: 300 hp, 6:400 hp, 7: 500 hp, default: each type at 33.3 %)

continued

Category	Output data	Description
Vehicle	Types of loads in trucks	1~4 (Table 7-2)
	No exit or exit at driveway	Flag (0: no exit or 1: exit)
	Length of trucks	45.5, 55, 68.5, and 73.5 ft (default: each length at 25%)
	Speed in exiting	Right turn speed (mph)
	Deceleration in exiting	(mph/s)
	Vehicle status	Passing or not, exiting or not, at curve or not, at grade or not, …
	Speed	Speed at each time step (ft/s)
	Location	Location at each time step (ft)
Driver	Delay of safety reaction time	(sec)
	Desired speed	(mph)
	Critical gap time	(sec)
Statistics	Average travel speed	(mph)
	Percent time spent following	(%)
	Traffic volume	Observed traffic volume by vehicle types (passenger cars and trucks)
	Traffic flow rate	(vehicles)
	Density	Hourly traffic flow rate (vph)
	Number of passes	(veh/mi/ln)
	Passing time	Integer
		(sec)
Graphical output	Vehicle trajectories	Location of each vehicle at each time step in time-space diagram

APPENDIX D: VERIFICATION OF TWOSIM

Regression analysis for average travel speed of the first dummy vehicle

(Refer to Table 5-7)

SUMMARY OUTPUT

Regression Statistics	
Multiple R	0.931910281
R Square	0.868456772
Adjusted R Squar	0.80559326
Standard Error	1.647138262
Observations	20

ANOVA

	df	*SS*	*MS*	*F*	*Significance F*
Regression	2	322.4128398	161.20642	59.4185736	2.12891E-08
Residual	18	48.83516019	2.7130645		
Total	20	371.248			

	Coefficients	*Standard Error*	*t Stat*	*P-value*	*Lower 95%*	*Upper 95%*	*Lower 95.0%*	*Upper 95.0%*
X Variable 1	-0.006795304	0.00103643	-6.556455	3.6799E-06	-0.008972763	-0.004617844	-0.008972763	-0.004617844
X Variable 2	-0.002561782	0.001074966	-2.383128	0.02839216	-0.004820204	-0.00030336	-0.004820204	-0.00030336

Akcelik's M3A headway distribution

Chi-square test is performed to evaluate whether TWOSIM replicates the M3A distribution. Table D-1 shows that it is concluded that the TWOSIM's distribution replicates Akcelik's M3A distribution.

Table D- 1 Comparison of probability density with the probability of arrival headway

Headway (sec)	Akcelik M3A		TWOSIM Outcomes		$(f_t - f)^2/f$
	Probability (%)	Frequency (f_t)	Probability (%)	Frequency (f)	
0.0	0.00	0	0.00	0	0
1.5	39.34	295	41.20	309	0.66
2.0	38.58	289	38.00	285	0.07
2.5	14.04	105	13.73	103	0.05
3.0	5.11	38	4.93	37	0.05
3.5	1.86	14	1.21	9	1.76
4.0	0.68	8	0.40	3(7)	0.13
4.5	0.25	0	0.40	3	0.00

continued

Headway (sec)	Akcelik M3A		TWOSIM Outcomes		$(f_t - f)^2/f$
	Probability (%)	Frequency (f_t)	Probability (%)	Frequency	
5.0	0.09	0	0.00	0	0.00
5.5	0.03	0	0.13	1	0.00
6.0	0.01	0	0.00	0	0.00
45.7	0.01	0	0.00	0	0.00
Total	100.00	750	100.00	750	2.70
$\chi^2_{crit} = 11.1 \; at \; \alpha = 0.05$, since $\chi^2_{CALC} = 2.7 < \chi^2_{crit}$, Do not reject H_o.					

Maximum acceleration rates

Table D-2 shows that TWOSIM assigned maximum acceleration rates to all vehicles simulated as given probability specifies.

Table D- 2 Comparison built-in probability density with probability of assigned maximum acceleration by the algorithm in TWOSIM

TWOSIM Car type	Maximum acceleration rate (ft/s^2)	Probability density (%)[1]	TWOSIM Arrival headways	
			Probability (%)[2]	Frequency
1	6.4~8.0	17.8	17.0	61
2	8.1~10.0	42.6	41.9	151
3	10.1~12.0	3.9	3.0	14
4	12.1~14.0	17.8	18.9	68
5	14.1~16.0	5.7	6.4	23
6	16.1~18.0	7.4	7.5	27
7	18.1~20.0	4.4	3.9	14
8	20.1~23.3	0.4	0.5	1
Total		100.0	100.0	360

Note: [1] Built-in probability density in TWOSIM

[2] Probability of maximum acceleration rates calculated with outcome headways assigned by the algorithm in TWOSIM

Effective size of vehicles

A Chi-square test was conducted to test if the outcomes of effective size of passenger cars by TWOSIM are normally distributed (Figure D-1). The resulting test statistic is obtained to be 0.0 and the chi-square critical value is 3.8 at level of significance, 0.05 and 1 degree of freedom.

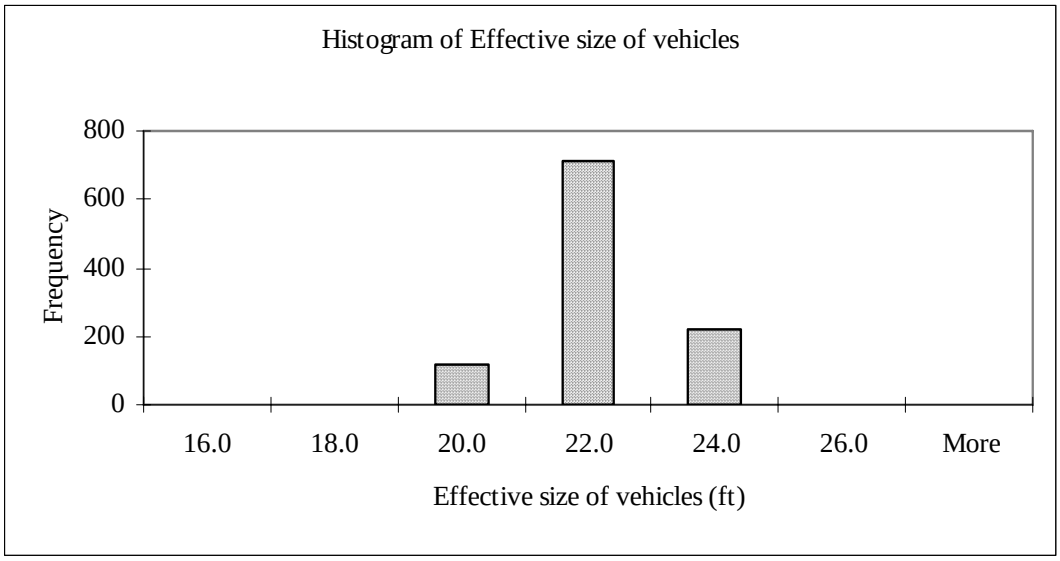

Figure D- 1 Histogram of effective size of vehicles

Desired speeds

A Chi-square test was conducted to verify that the desired speed in TWOSIM follows the normal distribution. The test statistic is obtained to be 6.3 and the chi-square critical value is 11.1 at level of significance, 0.05, with 5 degree of freedom. Since the statistic is smaller than the critical value, it is concluded that there is significant evidence that the distribution of desired speeds generated in TWOSIM is identical to the normal distribution.

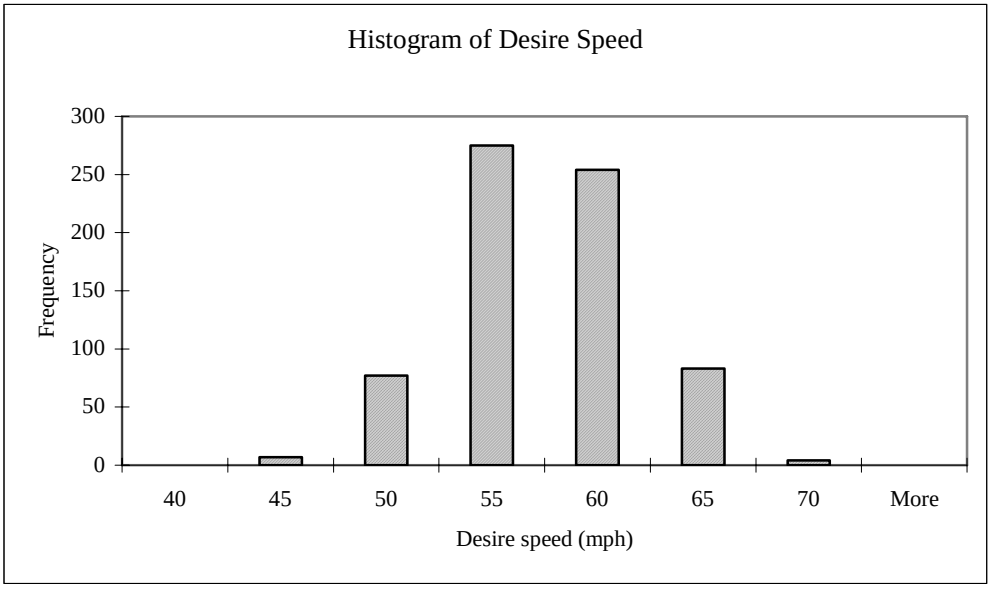

Figure D- 2 Histogram of desire speed

APPENDIX E: HYPOTHESIS TEST

Hypothesis tests are performed to examine if there is a significant difference between capacities estimated with TWOSIM I as a function of the average free flow speed. The Type 1 error is 0.05. The hypothesis test is as follows:

$$H_O : \mu_1 - \mu_2 = 0$$
$$H_A : \mu_1 - \mu_2 \neq 0$$

where,

μ_1, μ_2 : two base capacities at given average free flow speed to be compared

From the comparison of base capacities in Table 5-10, *p*-values are provided in Table E-1. These results show that all null hypotheses are rejected and there is statistical difference between every pair of base capacities. Therefore, base capacity is statistically different for each average free flow speed.

Table E- 1 Result of *t*-test for base capacities as a function of average free flow speed

p-value		Average free flow speed (mph)			
		40	50	60	70
Average free flow speed (mph)	40	NA	1.06e-38	1.44e-44	4.45e-20
	50	1.06e-38	NA	1.68e-27	8.51e-8
	60	1.44e-44	1.68e-27	NA	0.002
	70	4.45e-20	8.51e-8	0.002	NA

Table 5-11 is examined. In Table E-2, although no significant difference is found between the base capacity at 0 mph standard deviation of desired speed (STDD) and the base capacity at 4 mph STDD, there is significant difference between the base capacity at both 0 mph and 4 mph STDD and 8 mph STDD. Therefore, the standard deviation of desired speed is found to have an impact on the base capacity of two-lane, two-way

highways. The higher the standard deviation the desired speeds have, the lower the base capacity is.

Table E- 2 Result of *t*-test for base capacities as a function of standard deviation of desired speed

p-value		Standard deviation of desired speed (mph)		
		0	4	8
Standard deviation of desired speed (mph)	0	NA	0.58	3.21e-7
	4	0.58	NA	5.13e-7
	8	3.21e-7	5.13e-7	NA

Table 5-12 is examined. When all drivers have identical delay of safety reaction time and the delay of safety reaction time varies, it is found that there is significant difference in the base capacities.

Table E- 3 Result of *t*-test for base capacities with delay of safety reaction time

p-value		Delay of safety reaction time (sec)		
		0.07	0.78	1.14
Delay of safety reaction time (sec)	0.07	NA	0.002	3.44e-31
	0.78	0.002	NA	3.13e-29
	1.14	3.44e-31	3.13e-29	NA

Table 5-13 is examined. Table E-4 shows that when the length of segment varies, there is no significant difference in base capacity.

Table E- 4 Result of *t*-test for base capacities with length of segment

p-value		Length of segment (mile)			
		1	2	3	4
Length of segment (mile)	1	NA	0.208	0.656	0.283
	2	0.208	NA	0.377	0.948
	3	0.656	0.377	NA	0.477
	4	0.283	0.948	0.477	NA

Table 7-11 is examined. It is found that there is no significant difference in capacity when the radius of driveway curb varies.

Table E- 5 Result of *t*-test for capacities with radius of driveway curb

p-value		Radius of driveway curb (ft)		
		20	30	45
Radius of driveway curb (ft)	20	NA	0.084	0.077
	30	0.084	NA	0.794
	45	0.077	0.794	NA

Table 7-12 is examined. It is found that there is significant difference in capacities when radius of horizontal curve varies.

Table E- 6 Result of *t*-test for capacities with radius of horizontal curve

p-value		Radius of horizontal curve (ft)				
		100	300	400	500	1000
Radius of horizontal curve (ft)	100	NA	3.32e-26	3.22e-22	7.67e-40	1.28e-42
	300	3.32e-26	NA	1.57e-5	3.38e-18	6.21e-23
	400	3.22e-22	1.57e-5	NA	1.06e-6	6.14e-12
	500	7.67e-40	3.38e-18	1.06e-6	NA	4.76e-9
	1000	1.28e-42	6.21e-23	6.14e-12	4.76e-9	NA

Table 7-13 is examined. It is found that there is significant difference in capacity when the grade of the segment varies, when there is at least 10 percent truck traffic.

Table E- 7 Result of *t*-test for capacities with grade of upgrade segment

p-value		Grade of upgrade segment (%)		
		4	6	8
Grade of upgrade segment (%)	4	NA	2.93e-8	4.68e-14
	6	2.93e-8	NA	9.24e-6
	8	4.68e-14	9.24e-6	NA

Table 7-14 is examined. It is found that there is significant difference in capacities when maximum superelevation of horizontal curve varies.

Table E- 8 Result of *t*-test for capacities with maximum superelevation of horizontal curve

p-value		Maximum superelevation of horizontal curve (%)		
		4	7	10
Maximum superelevation of horizontal curve (%)	4	NA	1.21e-7	4.86e-20
	7	1.21e-7	NA	1.89e-10
	10	4.86e-20	1.89e-10	NA

Table 7-15 is examined. It is found that there is significant difference in capacities when the radius of horizontal curve varies in combination with varying percent of trucks.

Table 7-16 is examined. Like the result of Table E-5, the curb radius of driveway was found to have little impact on capacity. On the other hand, the change in percent of truck with the same radius is shown to have significant impact on capacity. Three cases are not rejected. Case 1 (1 in Table E-11) and Case 2 (2 in Table E-11) that have same truck percent and different radius shows that the radius of curb has no impact on capacity. Case 3 (3 in Table E-11) that has different radius and different truck percent shows that

there is no significant result even if Case 4 (4 in Table E-11), the same case gives opposite result. Consequently, it is found that the truck percent has significant impact on capacity, but the different radius does not. According to the result of Case 3, the impact by higher truck percent at certain truck percents (10 and 20 percent) on capacity appears to be offset by increased radius of driveway. More detailed tests will be recommended as future study.

Table E- 9 Result of *t*-test for capacities with radius of horizontal curve with percent of trucks

p-value		Combination of radius of horizontal curve and percent of trucks (ft, %)								
		100, 0	100, 10	100, 20	500, 0	500,10	500, 20	1000, 0	1000, 10	1000, 20
1Combinat-ion of radius of horizontal curve and percent of trucks	100,0	NA	1.1e-6	1.9e-13	7.7e-40	2.3e-19	3.1e-7	1.3e-42	2.4e-22	1.1e-18
	100, 10	1.1e-6	NA	8.6e-6	1.1e-30	3.5e-19	1.2e-10	4.2e-36	2.1e-19	7.5e-16
	100, 20	1.9e-13	8.6e-6	NA	5.5e-31	1.7e-20	5.5e-14	2.4e-36	1.5e-19	5.5e-17
	500, 0	7.7e-40	1.1e-30	5.5e-31	NA	9.5e-11	7.0e-17	4.7e-9	0.0051	3.4e-17
	500, 10	2.3e-19	3.5e-19	1.7e-20	9.5e-11	NA	5.5e-7	4.3e-17	0.0002	0.0198
	500, 20	3.1e-7	1.2e-10	5.5e-14	7.0e-17	5.5e-7	NA	1.1e-22	6.2e-10	0.0013
	1000, 0	1.3e-42	4.2e-36	2.4e-36	4.7e-9	4.3e-17	1.1e-22	NA	8.0e-9	5.9e-22
	1000, 10	2.4e-22	2.1e-19	1.5e-19	0.0051	0.0002	6.2e-10	8.0e-9	NA	1.0e-7
	1000, 20	1.1e-18	7.5e-16	5.5e-17	3.4e-17	0.0198	0.0013	5.9e-22	1.0e-7	NA

Table E- 10 Result of *t*-test for capacities with radius of horizontal curve with percent of trucks

p-value		Combination of driveway curb radius and percent of trucks (ft, %)					
		30, 0	30, 10	30, 20	45, 0	45, 10	45, 20
Combination of driveway curb radius and percent of trucks (ft, %)	30, 0	NA	5.9e-8	1.1e-12	0.9280[1]	1.0e-5[4]	4.0e-9
	30, 10	5.9e-8	NA	0.0010	8.3e-8	0.0890[2]	0.1733[3]
	30, 20	1.1e-12	0.0010	NA	2.0e-12	8.1e-6	0.0374
	45, 0	0.9280	8.3e-8	2.0e-12	NA	1.3e-5	7.5e-9
	45, 10	1.0e-5	0.0890	8.1e-6	1.3e-5	NA	0.0030
	45, 20	4.0e-9	0.1733	0.0374	7.5e-9	0.0030	NA

Table 7-17 is examined. Most cases are rejected and the test shows that there is significant difference between the capacities for each combination of grade and truck percent. Case 1s (1 in Table E-12) that have same grade and 10 percent of difference in truck percent at certain truck percents (20 and 30 percent) are shown to have little impact on capacity. Case 2s (2 in Table E-12) shows that higher grade and lower truck percent does not have significant impact on capacity in certain grades and truck percents. More detailed examination is recommended in future study. Consequently, different grade is found to have significant impact on capacity as long as truck percent is equal. The do-not-reject cases raises questions that the impact by higher truck percent would not be significant at certain high truck percents with the same grade of upgrade section and the impact by higher grade on capacity appear to be offset by decreased truck percent. Most combinations of grade and truck percent are shown to have significant difference in their capacities.

Table E- 11 Result of *t*-test for capacities as a function of grade and percent of trucks

p-value		Combination of grade and percent of truck (%, %)								
		4, 10	4, 20	4, 30	6, 10	6, 20	6, 30	8, 10	8, 20	8, 30
Combination of grade and percent of truck (%, %)	4, 10	NA	2.3e-10	4.1e-10	4.2e-11	6.9e-23	1.4e-17	1.5e-18	8.2e-23	1.1e-26
	4, 20	2.3e-10	NA	0.0591[1]	0.0179	1.5e-11	1.0e-9	1.1e-9	6.8e-14	8.2e-18
	4, 30	4.1e-10	0.0591	NA	0.5858[2]	8.2e-6	1.4e-5	9.1e-5	1.5e-7	5.0e-11
	6, 10	4.2e-11	0.0179	0.5858	NA	4.9e-5	0.0002	9.2e-6	5.1e-10	2.8e-11
	6, 20	6.9e-23	1.5e-11	8.2e-6	4.9e-5	NA	0.1108[1]	0.0672[2]	3e-6	1.9e-10
	6, 30	1.4e-17	1.0e-9	1.4e-5	0.0002	0.1108	NA	0.8188[2]	0.0174	6.5e-6
	8, 10	1.5e-18	1.1e-9	9.1e-5	9.2e-6	0.0672	0.8188	NA	0.0049	0.0001
	8, 20	8.2e-23	6.8e-14	1.5e-7	5.1e-10	3e-6	0.0174	0.0049	NA	0.1195[1]
	8, 30	1.1e-26	8.2e-18	5.0e-11	2.8e-11	1.9e-10	6.5e-6	0.0001	0.1195	NA

Table 7-19 is examined. It is found that there is significant difference in capacity when the percent of truck varies, when a horizontal curve is present.

Table E- 12 Result of *t*-test for capacities as a function of percent of trucks at horizontal curve

p-value		Percent of truck at horizontal curve (%)		
		0	10	20
Percent of truck at horizontal curve (%)	0	NA	1.2e-5	2.7e-8
	10	1.2e-5	NA	1.9e-6
	20	2.7e-8	1.9e-6	NA

The following two hypothesis tests show that there is significant difference between two average flow rates and average travel speeds associated with Figure 6-11. It is concluded that the presence of passing zones has increasing impact on average flow rate

and improves traffic operations particularly when traffic condition are below capacity level.

Table E- 13 Test of means for average flow rate

	Var 1	Var 2
Mean	1745.2	1774.5
Variance	2122.1	1093.9
Observations	30	32
Pooled Variance	1590.9	
Hypothesized diff	0	
Degree of freedom	60	
t-value	-2.94	
P(T<=t) one side	0.0027	
t-value for one side	1.67	
P(T<=t) both sides	0.0053	
t-value for both sides	2.00	

Table E- 14 Test of means for average travel speed

	Var 1	Var 2
Mean	52.6	53.8
Variance	1.2	0.5
Observations	30	32
Pooled Variance	0.8	
Hypothesized diff	0	
Degree of freedom	60	
t-value	-4.99	
P(T<=t) one side	2.757E-06	
t-value for one side	1.67	
P(T<=t) both sides	5.515E-06	
t-value for both sides	2.00	

VITA

Joonhyo Kim

2250 Dartmouth St. #716, College Station, TX 77840
Phone: (979) 571-4513; E-mail: joonhyokimpsu@hanmail.net

EDUCATION

- Ph.D. Civil Engineering, The Pennsylvania State University, University Park, PA, August 2006
  Major: Transportation Engineering.
- M.E. Civil Engineering, Texas A&M University, College Station, TX, December 2001.
  Major: Transportation Engineering.
- B.S. Urban Engineering, Hanyang University, Seoul, South Korea, August 1987.

EMPLOYMENT

- Research Assistant — February 2005 – December 2005
  University of Florida, Gainesville, FL
- Research Assistant — November 2002 – June 2004
  Pennsylvania Transportation Institute, The Pennsylvania State University, University Park, PA
- Research Assistant — June 2002 – August 2002
  Texas Transportation Institute, 3135 TAMU, College Station, TX
- Grading Teaching Assistant — January 2001 – December 2001
  Texas A&M University, College Station, TX

PUBLICATIONS (Journals and Conference Proceedings)

- Kim, J. and Elefteriadou, L., "New microscopic simulation model for the estimation of capacity in two-lane two-way highways", Under preparation to be submitted to the ASCE Journal of Engineering. September 2006.
- Kim, J. and Elefteriadou, L., "Estimation of capacity in two-lane, two-way highways using a simulation model (TWOSIM)", Under preparation to be submitted to the Transportation Research Board. July 2006.

PROFESSIONAL AFFILIATIONS/ACTIVITIES

- Member, Institute of Transportation Engineers (2000- Present)
- Member, American Society of Civil Engineers (2000- Present)
- Member, Transportation Research Board (2000-Present)

SCHOLARSHIPS AND HONORS

- Scholarship, Hanyang University (1983)